Density Model for Bottlenose Dolphin (*Tursiops truncatus*) for the U.S. East Coast: Supplementary Report

Duke University Marine Geospatial Ecology Lab*

Model Version 4.4 - 2016-04-21

Citation

When referencing our methodology or results generally, please cite our open-access article:

Roberts JJ, Best BD, Mannocci L, Fujioka E, Halpin PN, Palka DL, Garrison LP, Mullin KD, Cole TVN, Khan CB, McLellan WM, Pabst DA, Lockhart GG (2016) Habitat-based cetacean density models for the U.S. Atlantic and Gulf of Mexico. Scientific Reports 6: 22615. doi: 10.1038/srep22615

To reference this specific model or Supplementary Report, please cite:

Roberts JJ, Best BD, Mannocci L, Fujioka E, Halpin PN, Palka DL, Garrison LP, Mullin KD, Cole TVN, Khan CB, McLellan WM, Pabst DA, Lockhart GG (2016) Density Model for Bottlenose Dolphin (*Tursiops truncatus*) for the U.S. East Coast Version 4.4, 2016-04-21, and Supplementary Report. Marine Geospatial Ecology Lab, Duke University, Durham, North Carolina.

Copyright and License

Revision History

Version	Date	Description of changes
1	2014-10-21	Initial version.
2	2014-11-13	Reconfigured detection hierarchy and adjusted NARWSS detection functions based on additional information from Tim Cole. Updated documentation.
3	2014-11-19	Removed CumVGPM180 predictor and refitted models.
4	2014-12-05	Fixed bug that applied the wrong detection function to segments NE_narwss_1999_widgeon_hapo dataset. Refitted model. Updated documentation.
4.1	2015-03-06	Updated the documentation. No changes to the model.
4.2	2015-05-14	Updated calculation of CVs. Switched density rasters to logarithmic breaks. No changes to the model.
4.3	2015-10-07	Updated the documentation. No changes to the model.
4.4	2016-04-21	Switched calculation of monthly 5% and 95% confidence interval rasters to the method used to produce the year-round rasters. (We intended this to happen in version 4.2 but I did not implement it properly.) No changes to the other rasters or the model itself.

*For questions, or to offer feedback about this model or report, please contact Jason Roberts (jason.roberts@duke.edu)

Survey Data

Survey	Period	Length (1000 km)	Hours	Sightings
NEFSC Aerial Surveys	1995-2008	70	412	82
NEFSC NARWSS Harbor Porpoise Survey	1999-1999	6	36	0
NEFSC North Atlantic Right Whale Sighting Survey	1999-2013	432	2330	45
NEFSC Shipboard Surveys	1995-2004	16	1143	177
NJDEP Aerial Surveys	2008-2009	11	60	92
NJDEP Shipboard Surveys	2008-2009	14	836	160
SEFSC Atlantic Shipboard Surveys	1992-2005	28	1731	372
SEFSC Mid Atlantic Tursiops Aerial Surveys	1995-2005	35	196	694
SEFSC Southeast Cetacean Aerial Surveys	1992-1995	8	42	212
UNCW Cape Hatteras Navy Surveys	2011-2013	19	125	108
UNCW Early Marine Mammal Surveys	2002-2002	18	98	347
UNCW Jacksonville Navy Surveys	2009-2013	66	402	315
UNCW Onslow Navy Surveys	2007-2011	49	282	144
UNCW Right Whale Surveys	2005-2008	114	586	1842
Virginia Aquarium Aerial Surveys	2012-2014	9	53	67
Total		895	8332	4657

Table 2: Survey effort and sightings used in this model. Effort is tallied as the cumulative length of on-effort transects and hours the survey team was on effort. Sightings are the number of on-effort encounters of the modeled species for which a perpendicular sighting distance (PSD) was available. Off effort sightings and those without PSDs were omitted from the analysis.

Season	Months	Length (1000 km)	Hours	Sightings
All_Year	All	897	8332	4657

Table 3: Survey effort and on-effort sightings having perpendicular sighting distances.

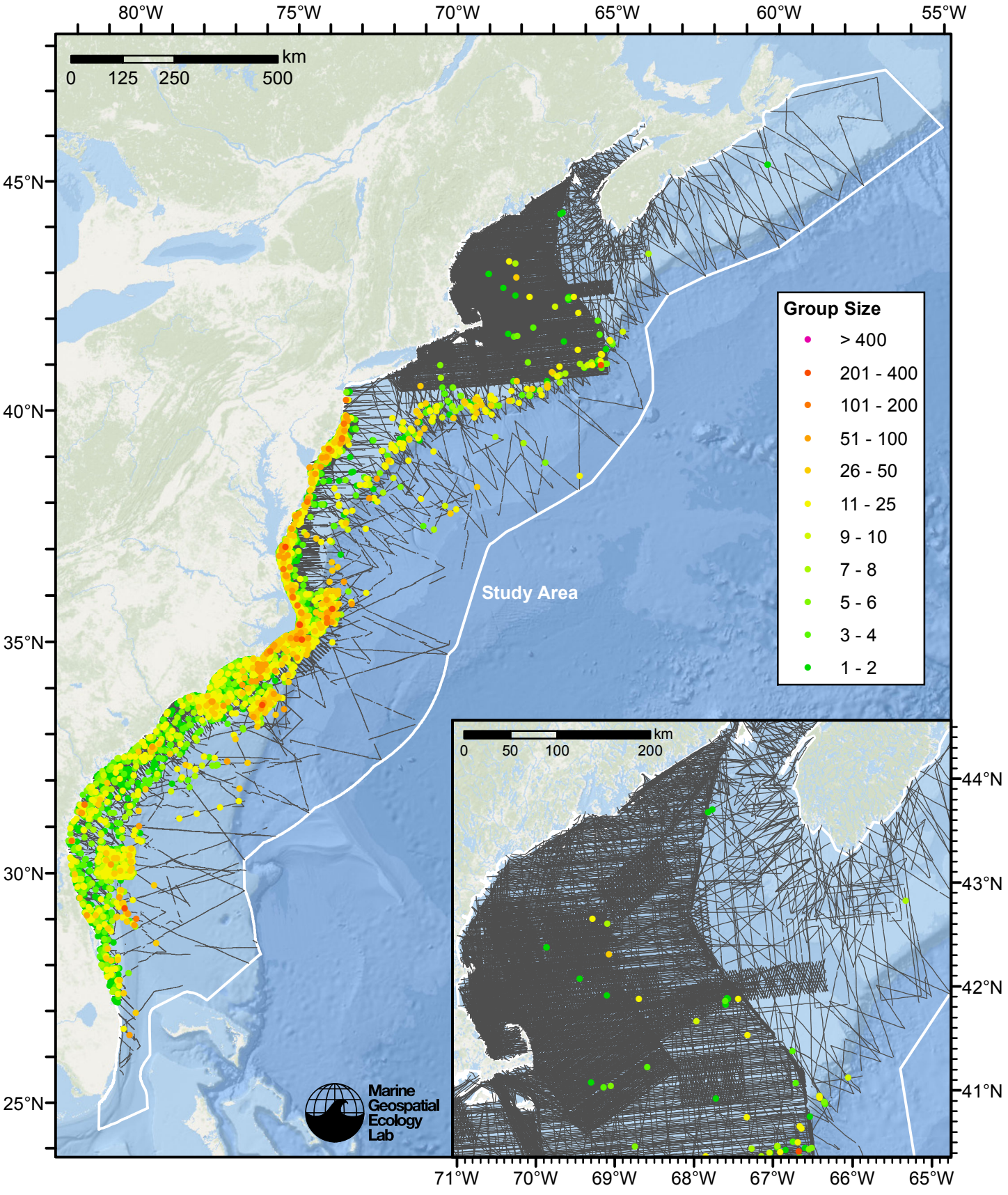

Figure 1: Bottlenose dolphin sightings and survey tracklines.

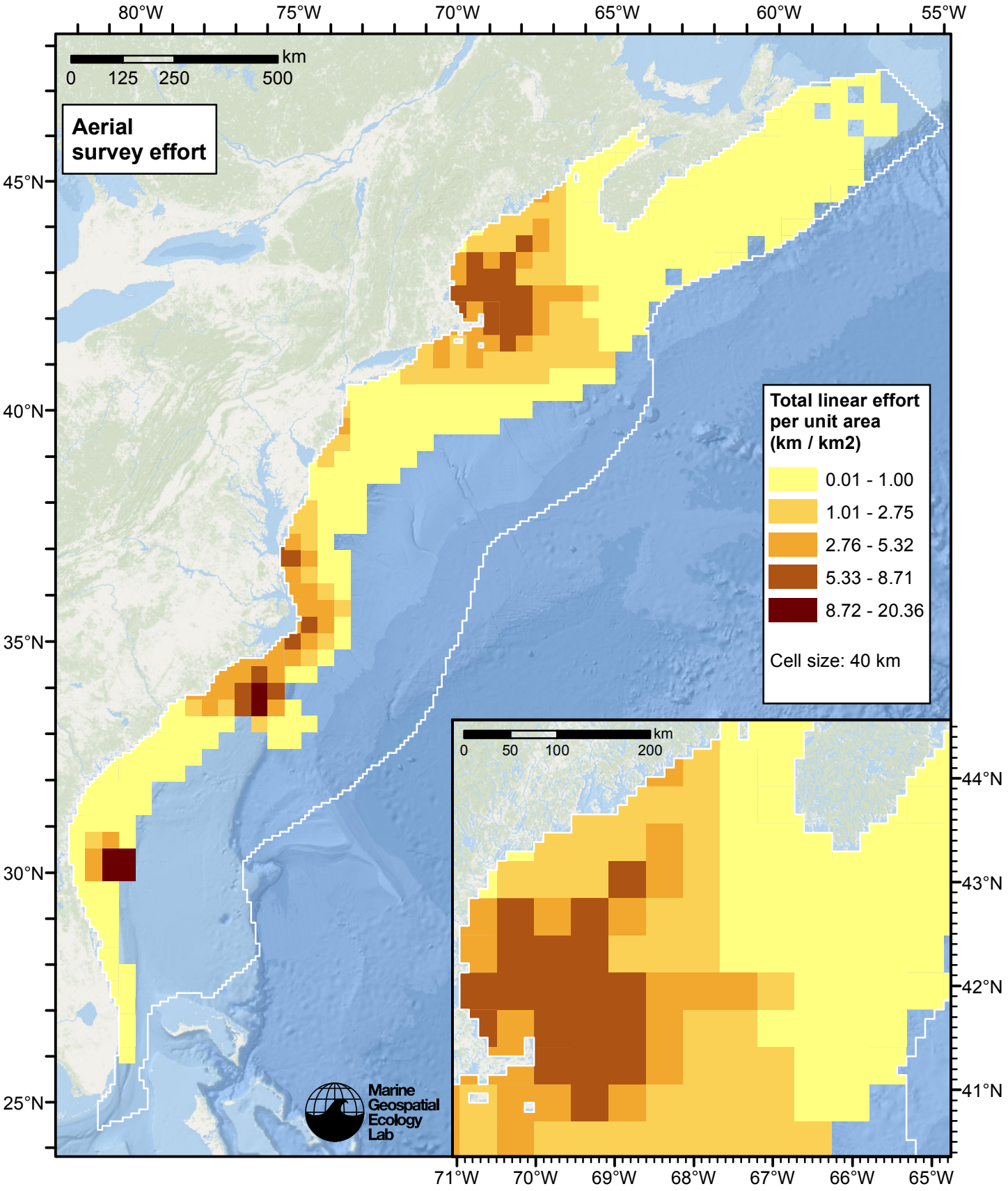

Figure 2: Aerial linear survey effort per unit area.

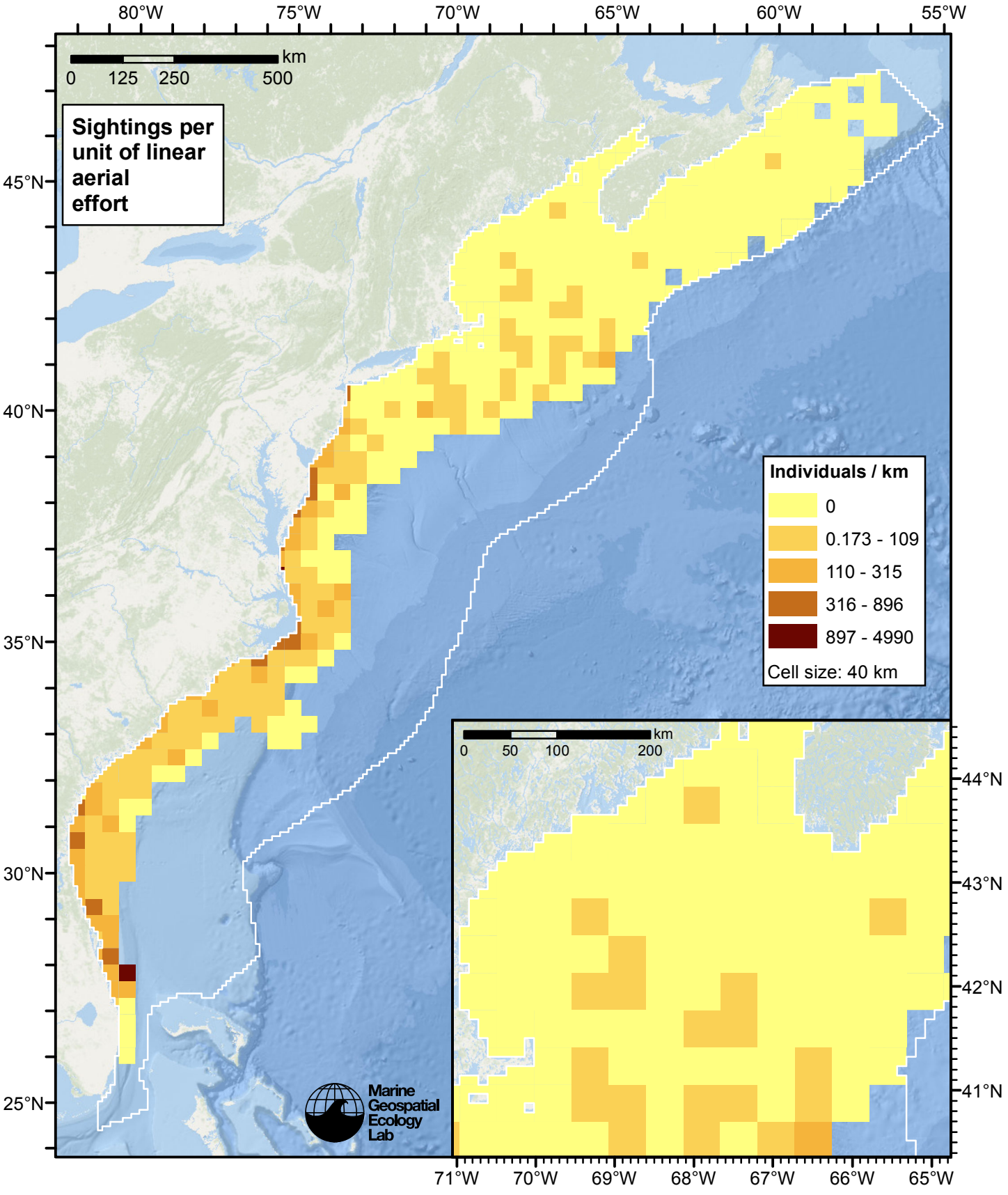

Figure 3: Bottlenose dolphin sightings per unit aerial linear survey effort.

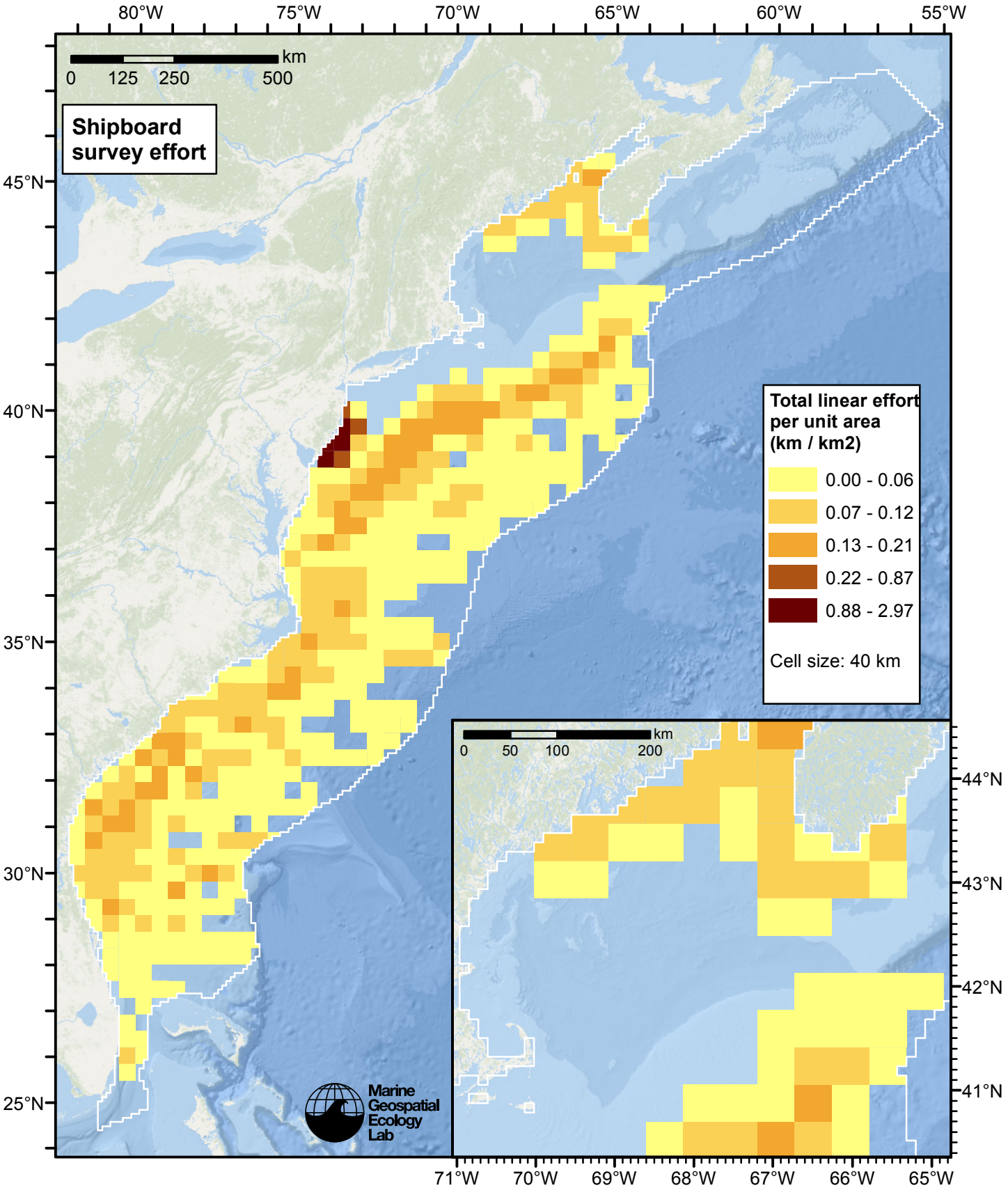

Figure 4: Shipboard linear survey effort per unit area.

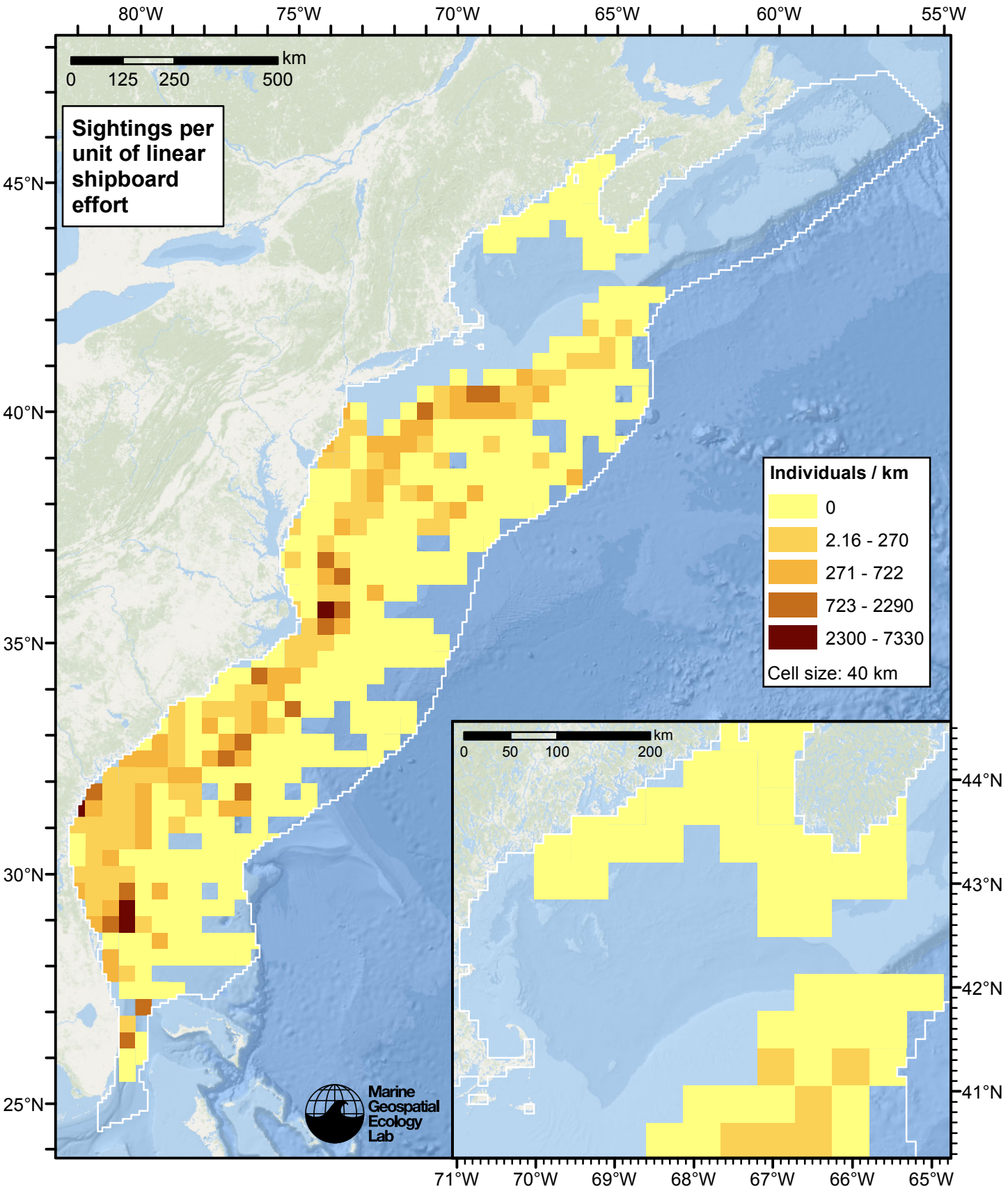

Figure 5: Bottlenose dolphin sightings per unit shipboard linear survey effort.

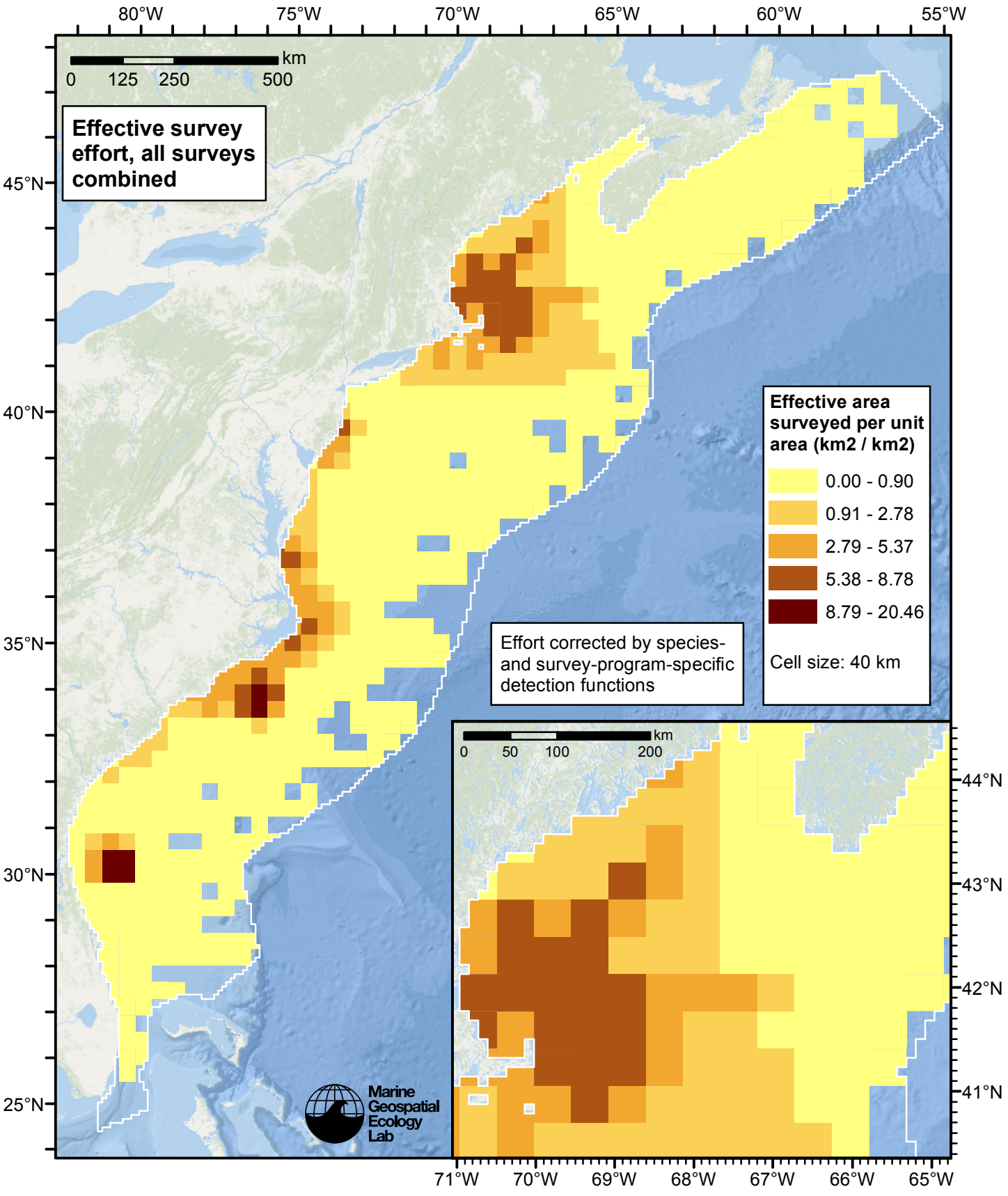

Figure 6: Effective survey effort per unit area, for all surveys combined. Here, effort is corrected by the species- and survey-program-specific detection functions used in fitting the density models.

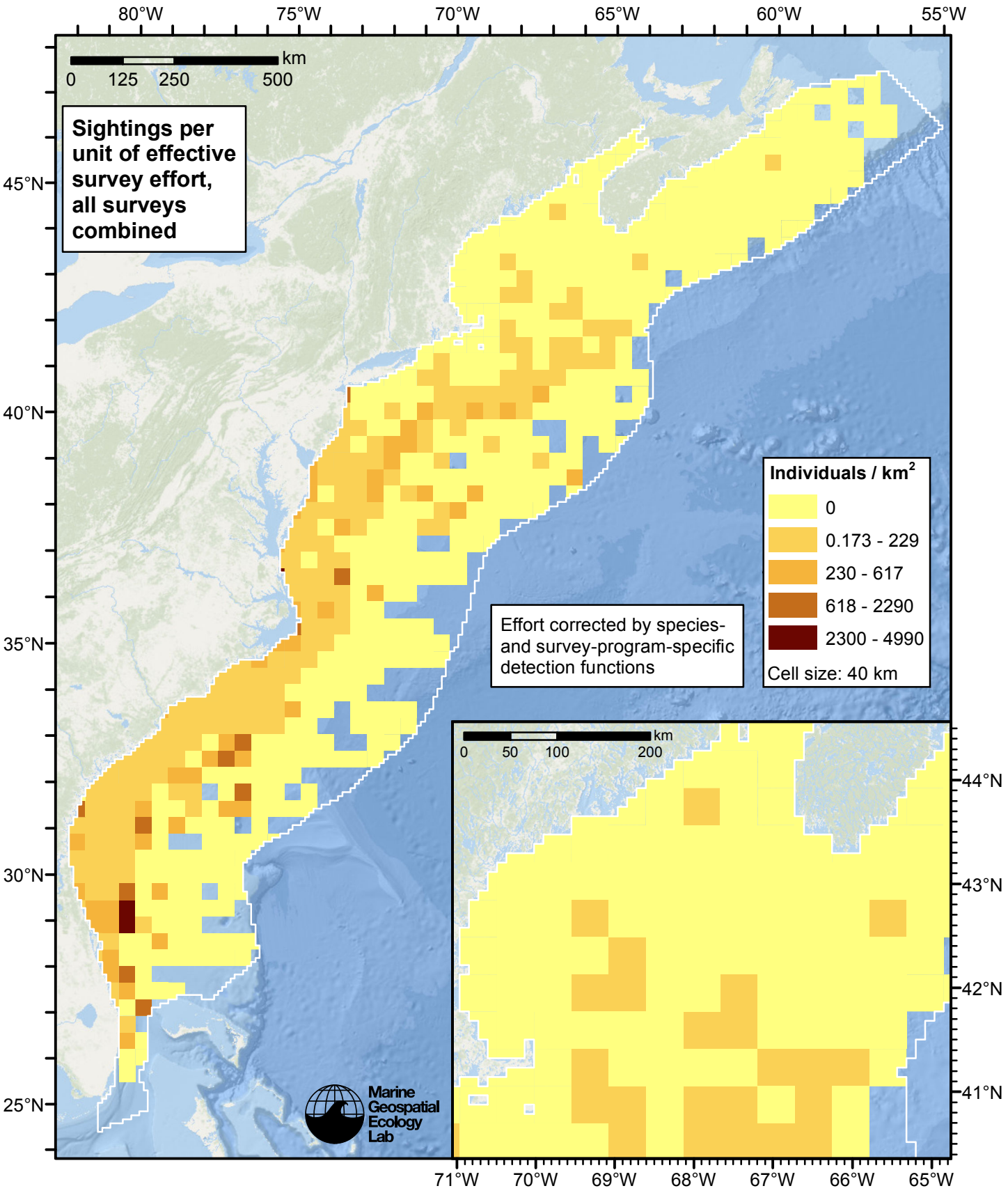

Figure 7: Bottlenose dolphin sightings per unit of effective survey effort, for all surveys combined. Here, effort is corrected by the species- and survey-program-specific detection functions used in fitting the density models.

Reclassification of Ambiguous Sightings

Observers occasionally experience difficulty identifying species, due to poor sighting conditions or phenotypic similarities between the possible choices. For example, observers may not always be able to distinguish fin whales from sei whales (Tim Cole, pers. comm.). When this happens, observers will report an ambiguous identification, such as "fin or sei whale".

In our density models, we handled ambiguous identifications in three ways:

1. For sightings with very generic identifications such as "large whale", we discarded the sightings. These sightings represented a clear minority when compared to those with definitive species identifications, but they are uncounted animals and our density models may therefore underestimate density to some degree.
2. For sightings of certain taxa in which a large majority of identifications were ambiguous (e.g. "Globicephala spp.") rather than specific (e.g. "Globicephala melas" or "Globicephala macrorhynchus"), it was not tractable to model the individual species so we modeled the generic taxon instead.
3. For sightings that reported an ambiguous identification of two species (e.g. "fin or sei whale") that are known to exhibit different habitat preferences or typically occur in different group sizes, and for which we had sufficient number of definitive sightings of both species, we fitted a predictive model that classified the ambiguous sightings into one species or the other.

This section describes how we utilized the third category of ambiguous sightings in the density models presented in this report.

For the predictive model, we used the cforest classifier (Hothorn et al. 2006), an elaboration of the classic random forest classifier (Breiman, 2001). First, we trained a binary classifier using the sightings that reported definitive species identifications (e.g. "fin whale" and "sei whale"). The training data included all on-effort sightings, not just those in the focal study area. We used the species ID as the response variable and oceanographic variables or group size as predictor variables, depending on the species. We used receiver operating characteristic (ROC) curve analysis to select a threshold for classifying the probabilistic predictions of species identifications made by the model into a binary result of one species or another; for the threshold, we selected the value that maximized the Youden index (see Perkins and Schisterman, 2006).

Then, for all sightings reporting the ambiguous identification, we reclassified the sighting as either one species or the other by processing the predictor values observed for that sighting through the fitted model. We then included the reclassified sightings in the detection functions and spatial models of density. The sightings reported elsewhere in this document incorporate both the definitive sightings and the reclassified sightings.

Reclassification of "Stenella frontalis/Tursiops truncatus" in the East Coast Region

Density Histograms

These plots show the per-species distribution of each predictor variable used in the reclassification model. When a variable exhibits a substantially different distribution for each species, it is a good candidate for classifying ambiguous sightings as one species or the other.

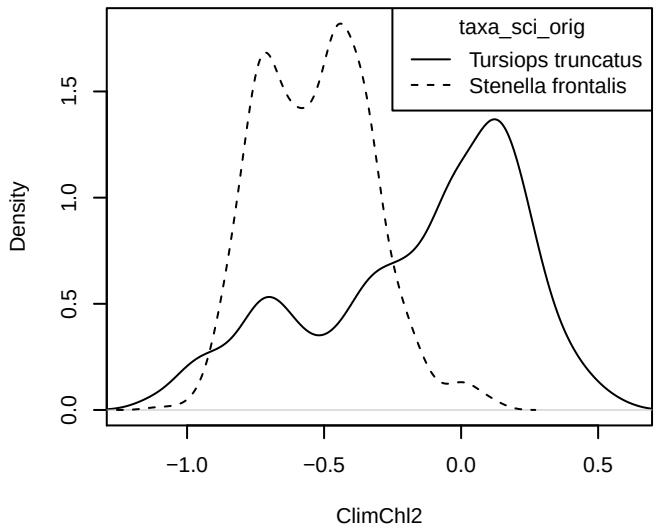
taxa_sci_orig
Tursiops truncatus
Stenella frontalis
Density
ClimChl2

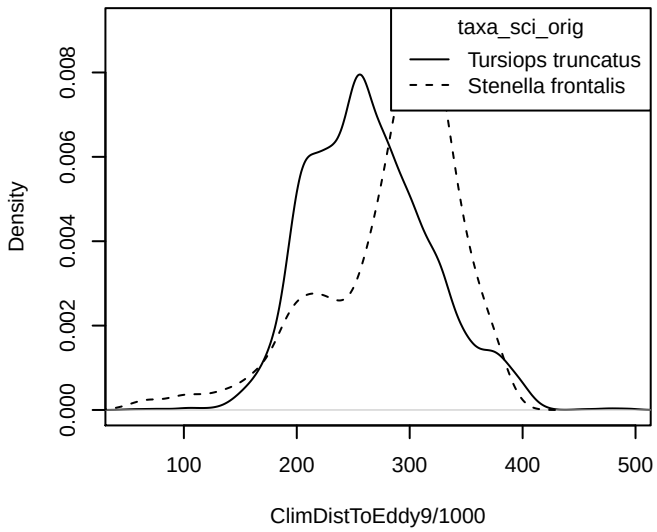
taxa_sci_orig
Tursiops truncatus
Stenella frontalis
Density
ClimDistToEddy9/1000

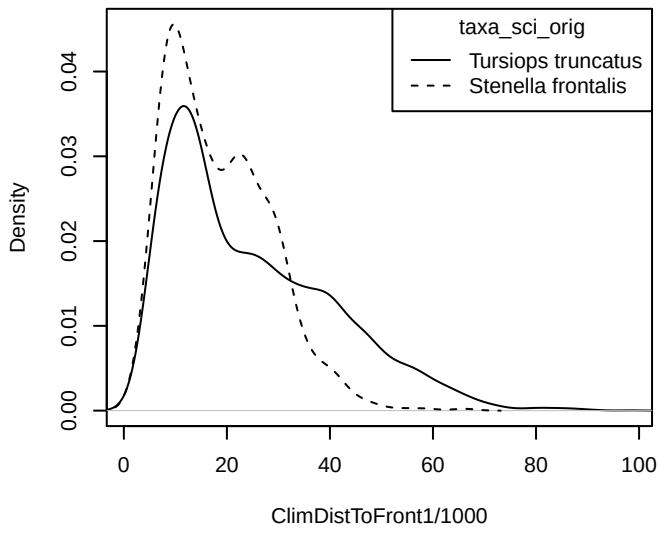
taxa_sci_orig
Tursiops truncatus
Stenella frontalis
Density
ClimDistToFront1/1000

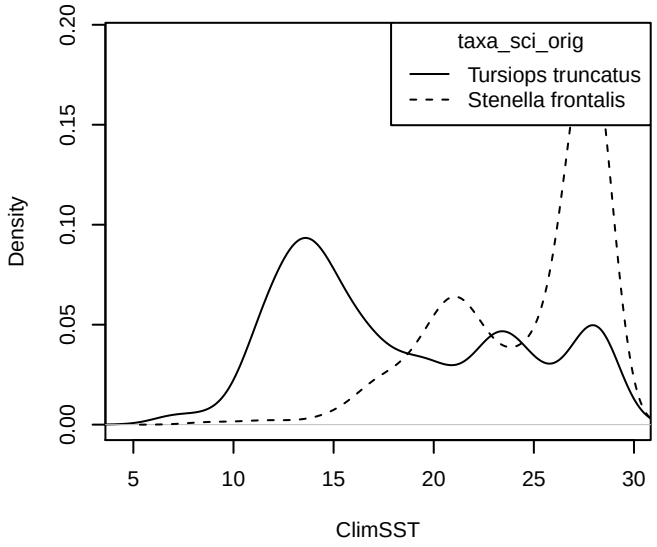
taxa_sci_orig
Tursiops truncatus
Stenella frontalis
Density
ClimSST

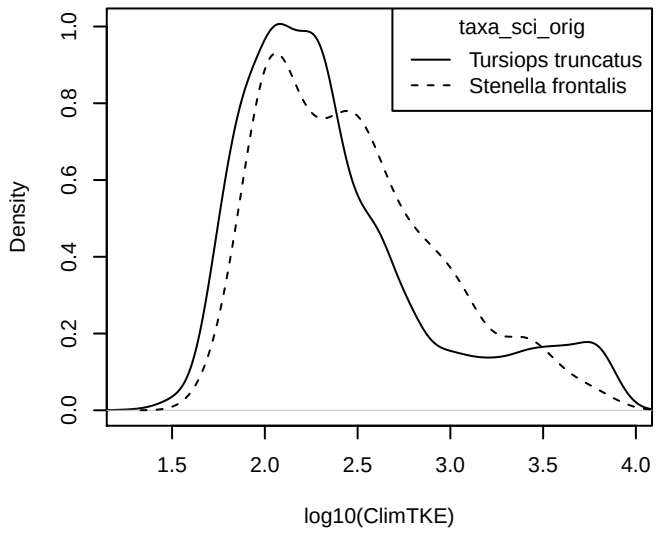
taxa_sci_orig
Tursiops truncatus
Stenella frontalis
Density
log10(ClimTKE)

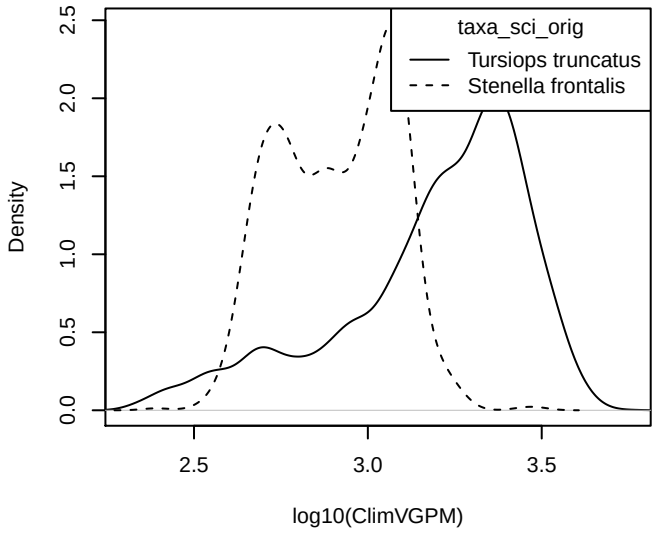
taxa_sci_orig
Tursiops truncatus
Stenella frontalis
Density
log10(ClimVGPM)

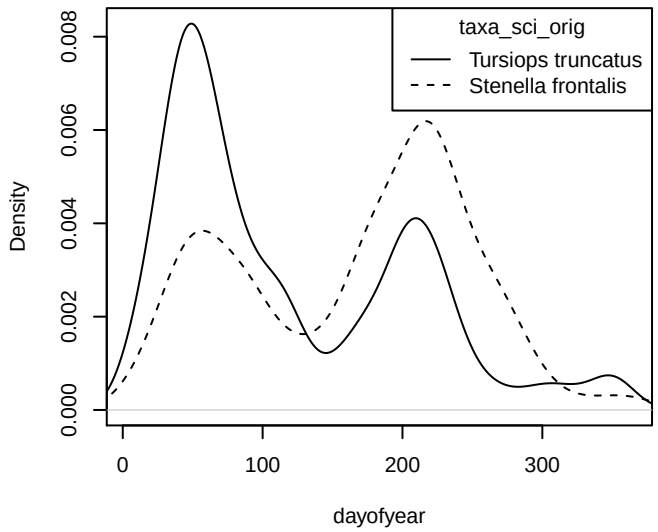

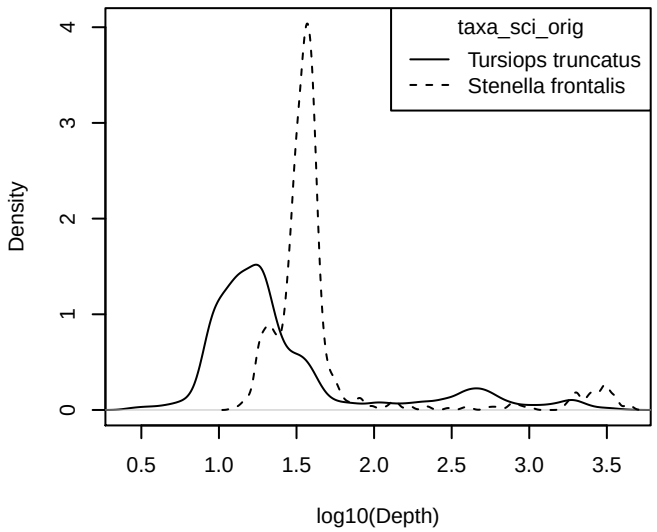

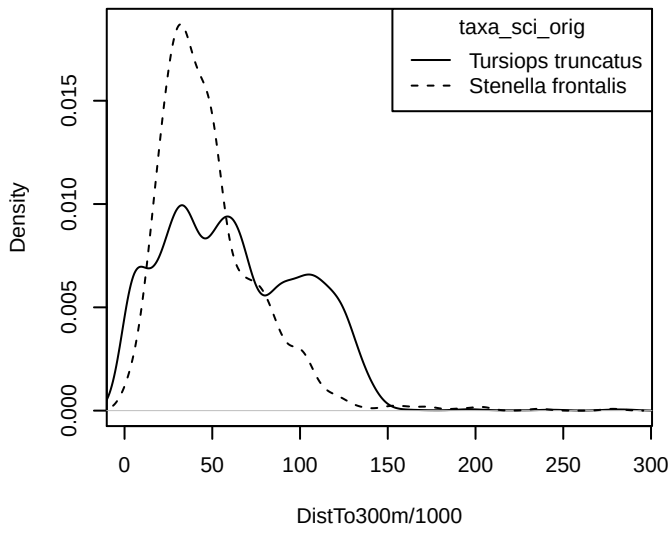

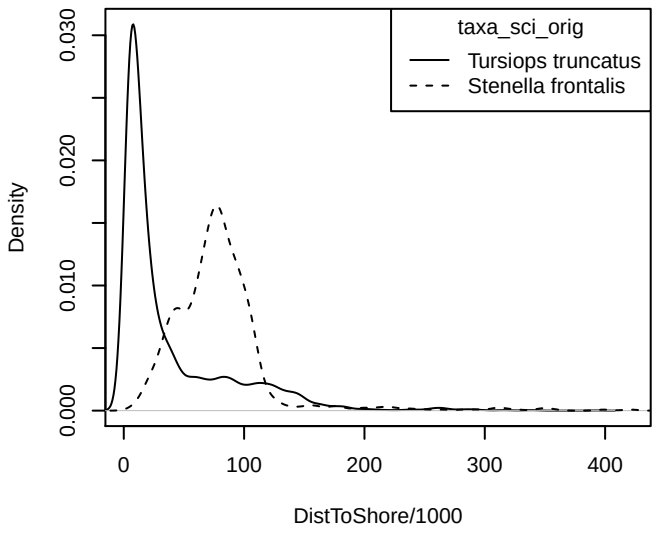

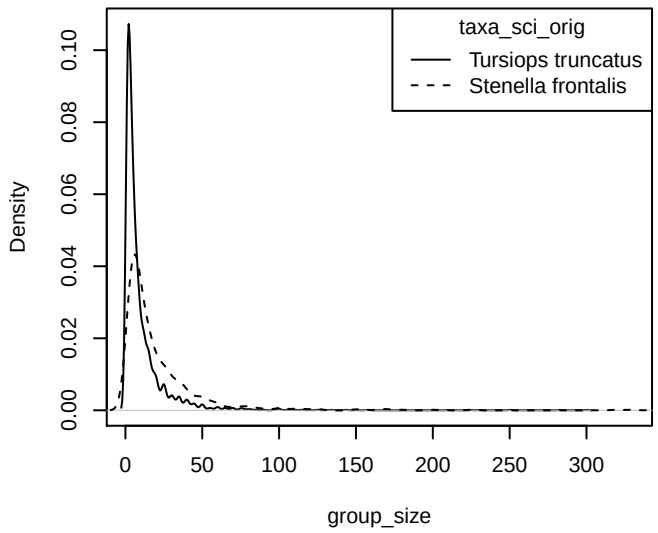

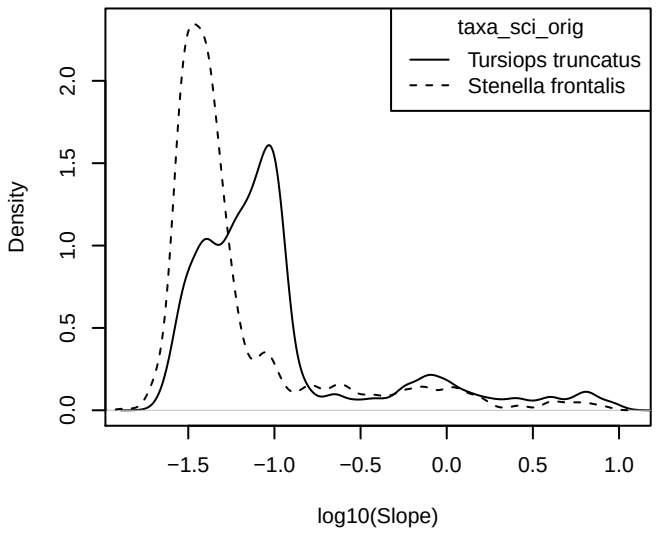

Statistical output

MODEL SUMMARY:

```
==============

     Random Forest using Conditional Inference Trees

Number of trees:  1000

Response:  factor(taxa_sci_orig)
Inputs:  group_size, dayofyear, Depth, Slope, DistToShore, DistTo300m, ClimSST, ClimDistToFront1, ClimChl2, Cl
Number of observations:  5265

Number of variables tried at each split: 5

Estimated predictor variable importance (conditional = FALSE):

                 Importance
ClimVGPM            0.02904
group_size          0.02416
ClimSST             0.02001
Slope               0.01773
DistToShore         0.01602
ClimChl2            0.01454
ClimTKE             0.01186
ClimDistToEddy9     0.01108
DistTo300m          0.00874
Depth               0.00641
ClimDistToFront1    0.00525
dayofyear           0.00353

MODEL PERFORMANCE SUMMARY:
==========================

Statistics calculated from the training data.

Area under the ROC curve (auc)           = 0.980
Mean cross-entropy (mxe)                 = 0.137
Precision-recall break-even point (prbe) = 0.966
Root-mean square error (rmse)            = 0.204

Cutoff selected by maximizing the Youden index = 0.838

Confusion matrix for that cutoff:

                             Actual Tursiops truncatus  Actual Stenella frontalis  Total
Predicted Tursiops truncatus                      4080                         47   4127
Predicted Stenella frontalis                       381                        757   1138
Total                                             4461                        804   5265

Model performance statistics for that cutoff:

Accuracy (acc)                              = 0.919
Error rate (err)                            = 0.081
Rate of positive predictions (rpp)          = 0.784
Rate of negative predictions (rnp)          = 0.216

True positive rate (tpr, or sensitivity)    = 0.915
False positive rate (fpr, or fallout)       = 0.058
True negative rate (tnr, or specificity)    = 0.942
False negative rate (fnr, or miss)          = 0.085
```

```
Positive prediction value (ppv, or precision) = 0.989
Negative prediction value (npv)               = 0.665
Prediction-conditioned fallout (pcfall)       = 0.011
Prediction-conditioned miss (pcmiss)          = 0.335

Matthews correlation coefficient (mcc)        = 0.748
Odds ratio (odds)                             = 172.478
SAR                                           = 0.701

Cohen's kappa (K)                             = 0.732
```

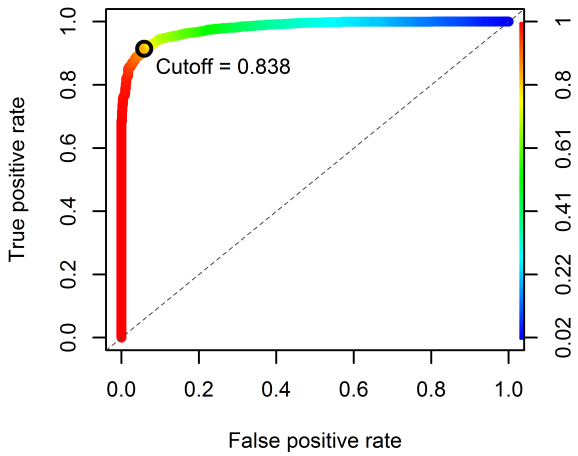

Figure 8: Receiver operating characteristic (ROC) curve illustrating the predictive performance of the model used to reclassify "Stenella frontalis/Tursiops truncatus" sightings into one species or the other.

Reclassifications Performed

Survey	Definitive T. truncatus Sightings	Definitive S. frontalis Sightings	Ambiguous Sightings	Reclassed to T. truncatus	Reclassed to S. frontalis
NEFSC Aerial Surveys	99	1	0	0	0
NEFSC North Atlantic Right Whale Sighting Survey	46	0	0	0	0
NEFSC Shipboard Surveys	184	16	0	0	0
NJDEP Aerial Surveys	92	0	0	0	0
NJDEP Shipboard Surveys	174	0	0	0	0
SEFSC Atlantic Shipboard Surveys	355	319	33	17	16
SEFSC Mid Atlantic Tursiops Aerial Surveys	693	101	20	11	9
SEFSC Southeast Cetacean Aerial Surveys	197	11	39	28	11
UNCW Cape Hatteras Navy Surveys	109	19	0	0	0
UNCW Early Marine Mammal Surveys	645	1	0	0	0
UNCW Jacksonville Navy Surveys	325	267	0	0	0

UNCW Onslow Navy Surveys	148	65	0	0	0
UNCW Right Whale Surveys	1847	5	0	0	0
Virginia Aquarium Aerial Surveys	67	0	0	0	0
Total	4981	805	92	56	36

Table 4: Counts of definitive sightings, ambiguous sightings, and what the ambiguous sightings were reclassified to. Note that this analysis was performed on all on-effort sightings, not just those in the focal study area. These counts may therefore be larger than those presented in the Survey Data section of this report, which are restricted to the focal study area.

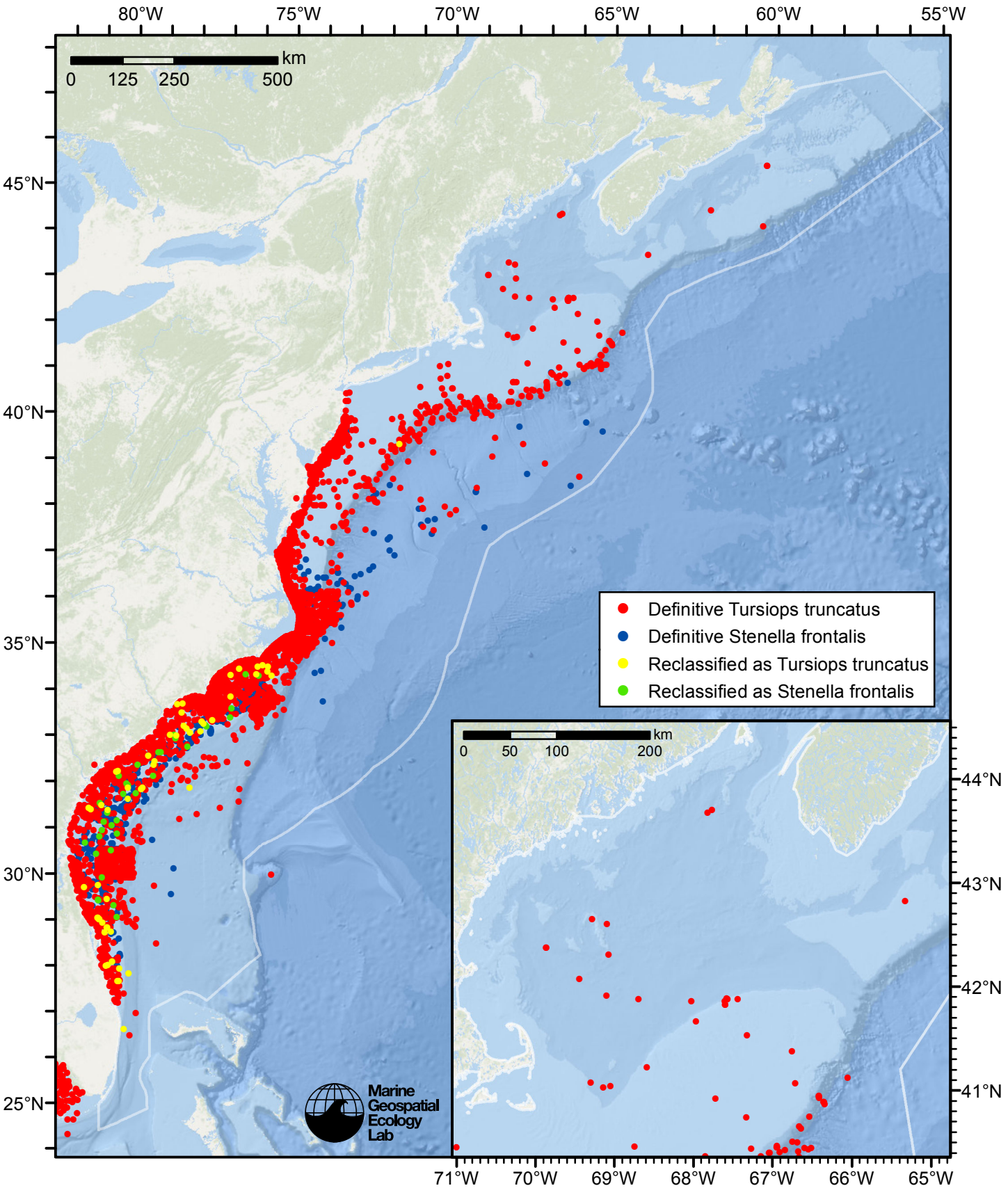

Figure 9: Definitive sightings used to train the model and ambiguous sightings reclassified by the model, by season.

Reclassification of "Stenella frontalis/Tursiops truncatus" in the Gulf of Mexico Region

Density Histograms

These plots show the per-species distribution of each predictor variable used in the reclassification model. When a variable exhibits a substantially different distribution for each species, it is a good candidate for classifying ambiguous sightings as one species or the other.

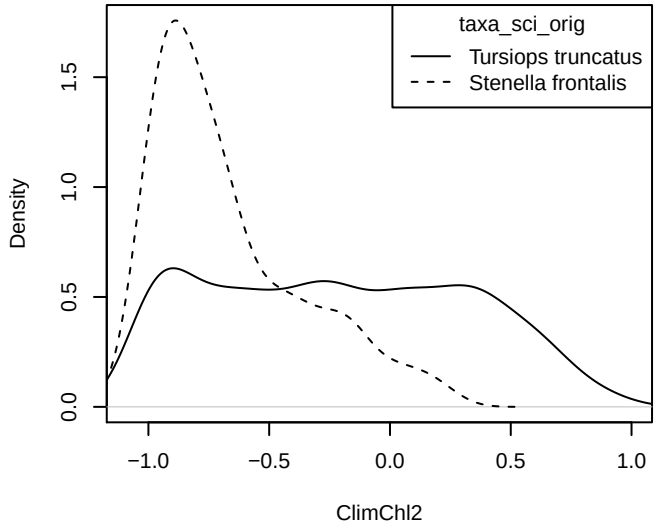

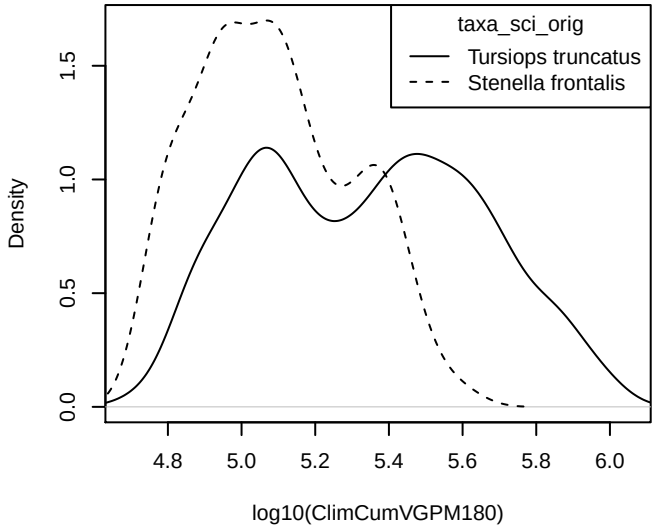

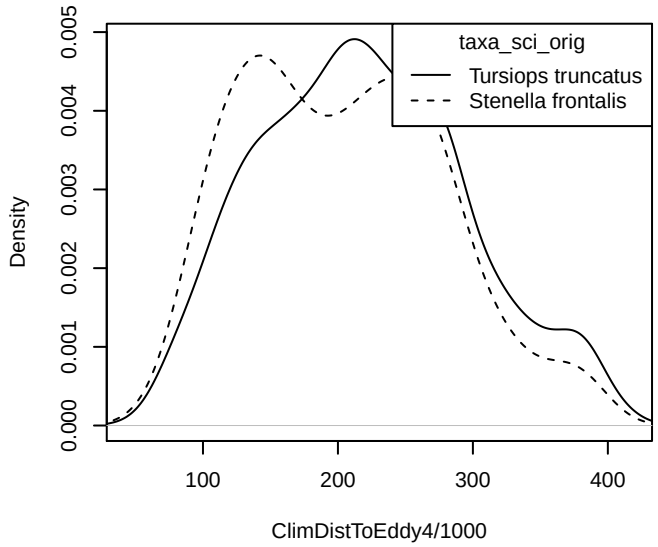

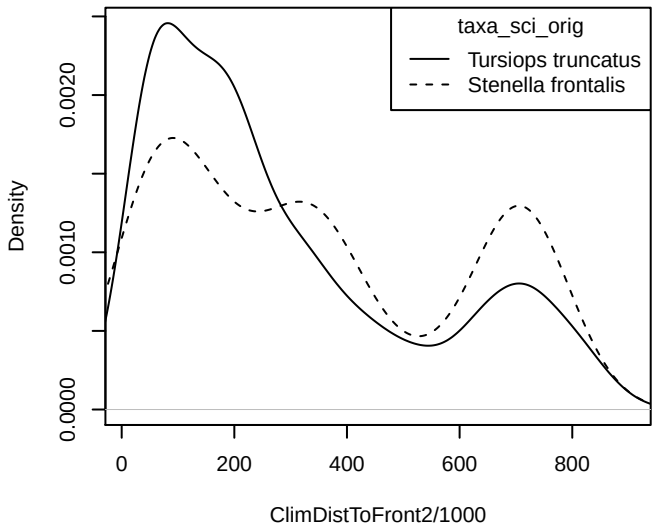

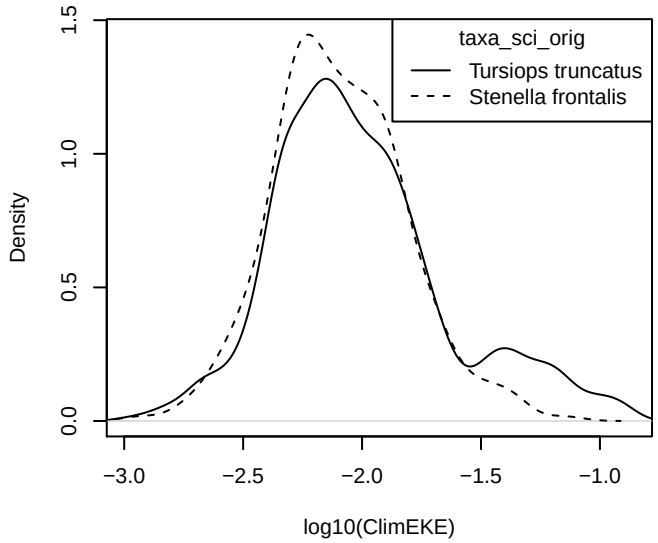
taxa_sci_orig
Tursiops truncatus
Stenella frontalis
Density
log10(ClimEKE)

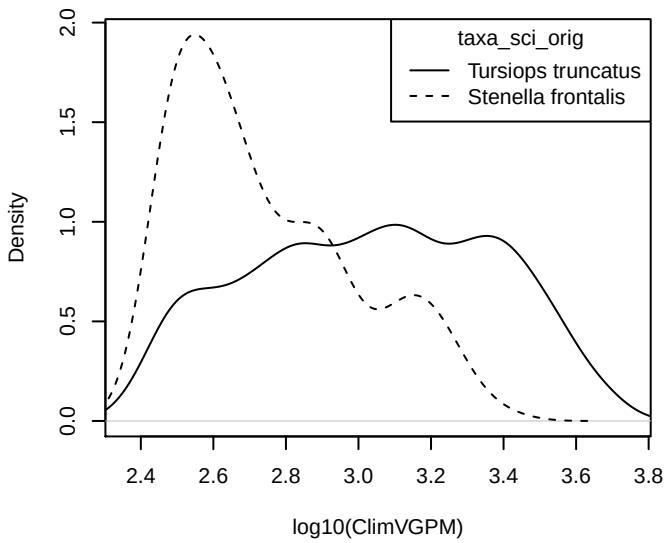
taxa_sci_orig
Tursiops truncatus
Stenella frontalis
Density
log10(ClimVGPM)

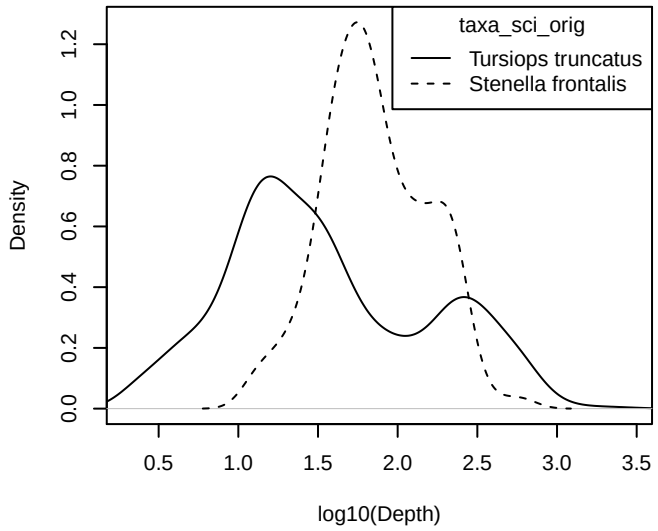
taxa_sci_orig
Tursiops truncatus
Stenella frontalis
Density
log10(Depth)

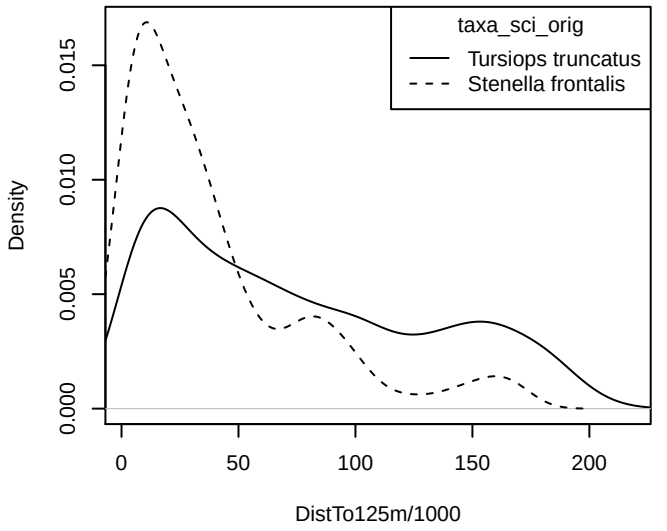
taxa_sci_orig
Tursiops truncatus
Stenella frontalis
Density
DistTo125m/1000

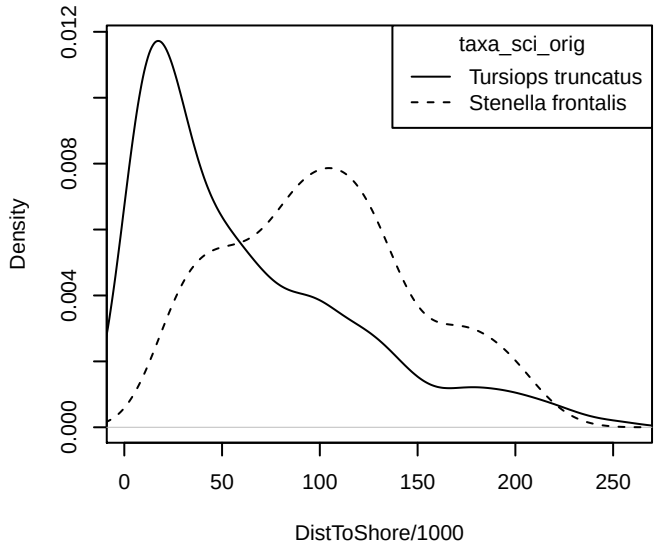
taxa_sci_orig
Tursiops truncatus
Stenella frontalis
Density
DistToShore/1000

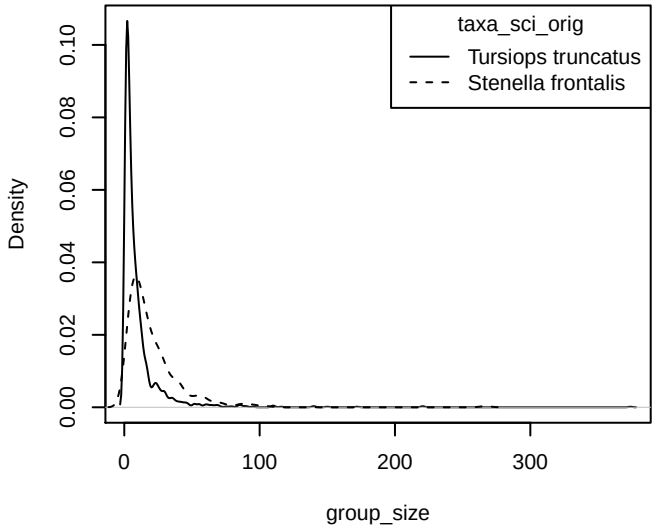
taxa_sci_orig
Tursiops truncatus
Stenella frontalis
Density
group_size

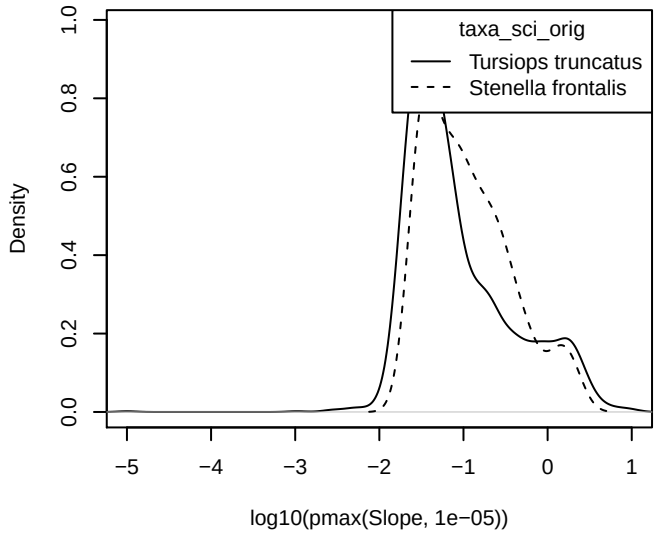

Statistical output

```
MODEL SUMMARY:
==============

     Random Forest using Conditional Inference Trees

Number of trees:  1000

Response:  factor(taxa_sci_orig)
Inputs:  group_size, ClimChl2, Depth, ClimVGPM, DistTo125m, ClimCumVGPM180, Slope, DistToShore, ClimEKE, ClimD
Number of observations:  1959

Number of variables tried at each split: 5

Estimated predictor variable importance (conditional = FALSE):

                 Importance
group_size          0.04073
ClimChl2            0.03281
Depth               0.02925
ClimVGPM            0.01694
ClimDistToEddy4     0.00976
ClimCumVGPM180      0.00798
Slope               0.00759
DistTo125m          0.00619
ClimEKE             0.00433
DistToShore         0.00361
ClimDistToFront2    0.00314

MODEL PERFORMANCE SUMMARY:
==========================

Statistics calculated from the training data.

Area under the ROC curve (auc)           = 0.961
Mean cross-entropy (mxe)                 = 0.193
Precision-recall break-even point (prbe) = 0.951
Root-mean square error (rmse)            = 0.247
```

```
Cutoff selected by maximizing the Youden index = 0.910

Confusion matrix for that cutoff:

                            Actual Tursiops truncatus  Actual Stenella frontalis  Total
Predicted Tursiops truncatus                      1388                         17   1405
Predicted Stenella frontalis                       256                        298    554
Total                                             1644                        315   1959

Model performance statistics for that cutoff:

Accuracy (acc)                                = 0.861
Error rate (err)                              = 0.139
Rate of positive predictions (rpp)            = 0.717
Rate of negative predictions (rnp)            = 0.283

True positive rate (tpr, or sensitivity)      = 0.844
False positive rate (fpr, or fallout)         = 0.054
True negative rate (tnr, or specificity)      = 0.946
False negative rate (fnr, or miss)            = 0.156

Positive prediction value (ppv, or precision) = 0.988
Negative prediction value (npv)               = 0.538
Prediction-conditioned fallout (pcfall)       = 0.012
Prediction-conditioned miss (pcmiss)          = 0.462

Matthews correlation coefficient (mcc)        = 0.645
Odds ratio (odds)                             = 95.042
SAR                                           = 0.690

Cohen's kappa (K)                             = 0.605
```

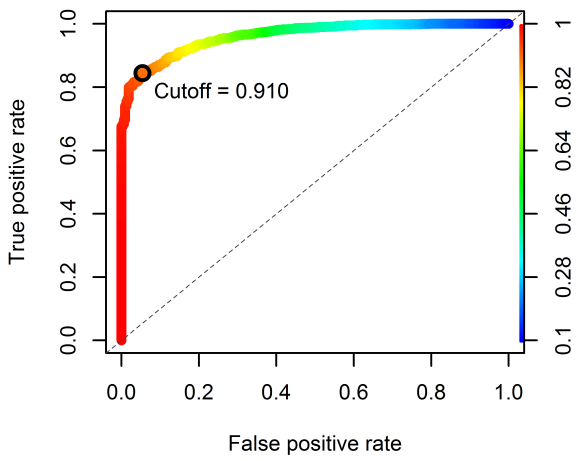

Figure 10: Receiver operating characteristic (ROC) curve illustrating the predictive performance of the model used to reclassify "Stenella frontalis/Tursiops truncatus" sightings into one species or the other.

Reclassifications Performed

Survey	Definitive T. truncatus Sightings	Definitive S. frontalis Sightings	Ambiguous Sightings	Reclassed to T. truncatus	Reclassed to S. frontalis
SEFSC Caribbean Shipboard Surveys	0	1	0	0	0
SEFSC GOMEX92-96 Aerial Surveys	608	21	19	15	4
SEFSC Gulf of Mexico Shipboard Surveys, 2003-2009	69	10	1	0	1
SEFSC GulfCet I Aerial Surveys	83	12	6	5	1
SEFSC GulfCet II Aerial Surveys	153	24	12	12	0
SEFSC GulfSCAT 2007 Aerial Surveys	327	15	5	5	0
SEFSC Oceanic CetShip Surveys	247	73	27	21	6
SEFSC Shelf CetShip Surveys	309	159	86	63	23
Total	1796	315	156	121	35

Table 5: Counts of definitive sightings, ambiguous sightings, and what the ambiguous sightings were reclassified to. Note that this analysis was performed on all on-effort sightings, not just those in the focal study area. These counts may therefore be larger than those presented in the Survey Data section of this report, which are restricted to the focal study area.

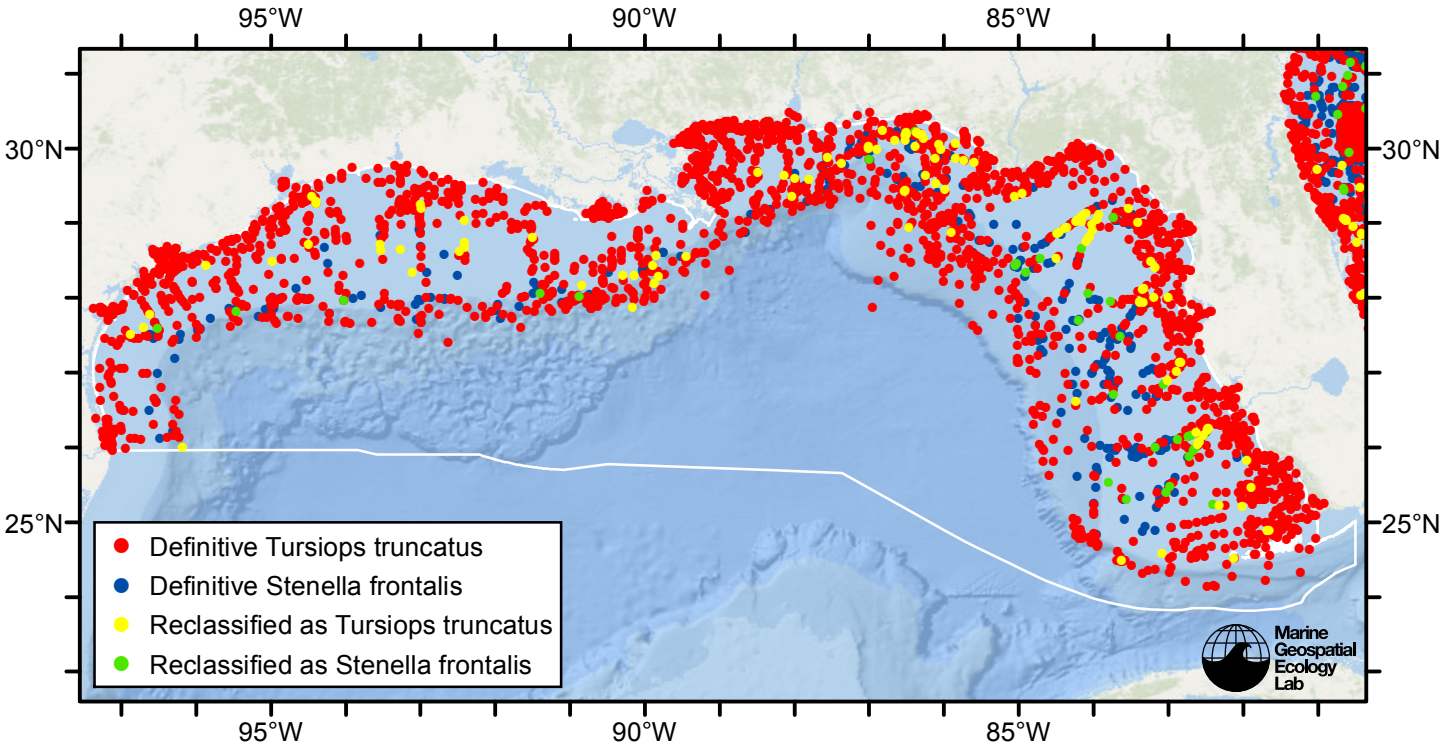

Figure 11: Definitive sightings used to train the model and ambiguous sightings reclassified by the model, by season.

Detection Functions

The detection hierarchy figures below show how sightings from multiple surveys were pooled to try to achieve Buckland et. al's (2001) recommendation that at least 60-80 sightings be used to fit a detection function. Leaf nodes, on the right, usually represent individual surveys, while the hierarchy to the left shows how they have been grouped according to how similar we believed the surveys were to each other in their detection performance.

At each node, the red or green number indicates the total number of sightings below that node in the hierarchy, and is colored green if 70 or more sightings were available, and red otherwise. If a grouping node has zero sightings–i.e. all of the surveys within it had zero sightings–it may be collapsed and shown as a leaf to save space.

Each histogram in the figure indicates a node where a detection function was fitted. The actual detection functions do not appear in this figure; they are presented in subsequent sections. The histogram shows the frequency of sightings by perpendicular sighting distance for all surveys contained by that node. Each survey (leaf node) recieves the detection function that is closest to it up the hierarchy. Thus, for common species, sufficient sightings may be available to fit detection functions deep in the hierarchy, with each function applying to only a few surveys, thereby allowing variability in detection performance between surveys to be addressed relatively finely. For rare species, so few sightings may be available that we have to pool many surveys together to try to meet Buckland's recommendation, and fit only a few coarse detection functions high in the hierarchy.

A blue Proxy Species tag indicates that so few sightings were available that, rather than ascend higher in the hierarchy to a point that we would pool grossly-incompatible surveys together, (e.g. shipboard surveys that used big-eye binoculars with those that used only naked eyes) we pooled sightings of similar species together instead. The list of species pooled is given in following sections.

Shipboard Surveys

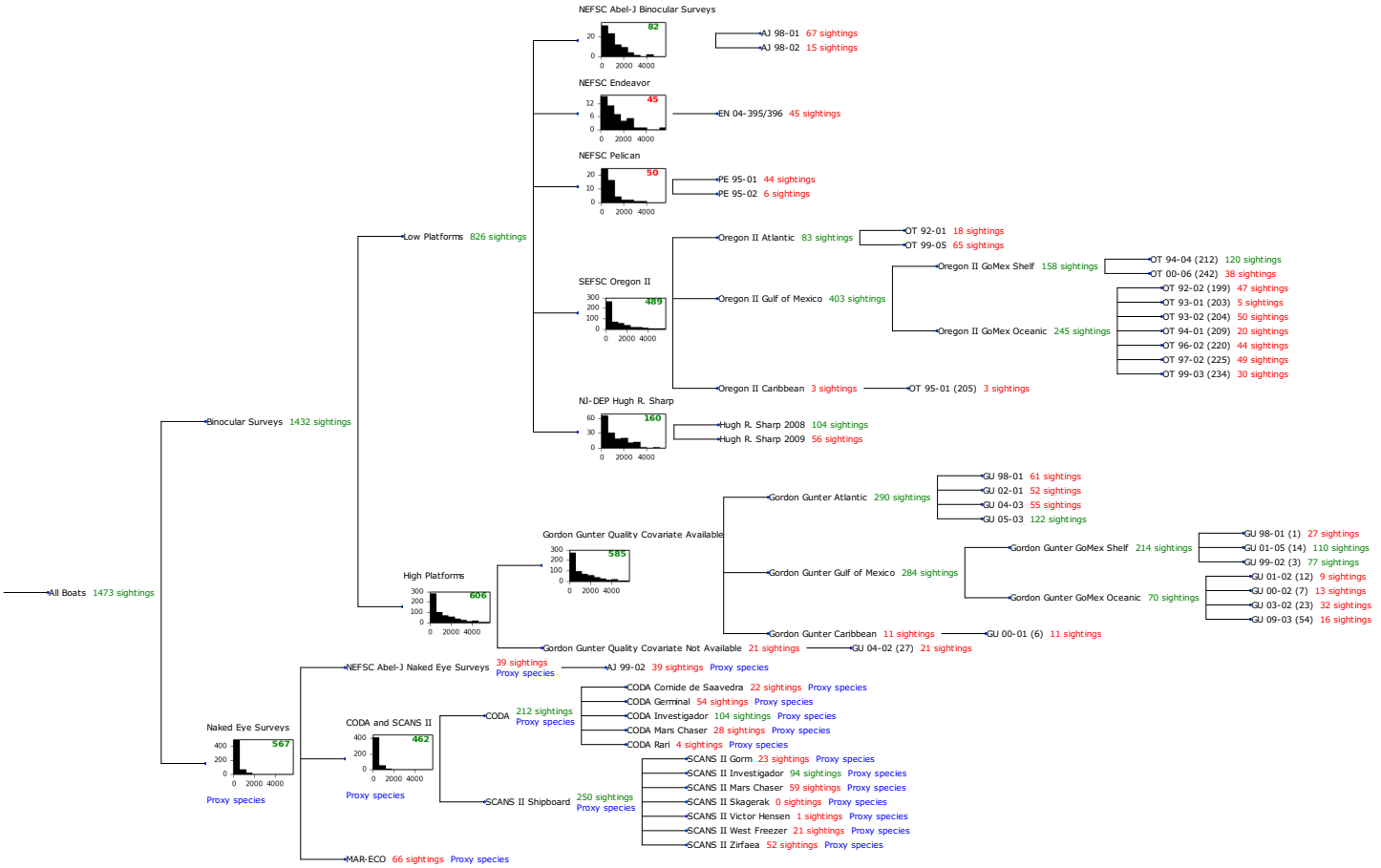

Figure 12: Detection hierarchy for shipboard surveys

NEFSC Abel-J Binocular Surveys

The sightings were right truncated at 4000m.

Covariate	Description
beaufort	Beaufort sea state.
quality	Survey-specific index of the quality of observation conditions, utilizing relevant factors other than Beaufort sea state (see methods).
size	Estimated size (number of individuals) of the sighted group.

Table 6: Covariates tested in candidate "multi-covariate distance sampling" (MCDS) detection functions.

Key	Adjustment	Order	Covariates	Succeeded	Δ AIC	Mean ESHW (m)
hn			beaufort	Yes	0.00	1505
hn			beaufort, size	Yes	0.42	1503
hn	cos	3		Yes	0.70	1234
hn				Yes	1.25	1512
hn			size	Yes	1.85	1514
hn	cos	2		Yes	2.66	1405
hn			quality	Yes	3.20	1511
hn	herm	4		Yes	3.25	1510
hn			quality, size	Yes	3.77	1515
hr			beaufort	Yes	5.76	1552
hr				Yes	6.04	1490
hr			beaufort, size	Yes	7.31	1603
hr			quality	Yes	7.59	1462
hr			beaufort, quality	Yes	7.70	1544
hr			size	Yes	7.99	1495
hr			quality, size	Yes	9.58	1465
hr	poly	2		Yes	90.73	20
hr	poly	4		No		
hn			beaufort, quality	No		
hr			beaufort, quality, size	No		
hn			beaufort, quality, size	No		

Table 7: Candidate detection functions for NEFSC Abel-J Binocular Surveys. The first one listed was selected for the density model.

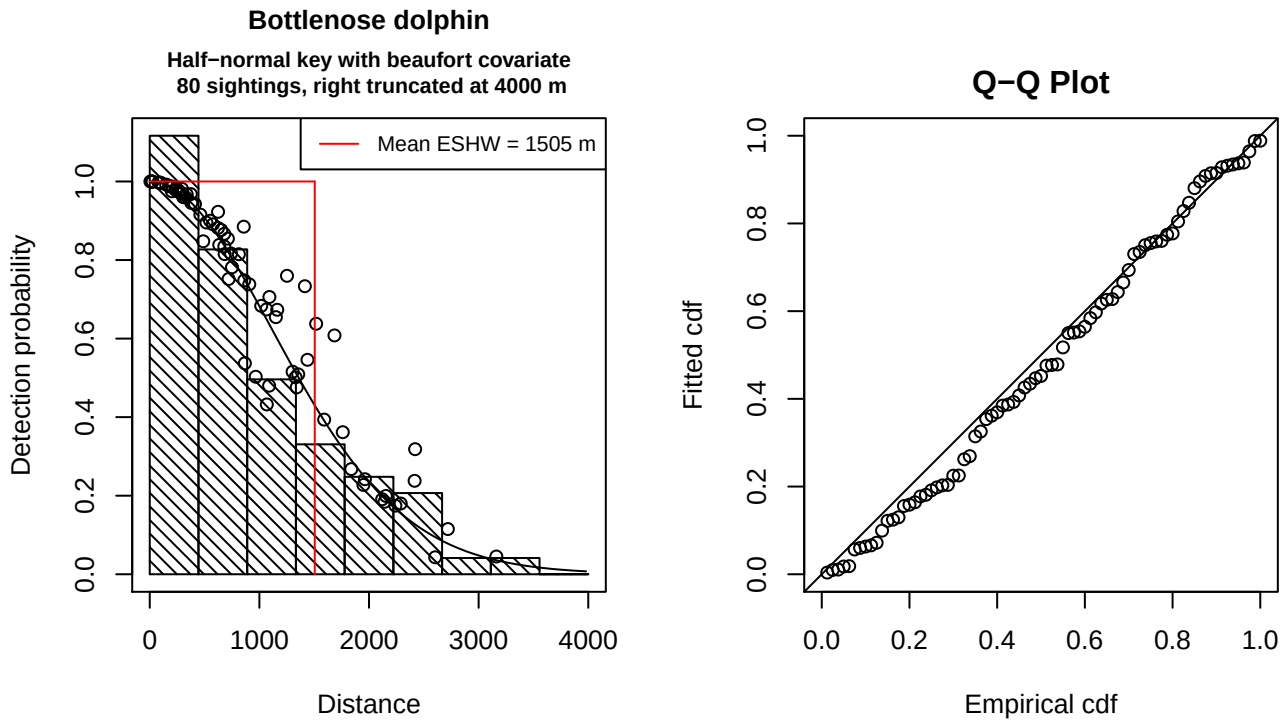

Figure 13: Detection function for NEFSC Abel-J Binocular Surveys that was selected for the density model

Statistical output for this detection function:

```
Summary for ds object
Number of observations :  80
Distance range         :  0  -  4000
AIC                    :  1251.223

Detection function:
 Half-normal key function

Detection function parameters
Scale Coefficients:
             estimate        se
(Intercept)  7.8680200 0.6271920
beaufort    -0.2882772 0.2270839

                      Estimate          SE        CV
Average p             0.3675535  0.03107941 0.0845575
N in covered region 217.6553959 26.80274858 0.1231430
```

Additional diagnostic plots:

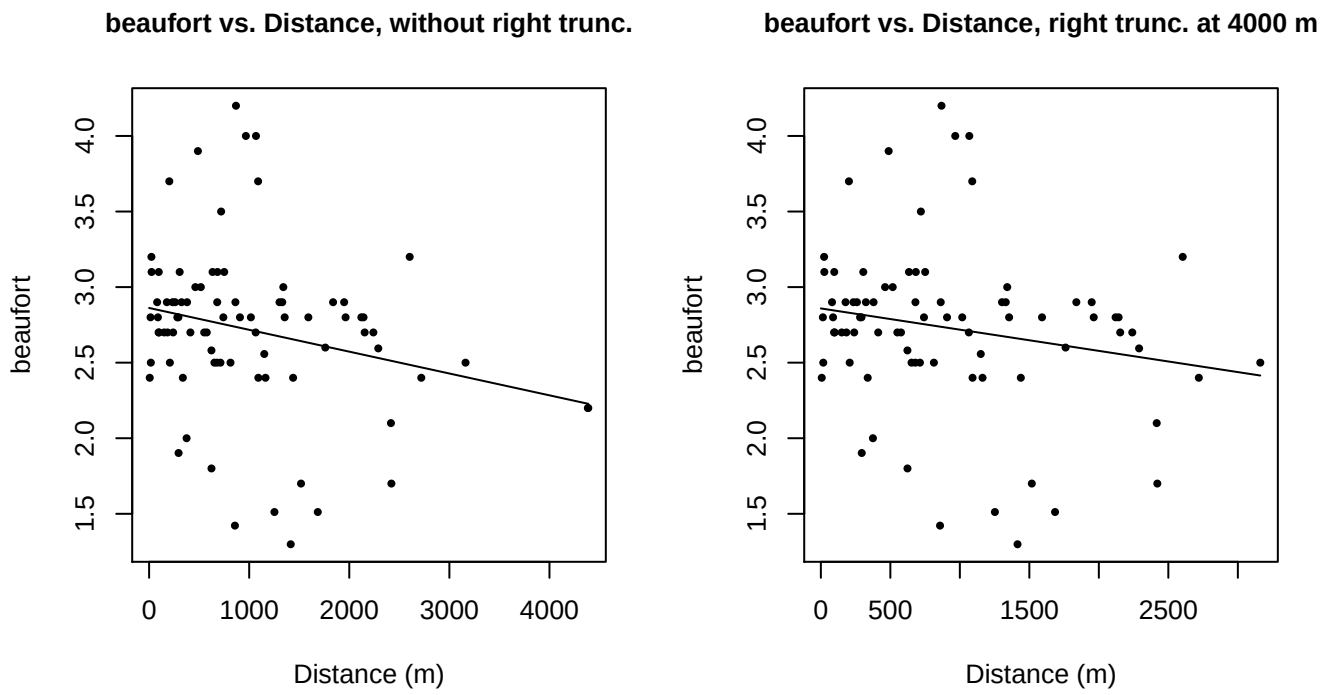

Figure 14: Scatterplots showing the relationship between Beaufort sea state and perpendicular sighting distance, for all sightings (left) and only those not right truncated (right). The line is a simple linear regression.

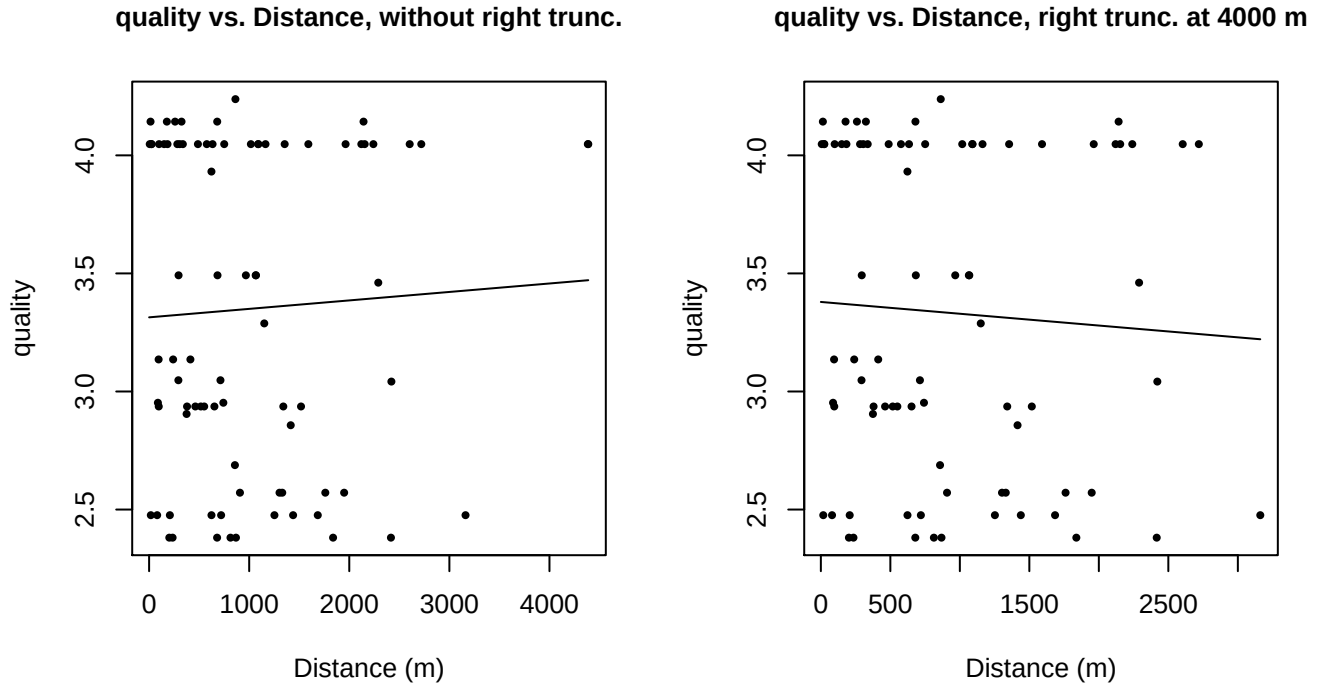

Figure 15: Scatterplots showing the relationship between the survey-specific index of the quality of observation conditions and perpendicular sighting distance, for all sightings (left) and only those not right truncated (right). Low values of the quality index correspond to better observation conditions. The line is a simple linear regression.

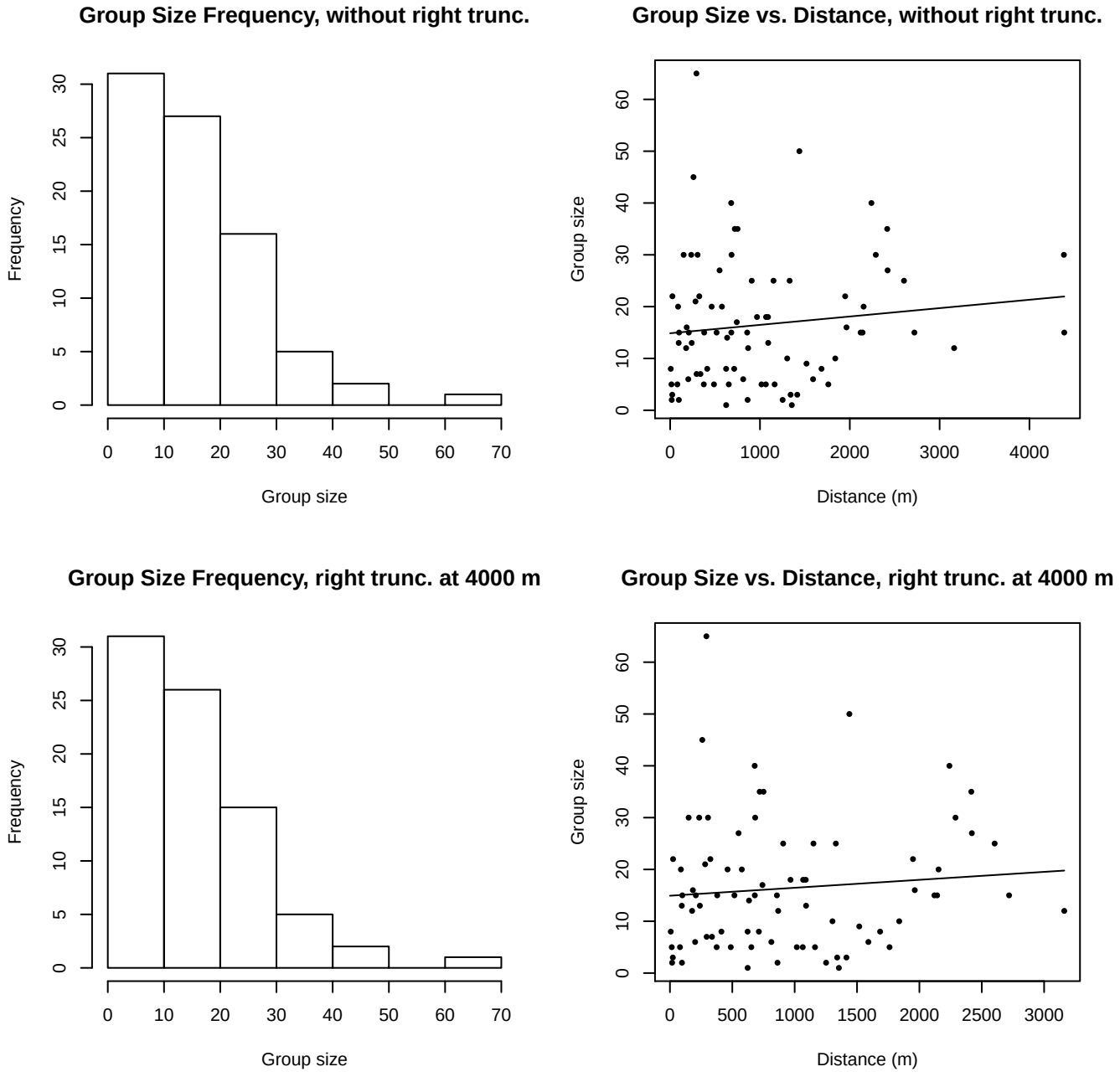

Figure 16: Histograms showing group size frequency and scatterplots showing the relationship between group size and perpendicular sighting distance, for all sightings (top row) and only those not right truncated (bottom row). In the scatterplot, the line is a simple linear regression.

NEFSC Endeavor

The sightings were right truncated at 4000m.

Covariate	Description
beaufort	Beaufort sea state.
quality	Survey-specific index of the quality of observation conditions, utilizing relevant factors other than Beaufort sea state (see methods).
size	Estimated size (number of individuals) of the sighted group.

Table 8: Covariates tested in candidate "multi-covariate distance sampling" (MCDS) detection functions.

Key	Adjustment	Order	Covariates	Succeeded	Δ AIC	Mean ESHW (m)
hn				Yes	0.00	1982
hn	cos	2		Yes	1.23	1715
hr				Yes	1.37	1932
hn			size	Yes	1.65	1980
hn	cos	3		Yes	1.69	1781
hn	herm	4		Yes	1.95	1975
hr	poly	2		Yes	3.36	1893
hr	poly	4		Yes	3.37	1932
hr			beaufort	No		
hn			beaufort	No		
hr			quality	No		
hn			quality	No		
hr			size	No		
hr			beaufort, quality	No		
hn			beaufort, quality	No		
hr			beaufort, size	No		
hn			beaufort, size	No		
hr			quality, size	No		
hn			quality, size	No		
hr			beaufort, quality, size	No		
hn			beaufort, quality, size	No		

Table 9: Candidate detection functions for NEFSC Endeavor. The first one listed was selected for the density model.

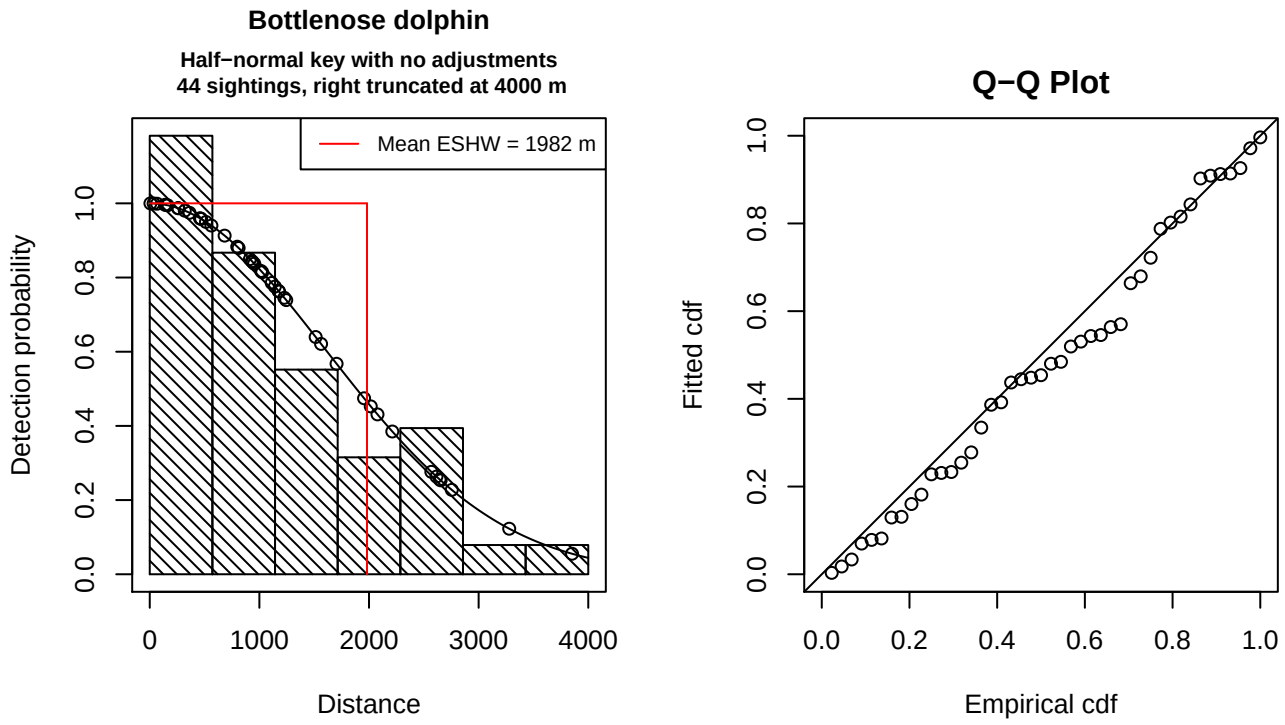

Figure 17: Detection function for NEFSC Endeavor that was selected for the density model

Statistical output for this detection function:

```
Summary for ds object
Number of observations :  44
Distance range         :  0  -  4000
AIC                    :  710.153

Detection function:
 Half-normal key function

Detection function parameters
Scale Coefficients:
            estimate        se
(Intercept) 7.378519 0.1203477

                     Estimate          SE        CV
Average p            0.4954395  0.05429789 0.1095954
N in covered region 88.8100379 13.60807385 0.1532268
```

Additional diagnostic plots:

Figure 18: Scatterplots showing the relationship between Beaufort sea state and perpendicular sighting distance, for all sightings (left) and only those not right truncated (right). The line is a simple linear regression.

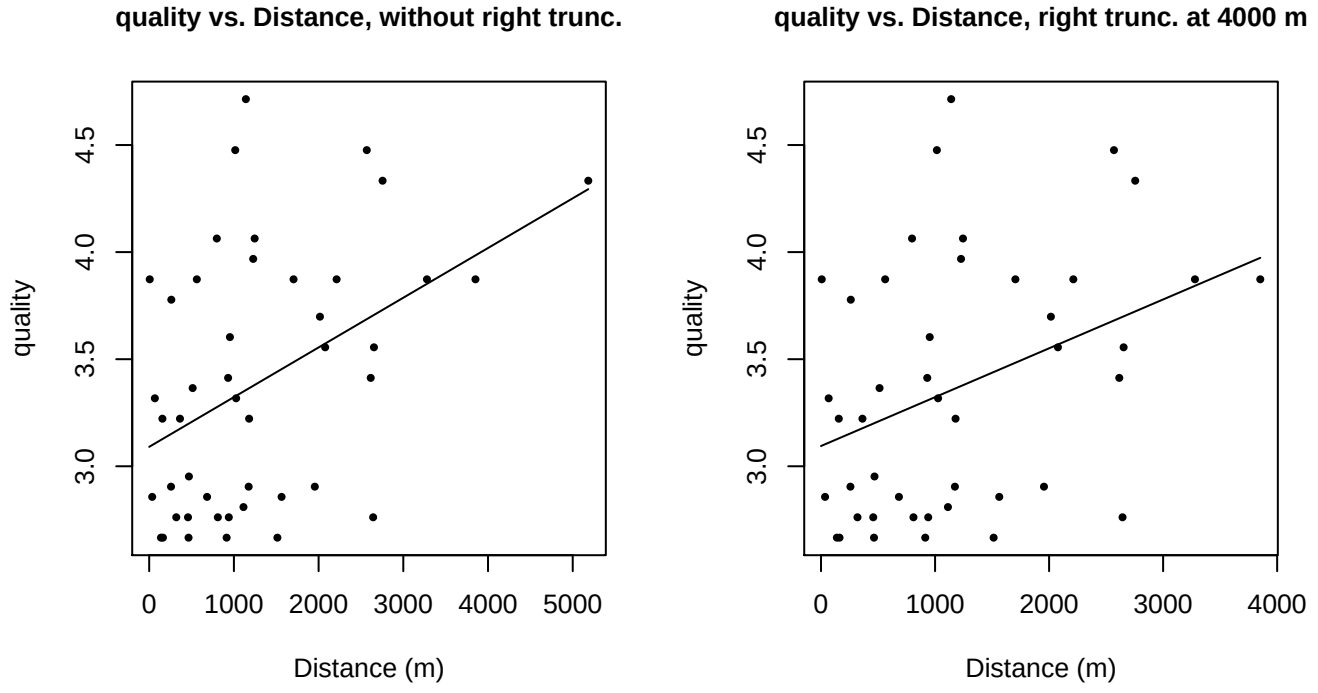

Figure 19: Scatterplots showing the relationship between the survey-specific index of the quality of observation conditions and perpendicular sighting distance, for all sightings (left) and only those not right truncated (right). Low values of the quality index correspond to better observation conditions. The line is a simple linear regression.

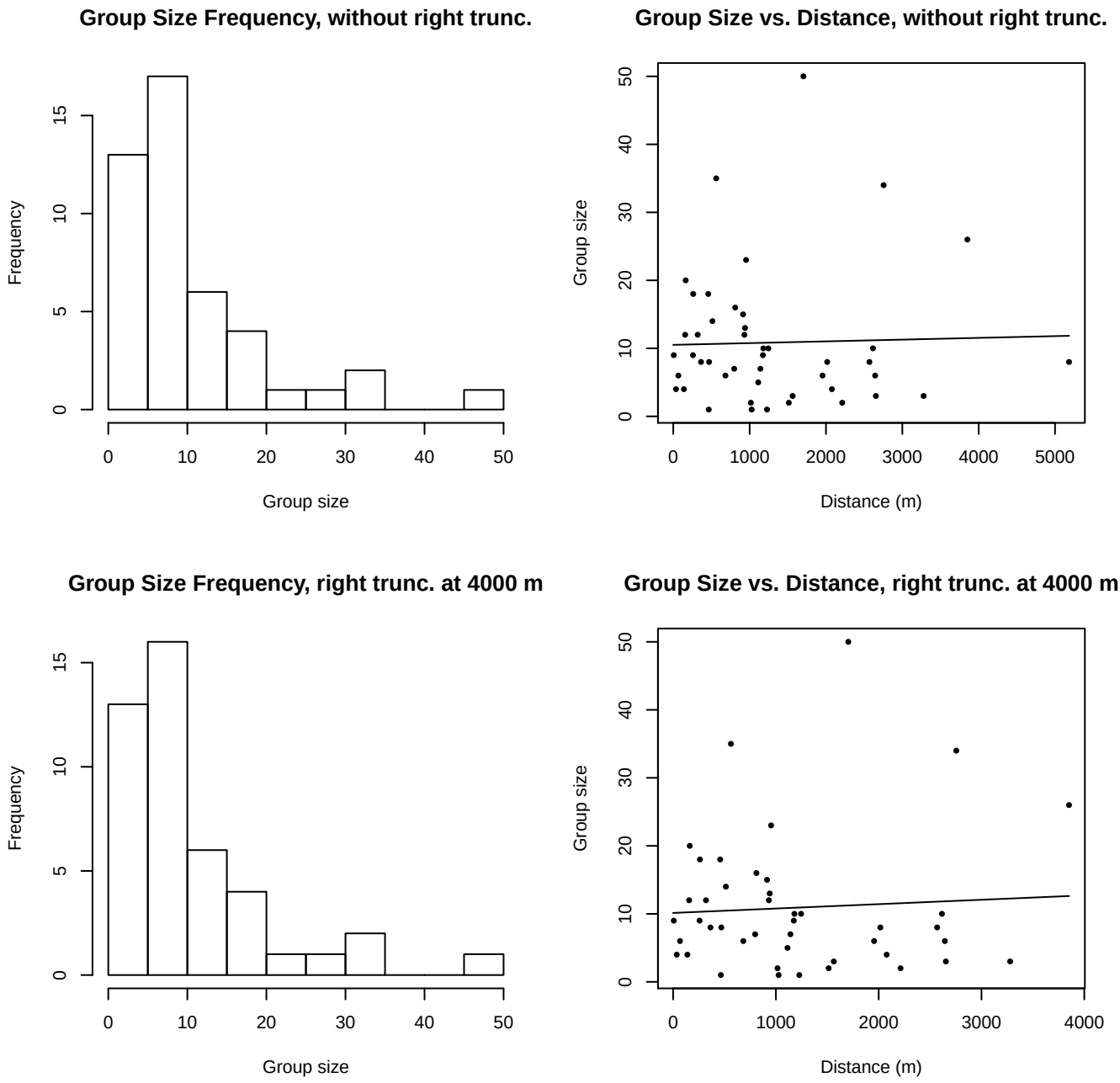

Figure 20: Histograms showing group size frequency and scatterplots showing the relationship between group size and perpendicular sighting distance, for all sightings (top row) and only those not right truncated (bottom row). In the scatterplot, the line is a simple linear regression.

NEFSC Pelican

The sightings were right truncated at 4000m.

Covariate	Description
beaufort	Beaufort sea state.
size	Estimated size (number of individuals) of the sighted group.

Table 10: Covariates tested in candidate "multi-covariate distance sampling" (MCDS) detection functions.

Key	Adjustment	Order	Covariates	Succeeded	Δ AIC	Mean ESHW (m)
hr			size	Yes	0.00	1197
hn	cos	2		Yes	0.00	1101
hr				Yes	0.22	1120
hr			beaufort	Yes	1.55	1142
hr			beaufort, size	Yes	1.97	1196
hn			size	Yes	2.22	1420
hr	poly	4		Yes	2.27	1150
hn			beaufort, size	Yes	2.29	1393
hr	poly	2		Yes	2.36	1184
hn			beaufort	Yes	4.52	1420
hn	cos	3		Yes	5.41	1104
hn				Yes	6.67	1455
hn	herm	4		Yes	8.56	1453

Table 11: Candidate detection functions for NEFSC Pelican. The first one listed was selected for the density model.

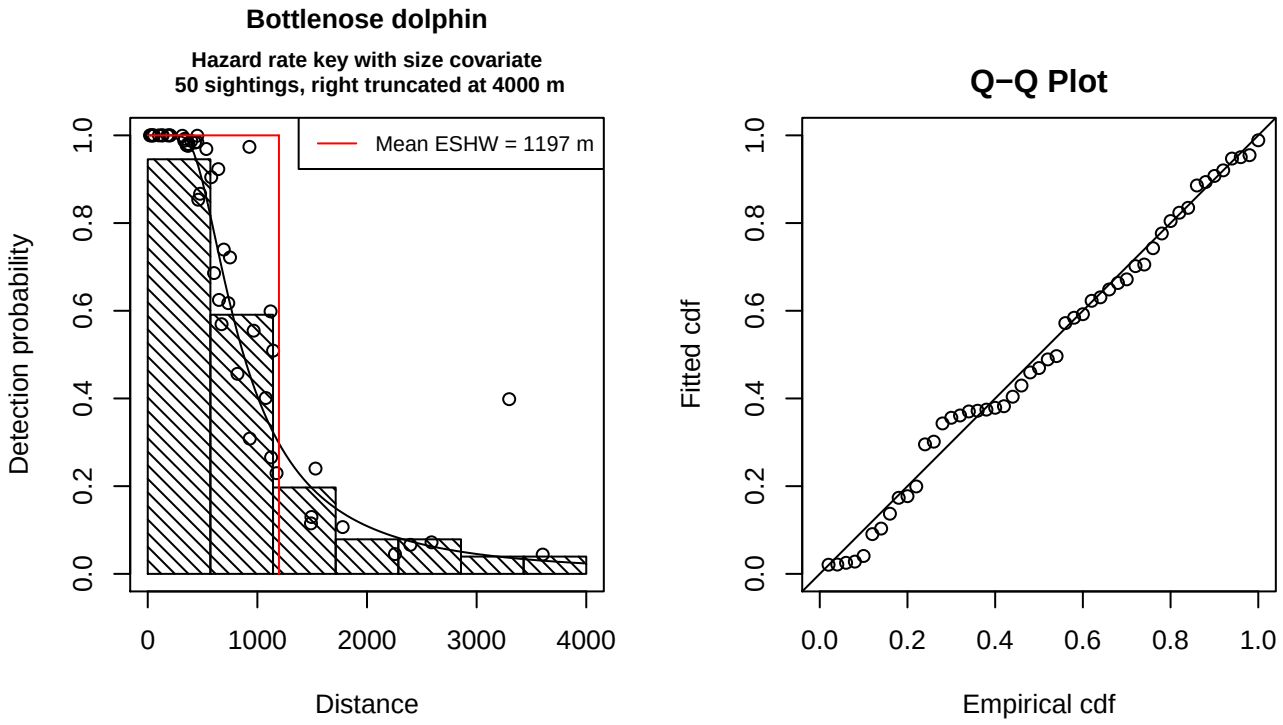

Figure 21: Detection function for NEFSC Pelican that was selected for the density model

Statistical output for this detection function:

```
Summary for ds object
```

```
Number of observations :  50
Distance range         :  0  -  4000
AIC                    :  773.2273

Detection function:
 Hazard-rate key function

Detection function parameters
Scale Coefficients:
             estimate        se
(Intercept) 6.3819640 0.3111936
size        0.2843228 0.1528551

Shape parameters:
             estimate        se
(Intercept) 0.8529645 0.2506987

                      Estimate          SE        CV
Average p             0.281388  0.04832536 0.1717392
N in covered region 177.690585 37.36715380 0.2102934
```

Additional diagnostic plots:

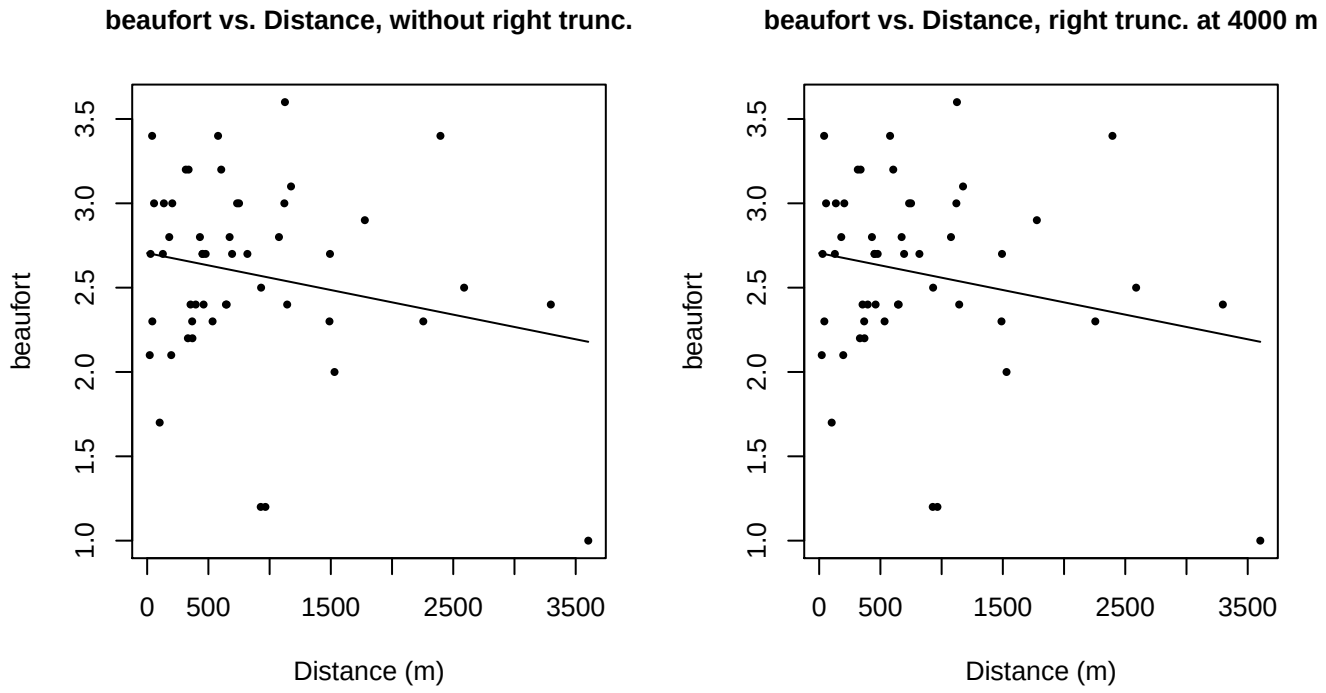

Figure 22: Scatterplots showing the relationship between Beaufort sea state and perpendicular sighting distance, for all sightings (left) and only those not right truncated (right). The line is a simple linear regression.

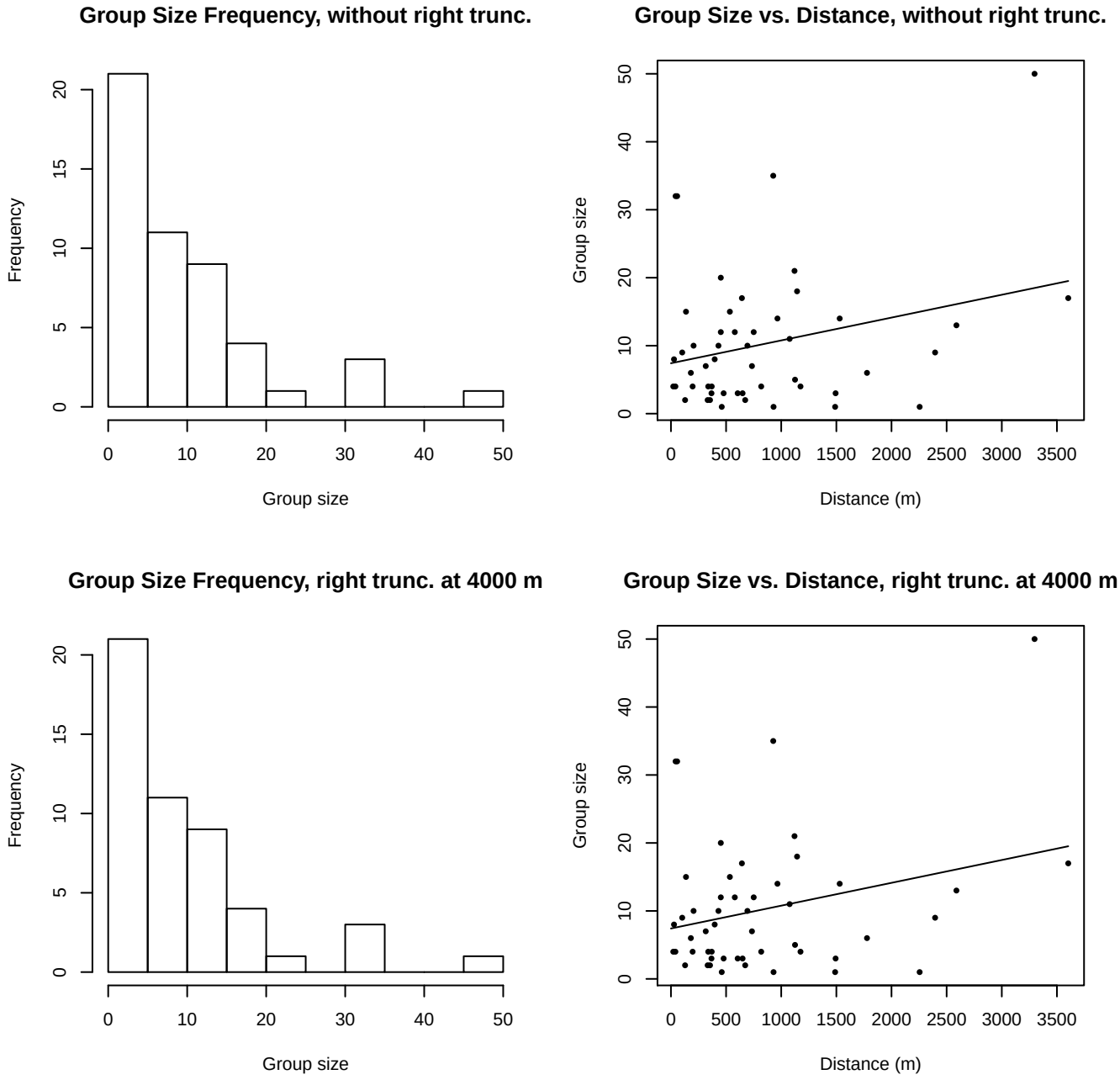

Figure 23: Histograms showing group size frequency and scatterplots showing the relationship between group size and perpendicular sighting distance, for all sightings (top row) and only those not right truncated (bottom row). In the scatterplot, the line is a simple linear regression.

SEFSC Oregon II

The sightings were right truncated at 4000m.

Covariate	Description
beaufort	Beaufort sea state.
quality	Survey-specific index of the quality of observation conditions, utilizing relevant factors other than Beaufort sea state (see methods).
size	Estimated size (number of individuals) of the sighted group.

Table 12: Covariates tested in candidate "multi-covariate distance sampling" (MCDS) detection functions.

Key	Adjustment	Order	Covariates	Succeeded	Δ AIC	Mean ESHW (m)
hr			beaufort, quality, size	Yes	0.00	423
hr			beaufort, size	Yes	1.81	410
hr			beaufort, quality	Yes	13.83	359
hr			beaufort	Yes	16.49	344
hr			quality, size	Yes	21.53	308
hr			size	Yes	26.51	276
hr			quality	Yes	34.43	265
hr				Yes	42.58	228
hn	cos	3		Yes	211.33	1112
hn	cos	2		Yes	220.06	1266
hn			beaufort, quality, size	Yes	252.47	1626
hn			beaufort, size	Yes	254.51	1631
hn			quality, size	Yes	264.40	1634
hn			size	Yes	268.82	1637
hn			beaufort, quality	Yes	272.47	1637
hn			beaufort	Yes	277.23	1641
hn			quality	Yes	280.46	1644
hn				Yes	287.10	1647
hn	herm	4		Yes	287.82	1643
hr	poly	2		No		
hr	poly	4		No		

Table 13: Candidate detection functions for SEFSC Oregon II. The first one listed was selected for the density model.

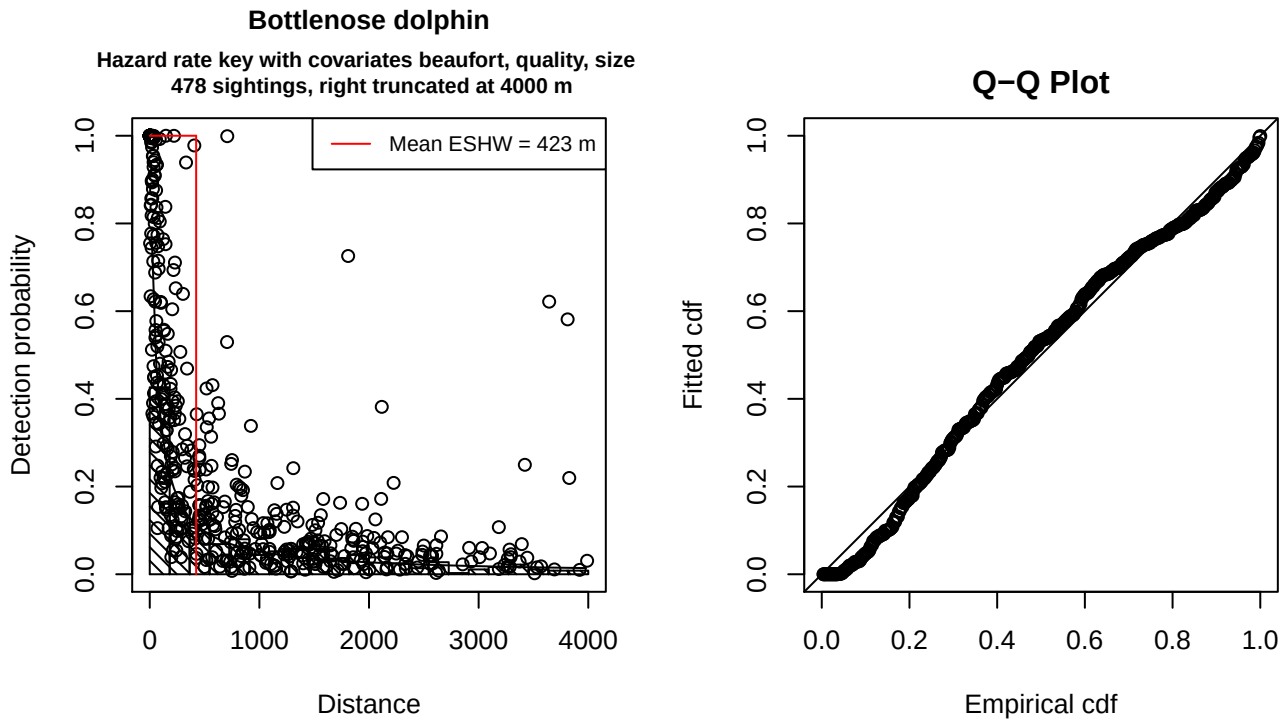

Figure 24: Detection function for SEFSC Oregon II that was selected for the density model

Statistical output for this detection function:

```
Summary for ds object
Number of observations :  478
Distance range         :  0  -  4000
AIC                    :  7262.16

Detection function:
 Hazard-rate key function

Detection function parameters
Scale Coefficients:
             estimate        se
(Intercept)  5.5026964 0.4212720
beaufort    -0.5435437 0.1033765
quality     -0.2515070 0.1252423
size         0.6785389 0.1649255

Shape parameters:
            estimate         se
(Intercept)        0 0.05338445

                         Estimate           SE        CV
Average p            5.977685e-02 7.429875e-03 0.1242935
N in covered region 7.996407e+03 1.058194e+03 0.1323337
```

Additional diagnostic plots:

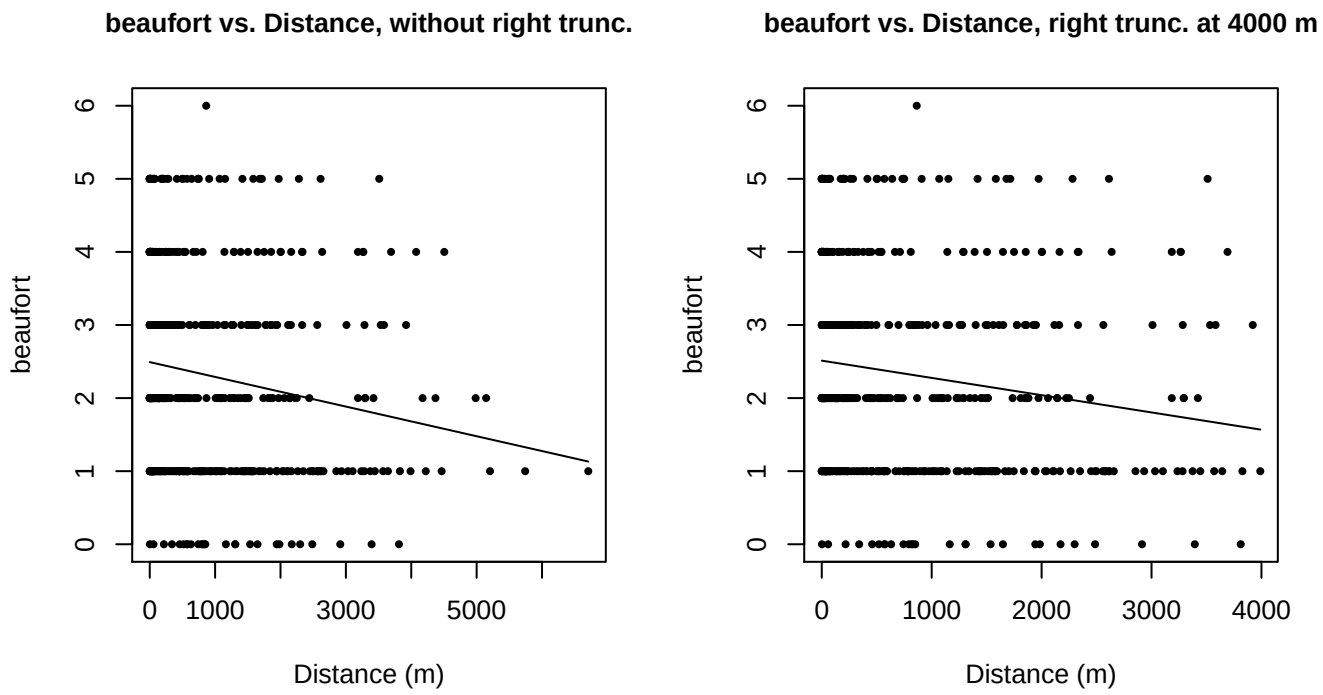

Figure 25: Scatterplots showing the relationship between Beaufort sea state and perpendicular sighting distance, for all sightings (left) and only those not right truncated (right). The line is a simple linear regression.

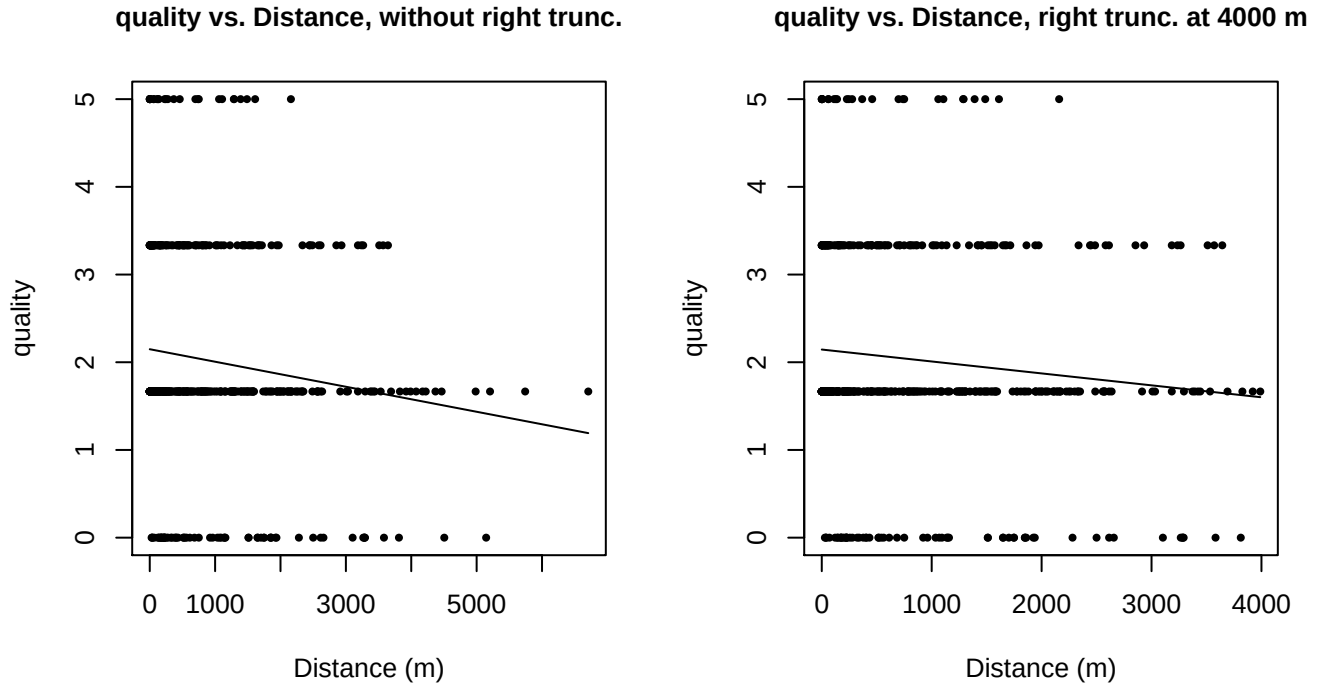

Figure 26: Scatterplots showing the relationship between the survey-specific index of the quality of observation conditions and perpendicular sighting distance, for all sightings (left) and only those not right truncated (right). Low values of the quality index correspond to better observation conditions. The line is a simple linear regression.

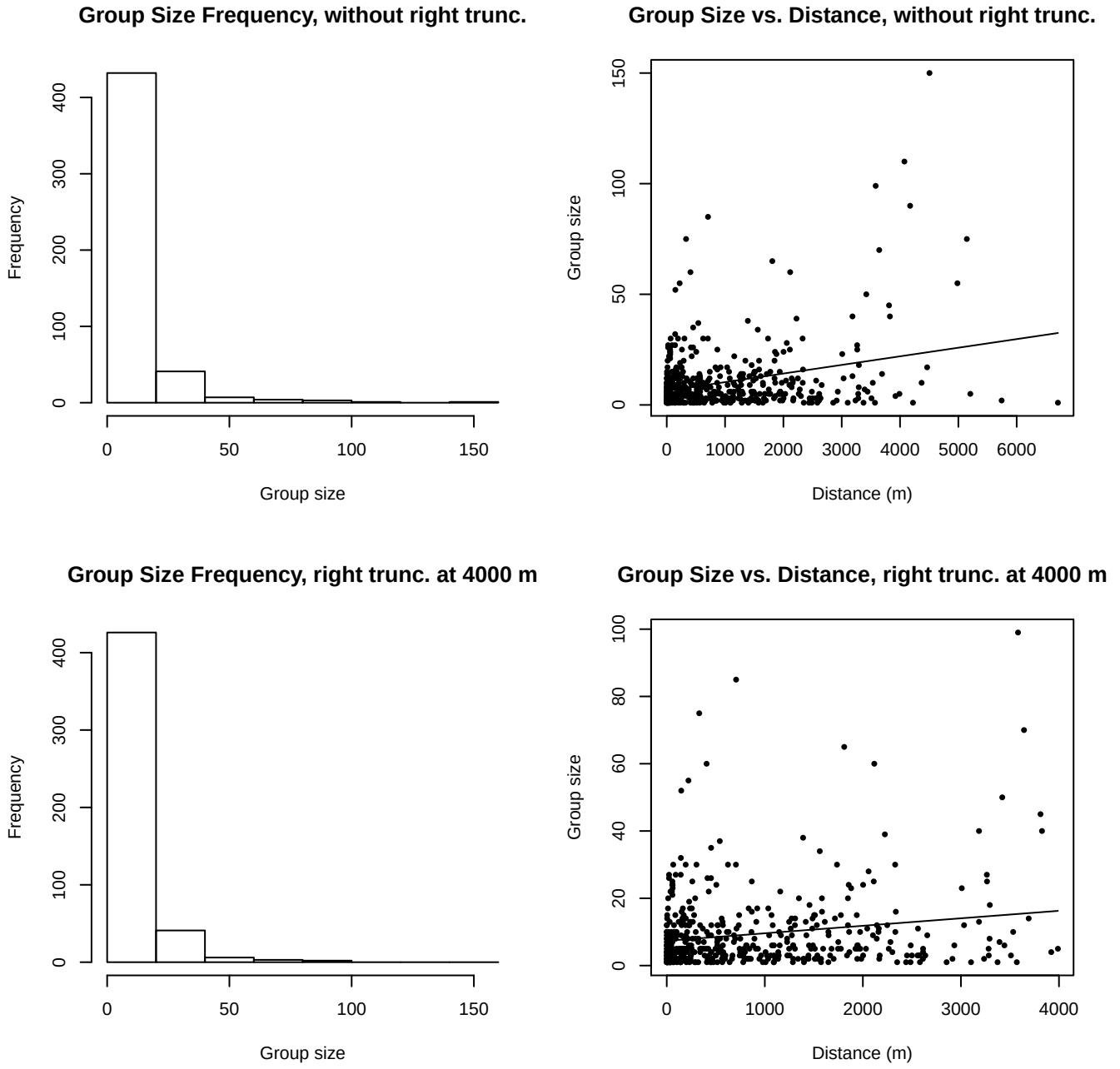

Figure 27: Histograms showing group size frequency and scatterplots showing the relationship between group size and perpendicular sighting distance, for all sightings (top row) and only those not right truncated (bottom row). In the scatterplot, the line is a simple linear regression.

NJ-DEP Hugh R. Sharp

The sightings were right truncated at 4000m.

Covariate	Description
beaufort	Beaufort sea state.
quality	Survey-specific index of the quality of observation conditions, utilizing relevant factors other than Beaufort sea state (see methods).
size	Estimated size (number of individuals) of the sighted group.

Table 14: Covariates tested in candidate "multi-covariate distance sampling" (MCDS) detection functions.

Key	Adjustment	Order	Covariates	Succeeded	Δ AIC	Mean ESHW (m)
hr			beaufort, size	Yes	0.00	1431
hr			beaufort, quality, size	Yes	1.32	1472
hr			beaufort	Yes	2.05	1188
hn			beaufort, size	Yes	2.17	1885
hn	cos	3		Yes	2.49	1321
hr			beaufort, quality	Yes	2.61	1349
hn			beaufort, quality, size	Yes	4.12	1881
hr			size	Yes	4.35	1209
hr			quality, size	Yes	5.18	1184
hr				Yes	6.35	897
hn			beaufort	Yes	6.49	1828
hr			quality	Yes	6.74	934
hn			beaufort, quality	Yes	8.35	1823
hn			quality, size	Yes	9.04	1878
hn	cos	2		Yes	10.36	1555
hn			size	Yes	10.43	1874
hn			quality	Yes	12.70	1839
hn				Yes	13.97	1844
hn	herm	4		Yes	15.90	1839
hr	poly	2		No		
hr	poly	4		No		

Table 15: Candidate detection functions for NJ-DEP Hugh R. Sharp. The first one listed was selected for the density model.

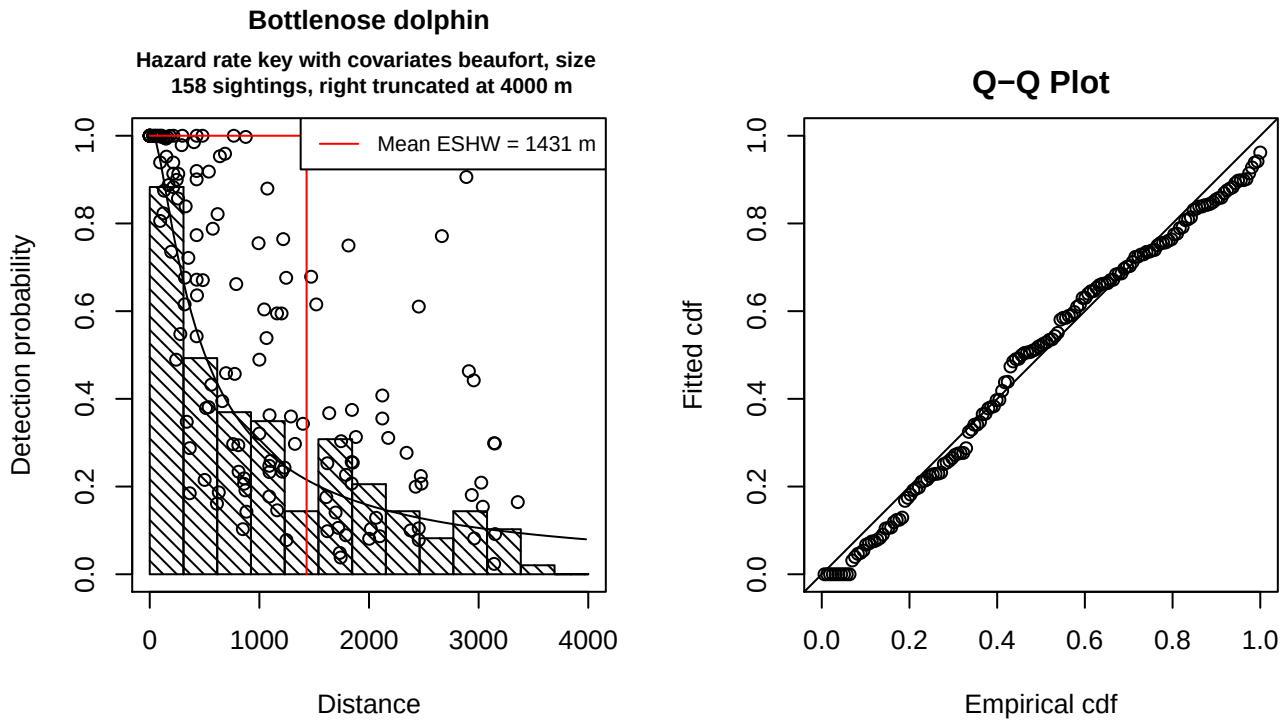

Figure 28: Detection function for NJ-DEP Hugh R. Sharp that was selected for the density model

Statistical output for this detection function:

```
Summary for ds object
Number of observations :  158
Distance range         :  0  -  4000
AIC                    :  2513.341

Detection function:
 Hazard-rate key function

Detection function parameters
Scale Coefficients:
             estimate        se
(Intercept)  6.8556257 0.4941651
beaufort    -0.5037474 0.1672603
size         0.9144847 0.3918243

Shape parameters:
             estimate        se
(Intercept) 0.2398386 0.1759367

                       Estimate           SE        CV
Average p             0.2495933   0.04730576 0.1895313
N in covered region 633.0297257 128.73310956 0.2033603
```

Additional diagnostic plots:

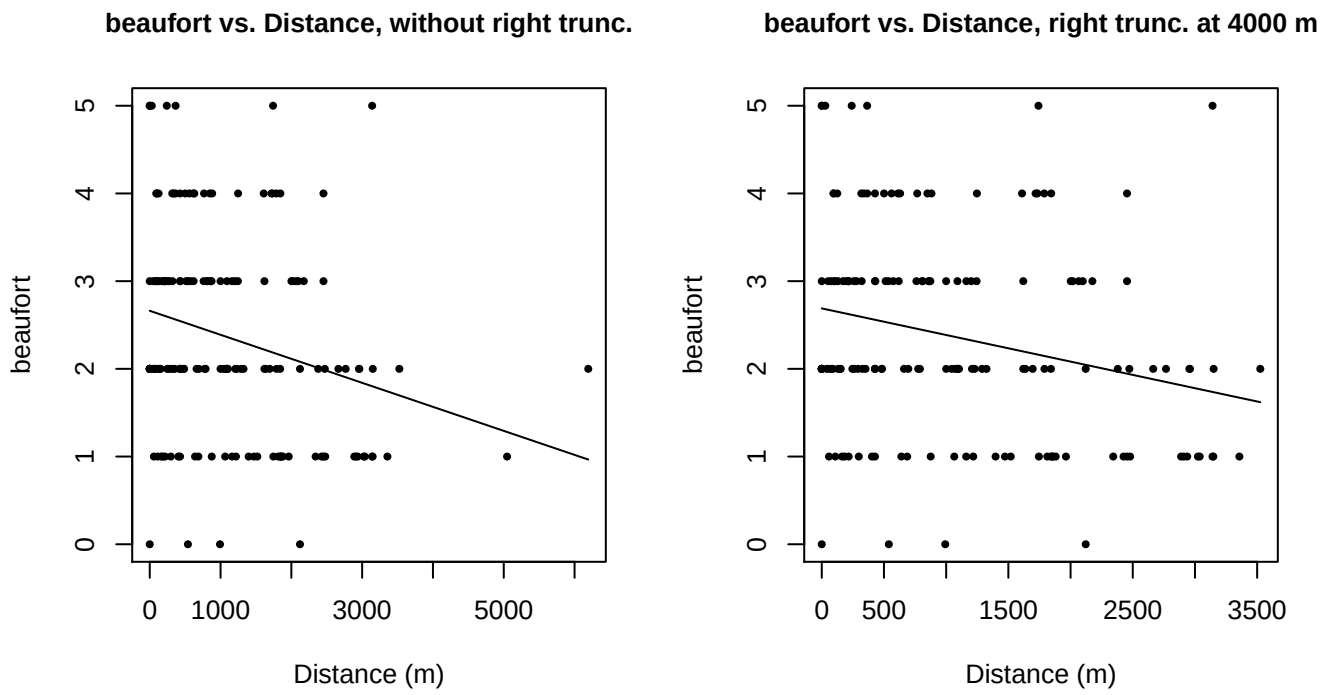

Figure 29: Scatterplots showing the relationship between Beaufort sea state and perpendicular sighting distance, for all sightings (left) and only those not right truncated (right). The line is a simple linear regression.

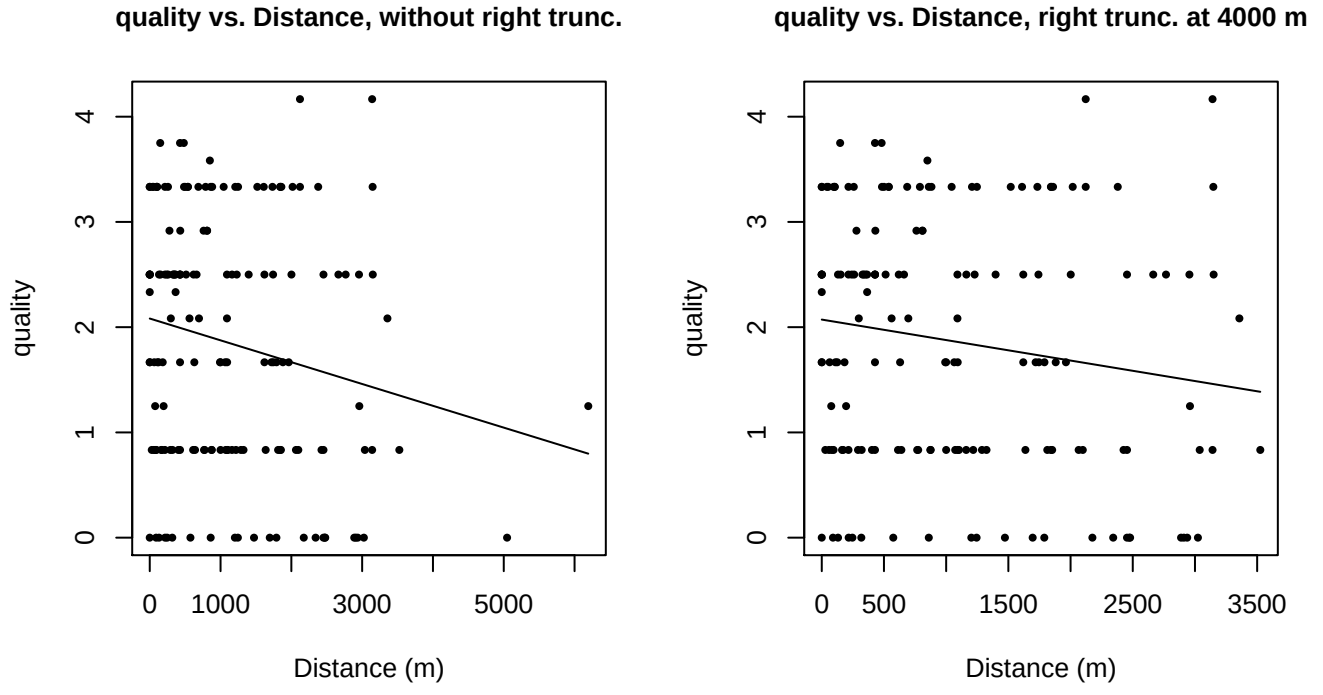

Figure 30: Scatterplots showing the relationship between the survey-specific index of the quality of observation conditions and perpendicular sighting distance, for all sightings (left) and only those not right truncated (right). Low values of the quality index correspond to better observation conditions. The line is a simple linear regression.

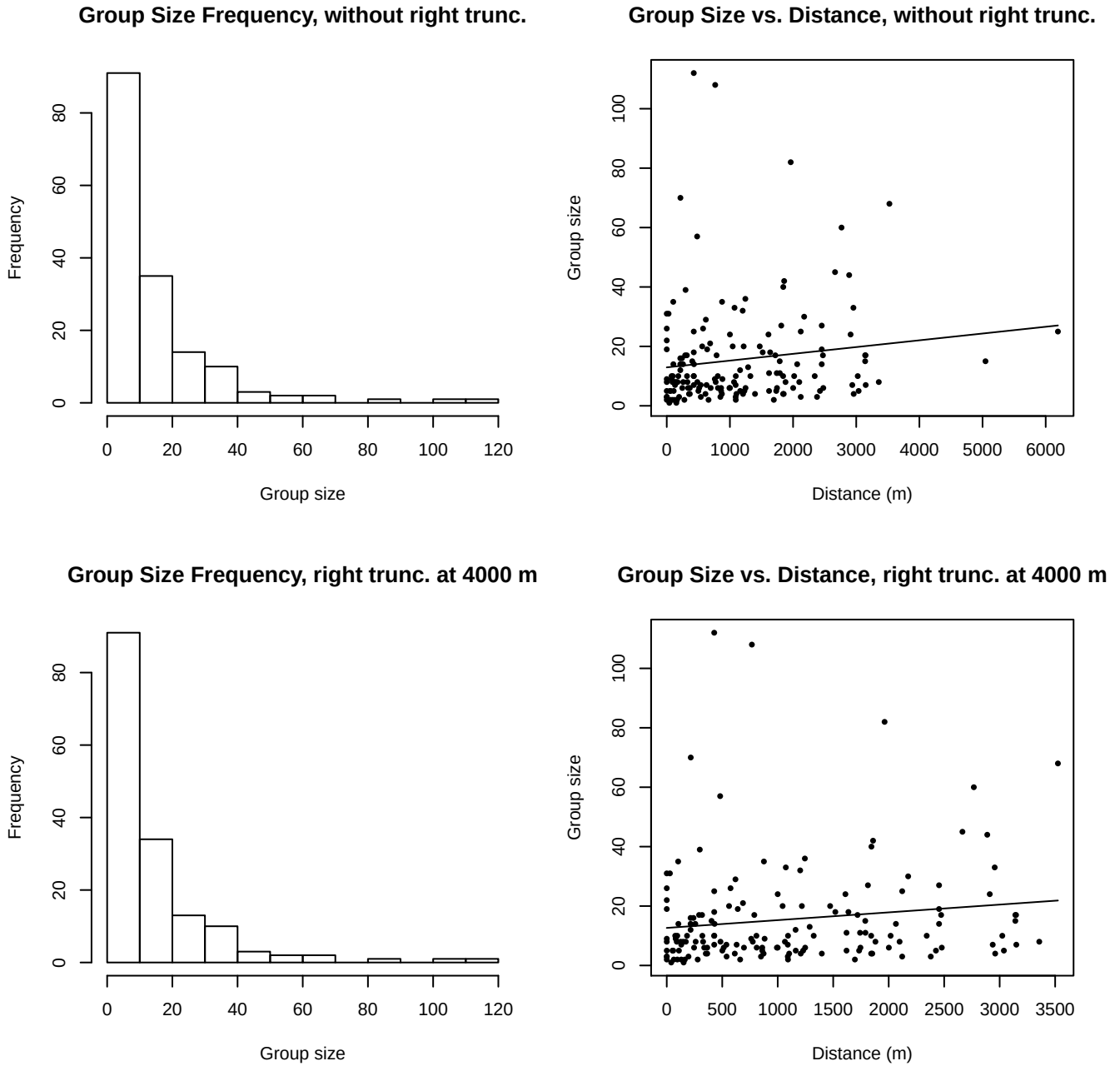

Figure 31: Histograms showing group size frequency and scatterplots showing the relationship between group size and perpendicular sighting distance, for all sightings (top row) and only those not right truncated (bottom row). In the scatterplot, the line is a simple linear regression.

High Platforms

The sightings were right truncated at 5000m.

Covariate	Description
beaufort	Beaufort sea state.
size	Estimated size (number of individuals) of the sighted group.

Table 16: Covariates tested in candidate "multi-covariate distance sampling" (MCDS) detection functions.

Key	Adjustment	Order	Covariates	Succeeded	Δ AIC	Mean ESHW (m)
hr			beaufort, size	Yes	0.00	1001
hr			beaufort	Yes	28.50	782
hr			size	Yes	66.30	673
hr				Yes	95.04	453
hn			beaufort, size	Yes	193.73	2018
hn	cos	3		Yes	210.72	1406
hn	cos	2		Yes	212.55	1574
hn			beaufort	Yes	233.58	1987
hn			size	Yes	251.49	2040
hn				Yes	279.81	1998
hn	herm	4		Yes	280.42	1995
hr	poly	2		No		
hr	poly	4		No		

Table 17: Candidate detection functions for High Platforms. The first one listed was selected for the density model.

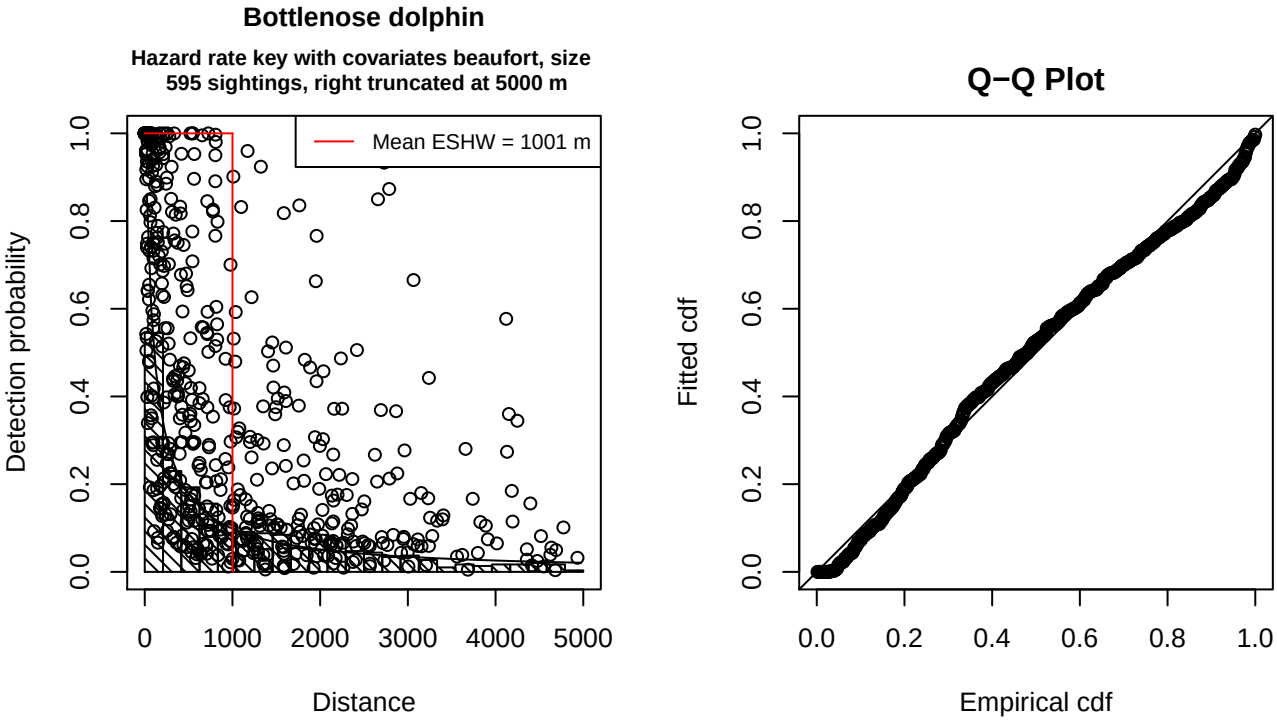

Figure 32: Detection function for High Platforms that was selected for the density model

Statistical output for this detection function:

```
Summary for ds object
```

```
Number of observations :  595
Distance range         :  0  -  5000
AIC                    :  9350.17

Detection function:
 Hazard-rate key function

Detection function parameters
Scale Coefficients:
             estimate        se
(Intercept)  6.9645860 0.2791044
beaufort    -0.8765275 0.0974669
size         1.2832927 0.2311812

Shape parameters:
             estimate         se
(Intercept) 0.1320332 0.05640665

                         Estimate           SE        CV
Average p              0.0839147   0.01106363 0.1318437
N in covered region 7090.5335680 980.38707905 0.1382670
```

Additional diagnostic plots:

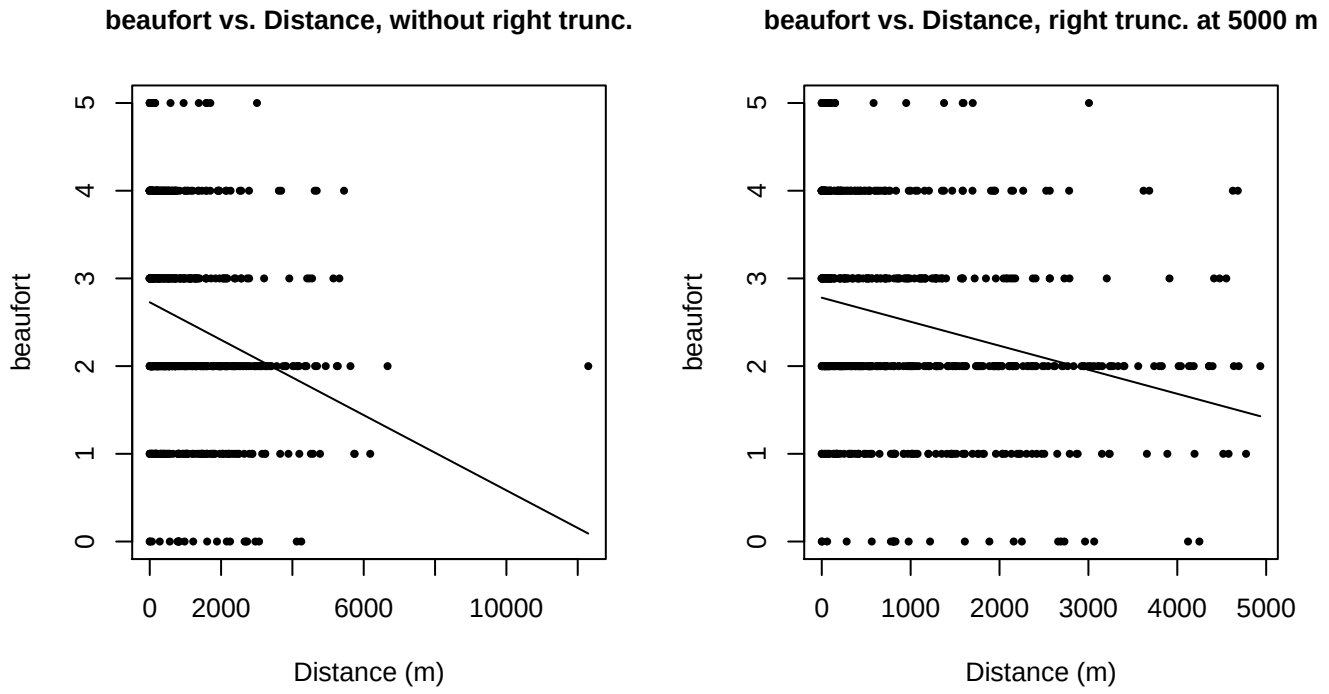

Figure 33: Scatterplots showing the relationship between Beaufort sea state and perpendicular sighting distance, for all sightings (left) and only those not right truncated (right). The line is a simple linear regression.

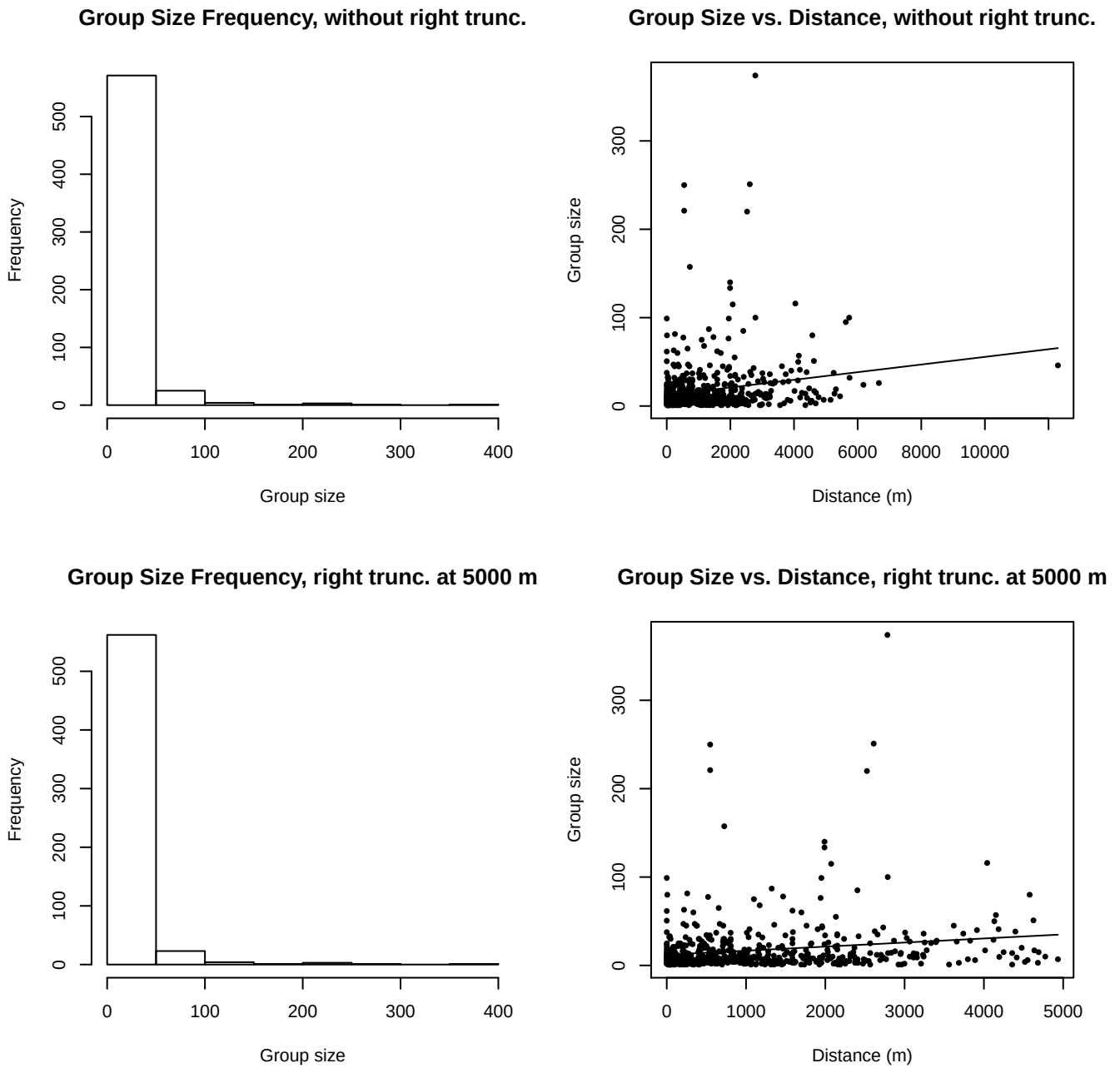

Figure 34: Histograms showing group size frequency and scatterplots showing the relationship between group size and perpendicular sighting distance, for all sightings (top row) and only those not right truncated (bottom row). In the scatterplot, the line is a simple linear regression.

Gordon Gunter Quality Covariate Available

The sightings were right truncated at 5000m.

Covariate	Description
beaufort	Beaufort sea state.
quality	Survey-specific index of the quality of observation conditions, utilizing relevant factors other than Beaufort sea state (see methods).
size	Estimated size (number of individuals) of the sighted group.

Table 18: Covariates tested in candidate "multi-covariate distance sampling" (MCDS) detection functions.

Key	Adjustment	Order	Covariates	Succeeded	Δ AIC	Mean ESHW (m)
hr			beaufort, quality, size	Yes	0.00	1057
hr			beaufort, size	Yes	0.92	1023
hr			beaufort	Yes	31.84	787
hr			beaufort, quality	Yes	32.40	800
hr			quality, size	Yes	42.91	762
hr			size	Yes	57.27	683
hr			quality	Yes	73.57	534
hr				Yes	88.09	463
hn			beaufort, size	Yes	176.57	2002
hn			beaufort, quality, size	Yes	178.52	2000
hn	cos	3		Yes	193.39	1400
hn	cos	2		Yes	197.63	1575
hn			beaufort	Yes	209.82	1976
hn			beaufort, quality	Yes	210.19	1977
hn			quality, size	Yes	231.81	2014
hn			size	Yes	234.23	2029
hn			quality	Yes	253.99	1988
hn				Yes	260.03	1989
hn	herm	4		Yes	260.74	1985
hr	poly	2		No		
hr	poly	4		No		

Table 19: Candidate detection functions for Gordon Gunter Quality Covariate Available. The first one listed was selected for the density model.

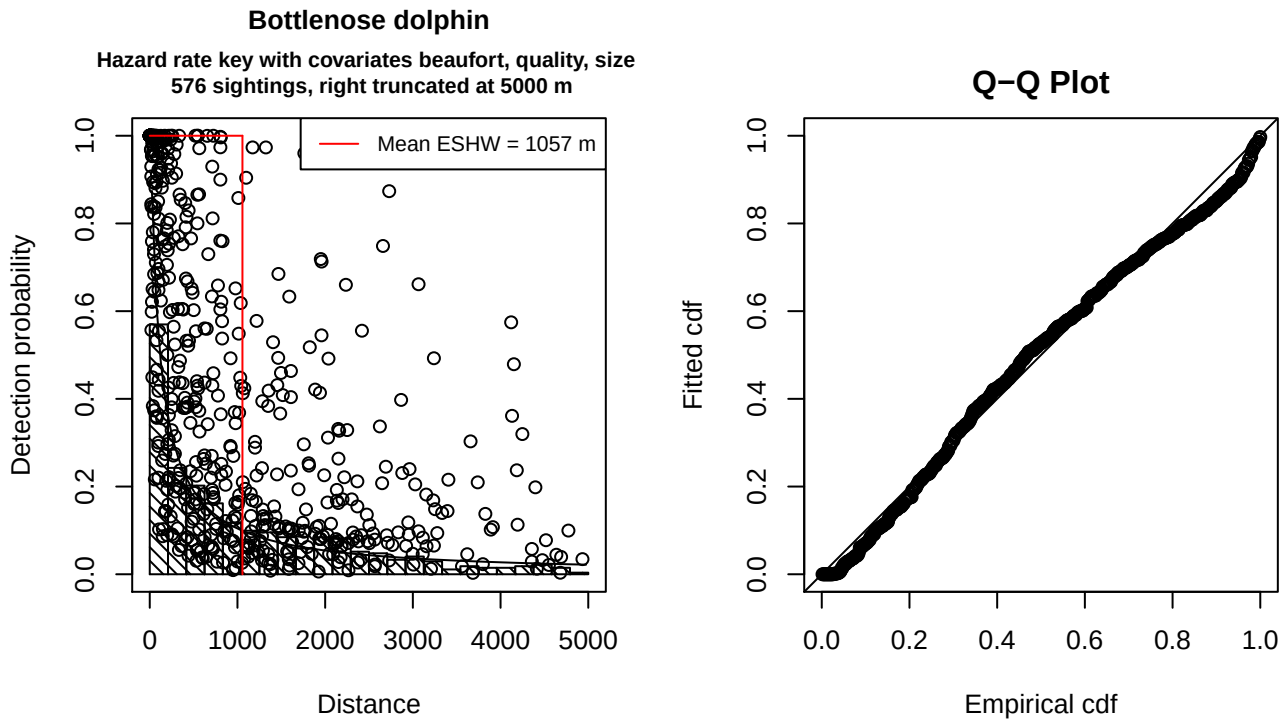

Figure 35: Detection function for Gordon Gunter Quality Covariate Available that was selected for the density model

Statistical output for this detection function:

```
Summary for ds object
Number of observations :  576
Distance range         :  0  -  5000
AIC                    :  9057.588

Detection function:
 Hazard-rate key function

Detection function parameters
Scale Coefficients:
             estimate         se
(Intercept)  7.1448192 0.29997342
beaufort    -0.7643044 0.10907324
quality     -0.1838412 0.09913961
size         1.4231059 0.26038370

Shape parameters:
             estimate         se
(Intercept) 0.1544527 0.05933841

                         Estimate           SE        CV
Average p            8.822243e-02   0.01197154 0.1356973
N in covered region 6.528952e+03 928.18022775 0.1421637
```

Additional diagnostic plots:

Figure 36: Scatterplots showing the relationship between Beaufort sea state and perpendicular sighting distance, for all sightings (left) and only those not right truncated (right). The line is a simple linear regression.

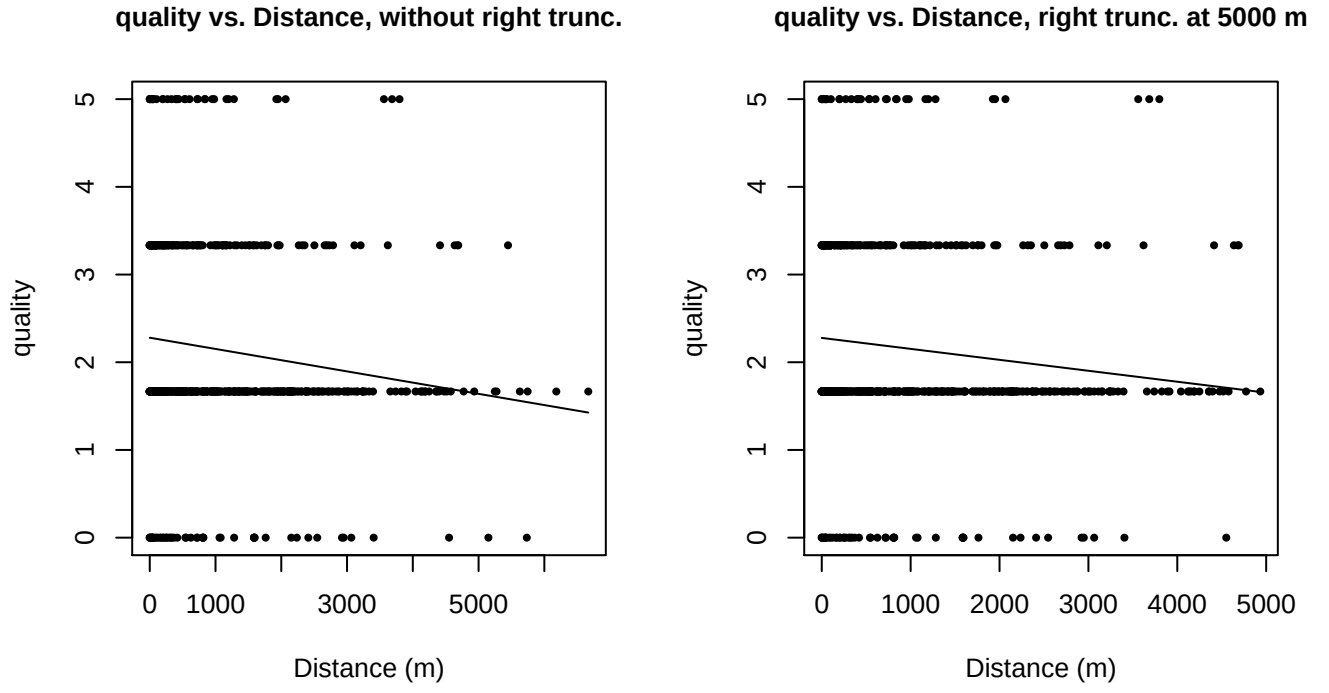

Figure 37: Scatterplots showing the relationship between the survey-specific index of the quality of observation conditions and perpendicular sighting distance, for all sightings (left) and only those not right truncated (right). Low values of the quality index correspond to better observation conditions. The line is a simple linear regression.

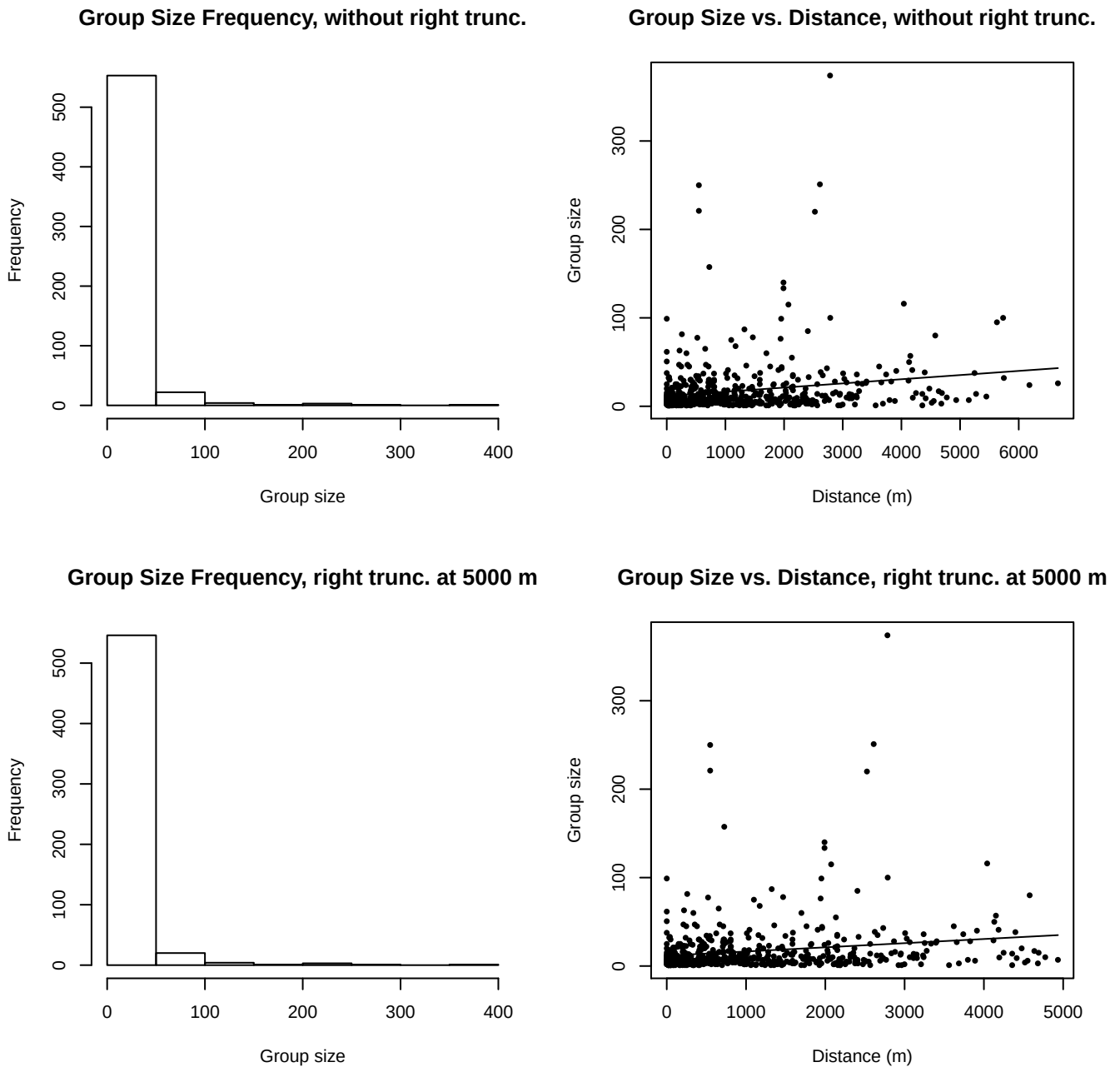

Figure 38: Histograms showing group size frequency and scatterplots showing the relationship between group size and perpendicular sighting distance, for all sightings (top row) and only those not right truncated (bottom row). In the scatterplot, the line is a simple linear regression.

Naked Eye Surveys

Because this taxon was sighted too infrequently to fit a detection function to its sightings alone, we fit a detection function to the pooled sightings of several other species that we believed would exhibit similar detectability. These "proxy species" are listed below.

Reported By Observer	Common Name	n
Delphinus delphis	Short-beaked common dolphin	255
Delphinus delphis/Lagenorhynchus acutus	Short-beaked common or Atlantic white-sided dolphin	0

Delphinus delphis/Stenella	Short-beaked common dolphin or Stenella spp.	0
Delphinus delphis/Stenella coeruleoalba	Short-beaked common or striped dolphin	72
Grampus griseus	Risso's dolphin	9
Grampus griseus/Tursiops truncatus	Risso's or Bottlenose dolphin	0
Lagenodelphis hosei	Fraser's dolphin	0
Lagenorhynchus acutus	Atlantic white-sided dolphin	102
Lagenorhynchus albirostris	White-beaked dolphin	36
Lagenorhynchus albirostris/Lagenorhynchus acutus	White-beaked or white-sided dolphin	4
Stenella	Unidentified Stenella	0
Stenella attenuata	Pantropical spotted dolphin	0
Stenella attenuata/frontalis	Pantropical or Atlantic spotted dolphin	0
Stenella clymene	Clymene dolphin	0
Stenella coeruleoalba	Striped dolphin	48
Stenella frontalis	Atlantic spotted dolphin	0
Stenella frontalis/Tursiops truncatus	Atlantic spotted or Bottlenose dolphin	0
Stenella longirostris	Spinner dolphin	0
Steno bredanensis	Rough-toothed dolphin	0
Steno bredanensis/Tursiops truncatus	Bottlenose or rough-toothed dolphin	0
Tursiops truncatus	Bottlenose dolphin	41
Total		567

Table 20: Proxy species used to fit detection functions for Naked Eye Surveys. The number of sightings, n, is before truncation.

The sightings were right truncated at 1000m.

Covariate	Description
beaufort	Beaufort sea state.
size	Estimated size (number of individuals) of the sighted group.

Table 21: Covariates tested in candidate "multi-covariate distance sampling" (MCDS) detection functions.

Key	Adjustment	Order	Covariates	Succeeded	Δ AIC	Mean ESHW (m)
hr			beaufort, size	Yes	0.00	329
hr			beaufort	Yes	5.52	306
hr			size	Yes	7.76	330
hr	poly	2		Yes	8.35	253
hr	poly	4		Yes	11.34	266
hn	cos	2		Yes	14.63	339
hr				Yes	14.95	308

hn	cos	3		Yes	29.74	330
hn			beaufort, size	Yes	33.37	434
hn			size	Yes	39.64	433
hn			beaufort	Yes	47.43	427
hn				Yes	53.26	426
hn	herm	4		Yes	54.28	425

Table 22: Candidate detection functions for Naked Eye Surveys. The first one listed was selected for the density model.

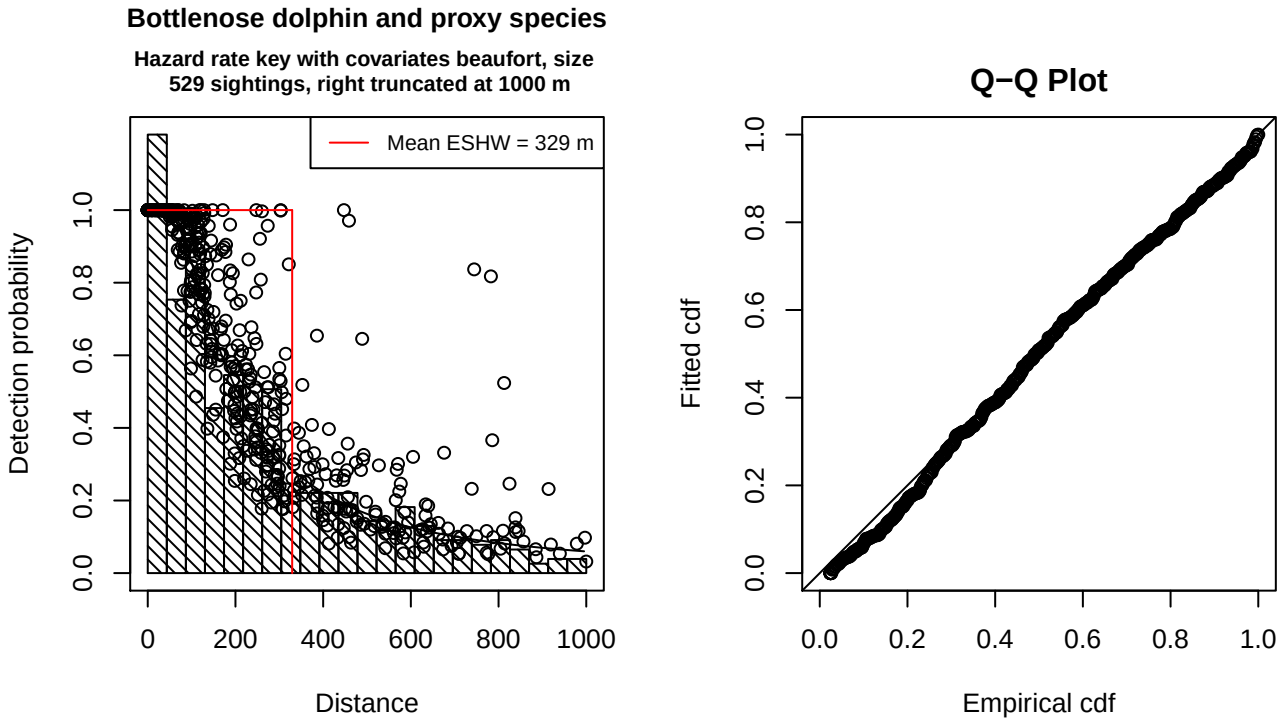

Figure 39: Detection function for Naked Eye Surveys that was selected for the density model

Statistical output for this detection function:

```
Summary for ds object
Number of observations :  529
Distance range         :  0  -  1000
AIC                    :  6866.942

Detection function:
 Hazard-rate key function

Detection function parameters
Scale Coefficients:
             estimate         se
(Intercept)  5.4796299 0.21489966
beaufort    -0.2095913 0.06594519
size         0.5152091 0.16341040
```

```
Shape parameters:
             estimate         se
(Intercept) 0.4966405 0.08804302

                         Estimate           SE         CV
Average p                0.2987683   0.02050381 0.06862779
N in covered region 1770.6030180 138.21190973 0.07805923
```

Additional diagnostic plots:

Figure 40: Scatterplots showing the relationship between Beaufort sea state and perpendicular sighting distance, for all sightings (left) and only those not right truncated (right). The line is a simple linear regression.

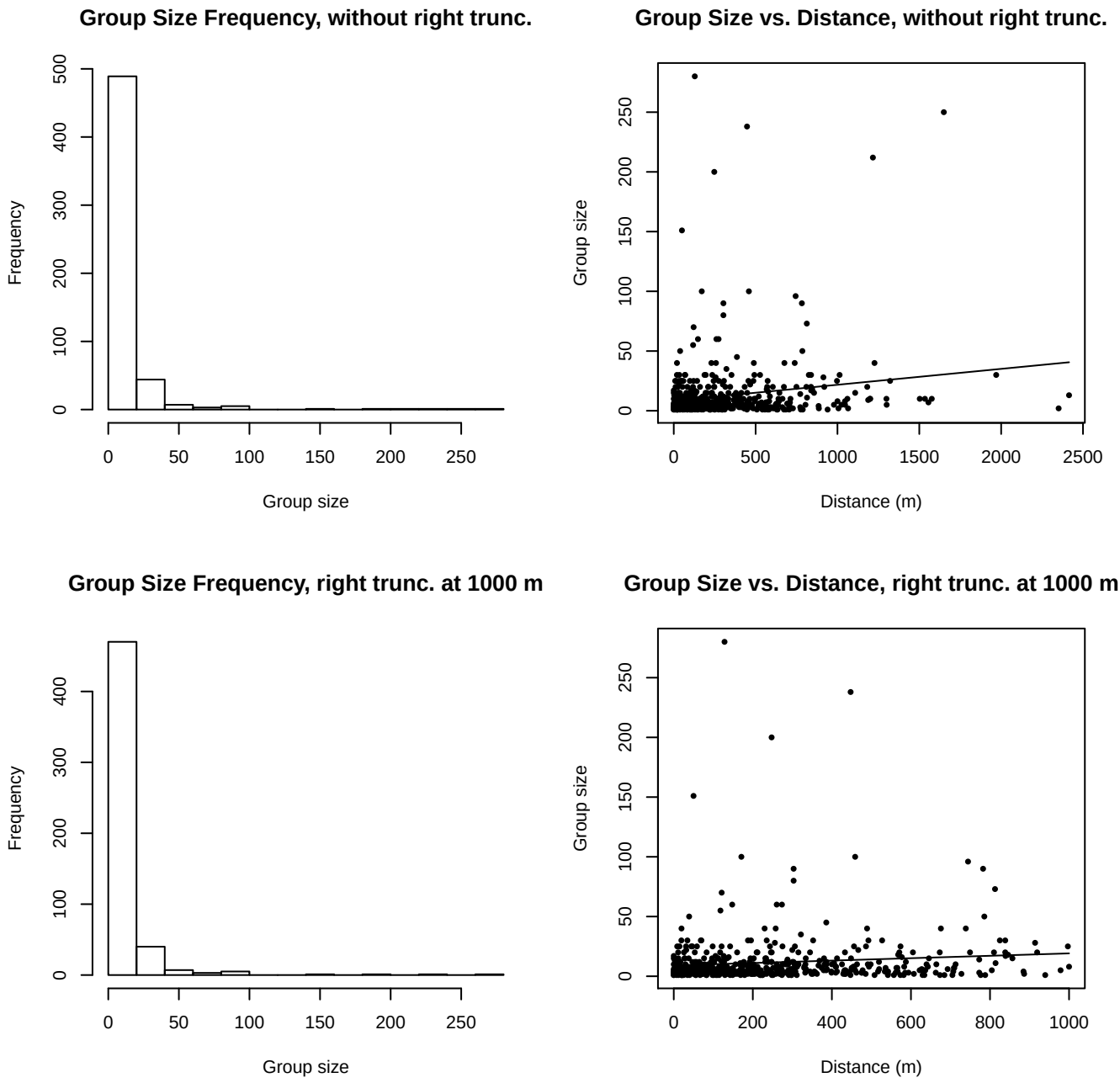

Figure 41: Histograms showing group size frequency and scatterplots showing the relationship between group size and perpendicular sighting distance, for all sightings (top row) and only those not right truncated (bottom row). In the scatterplot, the line is a simple linear regression.

CODA and SCANS II

Because this taxon was sighted too infrequently to fit a detection function to its sightings alone, we fit a detection function to the pooled sightings of several other species that we believed would exhibit similar detectability. These "proxy species" are listed below.

Reported By Observer	Common Name	n
Delphinus delphis	Short-beaked common dolphin	227
Delphinus delphis/Lagenorhynchus acutus	Short-beaked common or Atlantic white-sided dolphin	0

Delphinus delphis/Stenella	Short-beaked common dolphin or Stenella spp.	0
Delphinus delphis/Stenella coeruleoalba	Short-beaked common or striped dolphin	57
Grampus griseus	Risso's dolphin	9
Grampus griseus/Tursiops truncatus	Risso's or Bottlenose dolphin	0
Lagenodelphis hosei	Fraser's dolphin	0
Lagenorhynchus acutus	Atlantic white-sided dolphin	56
Lagenorhynchus albirostris	White-beaked dolphin	32
Lagenorhynchus albirostris/Lagenorhynchus acutus	White-beaked or white-sided dolphin	4
Stenella	Unidentified Stenella	0
Stenella attenuata	Pantropical spotted dolphin	0
Stenella attenuata/frontalis	Pantropical or Atlantic spotted dolphin	0
Stenella clymene	Clymene dolphin	0
Stenella coeruleoalba	Striped dolphin	36
Stenella frontalis	Atlantic spotted dolphin	0
Stenella frontalis/Tursiops truncatus	Atlantic spotted or Bottlenose dolphin	0
Stenella longirostris	Spinner dolphin	0
Steno bredanensis	Rough-toothed dolphin	0
Steno bredanensis/Tursiops truncatus	Bottlenose or rough-toothed dolphin	0
Tursiops truncatus	Bottlenose dolphin	41
Total		462

Table 23: Proxy species used to fit detection functions for CODA and SCANS II. The number of sightings, n, is before truncation.

The sightings were right truncated at 1000m.

Covariate	Description
beaufort	Beaufort sea state.
quality	Survey-specific index of the quality of observation conditions, utilizing relevant factors other than Beaufort sea state (see methods).
size	Estimated size (number of individuals) of the sighted group.

Table 24: Covariates tested in candidate "multi-covariate distance sampling" (MCDS) detection functions.

Key	Adjustment	Order	Covariates	Succeeded	Δ AIC	Mean ESHW (m)
hr			quality, size	Yes	0.00	326
hr			quality	Yes	0.85	325
hr	poly	2		Yes	2.85	257
hr			beaufort, size	Yes	3.50	319
hr			beaufort	Yes	4.73	315

hr	poly	4		Yes	5.08	288
hn	cos	2		Yes	5.71	335
hr			size	Yes	6.16	322
hr				Yes	7.78	319
hn	cos	3		Yes	15.49	324
hn			quality, size	Yes	21.34	416
hn			beaufort, size	Yes	22.76	417
hn			beaufort, quality, size	Yes	23.17	416
hn			quality	Yes	25.50	413
hn			size	Yes	26.46	418
hn			beaufort, quality	Yes	27.47	413
hn			beaufort	Yes	28.47	414
hn				Yes	32.88	414
hn	herm	4		Yes	34.17	413
hr			beaufort, quality	No		
hr			beaufort, quality, size	No		

Table 25: Candidate detection functions for CODA and SCANS II. The first one listed was selected for the density model.

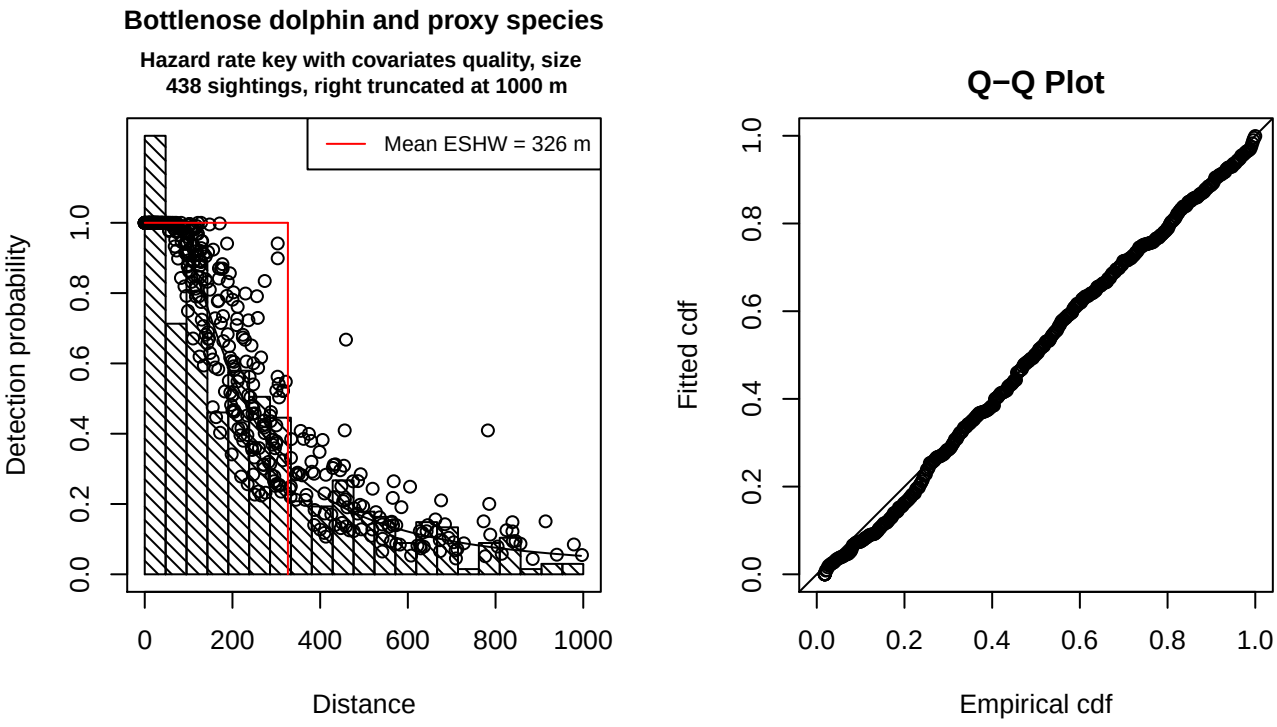

Figure 42: Detection function for CODA and SCANS II that was selected for the density model

Statistical output for this detection function:

```
Summary for ds object
Number of observations :  438
Distance range         :  0  -  1000
AIC                    :  5674.066

Detection function:
 Hazard-rate key function

Detection function parameters
Scale Coefficients:
             estimate         se
(Intercept)  5.4624136 0.17286880
quality     -0.1426257 0.05036964
size         0.2194236 0.11538504

Shape parameters:
             estimate         se
(Intercept) 0.5741026 0.09733169

                         Estimate           SE         CV
Average p               0.3097732   0.02170451 0.07006582
N in covered region 1413.9378602 114.19755693 0.08076561
```

Additional diagnostic plots:

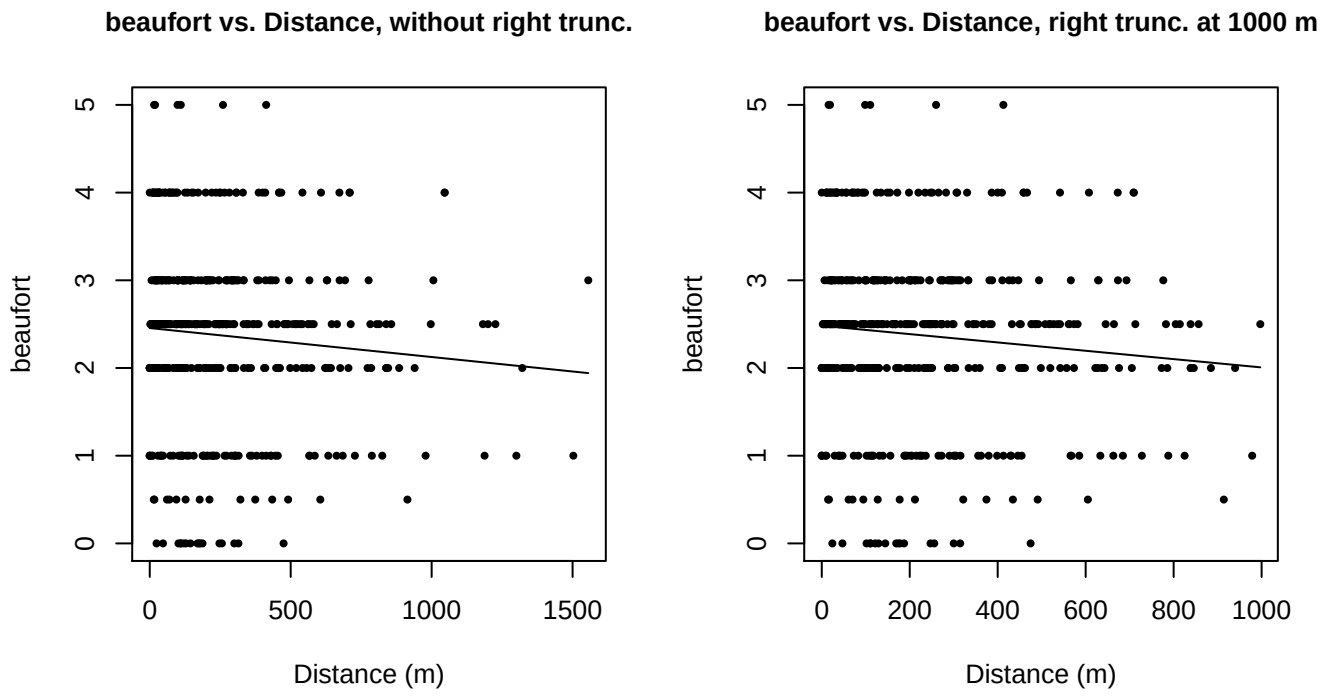

Figure 43: Scatterplots showing the relationship between Beaufort sea state and perpendicular sighting distance, for all sightings (left) and only those not right truncated (right). The line is a simple linear regression.

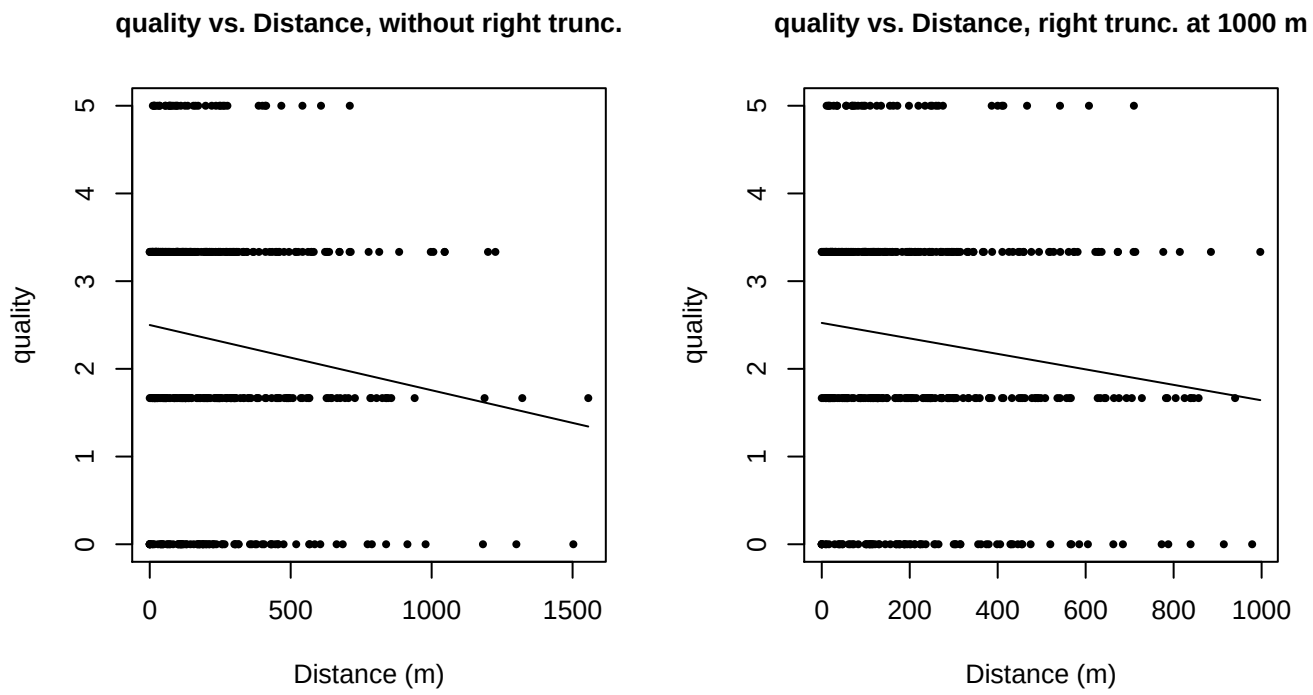

Figure 44: Scatterplots showing the relationship between the survey-specific index of the quality of observation conditions and perpendicular sighting distance, for all sightings (left) and only those not right truncated (right). Low values of the quality index correspond to better observation conditions. The line is a simple linear regression.

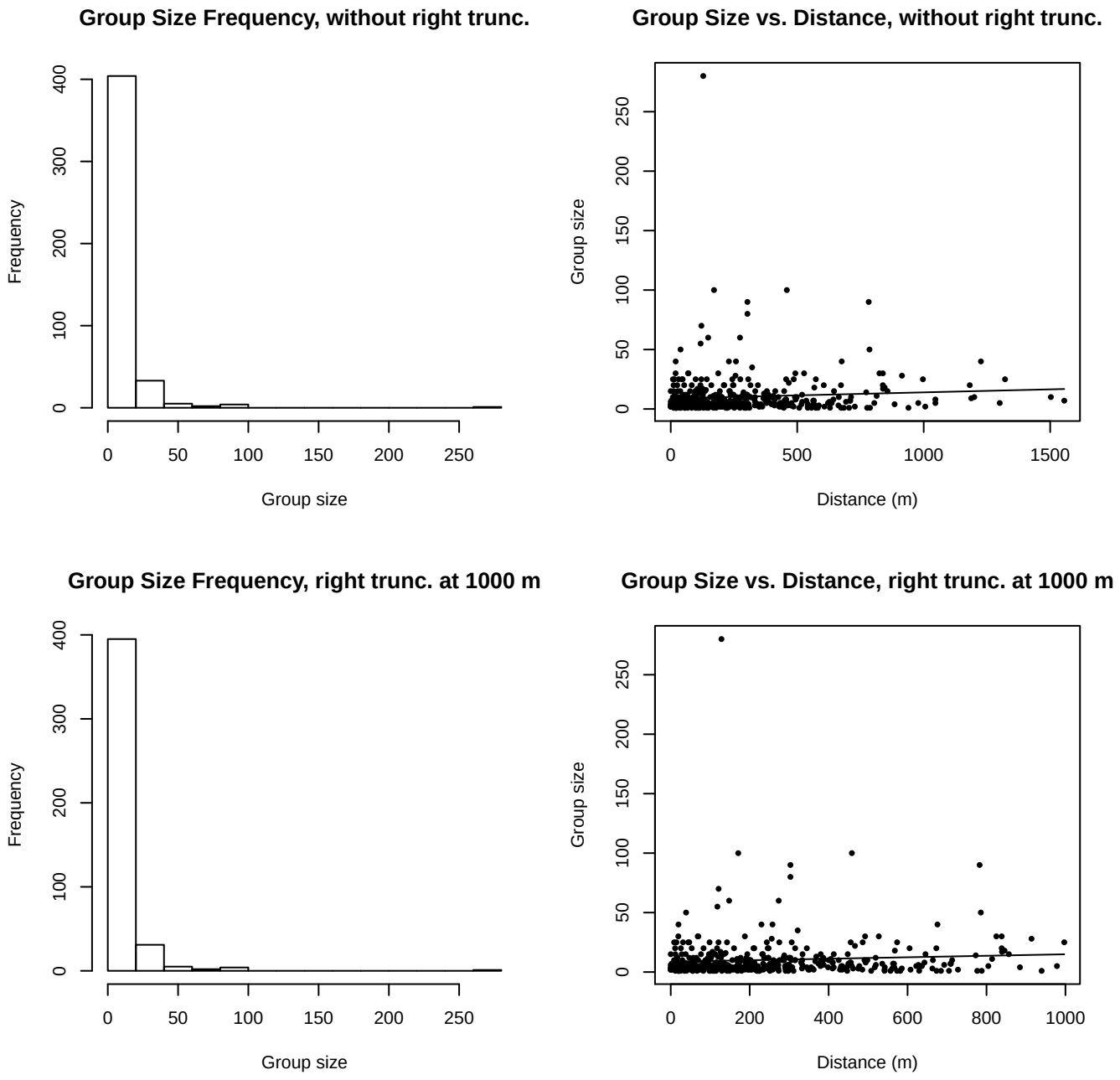

Figure 45: Histograms showing group size frequency and scatterplots showing the relationship between group size and perpendicular sighting distance, for all sightings (top row) and only those not right truncated (bottom row). In the scatterplot, the line is a simple linear regression.

Aerial Surveys

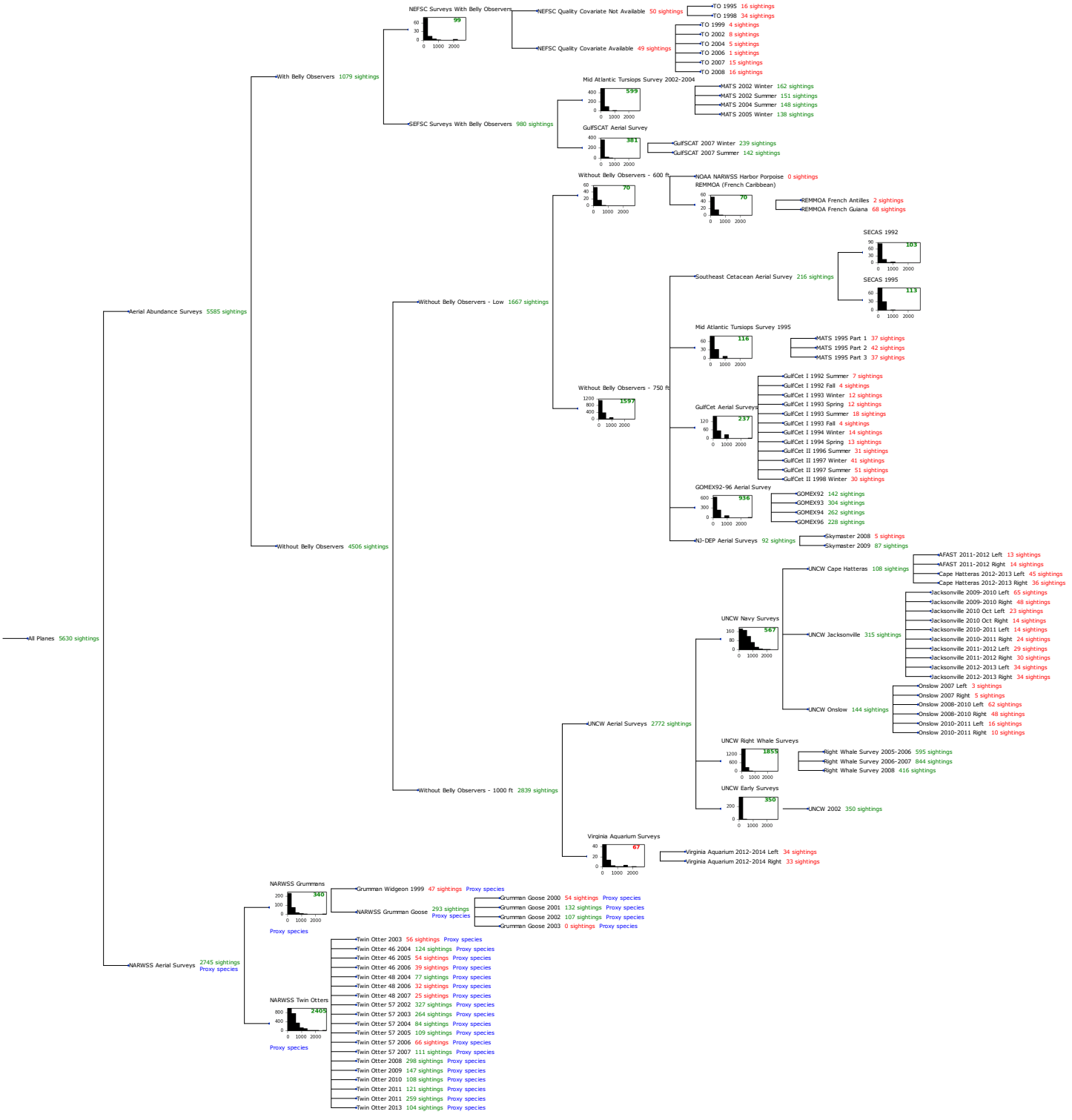

Figure 46: Detection hierarchy for aerial surveys

NEFSC Surveys With Belly Observers

The sightings were right truncated at 900m.

Covariate	Description

beaufort	Beaufort sea state.
size	Estimated size (number of individuals) of the sighted group.

Table 26: Covariates tested in candidate "multi-covariate distance sampling" (MCDS) detection functions.

Key	Adjustment	Order	Covariates	Succeeded	Δ AIC	Mean ESHW (m)
hr				Yes	0.00	310
hr			beaufort	Yes	1.67	309
hn	cos	2		Yes	1.67	241
hr			size	Yes	1.90	312
hr	poly	2		Yes	2.00	310
hr	poly	4		Yes	2.00	310
hr			beaufort, size	Yes	3.54	312
hn			size	Yes	9.69	317
hn				Yes	11.03	316
hn			beaufort, size	Yes	11.57	318
hn	herm	4		Yes	12.85	316
hn	cos	3		Yes	12.97	306
hn			beaufort	No		

Table 27: Candidate detection functions for NEFSC Surveys With Belly Observers. The first one listed was selected for the density model.

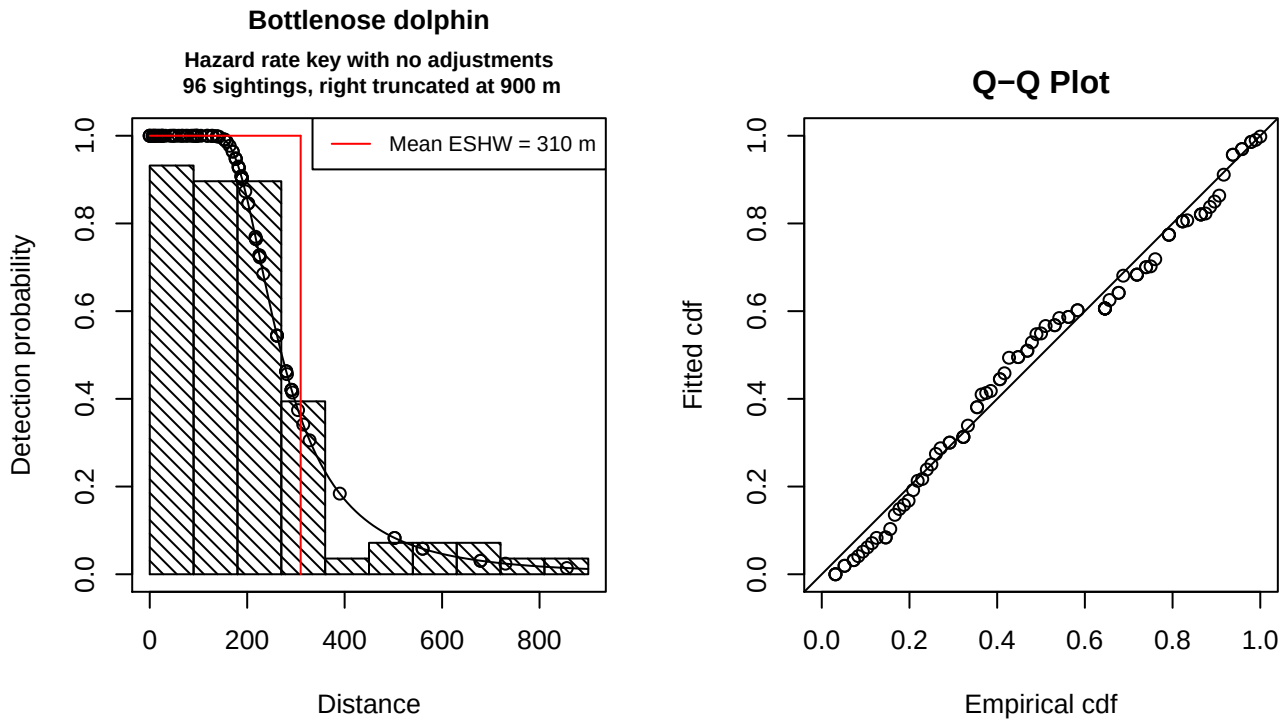

Figure 47: Detection function for NEFSC Surveys With Belly Observers that was selected for the density model

Statistical output for this detection function:

```
Summary for ds object
Number of observations :  96
Distance range         :  0  -  900
AIC                    :  1191.578

Detection function:
 Hazard-rate key function

Detection function parameters
Scale Coefficients:
            estimate        se
(Intercept) 5.493749 0.1267845

Shape parameters:
            estimate        se
(Intercept) 1.215614 0.1599951

                       Estimate          SE        CV
Average p              0.3441457  0.03303954 0.0960045
N in covered region 278.9515797 35.33852874 0.1266834
```

Additional diagnostic plots:

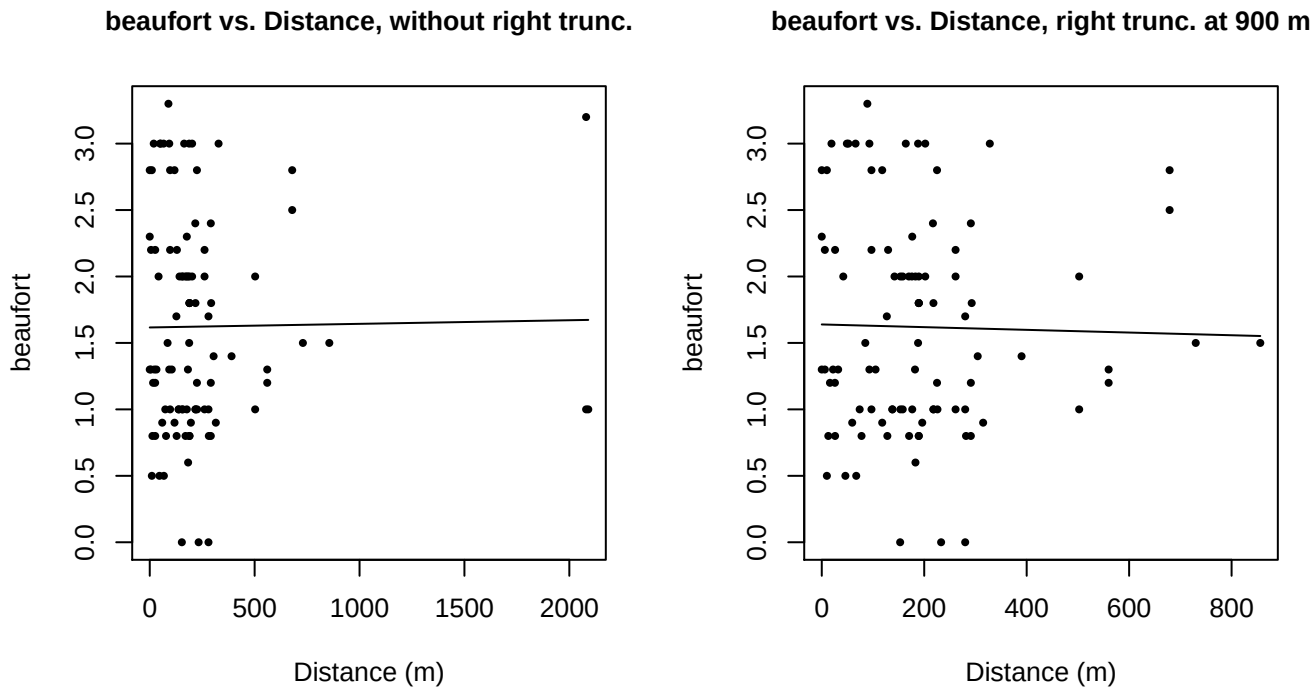

Figure 48: Scatterplots showing the relationship between Beaufort sea state and perpendicular sighting distance, for all sightings (left) and only those not right truncated (right). The line is a simple linear regression.

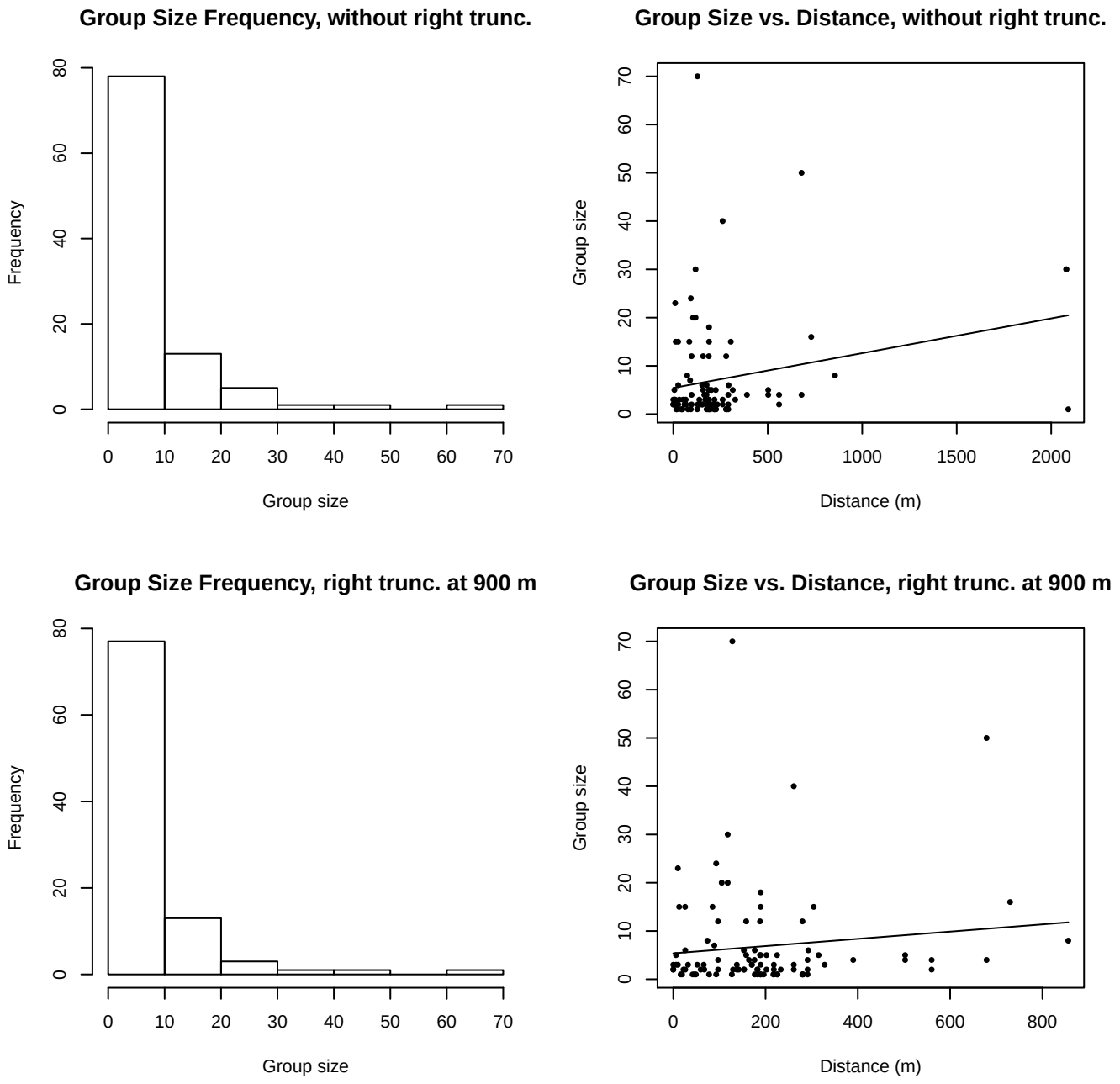

Figure 49: Histograms showing group size frequency and scatterplots showing the relationship between group size and perpendicular sighting distance, for all sightings (top row) and only those not right truncated (bottom row). In the scatterplot, the line is a simple linear regression.

Mid Atlantic Tursiops Survey 2002-2004

The sightings were right truncated at 1296m. The vertical sighting angles were heaped at 10 degree increments, so the candidate detection functions were fitted using linear bins scaled accordingly.

Covariate	Description
beaufort	Beaufort sea state.
quality	Survey-specific index of the quality of observation conditions, utilizing relevant factors other than Beaufort sea state (see methods).

size	Estimated size (number of individuals) of the sighted group.

Table 28: Covariates tested in candidate "multi-covariate distance sampling" (MCDS) detection functions.

Key	Adjustment	Order	Covariates	Succeeded	Δ AIC	Mean ESHW (m)
hr			beaufort, size	Yes	0.00	314
hr			beaufort	Yes	3.20	314
hn			beaufort, size	Yes	11.62	279
hr			size	Yes	12.92	314
hr				Yes	13.46	314
hn			beaufort, quality, size	Yes	13.61	279
hn			beaufort	Yes	13.78	279
hr	poly	4		Yes	15.47	314
hn	cos	2		Yes	16.46	273
hn	cos	3		Yes	24.29	260
hn				Yes	26.60	280
hn			size	Yes	27.55	280
hn	herm	4		Yes	28.57	280
hn			quality	Yes	28.60	280
hn			quality, size	Yes	29.53	280
hr	poly	2		No		
hr			quality	No		
hr			beaufort, quality	No		
hn			beaufort, quality	No		
hr			quality, size	No		
hr			beaufort, quality, size	No		

Table 29: Candidate detection functions for Mid Atlantic Tursiops Survey 2002-2004. The first one listed was selected for the density model.

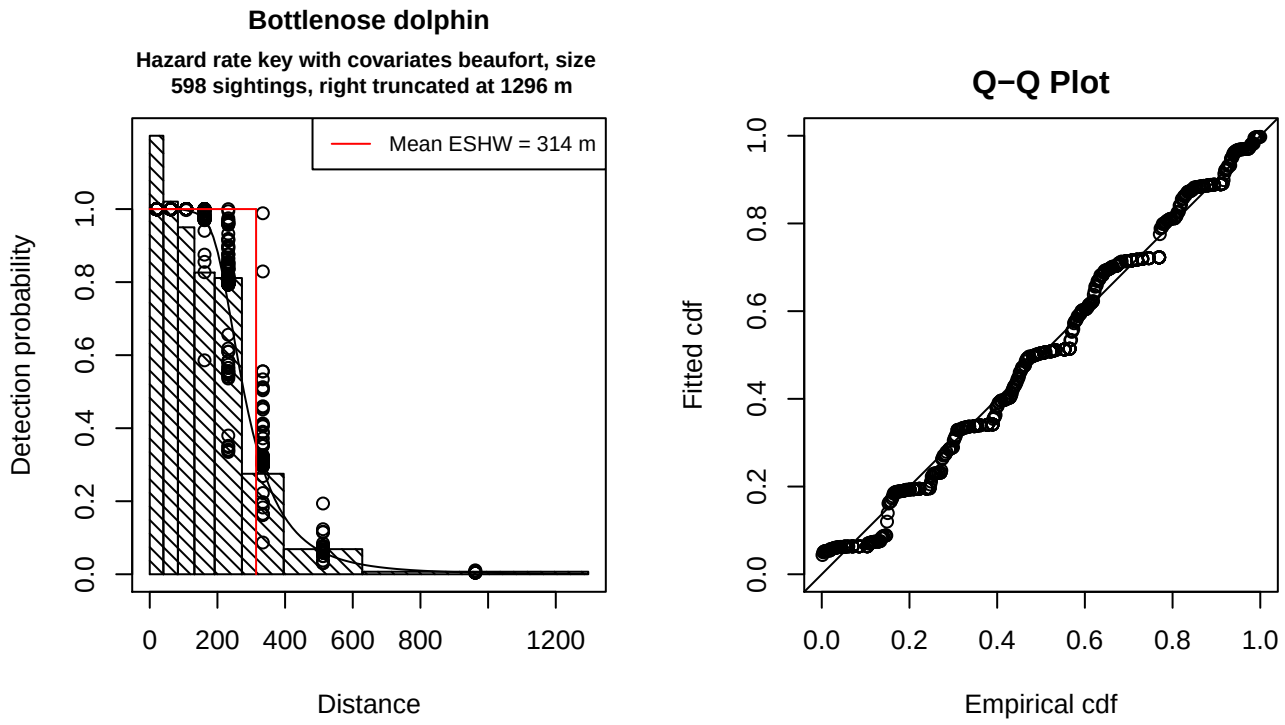

Figure 50: Detection function for Mid Atlantic Tursiops Survey 2002-2004 that was selected for the density model

Statistical output for this detection function:

```
Summary for ds object
Number of observations :  598
Distance range         :  0  -  1296
AIC                    :  2316.818

Detection function:
 Hazard-rate key function

Detection function parameters
Scale Coefficients:
               estimate         se
(Intercept)  5.72248163 0.07052517
beaufort    -0.16726126 0.04122532
size         0.07124364 0.03324356

Shape parameters:
            estimate         se
(Intercept) 1.415375 0.07632304

                        Estimate           SE         CV
Average p              0.2376071 7.857653e-03 0.03306994
N in covered region 2516.7593392 1.226967e+02 0.04875185
```

Additional diagnostic plots:

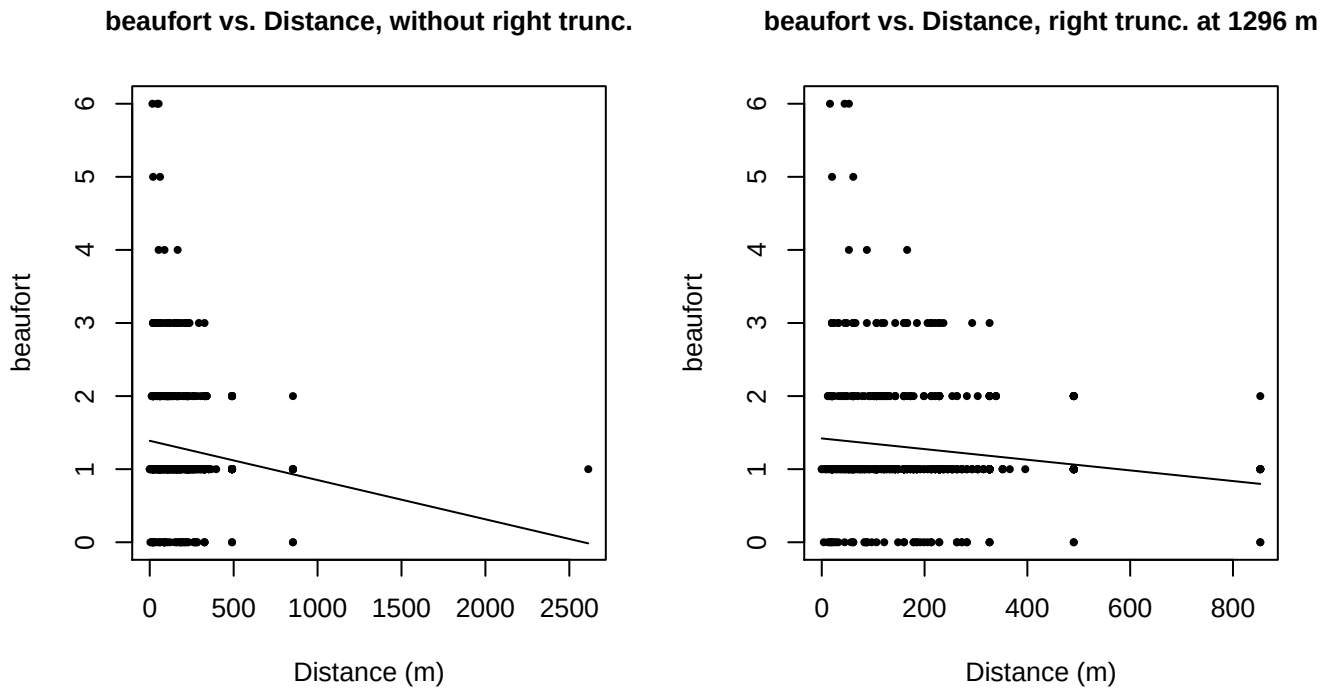

Figure 51: Scatterplots showing the relationship between Beaufort sea state and perpendicular sighting distance, for all sightings (left) and only those not right truncated (right). The line is a simple linear regression.

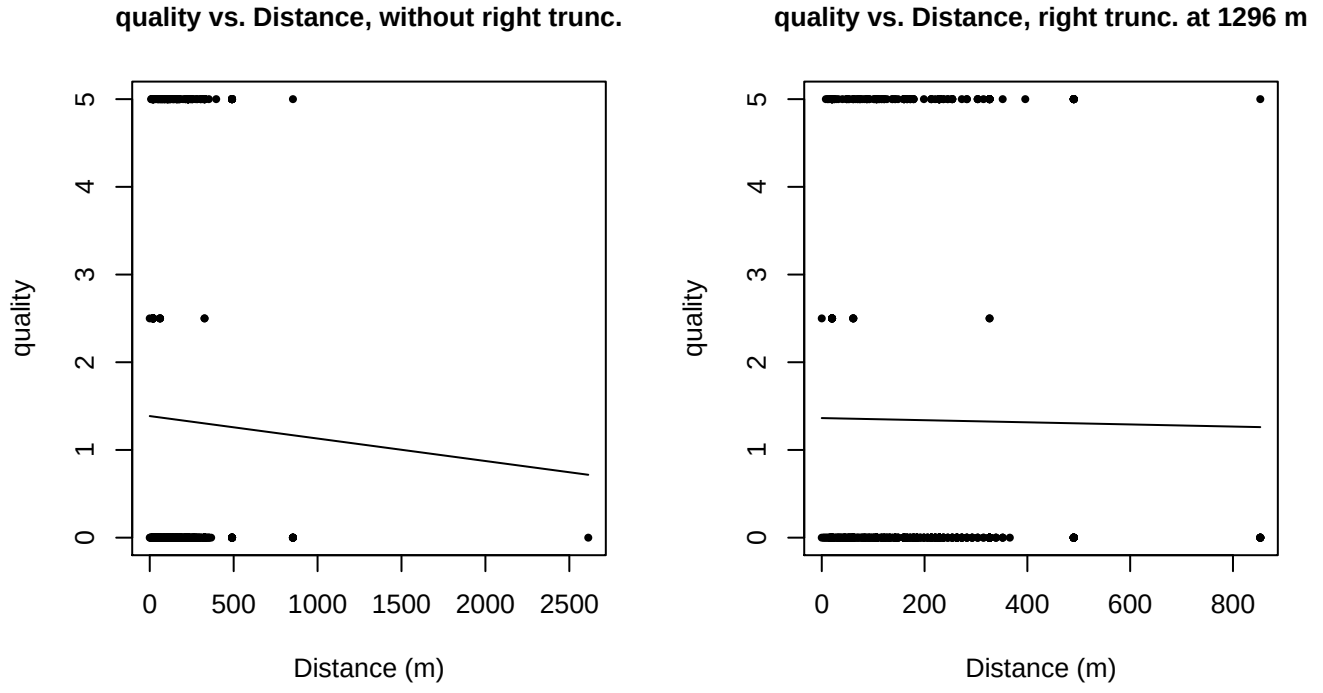

Figure 52: Scatterplots showing the relationship between the survey-specific index of the quality of observation conditions and perpendicular sighting distance, for all sightings (left) and only those not right truncated (right). Low values of the quality index correspond to better observation conditions. The line is a simple linear regression.

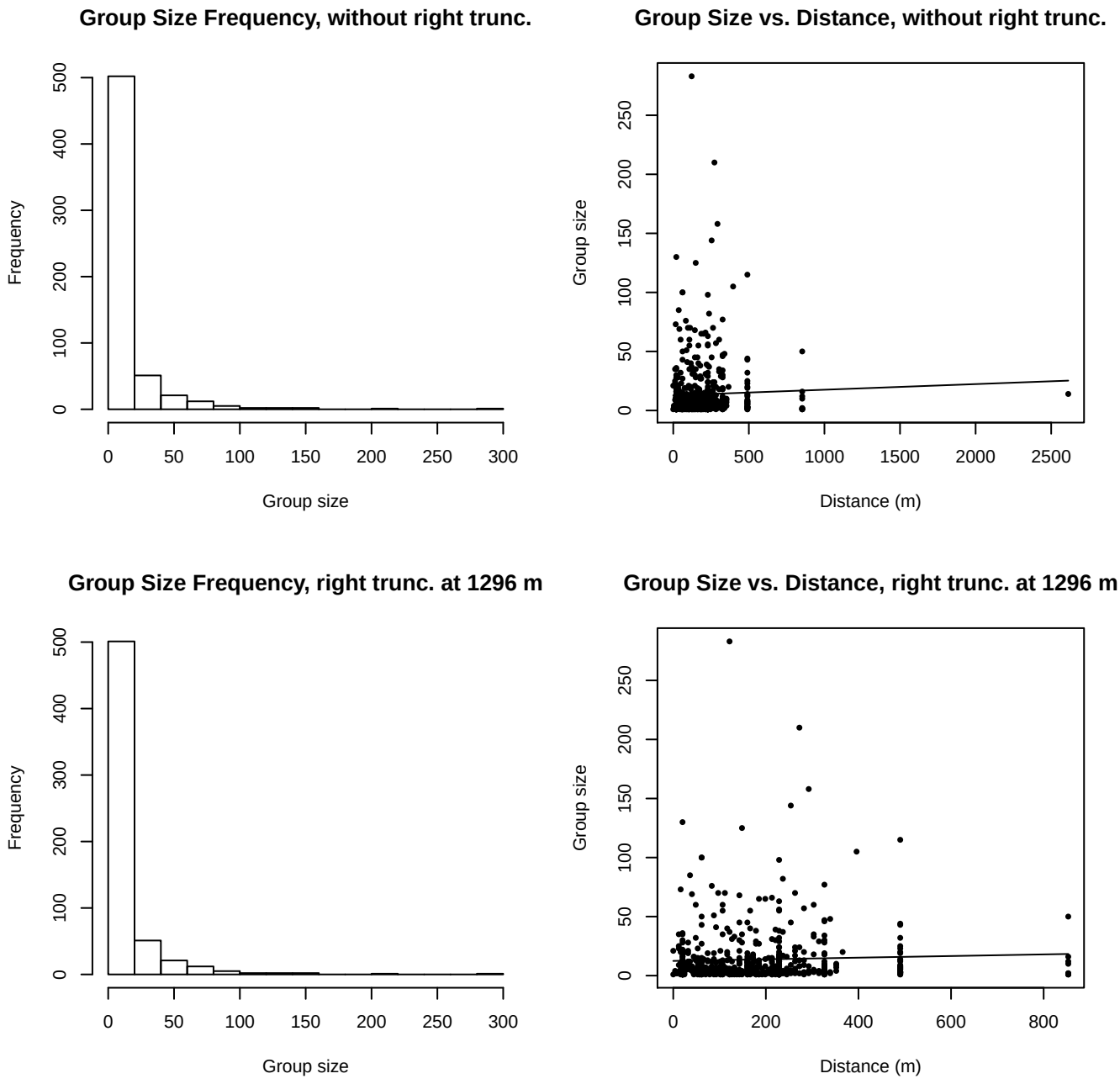

Figure 53: Histograms showing group size frequency and scatterplots showing the relationship between group size and perpendicular sighting distance, for all sightings (top row) and only those not right truncated (bottom row). In the scatterplot, the line is a simple linear regression.

GulfSCAT Aerial Survey

The sightings were right truncated at 628m.

Covariate	Description
beaufort	Beaufort sea state.
quality	Survey-specific index of the quality of observation conditions, utilizing relevant factors other than Beaufort sea state (see methods).
size	Estimated size (number of individuals) of the sighted group.

Table 30: Covariates tested in candidate "multi-covariate distance sampling" (MCDS) detection functions.

Key	Adjustment	Order	Covariates	Succeeded	Δ AIC	Mean ESHW (m)
hn	cos	3		Yes	0.00	225
hr			size	Yes	0.57	237
hn				Yes	1.36	199
hr				Yes	1.61	237
hn	cos	2		Yes	1.70	214
hn	herm	4		Yes	1.83	215
hn			size	Yes	1.83	198
hr			beaufort, size	Yes	2.07	238
hr	poly	4		Yes	2.60	233
hn			beaufort	Yes	3.30	199
hr			beaufort	Yes	3.30	238
hr	poly	2		Yes	3.65	237
hn			beaufort, size	Yes	3.69	198
hr			quality	No		
hn			quality	No		
hr			beaufort, quality	No		
hn			beaufort, quality	No		
hr			quality, size	No		
hn			quality, size	No		
hr			beaufort, quality, size	No		
hn			beaufort, quality, size	No		

Table 31: Candidate detection functions for GulfSCAT Aerial Survey. The first one listed was selected for the density model.

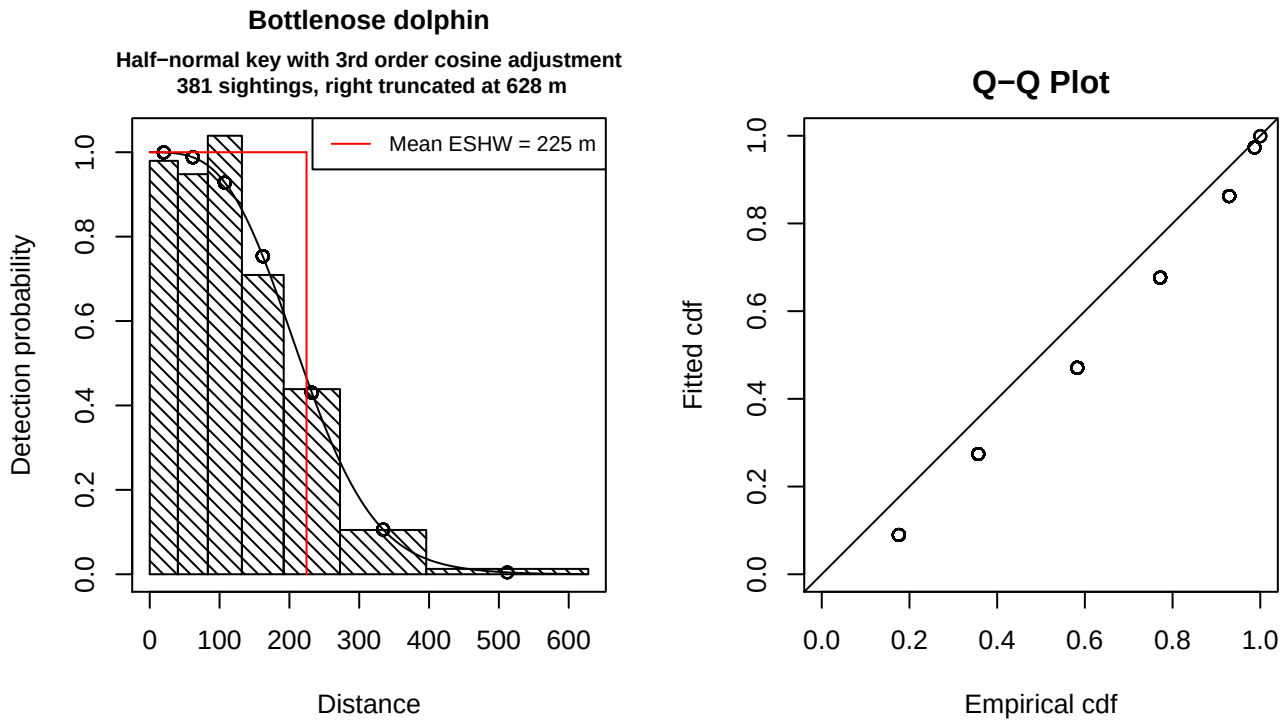

Figure 54: Detection function for GulfSCAT Aerial Survey that was selected for the density model

Statistical output for this detection function:

```
Summary for ds object
Number of observations :  381
Distance range         :  0  -  628
AIC                    :  1361.93

Detection function:
 Half-normal key function with cosine adjustment term of order 3

Detection function parameters
Scale Coefficients:
            estimate         se
(Intercept)  5.03541 0.03982634

Adjustment term parameter(s):
               estimate         se
cos, order 3 -0.1508097 0.08024846


Monotonicity constraints were enforced.
                        Estimate          SE         CV
Average p              0.3575448  0.02964342 0.08290827
N in covered region 1065.6007121 98.58974988 0.09252035

Monotonicity constraints were enforced.
```

Additional diagnostic plots:

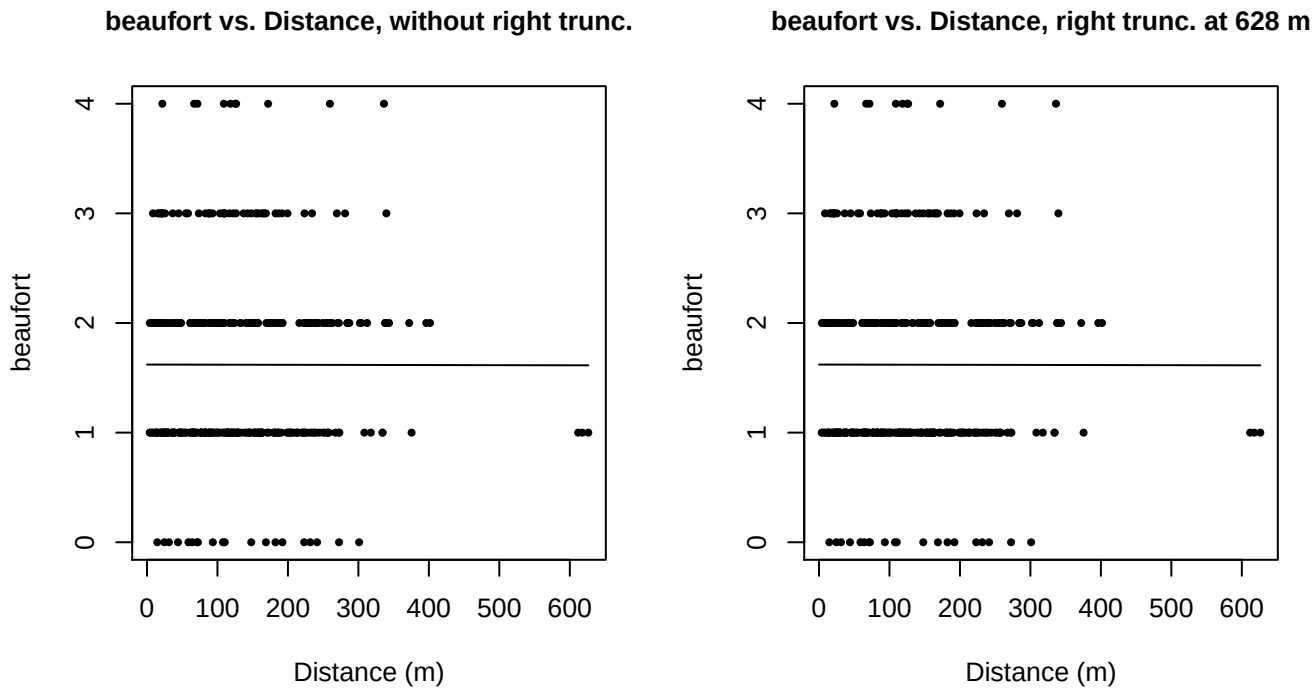

Figure 55: Scatterplots showing the relationship between Beaufort sea state and perpendicular sighting distance, for all sightings (left) and only those not right truncated (right). The line is a simple linear regression.

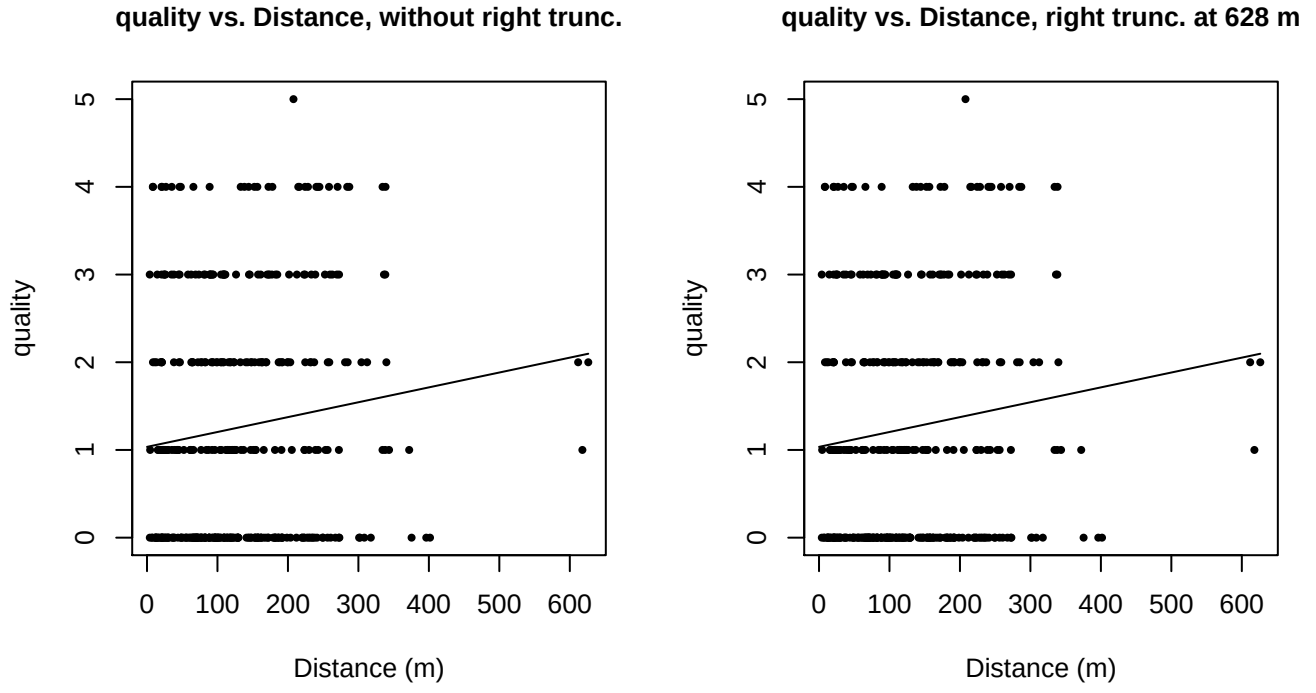

Figure 56: Scatterplots showing the relationship between the survey-specific index of the quality of observation conditions and perpendicular sighting distance, for all sightings (left) and only those not right truncated (right). Low values of the quality index correspond to better observation conditions. The line is a simple linear regression.

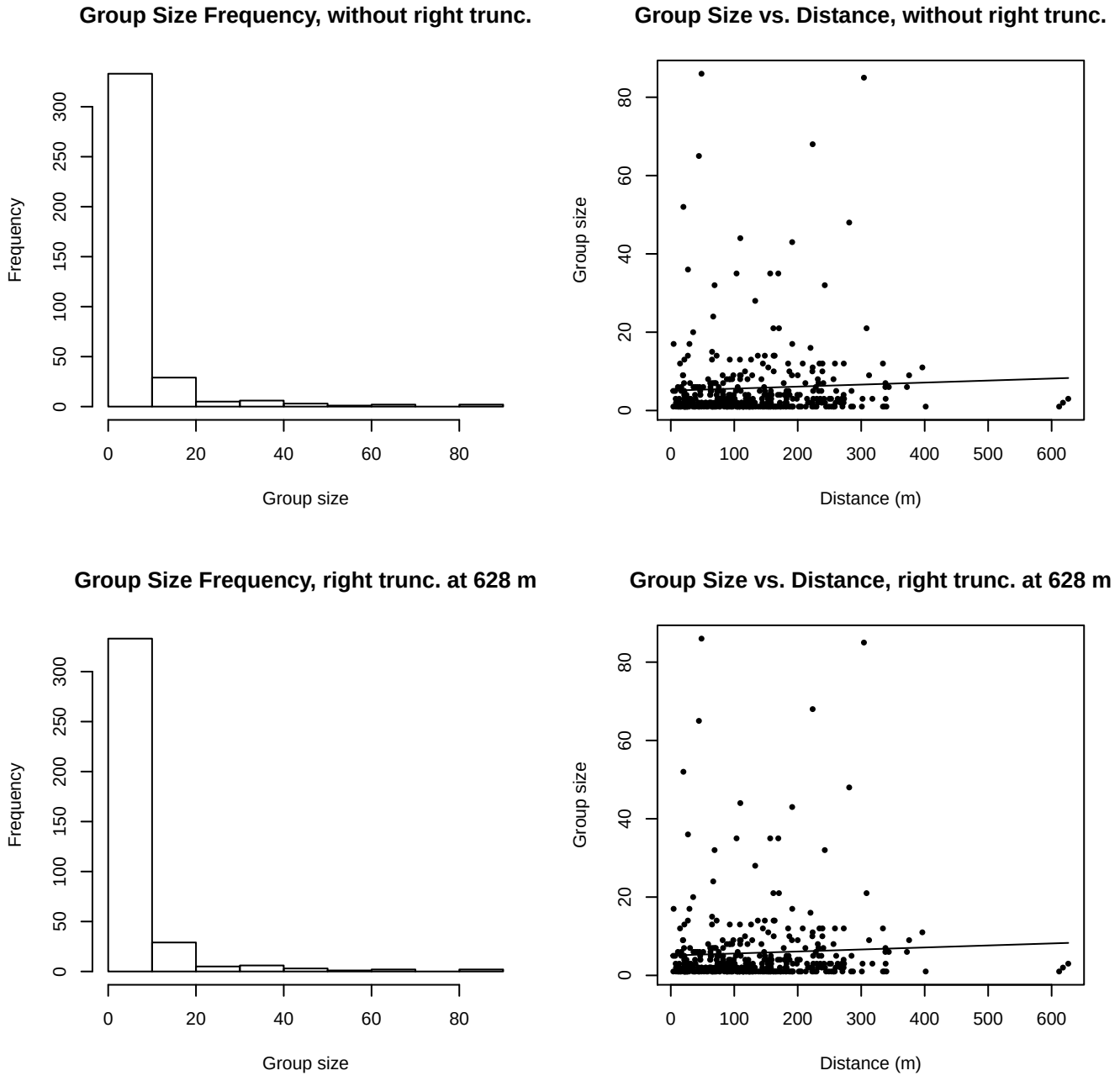

Figure 57: Histograms showing group size frequency and scatterplots showing the relationship between group size and perpendicular sighting distance, for all sightings (top row) and only those not right truncated (bottom row). In the scatterplot, the line is a simple linear regression.

Without Belly Observers - 600 ft

The sightings were right truncated at 800m.

Covariate	Description
beaufort	Beaufort sea state.
size	Estimated size (number of individuals) of the sighted group.

Table 32: Covariates tested in candidate "multi-covariate distance sampling" (MCDS) detection functions.

Key	Adjustment	Order	Covariates	Succeeded	Δ AIC	Mean ESHW (m)
hn				Yes	0.00	315
hr				Yes	0.39	355
hn	cos	3		Yes	0.82	347
hn	cos	2		Yes	1.44	354
hn	herm	4		Yes	1.55	355
hr	poly	4		Yes	1.89	353
hr	poly	2		Yes	2.39	355
hn			beaufort	No		
hr			beaufort	No		
hn			size	No		
hr			size	No		
hn			beaufort, size	No		
hr			beaufort, size	No		

Table 33: Candidate detection functions for Without Belly Observers - 600 ft. The first one listed was selected for the density model.

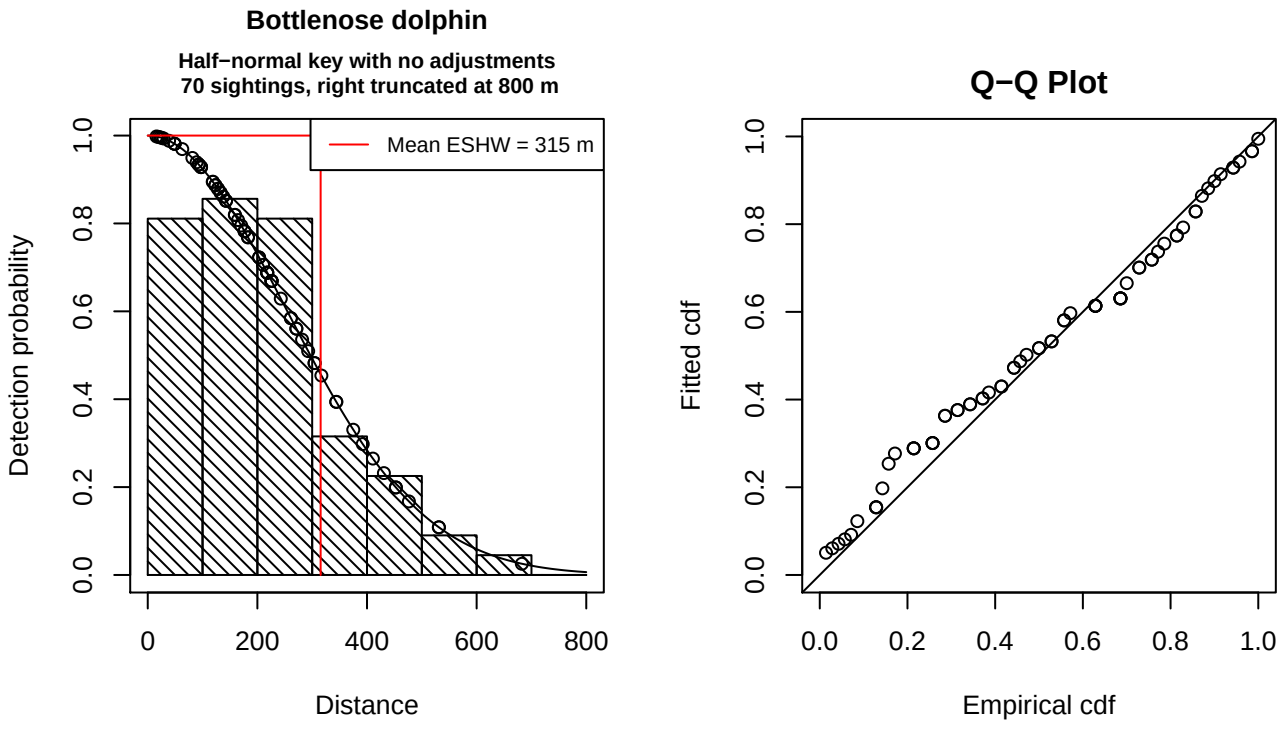

Figure 58: Detection function for Without Belly Observers - 600 ft that was selected for the density model

Statistical output for this detection function:

```
Summary for ds object
```

```
Number of observations :  70
Distance range         :  0  -  800
AIC                    :  876.3777

Detection function:
 Half-normal key function

Detection function parameters
Scale Coefficients:
             estimate         se
(Intercept)  5.52949 0.09235321

                        Estimate          SE         CV
Average p             0.3942252  0.03580923 0.09083444
N in covered region 177.5634687 23.08654291 0.13001854
```

Additional diagnostic plots:

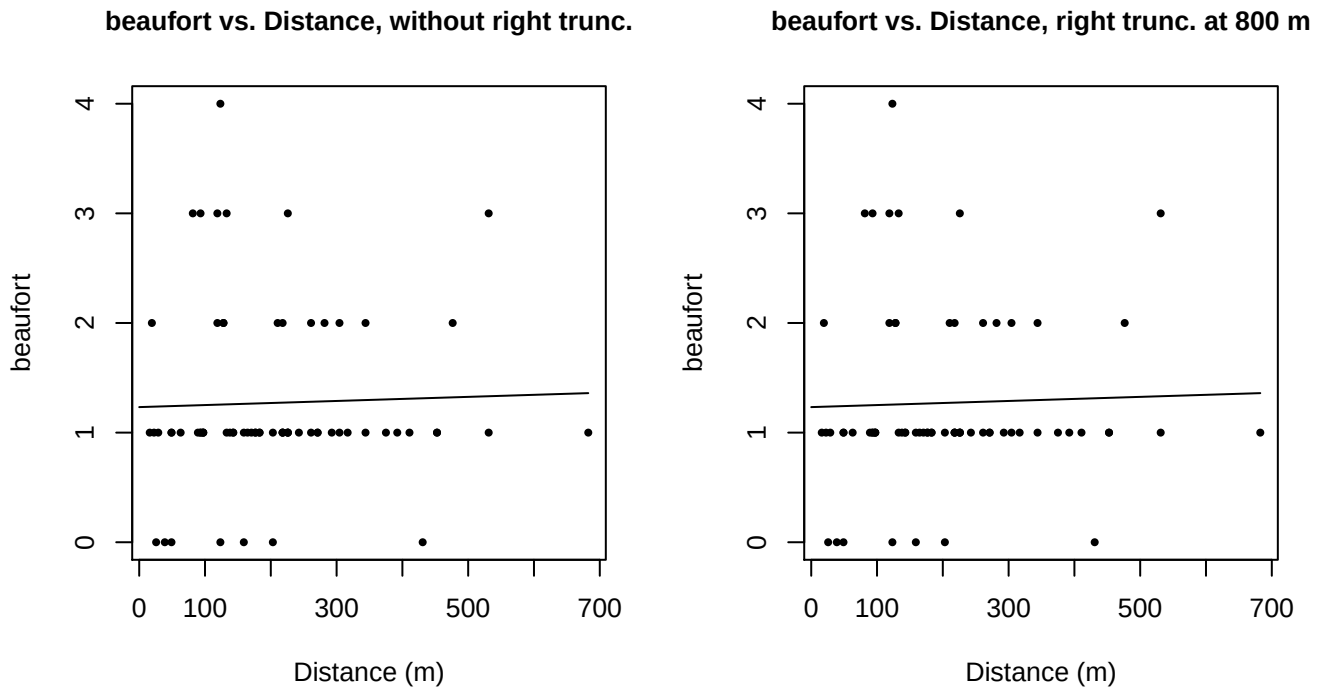

Figure 59: Scatterplots showing the relationship between Beaufort sea state and perpendicular sighting distance, for all sightings (left) and only those not right truncated (right). The line is a simple linear regression.

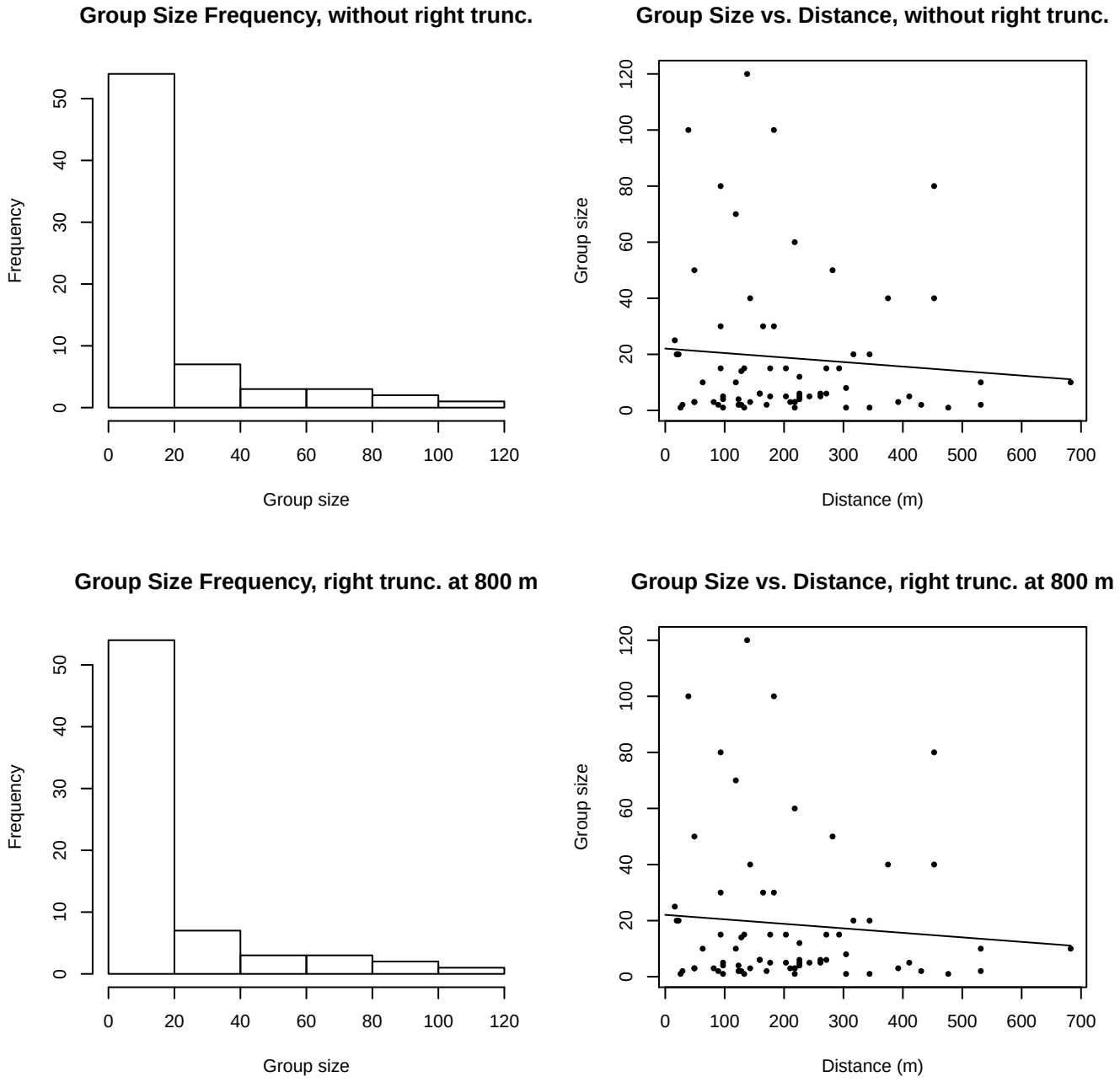

Figure 60: Histograms showing group size frequency and scatterplots showing the relationship between group size and perpendicular sighting distance, for all sightings (top row) and only those not right truncated (bottom row). In the scatterplot, the line is a simple linear regression.

REMMOA (French Caribbean)

The sightings were right truncated at 800m.

Covariate	Description
beaufort	Beaufort sea state.
quality	Survey-specific index of the quality of observation conditions, utilizing relevant factors other than Beaufort sea state (see methods).
size	Estimated size (number of individuals) of the sighted group.

Table 34: Covariates tested in candidate "multi-covariate distance sampling" (MCDS) detection functions.

Key	Adjustment	Order	Covariates	Succeeded	Δ AIC	Mean ESHW (m)
hr			quality	Yes	0.00	376
hn			quality	Yes	0.13	314
hn				Yes	0.62	315
hr				Yes	1.01	355
hn	cos	3		Yes	1.44	347
hr			beaufort, quality	Yes	2.00	376
hn	cos	2		Yes	2.06	354
hn	herm	4		Yes	2.18	355
hr	poly	4		Yes	2.51	353
hr	poly	2		Yes	2.84	345
hr			beaufort	No		
hn			beaufort	No		
hr			size	No		
hn			size	No		
hn			beaufort, quality	No		
hr			beaufort, size	No		
hn			beaufort, size	No		
hr			quality, size	No		
hn			quality, size	No		
hr			beaufort, quality, size	No		
hn			beaufort, quality, size	No		

Table 35: Candidate detection functions for REMMOA (French Caribbean). The first one listed was selected for the density model.

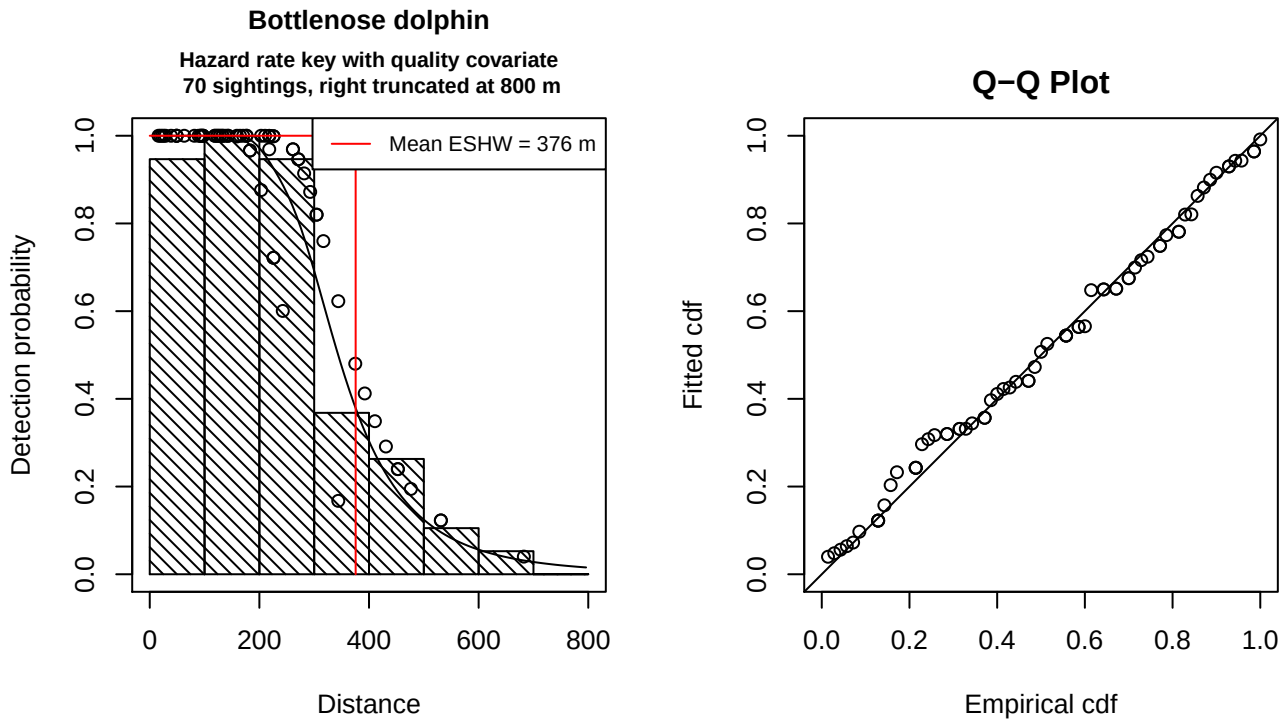

Figure 61: Detection function for REMMOA (French Caribbean) that was selected for the density model

Statistical output for this detection function:

```
Summary for ds object
Number of observations :  70
Distance range         :  0  -  800
AIC                    :  875.7539

Detection function:
 Hazard-rate key function

Detection function parameters
Scale Coefficients:
             estimate         se
(Intercept)  5.8349992 0.13321814
quality     -0.1447324 0.08959998

Shape parameters:
            estimate       se
(Intercept) 1.530251 0.317392

                       Estimate          SE         CV
Average p              0.4601637  0.04107147 0.08925405
N in covered region 152.1197789 19.12835431 0.12574535
```

Additional diagnostic plots:

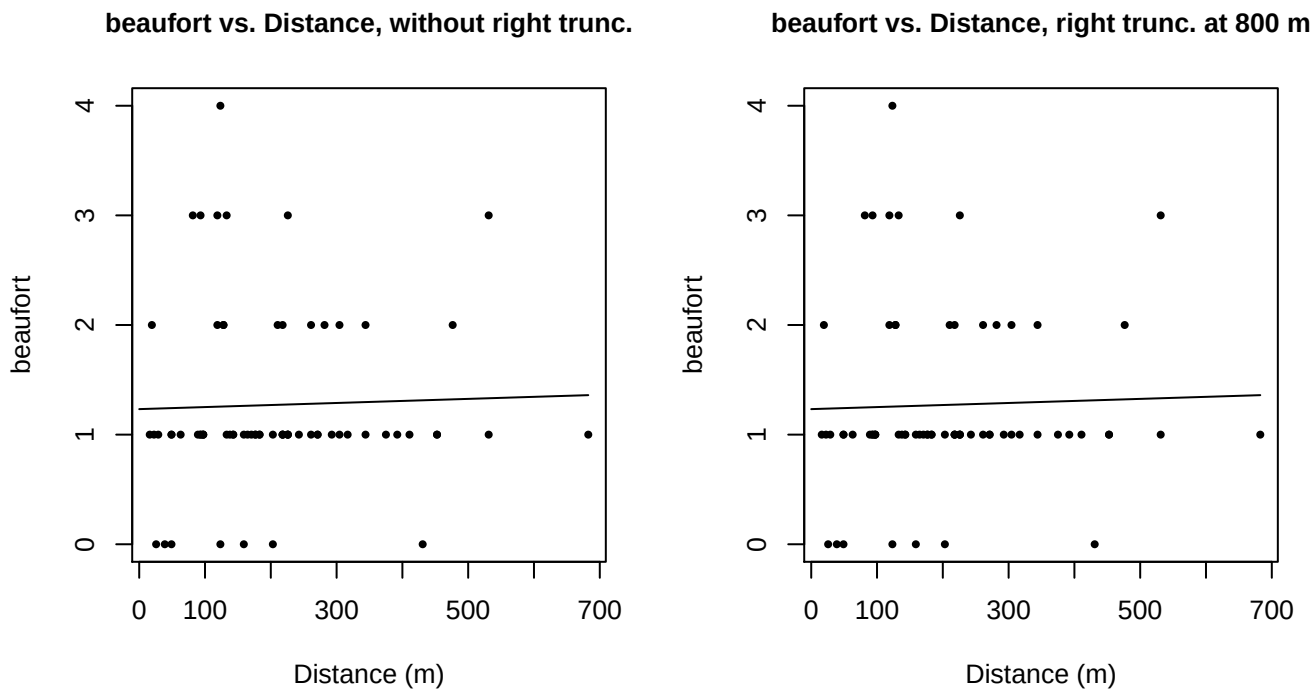

Figure 62: Scatterplots showing the relationship between Beaufort sea state and perpendicular sighting distance, for all sightings (left) and only those not right truncated (right). The line is a simple linear regression.

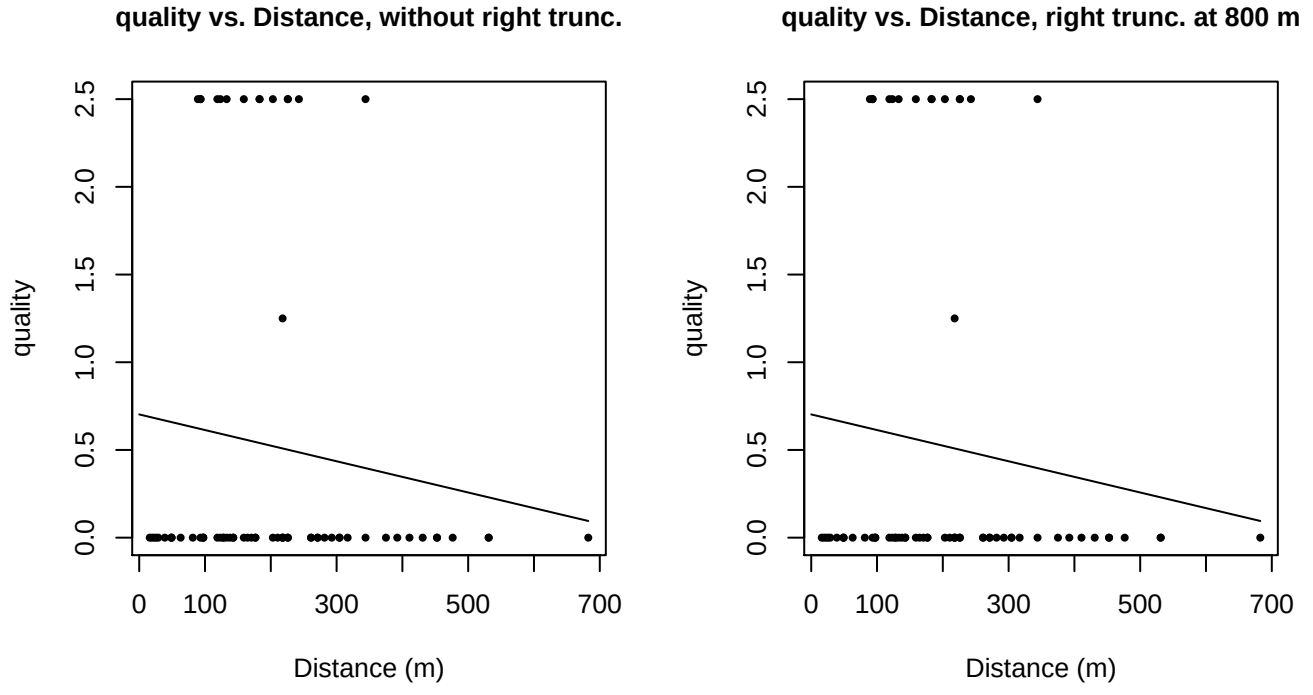

Figure 63: Scatterplots showing the relationship between the survey-specific index of the quality of observation conditions and perpendicular sighting distance, for all sightings (left) and only those not right truncated (right). Low values of the quality index correspond to better observation conditions. The line is a simple linear regression.

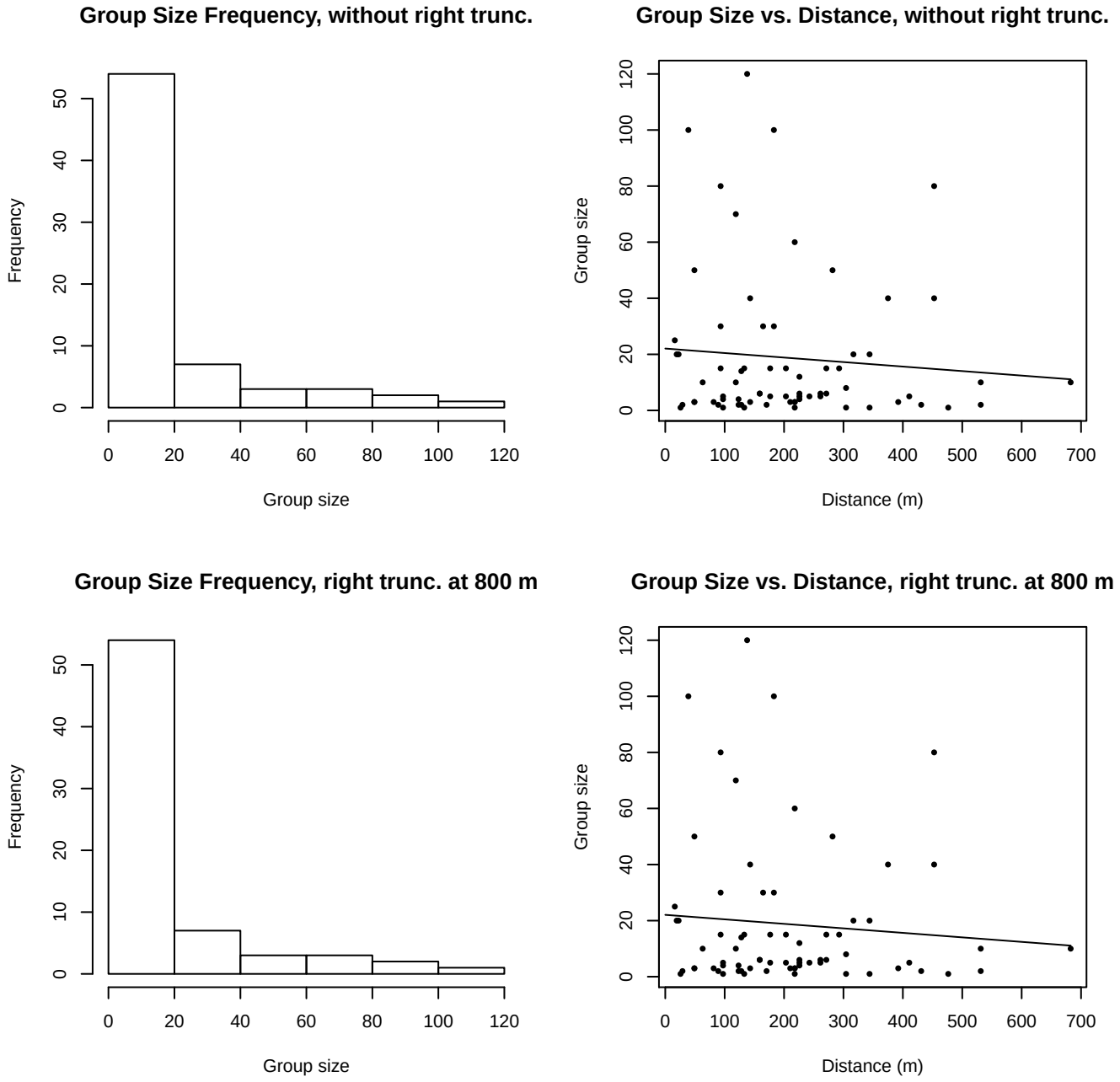

Figure 64: Histograms showing group size frequency and scatterplots showing the relationship between group size and perpendicular sighting distance, for all sightings (top row) and only those not right truncated (bottom row). In the scatterplot, the line is a simple linear regression.

Without Belly Observers - 750 ft

The sightings were right truncated at 1296m. The vertical sighting angles were heaped at 10 degree increments, so the candidate detection functions were fitted using linear bins scaled accordingly.

Covariate	Description
beaufort	Beaufort sea state.
size	Estimated size (number of individuals) of the sighted group.

Table 36: Covariates tested in candidate "multi-covariate distance sampling" (MCDS) detection functions.

Key	Adjustment	Order	Covariates	Succeeded	Δ AIC	Mean ESHW (m)
hr			size	Yes	0.00	385
hr				Yes	6.10	383
hr	poly	2		Yes	8.09	383
hr	poly	4		Yes	8.09	383
hn	cos	2		Yes	26.24	352
hn	cos	3		Yes	41.99	335
hn			size	Yes	75.35	401
hn				Yes	83.50	401
hn	herm	4		Yes	85.03	400
hr			beaufort	No		
hn			beaufort	No		
hr			beaufort, size	No		
hn			beaufort, size	No		

Table 37: Candidate detection functions for Without Belly Observers - 750 ft. The first one listed was selected for the density model.

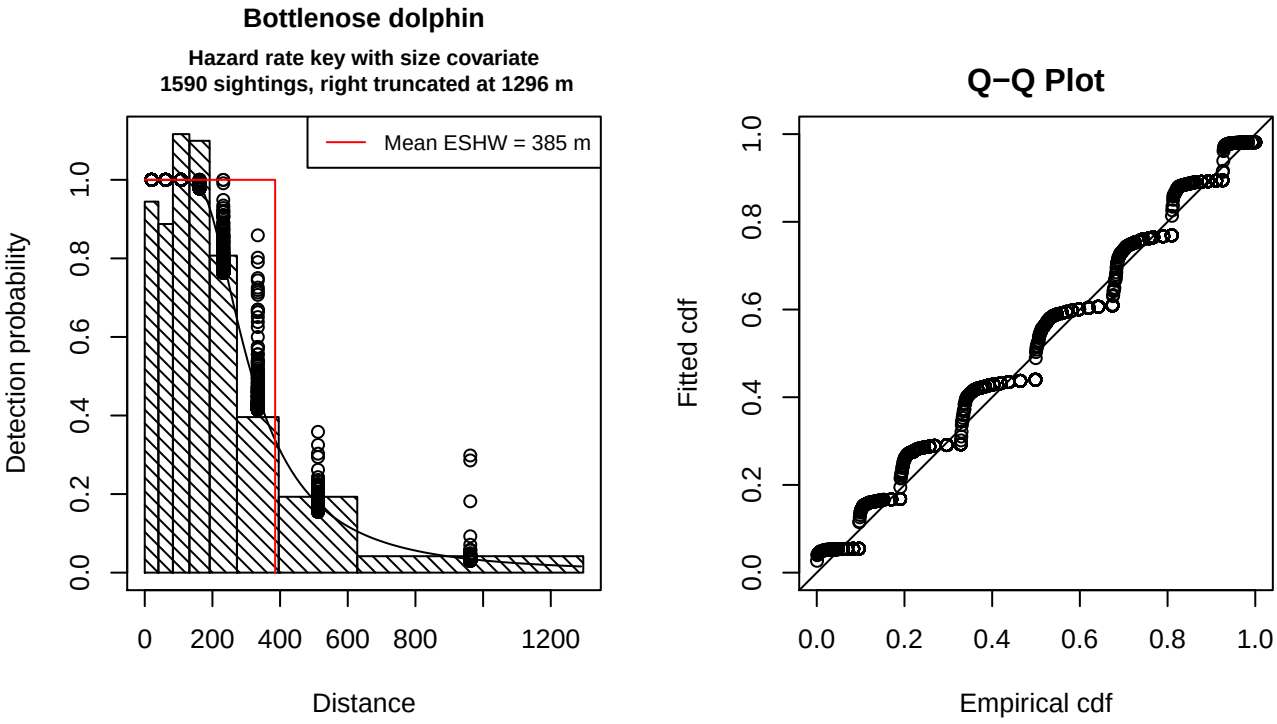

Figure 65: Detection function for Without Belly Observers - 750 ft that was selected for the density model

Statistical output for this detection function:

```
Summary for ds object
Number of observations :  1590
Distance range         :  0  -  1296
AIC                    :  6503.295

Detection function:
 Hazard-rate key function

Detection function parameters
Scale Coefficients:
             estimate         se
(Intercept) 5.57563026 0.04343791
size        0.08344291 0.02555223

Shape parameters:
             estimate         se
(Intercept) 0.9966795 0.04593339

                         Estimate           SE         CV
Average p                0.2956102 7.995006e-03 0.02704577
N in covered region 5378.7042741 1.844200e+02 0.03428707
```

Additional diagnostic plots:

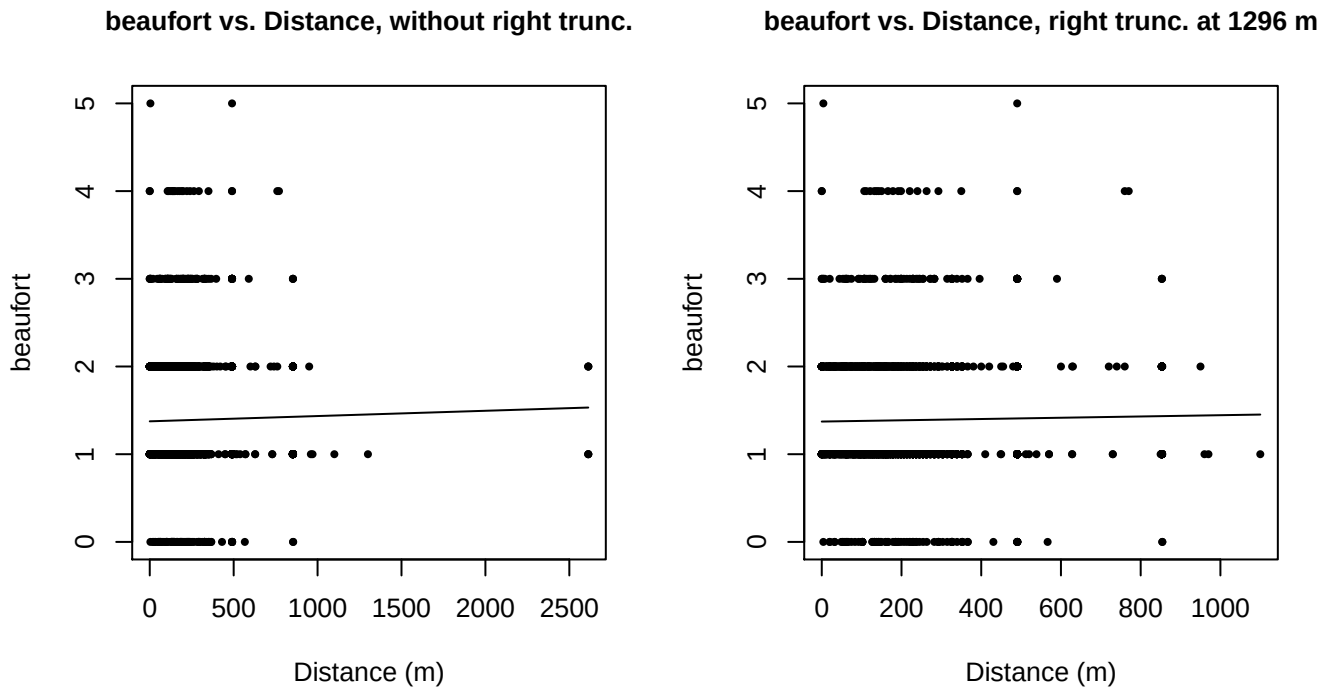

Figure 66: Scatterplots showing the relationship between Beaufort sea state and perpendicular sighting distance, for all sightings (left) and only those not right truncated (right). The line is a simple linear regression.

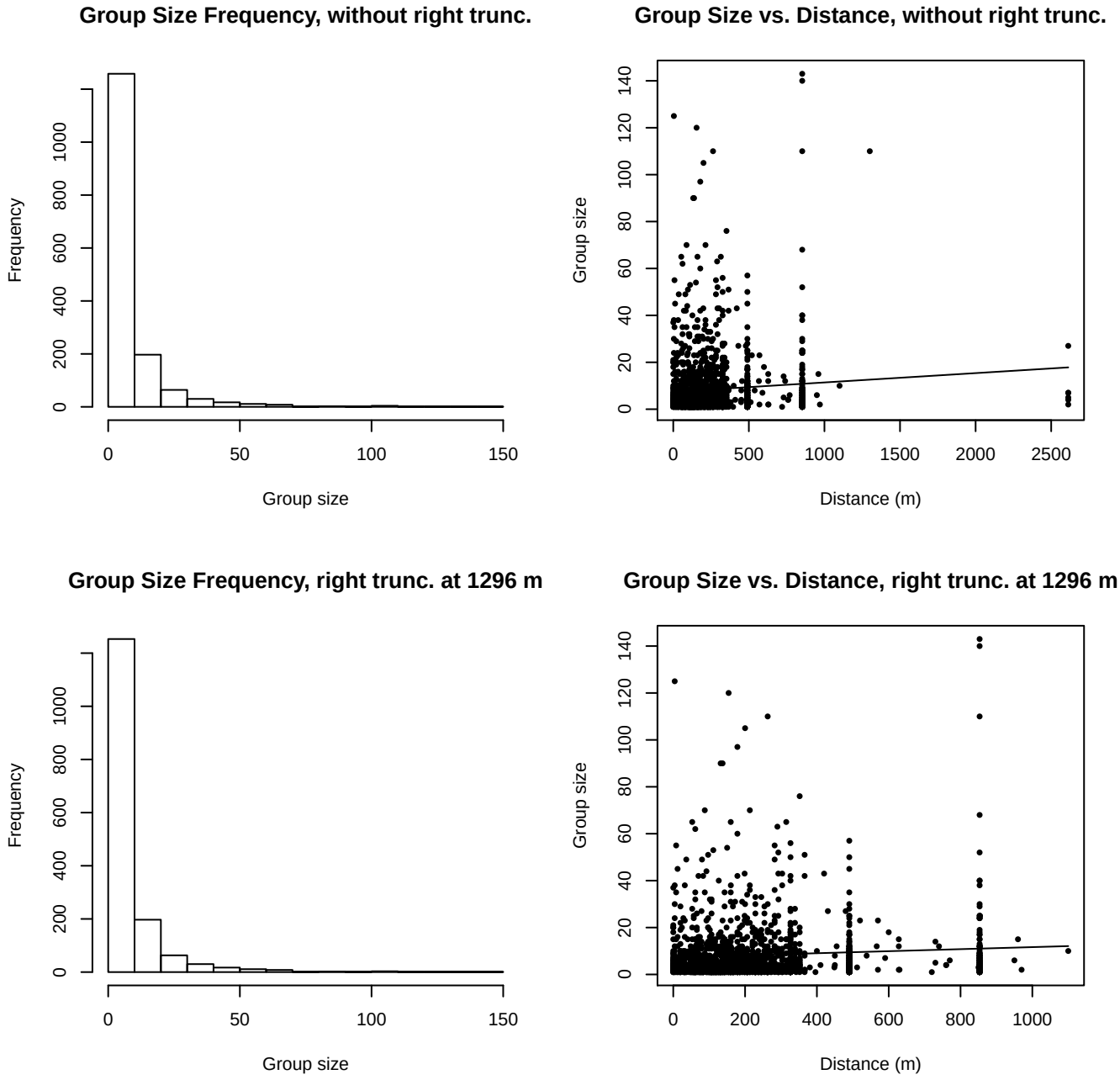

Figure 67: Histograms showing group size frequency and scatterplots showing the relationship between group size and perpendicular sighting distance, for all sightings (top row) and only those not right truncated (bottom row). In the scatterplot, the line is a simple linear regression.

SE_secas92

The sightings were right truncated at 900m. Due to a reduced frequency of sightings close to the trackline that plausibly resulted from the behavior of the observers and/or the configuration of the survey platform, the sightings were left truncted as well. Sightings closer than 40 m to the trackline were omitted from the analysis, and it was assumed that the the area closer to the trackline than this was not surveyed. This distance was estimated by inspecting histograms of perpendicular sighting distances. The vertical sighting angles were heaped at 10 degree increments, so the candidate detection functions were fitted using linear bins scaled accordingly.

Covariate	Description

beaufort	Beaufort sea state.
size	Estimated size (number of individuals) of the sighted group.

Table 38: Covariates tested in candidate "multi-covariate distance sampling" (MCDS) detection functions.

Key	Adjustment	Order	Covariates	Succeeded	Δ AIC	Mean ESHW (m)
hr			beaufort, size	Yes	0.00	256
hr			beaufort	Yes	0.39	254
hr			size	Yes	7.70	286
hr				Yes	13.04	218
hn			beaufort, size	Yes	14.83	348
hn	cos	2		Yes	14.89	193
hr	poly	2		Yes	15.04	218
hr	poly	4		Yes	15.04	216
hn			size	Yes	16.56	335
hn			beaufort	Yes	32.36	268
hn				Yes	35.93	271
hn	cos	3		Yes	36.28	224
hn	herm	4		Yes	37.50	271

Table 39: Candidate detection functions for SE_secas92. The first one listed was selected for the density model.

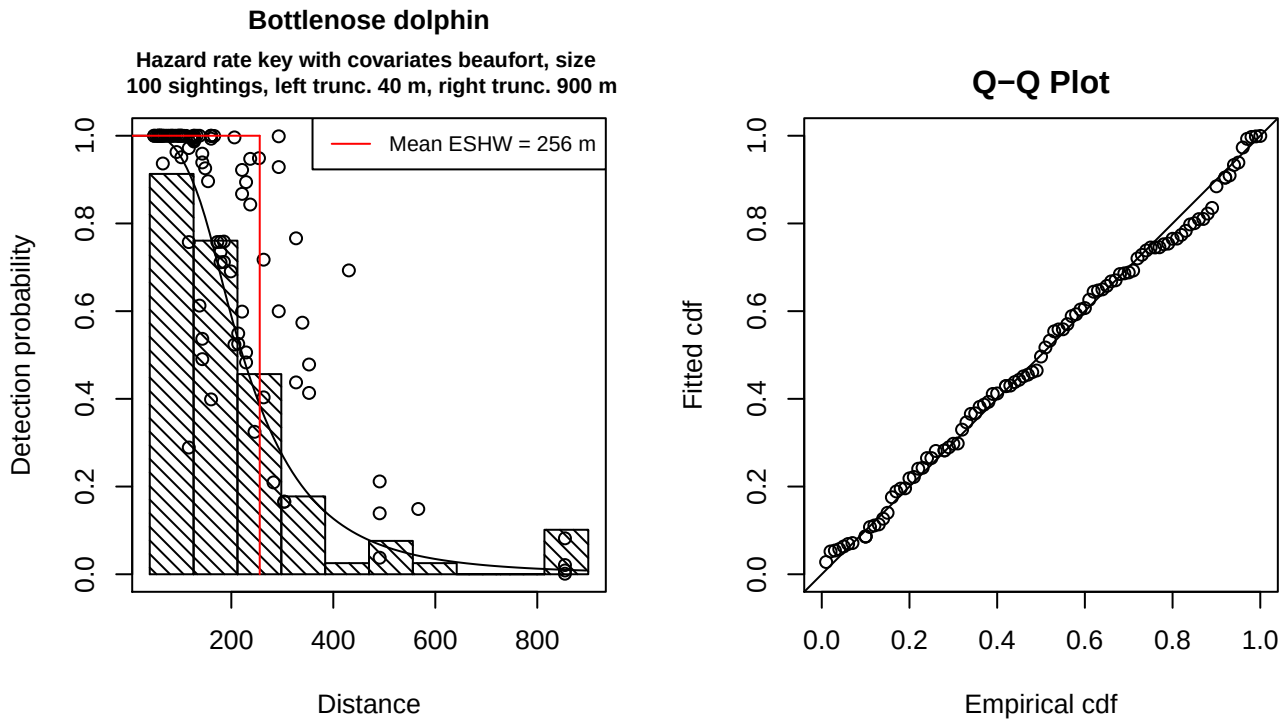

Figure 68: Detection function for SE_secas92 that was selected for the density model

Statistical output for this detection function:

```
Summary for ds object
Number of observations :  100
Distance range         :  40  -  900
AIC                    :  1200.912

Detection function:
 Hazard-rate key function

Detection function parameters
Scale Coefficients:
             estimate         se
(Intercept)  5.6195685 0.15410352
beaufort    -0.3914631 0.11597821
size         0.1450668 0.09081025

Shape parameters:
            estimate        se
(Intercept) 1.291198 0.1271422

                      Estimate          SE        CV
Average p             0.2423105  0.03018737 0.1245814
N in covered region 412.6937100 63.28554498 0.1533475
```

Additional diagnostic plots:

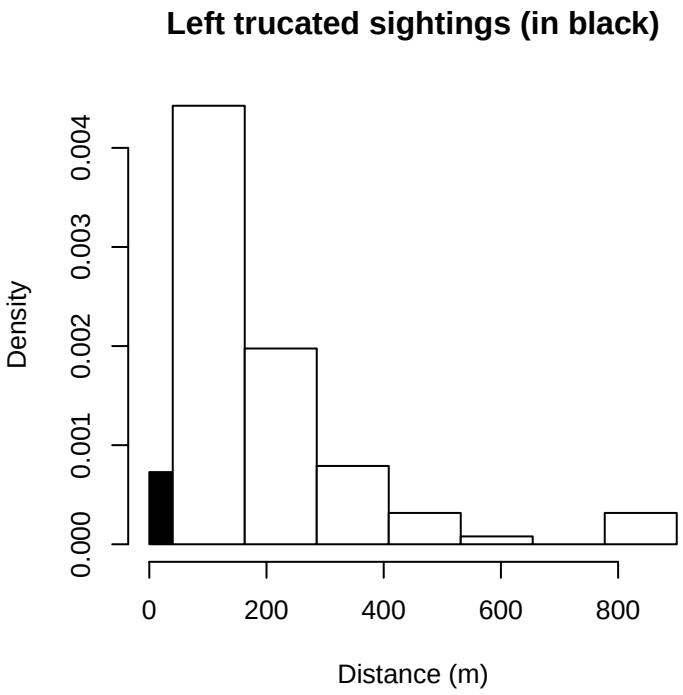

Figure 69: Density of sightings by perpendicular distance for SE_secas92. Black bars on the left show sightings that were left truncated.

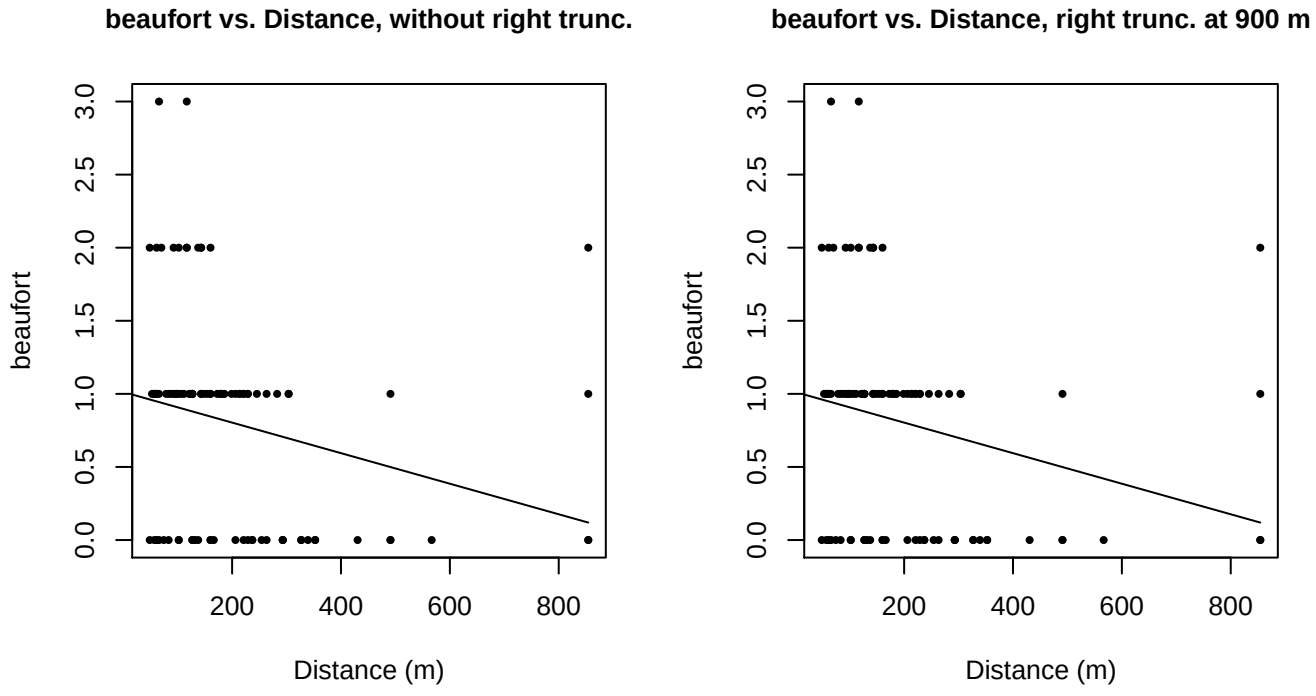

Figure 70: Scatterplots showing the relationship between Beaufort sea state and perpendicular sighting distance, for all sightings (left) and only those not right truncated (right). The line is a simple linear regression.

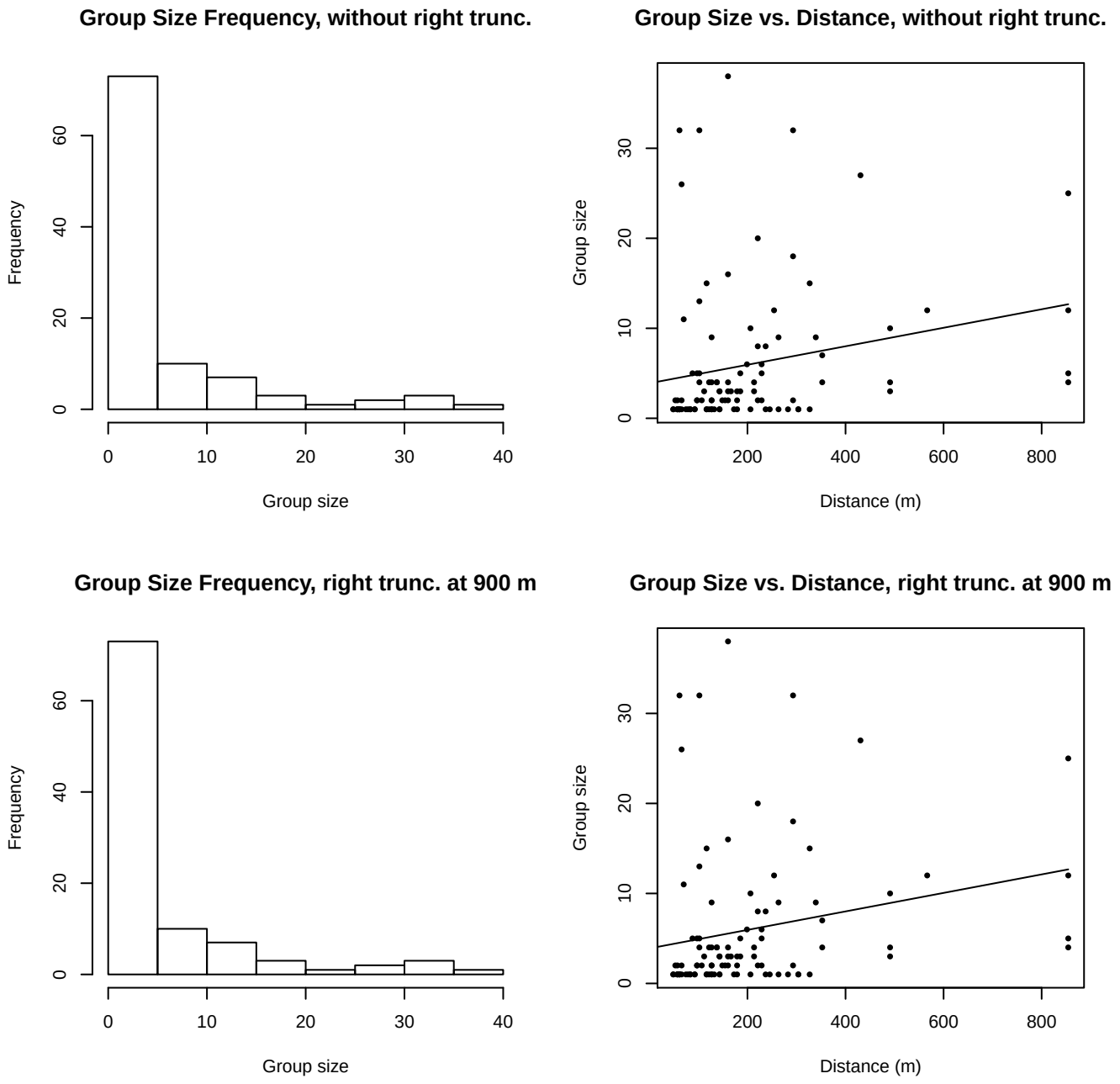

Figure 71: Histograms showing group size frequency and scatterplots showing the relationship between group size and perpendicular sighting distance, for all sightings (top row) and only those not right truncated (bottom row). In the scatterplot, the line is a simple linear regression.

SE_secas95

The sightings were right truncated at 900m. Due to a reduced frequency of sightings close to the trackline that plausibly resulted from the behavior of the observers and/or the configuration of the survey platform, the sightings were left truncted as well. Sightings closer than 40 m to the trackline were omitted from the analysis, and it was assumed that the the area closer to the trackline than this was not surveyed. This distance was estimated by inspecting histograms of perpendicular sighting distances. The vertical sighting angles were heaped at 10 degree increments, so the candidate detection functions were fitted using linear bins scaled accordingly.

Covariate	Description

beaufort	Beaufort sea state.
quality	Survey-specific index of the quality of observation conditions, utilizing relevant factors other than Beaufort sea state (see methods).
size	Estimated size (number of individuals) of the sighted group.

Table 40: Covariates tested in candidate "multi-covariate distance sampling" (MCDS) detection functions.

Key	Adjustment	Order	Covariates	Succeeded	Δ AIC	Mean ESHW (m)
hr				Yes	0.00	335
hn				Yes	0.33	305
hn	cos	3		Yes	1.68	345
hr			quality	Yes	1.71	332
hr	poly	2		Yes	1.97	332
hn			quality	Yes	1.99	305
hr	poly	4		Yes	2.00	335
hn	herm	4		Yes	2.22	304
hn	cos	2		Yes	2.30	299
hn			beaufort	No		
hr			beaufort	No		
hn			size	No		
hr			size	No		
hn			beaufort, quality	No		
hr			beaufort, quality	No		
hn			beaufort, size	No		
hr			beaufort, size	No		
hn			quality, size	No		
hr			quality, size	No		
hn			beaufort, quality, size	No		
hr			beaufort, quality, size	No		

Table 41: Candidate detection functions for SE_secas95. The first one listed was selected for the density model.

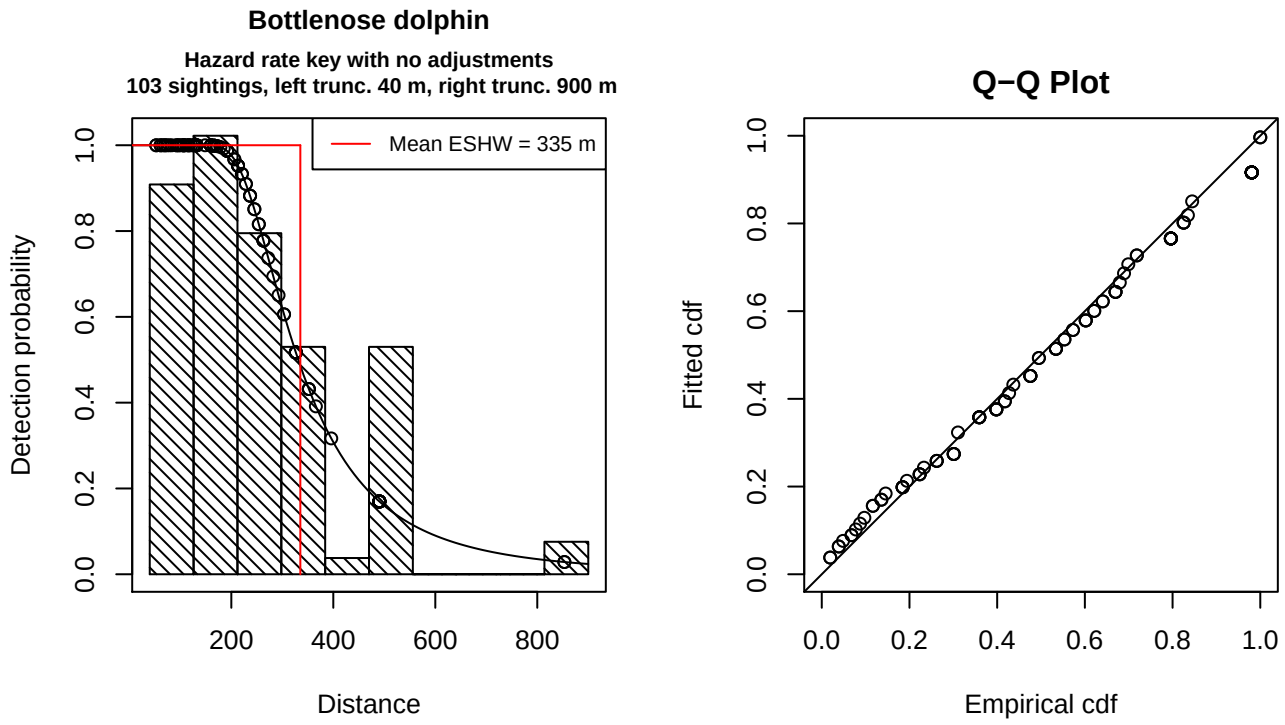

Figure 72: Detection function for SE_secas95 that was selected for the density model

Statistical output for this detection function:

```
Summary for ds object
Number of observations :  103
Distance range         :  40  -  900
AIC                    :  1294.824

Detection function:
 Hazard-rate key function

Detection function parameters
Scale Coefficients:
            estimate        se
(Intercept) 5.693681 0.1236017

Shape parameters:
            estimate        se
(Intercept) 1.210765 0.2087024

                       Estimate          SE         CV
Average p              0.3726091  0.03559214 0.09552141
N in covered region 276.4291340 34.09786089 0.12335118
```

Additional diagnostic plots:

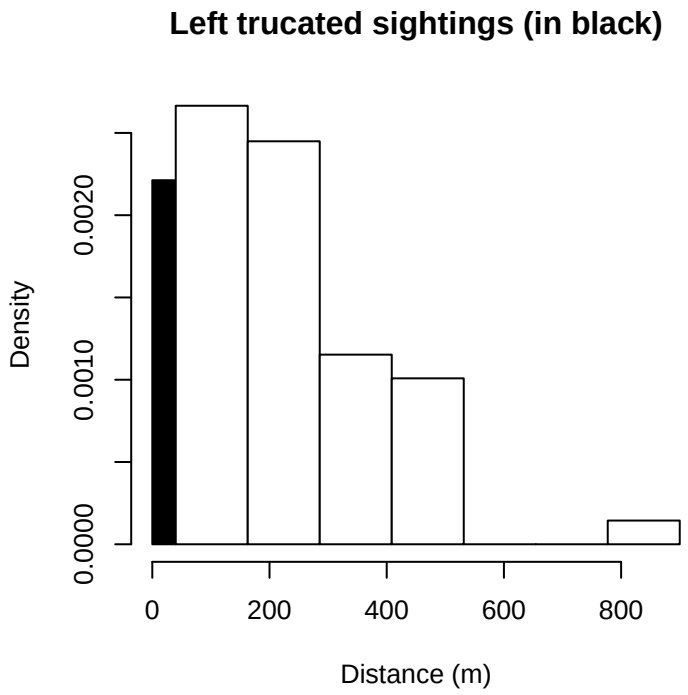

Figure 73: Density of sightings by perpendicular distance for SE_secas95. Black bars on the left show sightings that were left truncated.

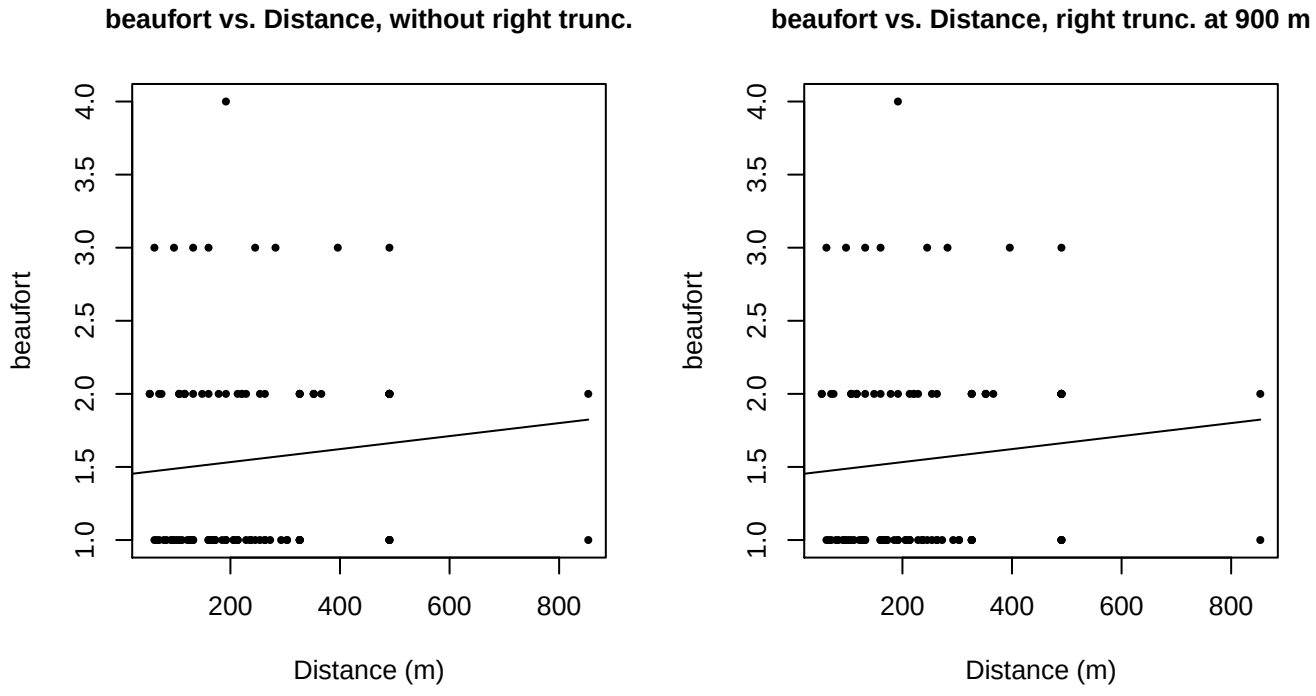

Figure 74: Scatterplots showing the relationship between Beaufort sea state and perpendicular sighting distance, for all sightings (left) and only those not right truncated (right). The line is a simple linear regression.

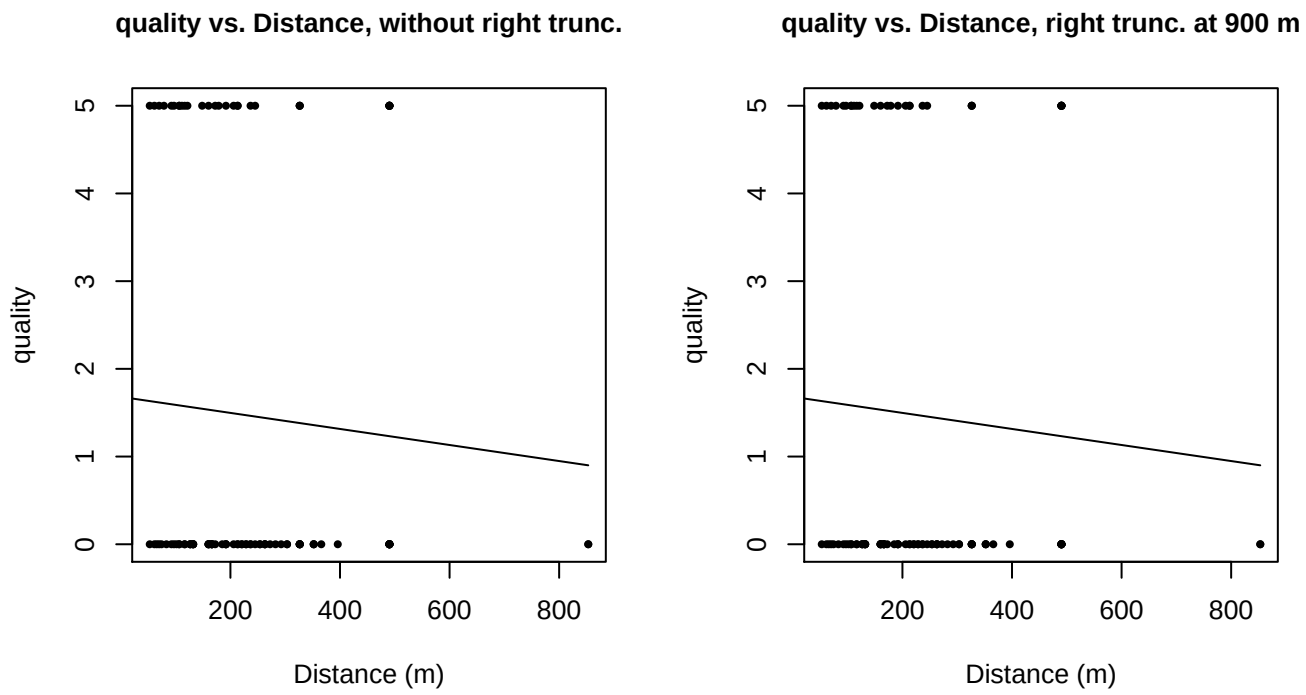

Figure 75: Scatterplots showing the relationship between the survey-specific index of the quality of observation conditions and perpendicular sighting distance, for all sightings (left) and only those not right truncated (right). Low values of the quality index correspond to better observation conditions. The line is a simple linear regression.

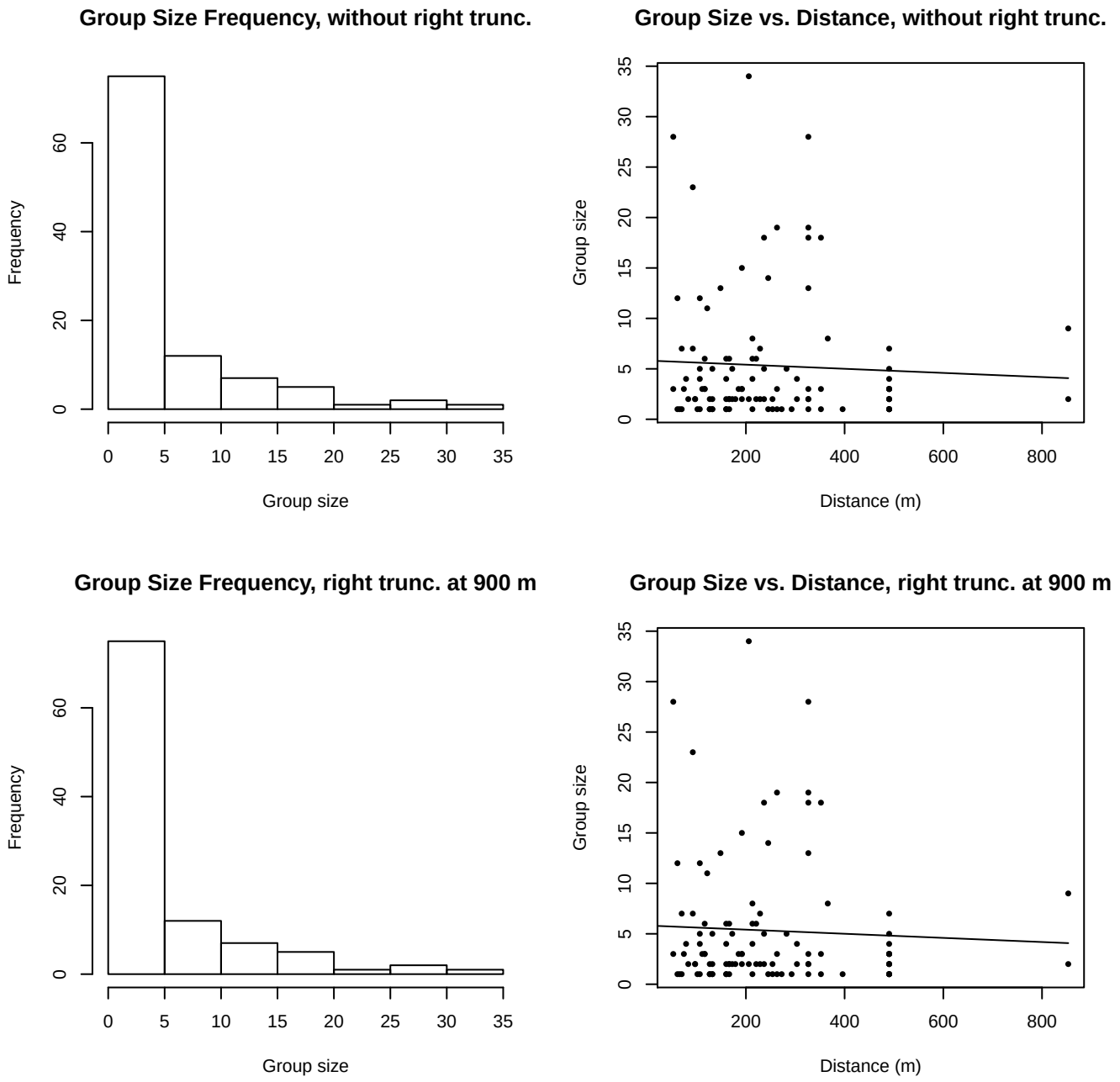

Figure 76: Histograms showing group size frequency and scatterplots showing the relationship between group size and perpendicular sighting distance, for all sightings (top row) and only those not right truncated (bottom row). In the scatterplot, the line is a simple linear regression.

Mid Atlantic Tursiops Survey 1995

The sightings were right truncated at 1296m. The vertical sighting angles were heaped at 10 degree increments, so the candidate detection functions were fitted using linear bins scaled accordingly.

Covariate	Description
beaufort	Beaufort sea state.
quality	Survey-specific index of the quality of observation conditions, utilizing relevant factors other than Beaufort sea state (see methods).

size	Estimated size (number of individuals) of the sighted group.

Table 42: Covariates tested in candidate "multi-covariate distance sampling" (MCDS) detection functions.

Key	Adjustment	Order	Covariates	Succeeded	Δ AIC	Mean ESHW (m)
hr				Yes	0.00	409
hr			quality	Yes	0.84	421
hr			size	Yes	1.65	413
hr	poly	4		Yes	1.99	410
hr	poly	2		Yes	1.99	410
hr			quality, size	Yes	2.75	421
hn	cos	2		Yes	3.02	325
hn			quality	Yes	5.93	386
hn				Yes	6.62	386
hn			quality, size	Yes	7.67	386
hn			size	Yes	7.83	386
hn	cos	3		Yes	8.46	369
hn	herm	4		Yes	8.59	386
hr			beaufort	No		
hn			beaufort	No		
hr			beaufort, quality	No		
hn			beaufort, quality	No		
hr			beaufort, size	No		
hn			beaufort, size	No		
hr			beaufort, quality, size	No		
hn			beaufort, quality, size	No		

Table 43: Candidate detection functions for Mid Atlantic Tursiops Survey 1995. The first one listed was selected for the density model.

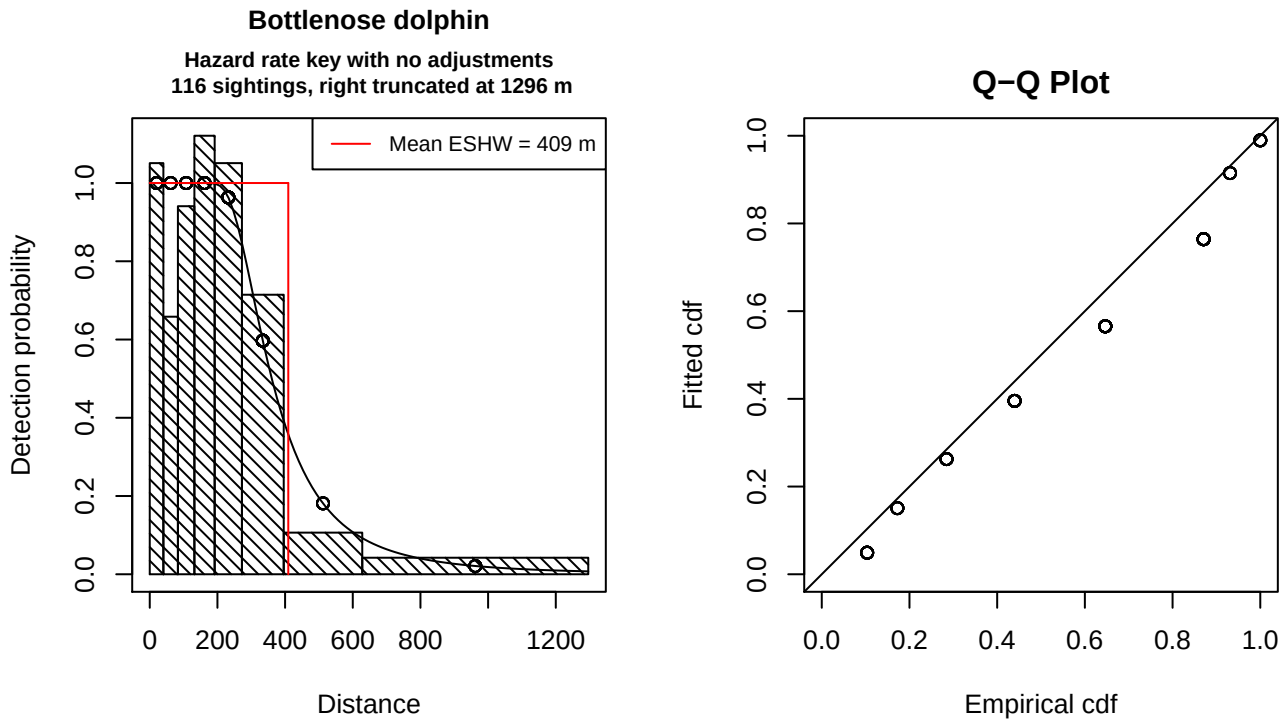

Figure 77: Detection function for Mid Atlantic Tursiops Survey 1995 that was selected for the density model

Statistical output for this detection function:

```
Summary for ds object
Number of observations :  116
Distance range         :  0  -  1296
AIC                    :  468.2075

Detection function:
 Hazard-rate key function

Detection function parameters
Scale Coefficients:
            estimate        se
(Intercept) 5.784778 0.1136719

Shape parameters:
            estimate        se
(Intercept) 1.266172 0.1583769

                       Estimate          SE         CV
Average p             0.3159489  0.02687407 0.08505826
N in covered region 367.1479370 42.07313491 0.11459450
```

Additional diagnostic plots:

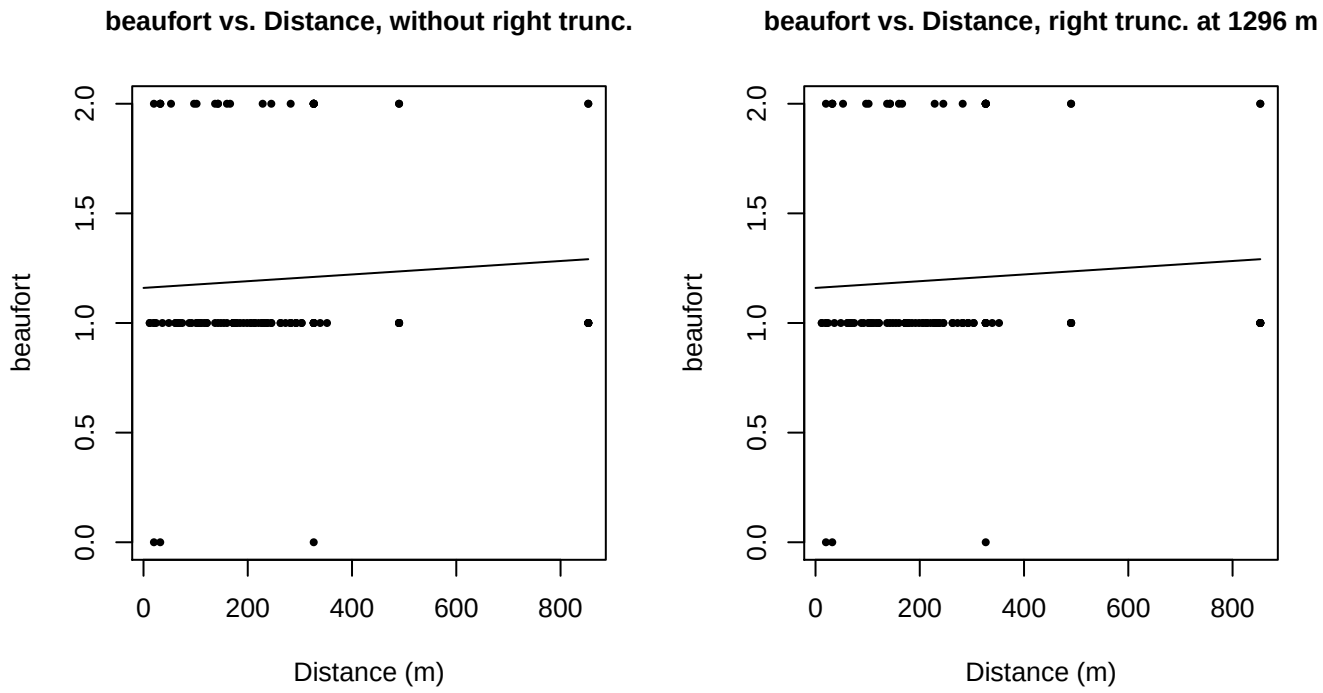

Figure 78: Scatterplots showing the relationship between Beaufort sea state and perpendicular sighting distance, for all sightings (left) and only those not right truncated (right). The line is a simple linear regression.

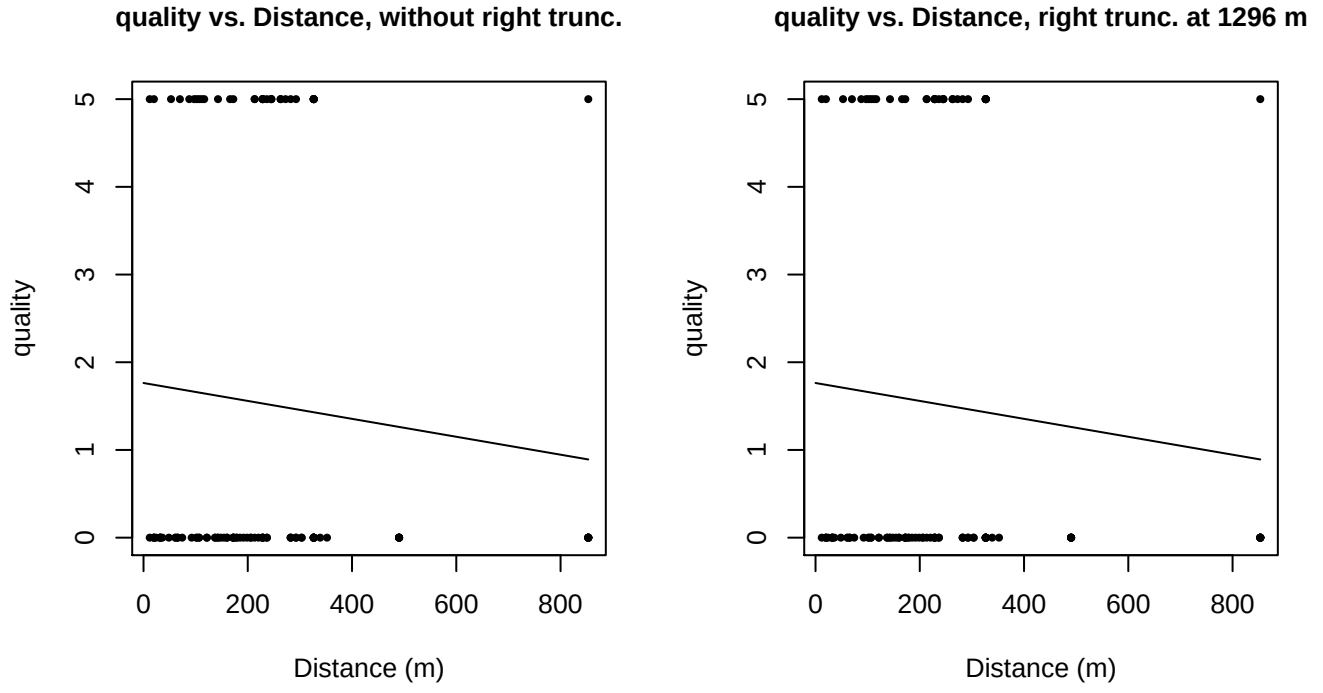

Figure 79: Scatterplots showing the relationship between the survey-specific index of the quality of observation conditions and perpendicular sighting distance, for all sightings (left) and only those not right truncated (right). Low values of the quality index correspond to better observation conditions. The line is a simple linear regression.

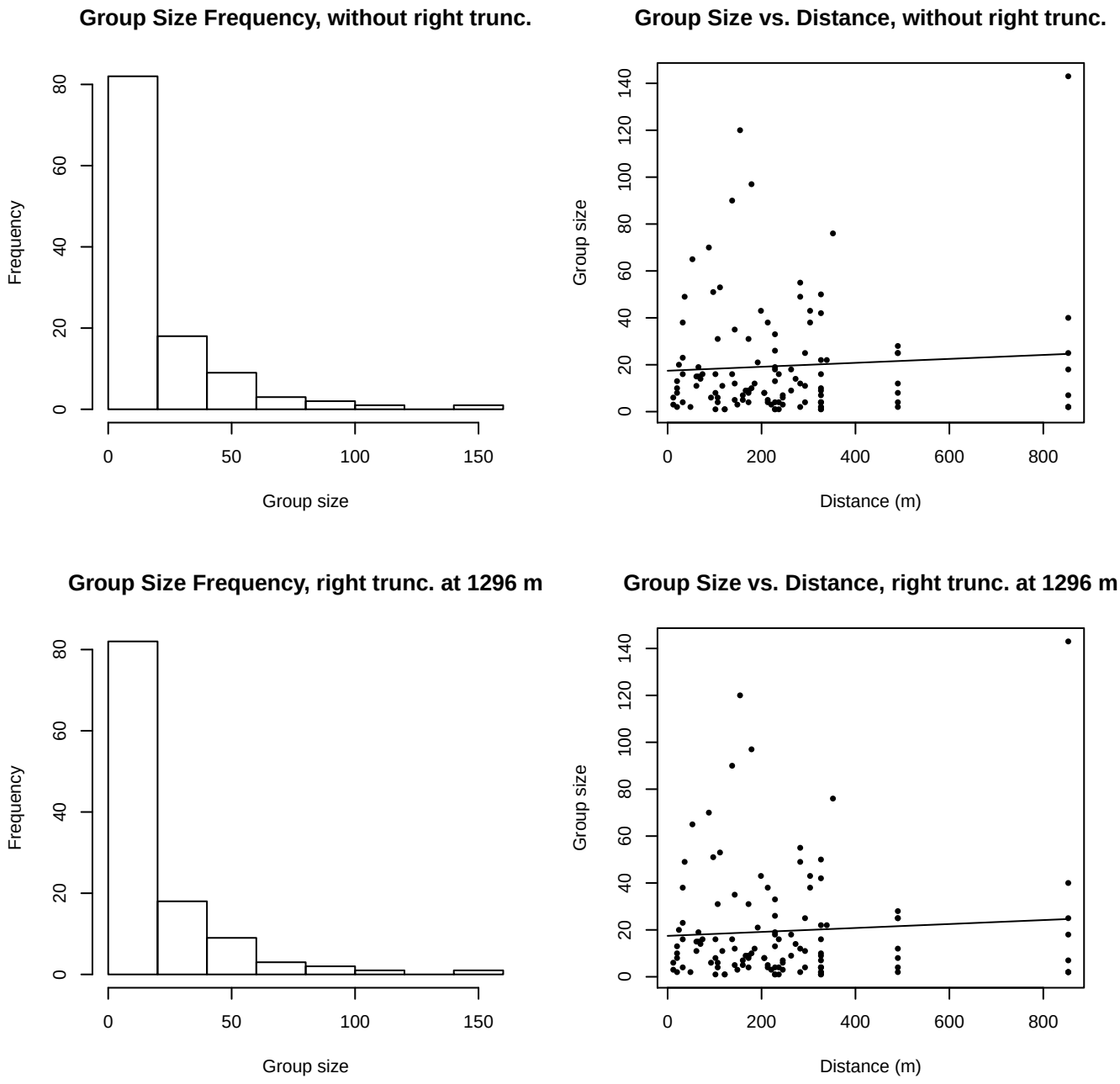

Figure 80: Histograms showing group size frequency and scatterplots showing the relationship between group size and perpendicular sighting distance, for all sightings (top row) and only those not right truncated (bottom row). In the scatterplot, the line is a simple linear regression.

GulfCet Aerial Surveys

The sightings were right truncated at 1296m. Due to a reduced frequency of sightings close to the trackline that plausibly resulted from the behavior of the observers and/or the configuration of the survey platform, the sightings were left truncted as well. Sightings closer than 40 m to the trackline were omitted from the analysis, and it was assumed that the the area closer to the trackline than this was not surveyed. This distance was estimated by inspecting histograms of perpendicular sighting distances. The vertical sighting angles were heaped at 10 degree increments, so the candidate detection functions were fitted using linear bins scaled accordingly.

Covariate	Description

beaufort	Beaufort sea state.
quality	Survey-specific index of the quality of observation conditions, utilizing relevant factors other than Beaufort sea state (see methods).
size	Estimated size (number of individuals) of the sighted group.

Table 44: Covariates tested in candidate "multi-covariate distance sampling" (MCDS) detection functions.

Key	Adjustment	Order	Covariates	Succeeded	Δ AIC	Mean ESHW (m)
hr			size	Yes	0.00	346
hn	cos	2		Yes	0.95	318
hr				Yes	1.73	333
hn	cos	3		Yes	3.66	278
hr	poly	2		Yes	3.73	333
hr	poly	4		Yes	4.20	317
hn			size	Yes	17.33	405
hn				Yes	21.19	404
hn	herm	4		Yes	23.06	404
hr			beaufort	No		
hn			beaufort	No		
hr			quality	No		
hn			quality	No		
hr			beaufort, quality	No		
hn			beaufort, quality	No		
hr			beaufort, size	No		
hn			beaufort, size	No		
hr			quality, size	No		
hn			quality, size	No		
hr			beaufort, quality, size	No		
hn			beaufort, quality, size	No		

Table 45: Candidate detection functions for GulfCet Aerial Surveys. The first one listed was selected for the density model.

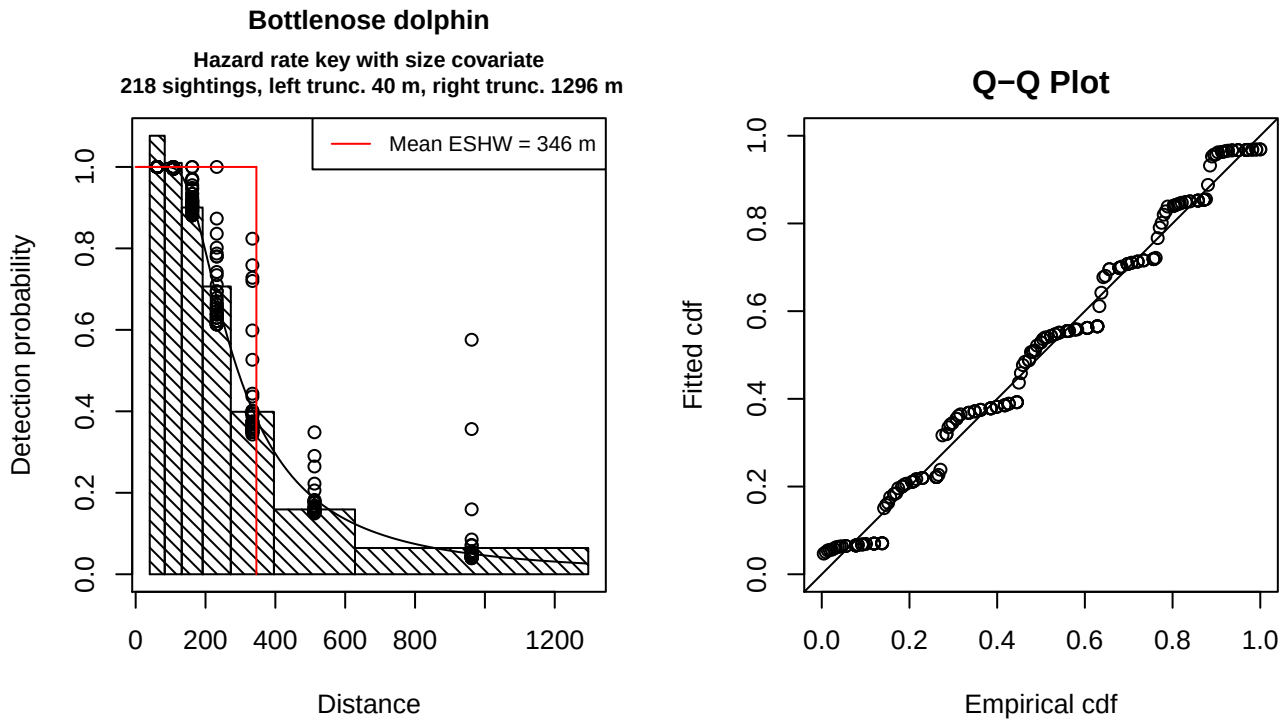

Figure 81: Detection function for GulfCet Aerial Surveys that was selected for the density model

Statistical output for this detection function:

```
Summary for ds object
Number of observations :  218
Distance range         :  40.30835  -  1296
AIC                    :  847.2577

Detection function:
 Hazard-rate key function

Detection function parameters
Scale Coefficients:
             estimate         se
(Intercept) 5.4148062 0.15146942
size        0.1832565 0.08934361

Shape parameters:
             estimate        se
(Intercept) 0.8065024 0.1166782

                       Estimate          SE        CV
Average p              0.2589319  0.02618002 0.1011078
N in covered region 841.9203026 98.39311604 0.1168675
```

Additional diagnostic plots:

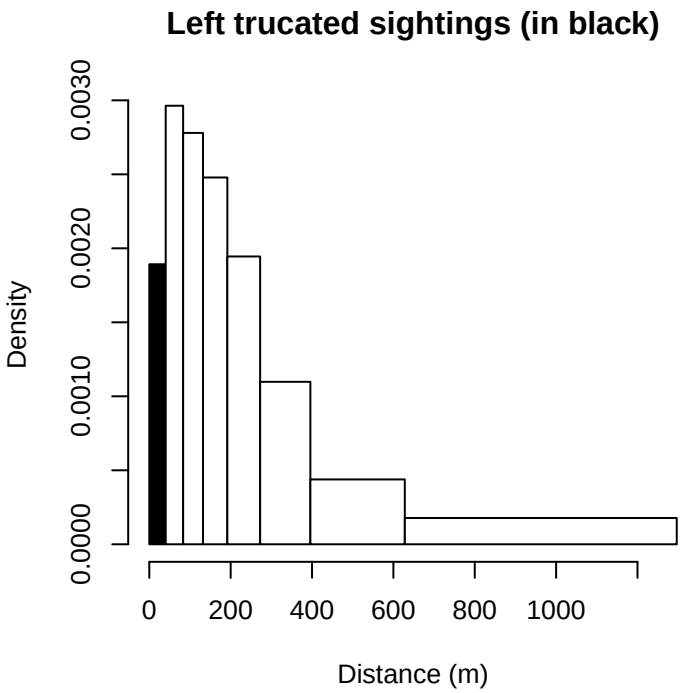

Figure 82: Density of sightings by perpendicular distance for GulfCet Aerial Surveys. Black bars on the left show sightings that were left truncated.

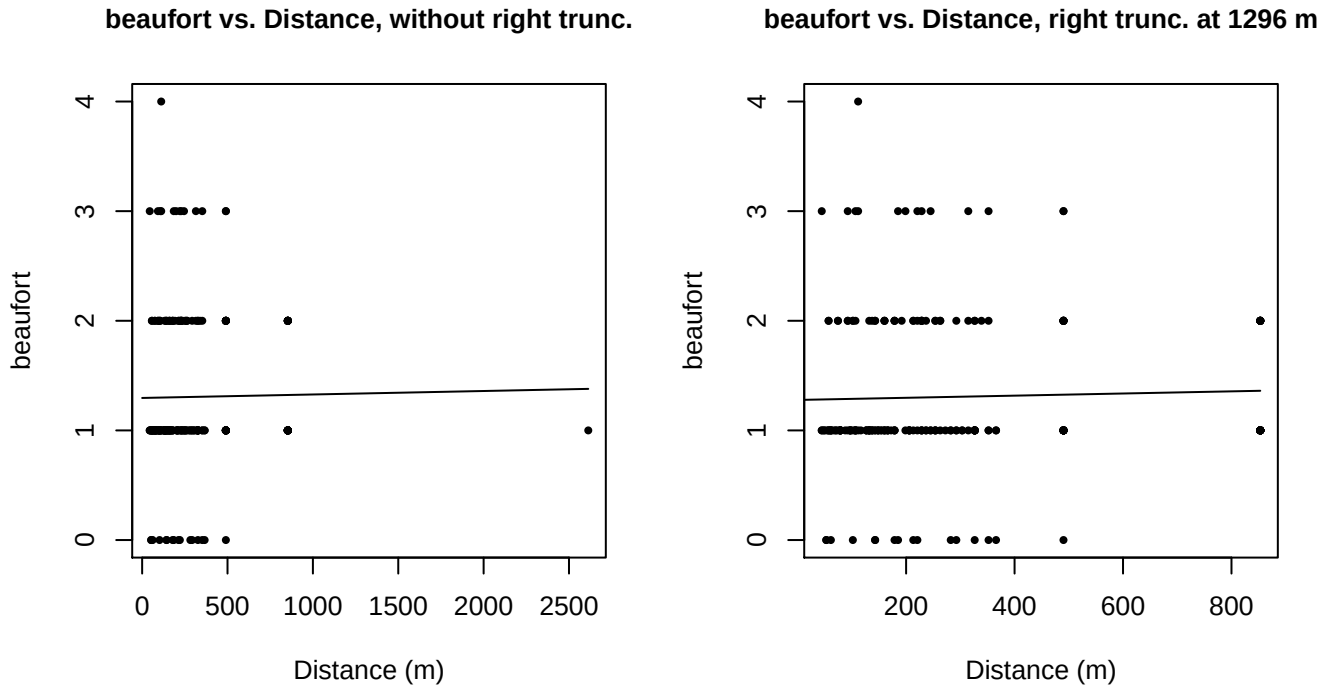

Figure 83: Scatterplots showing the relationship between Beaufort sea state and perpendicular sighting distance, for all sightings (left) and only those not right truncated (right). The line is a simple linear regression.

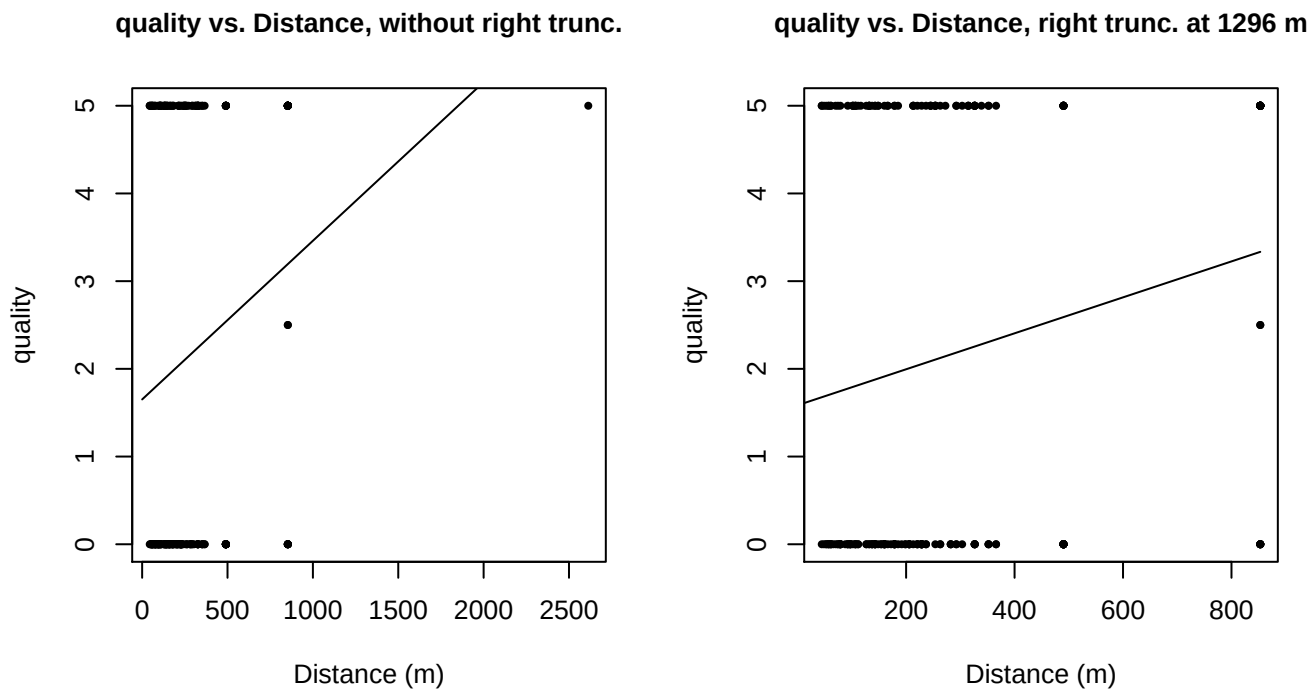

Figure 84: Scatterplots showing the relationship between the survey-specific index of the quality of observation conditions and perpendicular sighting distance, for all sightings (left) and only those not right truncated (right). Low values of the quality index correspond to better observation conditions. The line is a simple linear regression.

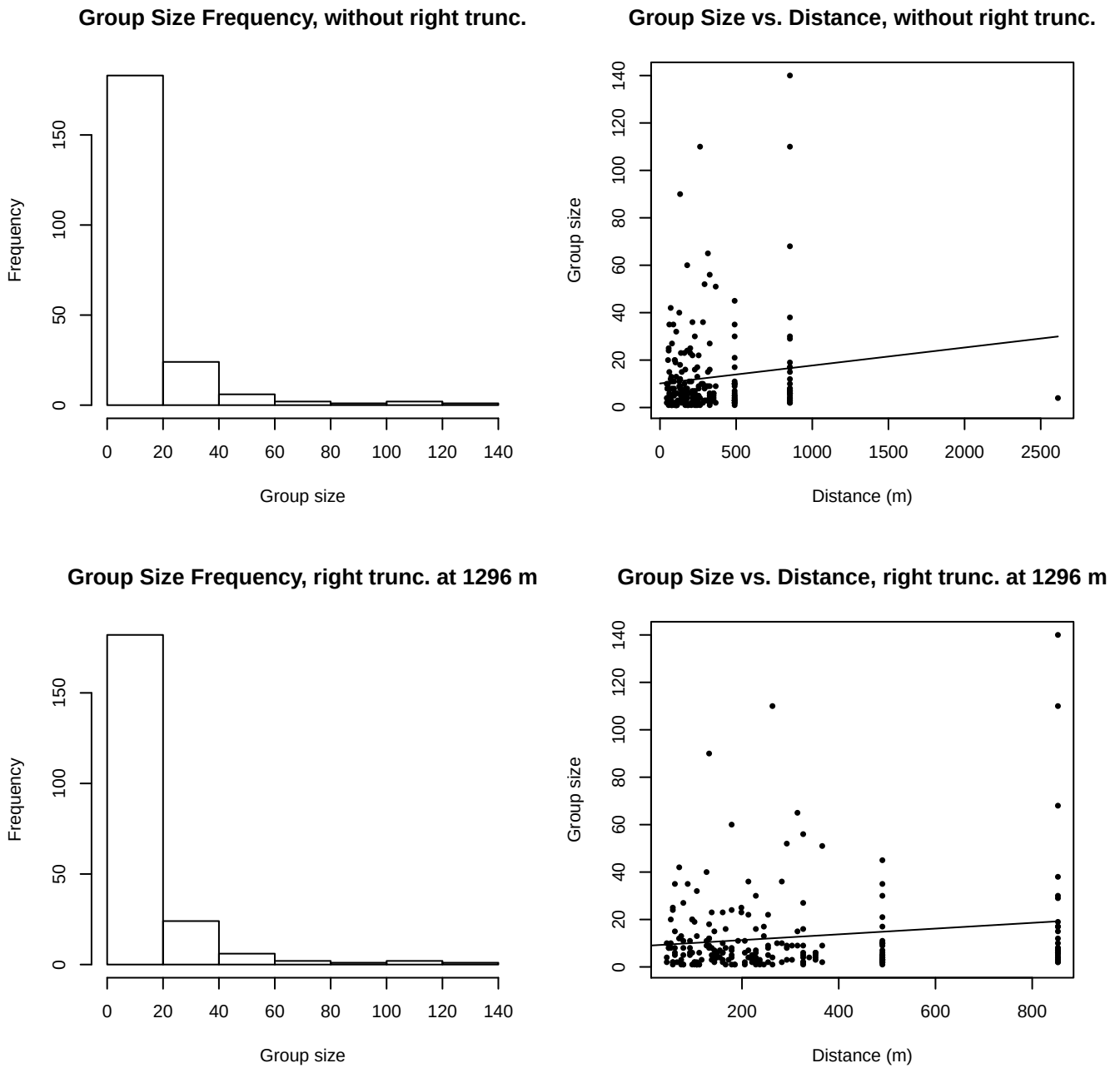

Figure 85: Histograms showing group size frequency and scatterplots showing the relationship between group size and perpendicular sighting distance, for all sightings (top row) and only those not right truncated (bottom row). In the scatterplot, the line is a simple linear regression.

GOMEX92-96 Aerial Survey

The sightings were right truncated at 1296m. Due to a reduced frequency of sightings close to the trackline that plausibly resulted from the behavior of the observers and/or the configuration of the survey platform, the sightings were left truncted as well. Sightings closer than 83 m to the trackline were omitted from the analysis, and it was assumed that the the area closer to the trackline than this was not surveyed. This distance was estimated by inspecting histograms of perpendicular sighting distances. The vertical sighting angles were heaped at 10 degree increments, so the candidate detection functions were fitted using linear bins scaled accordingly.

Covariate	Description

beaufort	Beaufort sea state.
quality	Survey-specific index of the quality of observation conditions, utilizing relevant factors other than Beaufort sea state (see methods).
size	Estimated size (number of individuals) of the sighted group.

Table 46: Covariates tested in candidate "multi-covariate distance sampling" (MCDS) detection functions.

Key	Adjustment	Order	Covariates	Succeeded	Δ AIC	Mean ESHW (m)
hr			size	Yes	0.00	280
hr				Yes	2.38	278
hn	cos	3		Yes	3.71	219
hr	poly	4		Yes	4.39	278
hr	poly	2		Yes	4.39	278
hn	cos	2		Yes	9.94	258
hn			size	Yes	40.32	306
hn				Yes	42.06	306
hn	herm	4		Yes	43.81	306
hr			beaufort	No		
hn			beaufort	No		
hr			quality	No		
hn			quality	No		
hr			beaufort, quality	No		
hn			beaufort, quality	No		
hr			beaufort, size	No		
hn			beaufort, size	No		
hr			quality, size	No		
hn			quality, size	No		
hr			beaufort, quality, size	No		
hn			beaufort, quality, size	No		

Table 47: Candidate detection functions for GOMEX92-96 Aerial Survey. The first one listed was selected for the density model.

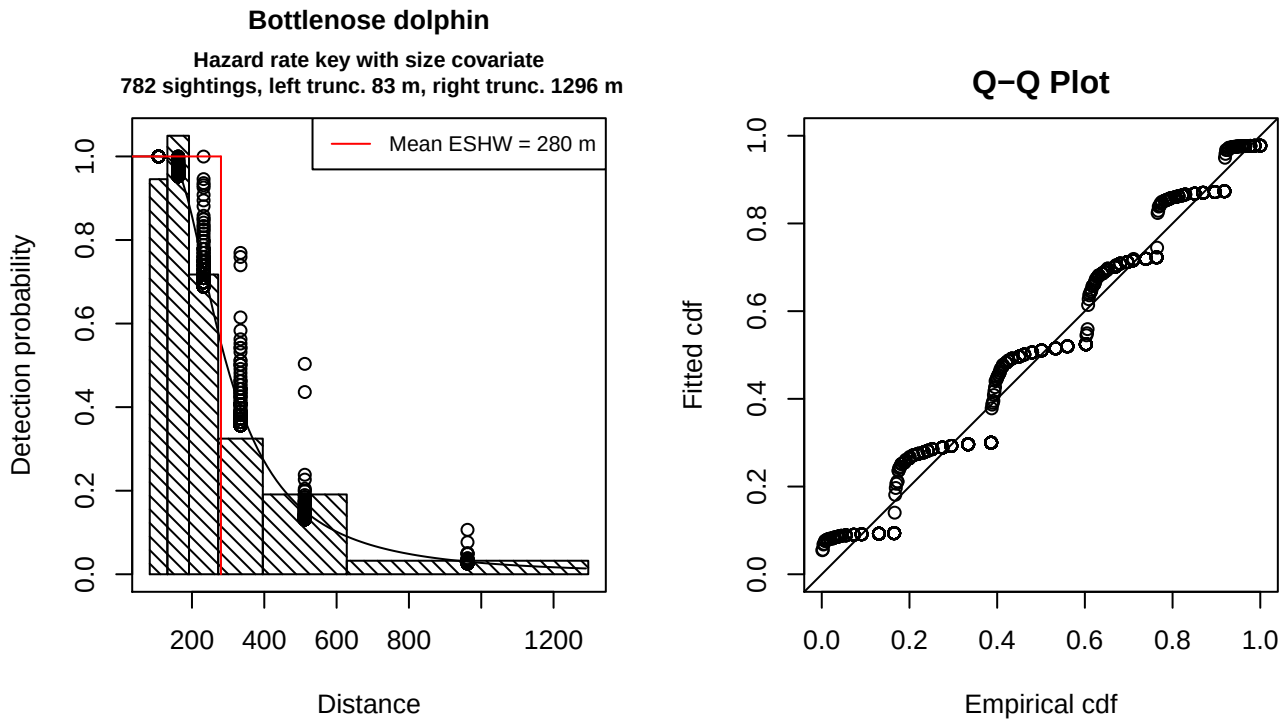

Figure 86: Detection function for GOMEX92-96 Aerial Survey that was selected for the density model

Statistical output for this detection function:

```
Summary for ds object
Number of observations :  782
Distance range         :  83.2036  -  1296
AIC                    :  2744.589

Detection function:
 Hazard-rate key function

Detection function parameters
Scale Coefficients:
             estimate         se
(Intercept) 5.49389431 0.06866783
size        0.08363174 0.03816366

Shape parameters:
             estimate         se
(Intercept) 0.9827602 0.05937892

                        Estimate           SE         CV
Average p              0.2140879   0.01175494 0.05490705
N in covered region 3652.7045766 231.66521158 0.06342293
```

Additional diagnostic plots:

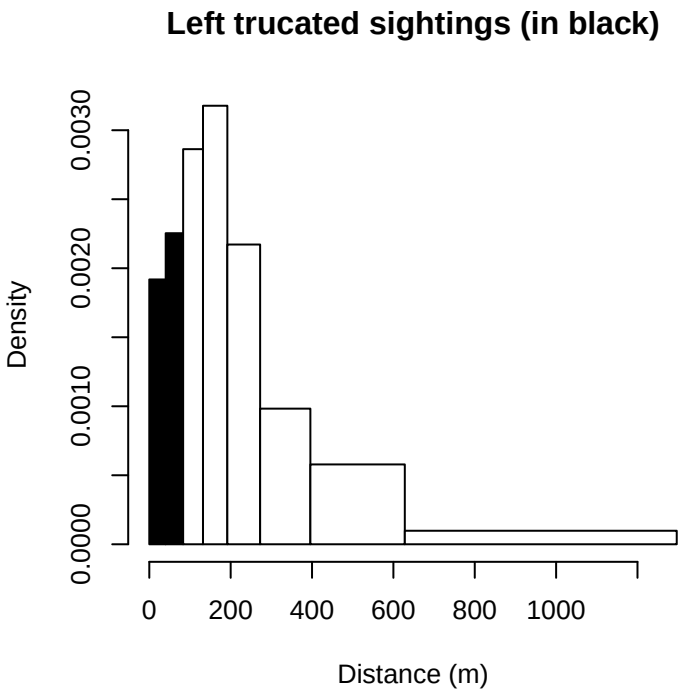

Figure 87: Density of sightings by perpendicular distance for GOMEX92-96 Aerial Survey. Black bars on the left show sightings that were left truncated.

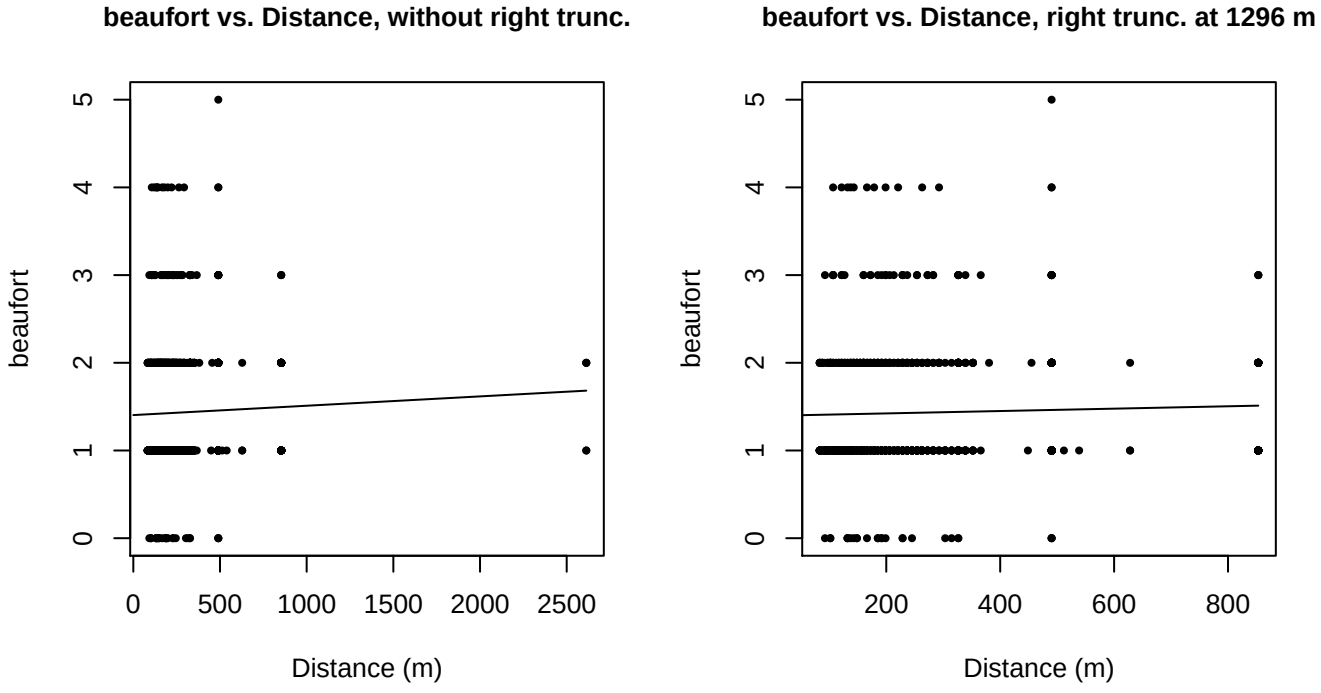

Figure 88: Scatterplots showing the relationship between Beaufort sea state and perpendicular sighting distance, for all sightings (left) and only those not right truncated (right). The line is a simple linear regression.

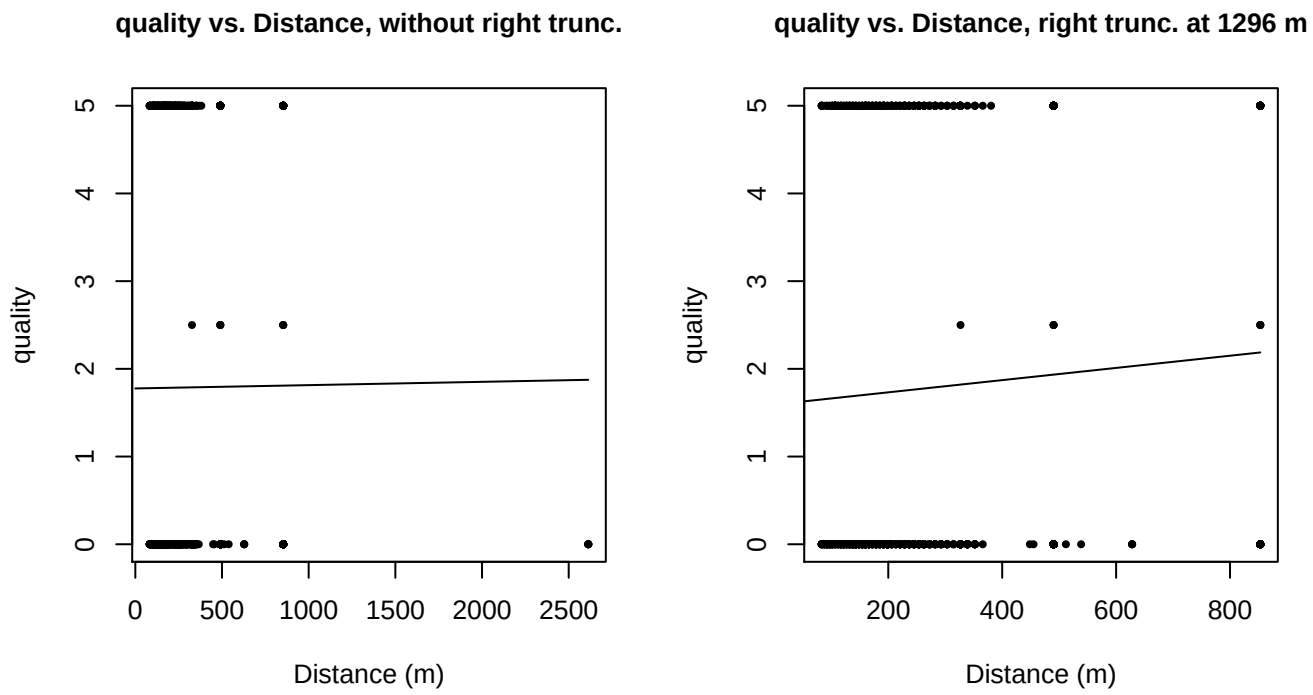

Figure 89: Scatterplots showing the relationship between the survey-specific index of the quality of observation conditions and perpendicular sighting distance, for all sightings (left) and only those not right truncated (right). Low values of the quality index correspond to better observation conditions. The line is a simple linear regression.

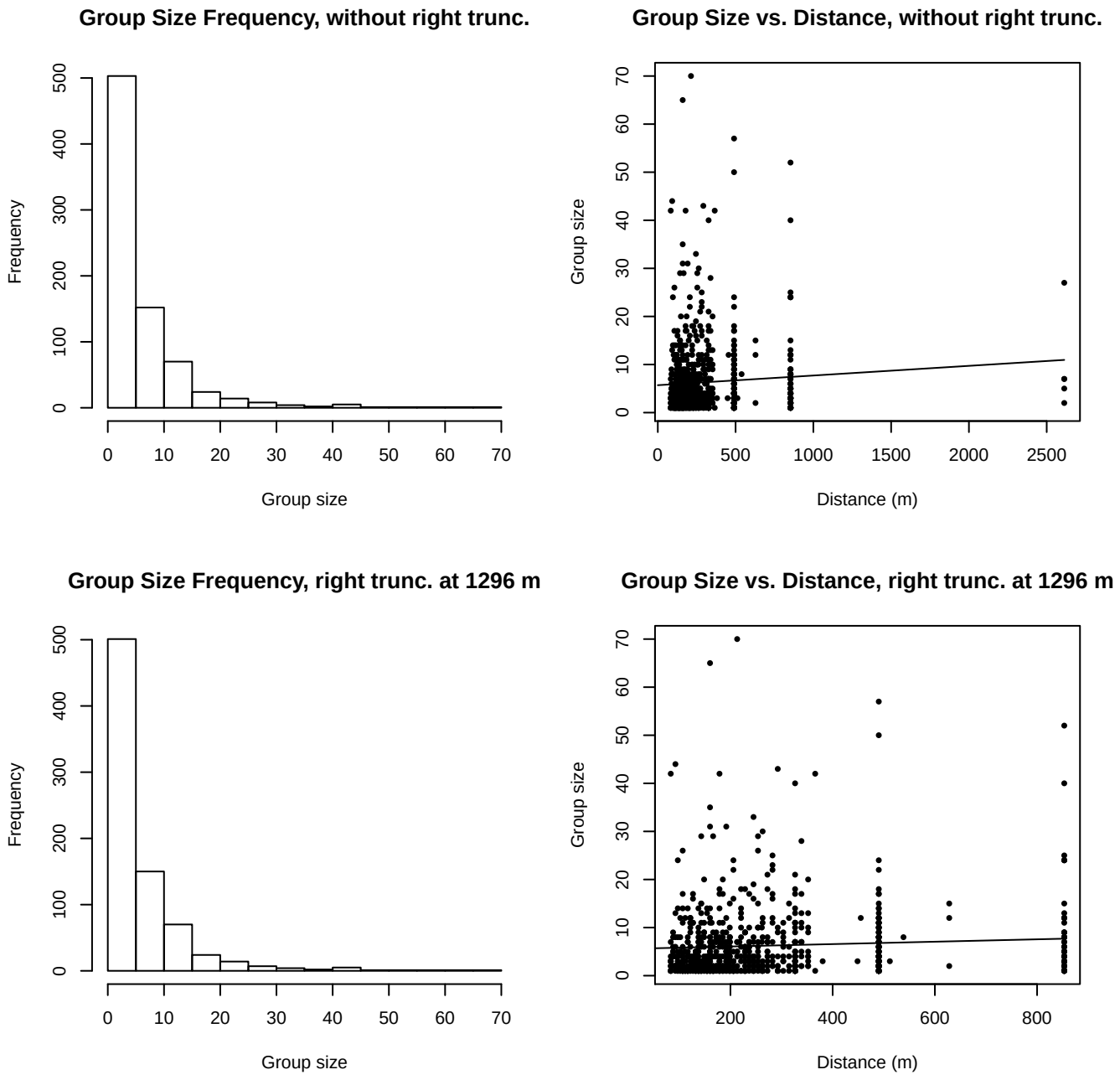

Figure 90: Histograms showing group size frequency and scatterplots showing the relationship between group size and perpendicular sighting distance, for all sightings (top row) and only those not right truncated (bottom row). In the scatterplot, the line is a simple linear regression.

UNCW Navy Surveys

The sightings were right truncated at 2000m.

Covariate	Description
beaufort	Beaufort sea state.
quality	Survey-specific index of the quality of observation conditions, utilizing relevant factors other than Beaufort sea state (see methods).
size	Estimated size (number of individuals) of the sighted group.

Table 48: Covariates tested in candidate "multi-covariate distance sampling" (MCDS) detection functions.

Key	Adjustment	Order	Covariates	Succeeded	Δ AIC	Mean ESHW (m)
hn			quality, size	Yes	0.00	760
hn			size	Yes	1.11	761
hn			beaufort, quality, size	Yes	1.62	761
hn			quality	Yes	2.55	760
hn	cos	2		Yes	2.64	817
hn	cos	3		Yes	2.65	833
hn			beaufort, size	Yes	2.81	761
hn	herm	4		Yes	3.13	811
hn				Yes	3.20	761
hr			quality, size	Yes	3.45	922
hn			beaufort, quality	Yes	4.45	761
hr			size	Yes	4.86	917
hn			beaufort	Yes	5.12	761
hr			beaufort, quality, size	Yes	5.42	924
hr	poly	4		Yes	7.25	894
hr			quality	Yes	7.69	916
hr				Yes	8.84	915
hr	poly	2		Yes	10.84	915
hr			beaufort	No		
hr			beaufort, quality	No		
hr			beaufort, size	No		

Table 49: Candidate detection functions for UNCW Navy Surveys. The first one listed was selected for the density model.

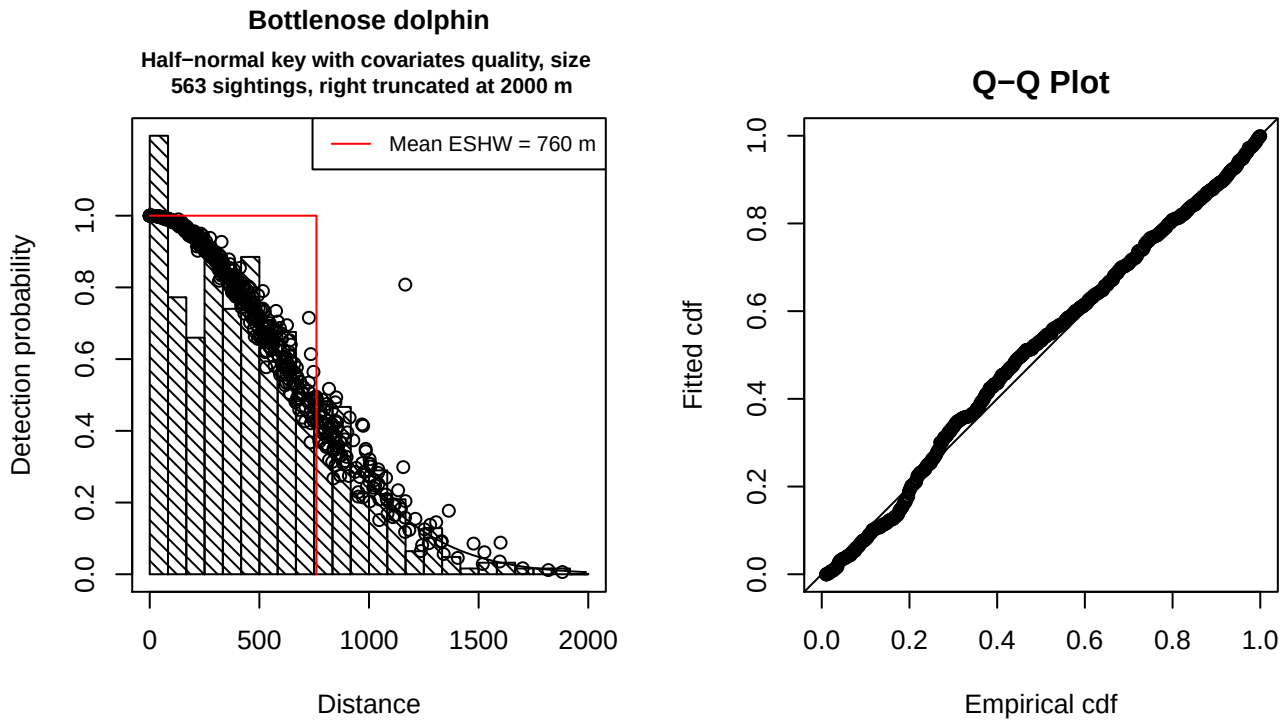

Figure 91: Detection function for UNCW Navy Surveys that was selected for the density model

Statistical output for this detection function:

```
Summary for ds object
Number of observations :  563
Distance range         :  0  -  2000
AIC                    :  8025.939

Detection function:
 Half-normal key function

Detection function parameters
Scale Coefficients:
               estimate         se
(Intercept)  6.40208533 0.06036240
quality     -0.04566216 0.02815651
size         0.07518915 0.04901212

                        Estimate         SE         CV
Average p              0.3774783  0.0121131 0.03208952
N in covered region 1491.4765306 69.0011376 0.04626364
```

Additional diagnostic plots:

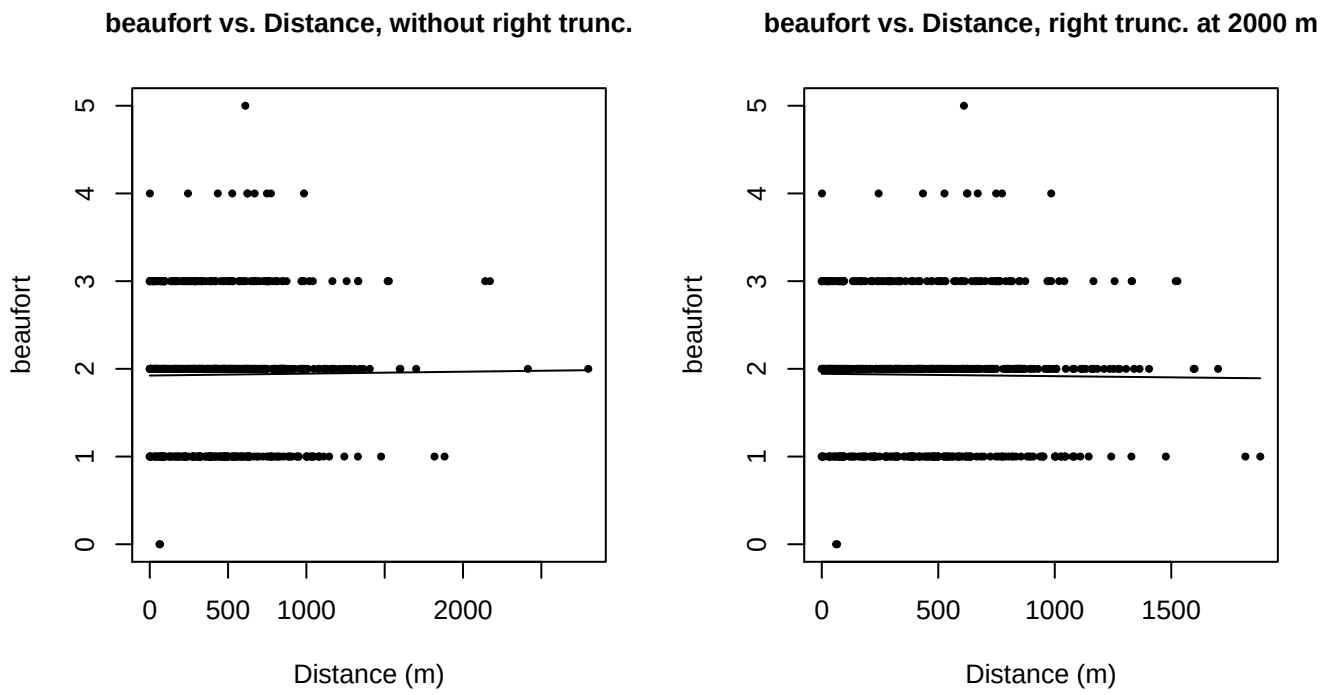

Figure 92: Scatterplots showing the relationship between Beaufort sea state and perpendicular sighting distance, for all sightings (left) and only those not right truncated (right). The line is a simple linear regression.

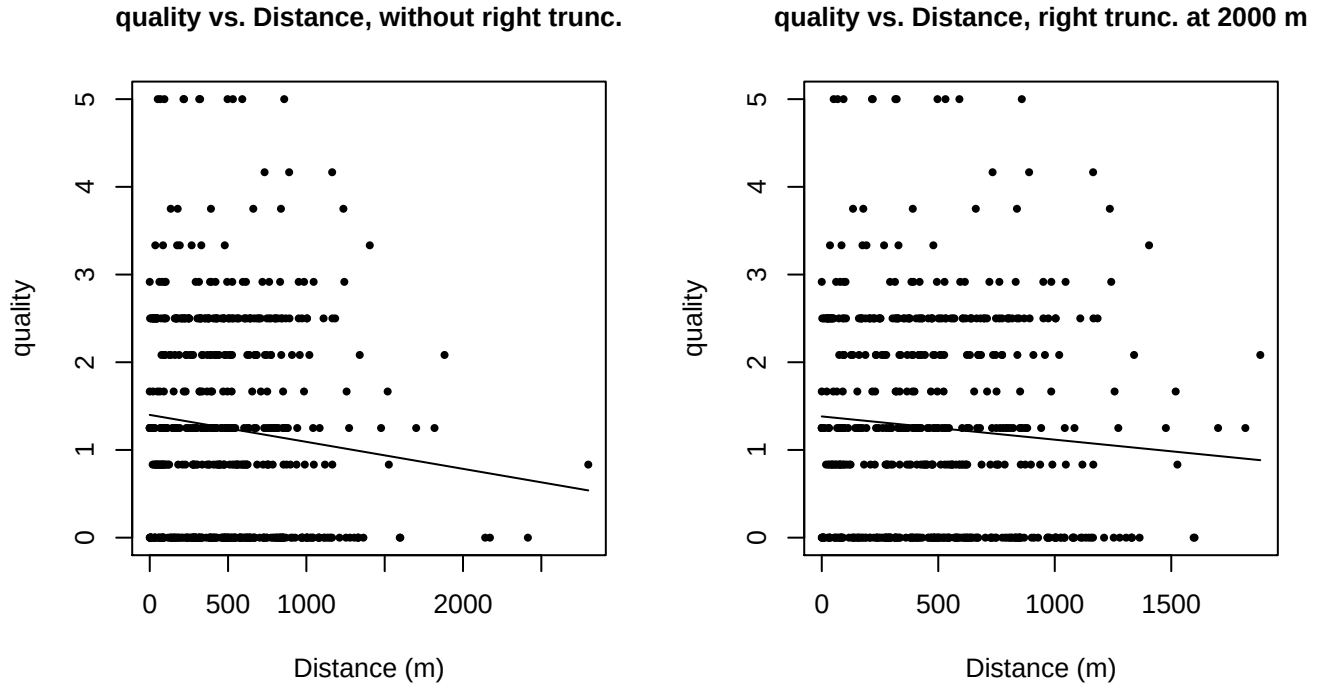

Figure 93: Scatterplots showing the relationship between the survey-specific index of the quality of observation conditions and perpendicular sighting distance, for all sightings (left) and only those not right truncated (right). Low values of the quality index correspond to better observation conditions. The line is a simple linear regression.

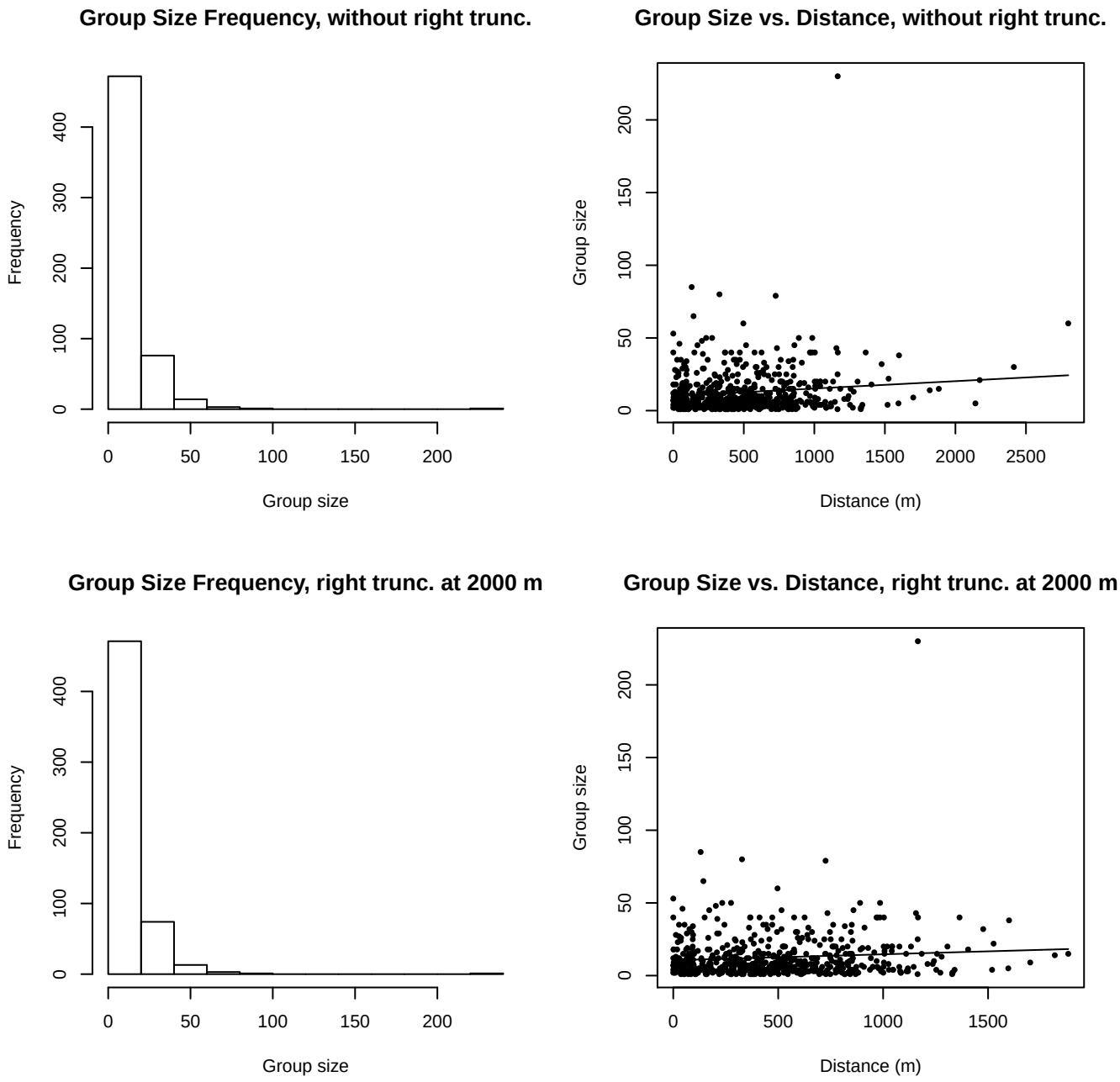

Figure 94: Histograms showing group size frequency and scatterplots showing the relationship between group size and perpendicular sighting distance, for all sightings (top row) and only those not right truncated (bottom row). In the scatterplot, the line is a simple linear regression.

UNCW Right Whale Surveys

The sightings were right truncated at 837m. Due to a reduced frequency of sightings close to the trackline that plausibly resulted from the behavior of the observers and/or the configuration of the survey platform, the sightings were left truncted as well. Sightings closer than 111 m to the trackline were omitted from the analysis, and it was assumed that the the area closer to the trackline than this was not surveyed. This distance was estimated by inspecting histograms of perpendicular sighting distances. The vertical sighting angles were heaped at 10 degree increments, so the candidate detection functions were fitted using linear bins scaled accordingly.

Covariate	Description

beaufort	Beaufort sea state.
quality	Survey-specific index of the quality of observation conditions, utilizing relevant factors other than Beaufort sea state (see methods).
size	Estimated size (number of individuals) of the sighted group.

Table 50: Covariates tested in candidate "multi-covariate distance sampling" (MCDS) detection functions.

Key	Adjustment	Order	Covariates	Succeeded	Δ AIC	Mean ESHW (m)
hr			beaufort	Yes	0.00	162
hr			beaufort, size	Yes	1.47	162
hr				Yes	2.85	161
hr	poly	2		Yes	4.85	161
hr	poly	4		Yes	4.85	161
hn	cos	2		Yes	62.07	87
hn	cos	3		Yes	78.34	117
hn	herm	4		Yes	79.92	103
hn				No		
hn			beaufort	No		
hn			quality	No		
hr			quality	No		
hn			size	No		
hr			size	No		
hn			beaufort, quality	No		
hr			beaufort, quality	No		
hn			beaufort, size	No		
hn			quality, size	No		
hr			quality, size	No		
hn			beaufort, quality, size	No		
hr			beaufort, quality, size	No		

Table 51: Candidate detection functions for UNCW Right Whale Surveys. The first one listed was selected for the density model.

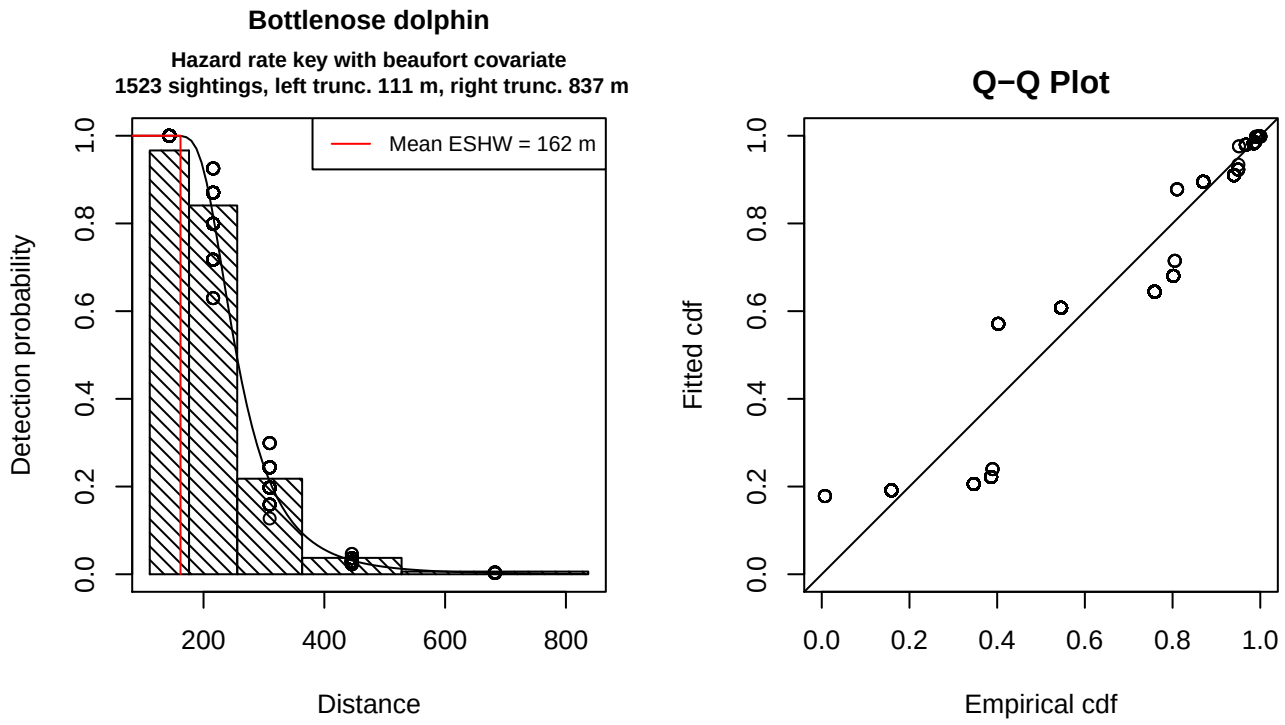

Figure 95: Detection function for UNCW Right Whale Surveys that was selected for the density model

Statistical output for this detection function:

```
Summary for ds object
Number of observations :  1523
Distance range         :  110.9381  -  837
AIC                    :  3630.412

Detection function:
 Hazard-rate key function

Detection function parameters
Scale Coefficients:
               estimate         se
(Intercept)  5.54751034 0.04112313
beaufort    -0.04349683 0.02080092

Shape parameters:
            estimate         se
(Intercept) 1.707925 0.04354036

                         Estimate           SE         CV
Average p               0.1928607 5.519347e-03 0.02861831
N in covered region 7896.8913338 2.900774e+02 0.03673311
```

Additional diagnostic plots:

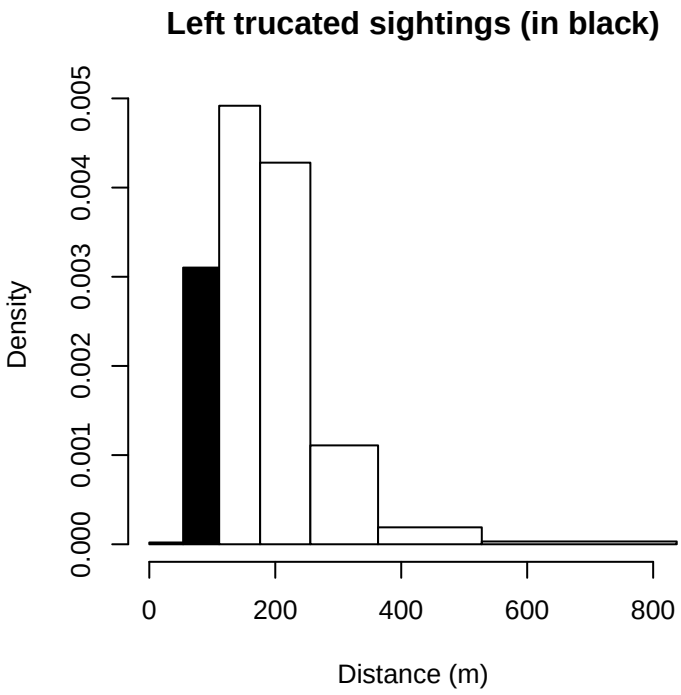

Figure 96: Density of sightings by perpendicular distance for UNCW Right Whale Surveys. Black bars on the left show sightings that were left truncated.

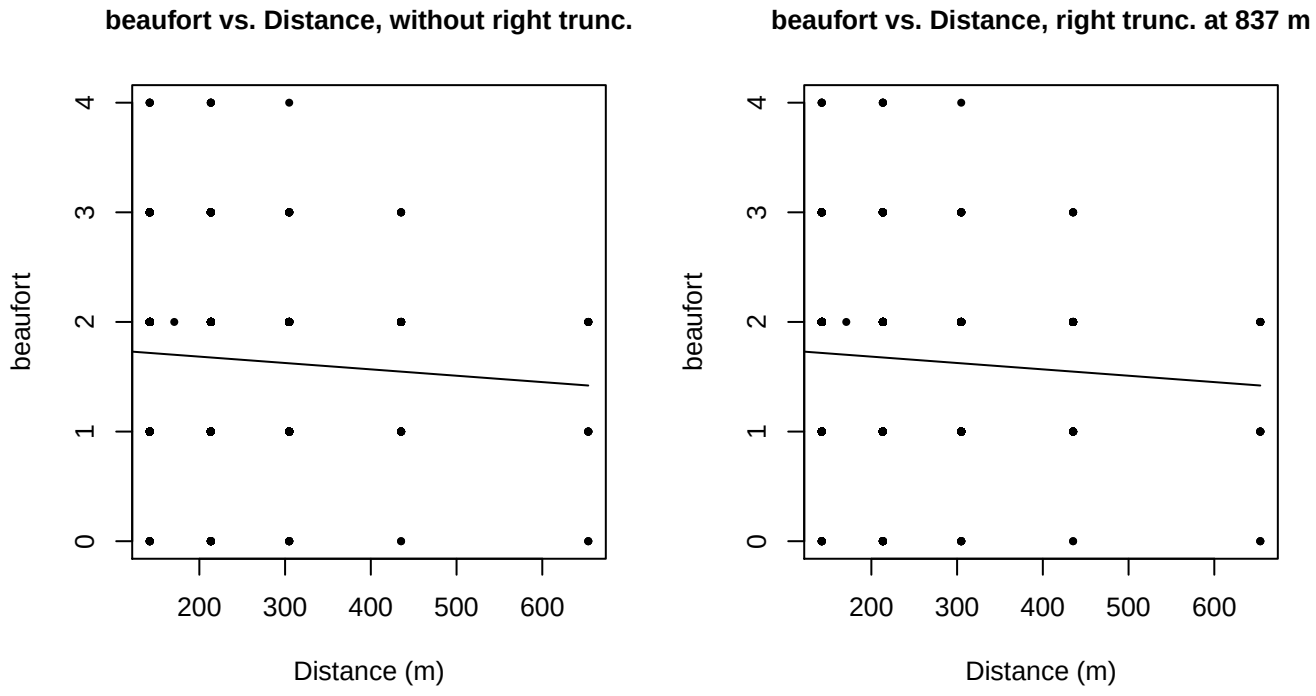

Figure 97: Scatterplots showing the relationship between Beaufort sea state and perpendicular sighting distance, for all sightings (left) and only those not right truncated (right). The line is a simple linear regression.

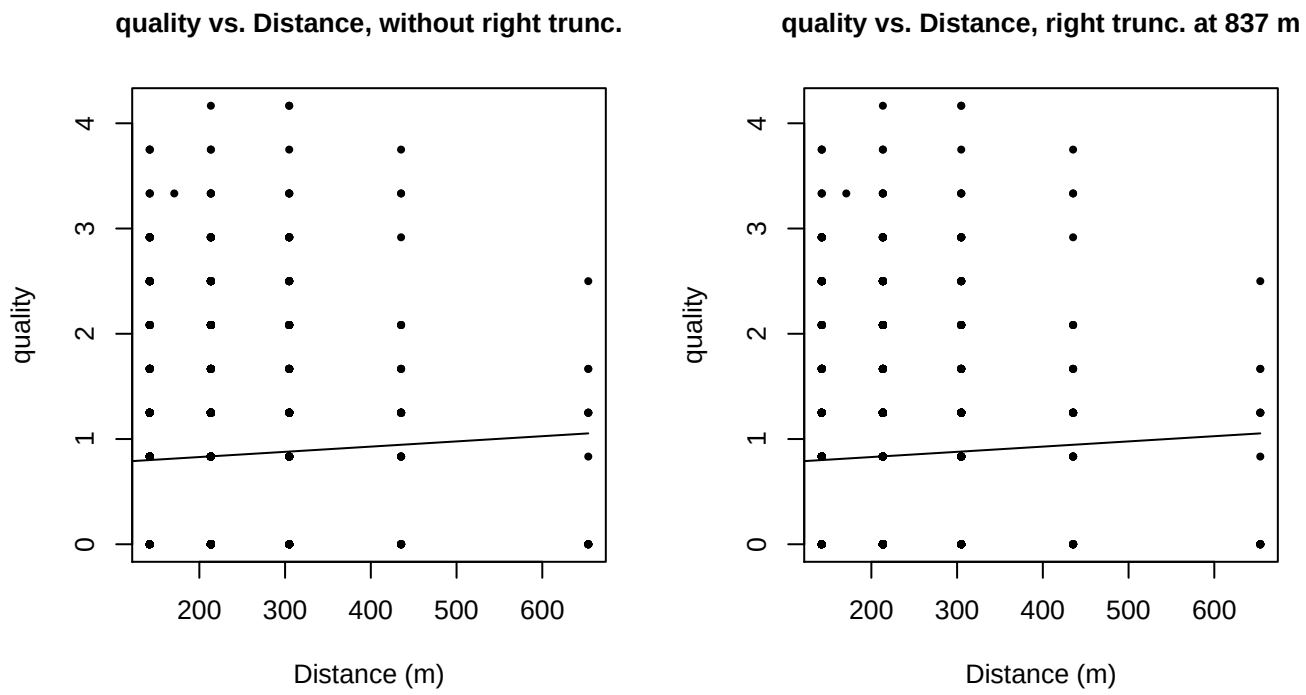

Figure 98: Scatterplots showing the relationship between the survey-specific index of the quality of observation conditions and perpendicular sighting distance, for all sightings (left) and only those not right truncated (right). Low values of the quality index correspond to better observation conditions. The line is a simple linear regression.

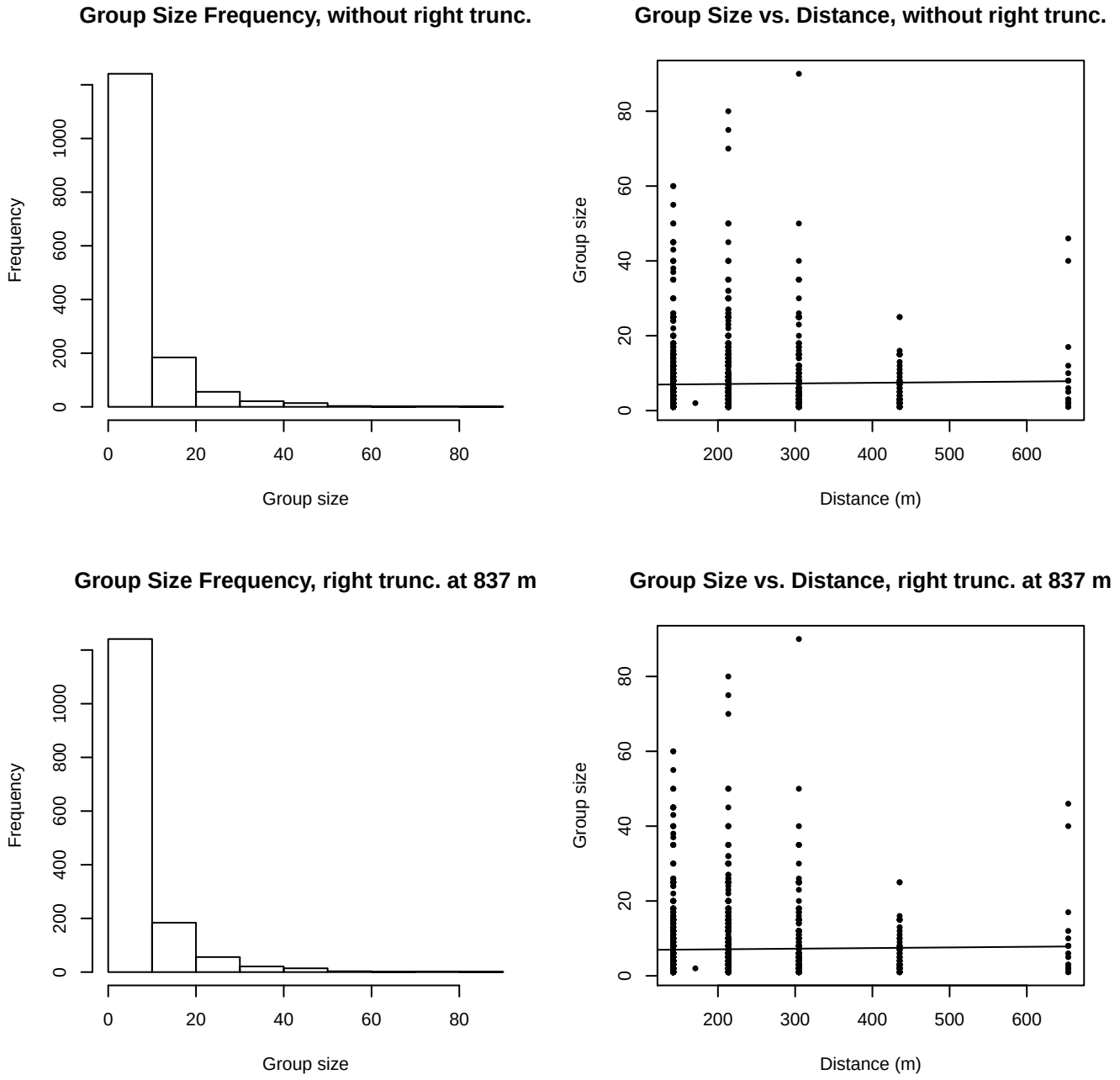

Figure 99: Histograms showing group size frequency and scatterplots showing the relationship between group size and perpendicular sighting distance, for all sightings (top row) and only those not right truncated (bottom row). In the scatterplot, the line is a simple linear regression.

UNCW Early Surveys

The sightings were right truncated at 397m. Due to a reduced frequency of sightings close to the trackline that plausibly resulted from the behavior of the observers and/or the configuration of the survey platform, the sightings were left truncted as well. Sightings closer than 13 m to the trackline were omitted from the analysis, and it was assumed that the the area closer to the trackline than this was not surveyed. This distance was estimated by inspecting histograms of perpendicular sighting distances.

Covariate	Description

beaufort	Beaufort sea state.
quality	Survey-specific index of the quality of observation conditions, utilizing relevant factors other than Beaufort sea state (see methods).
size	Estimated size (number of individuals) of the sighted group.

Table 52: Covariates tested in candidate "multi-covariate distance sampling" (MCDS) detection functions.

Key	Adjustment	Order	Covariates	Succeeded	Δ AIC	Mean ESHW (m)
hn			beaufort	Yes	0.00	152
hn	herm	4		Yes	0.77	171
hn	cos	2		Yes	1.55	172
hn				Yes	2.43	152
hn			quality	Yes	4.34	152
hn	cos	3		Yes	4.37	155
hr			beaufort	Yes	5.13	200
hr				Yes	12.32	195
hr			quality	Yes	14.22	194
hr	poly	2		Yes	14.41	194
hr	poly	4		No		
hr			size	No		
hn			size	No		
hr			beaufort, quality	No		
hn			beaufort, quality	No		
hr			beaufort, size	No		
hn			beaufort, size	No		
hr			quality, size	No		
hn			quality, size	No		
hr			beaufort, quality, size	No		
hn			beaufort, quality, size	No		

Table 53: Candidate detection functions for UNCW Early Surveys. The first one listed was selected for the density model.

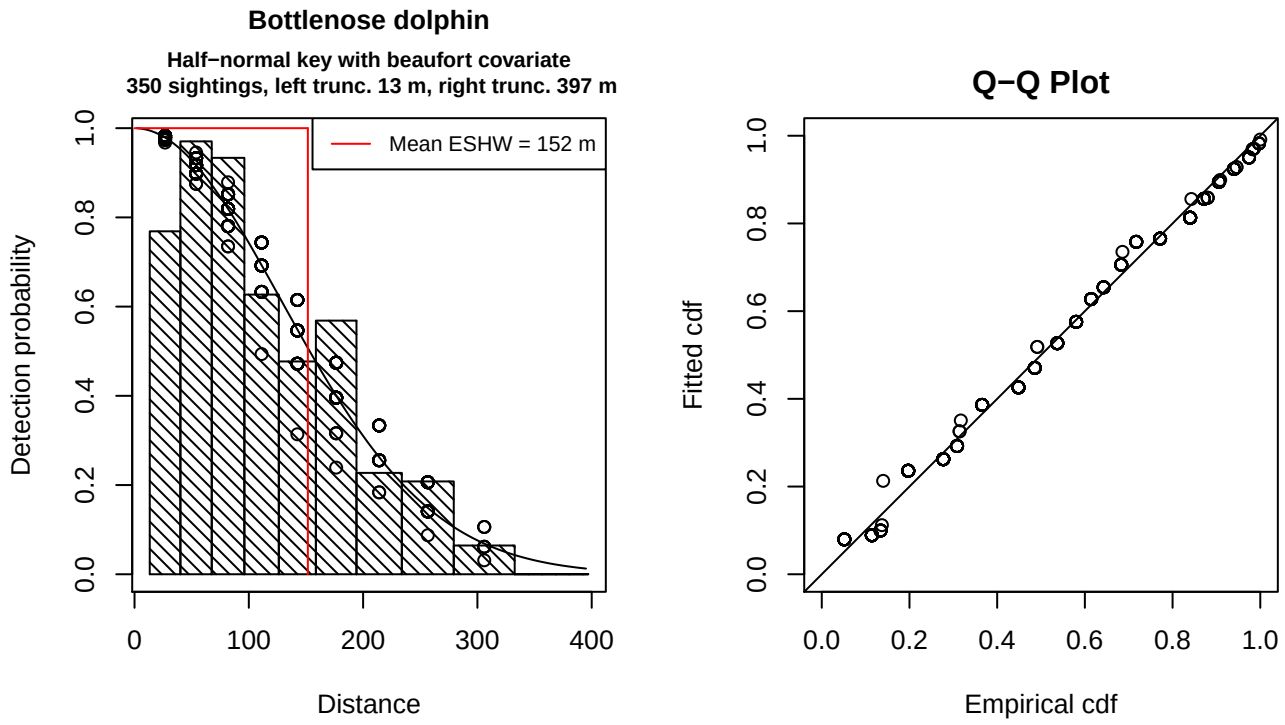

Figure 100: Detection function for UNCW Early Surveys that was selected for the density model

Statistical output for this detection function:

```
Summary for ds object
Number of observations :  350
Distance range         :  13.30786  -  397
AIC                    :  1474.598

Detection function:
 Half-normal key function

Detection function parameters
Scale Coefficients:
             estimate         se
(Intercept)  5.0814132 0.12575634
beaufort    -0.1085401 0.06178513

                      Estimate          SE         CV
Average p             0.3787064  0.01830693 0.04834068
N in covered region 924.1987081 59.33190523 0.06419821
```

Additional diagnostic plots:

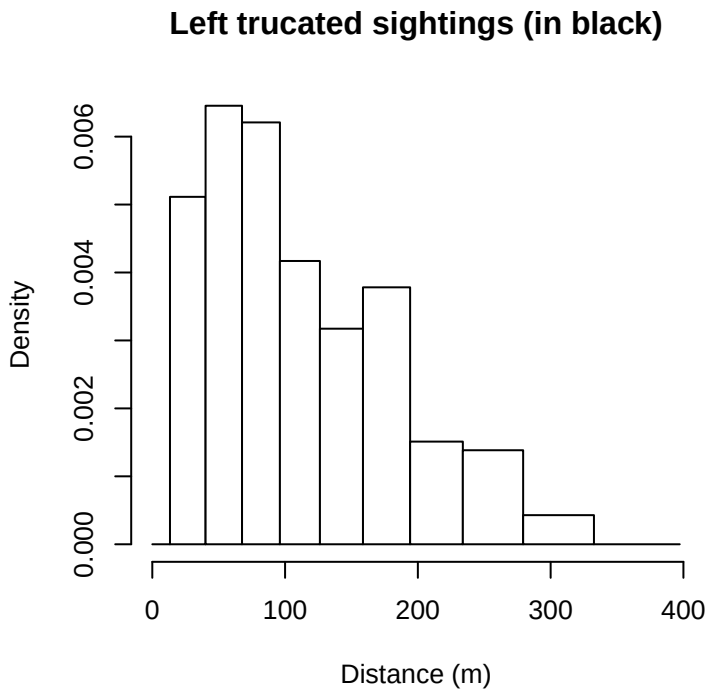

Figure 101: Density of sightings by perpendicular distance for UNCW Early Surveys. Black bars on the left show sightings that were left truncated.

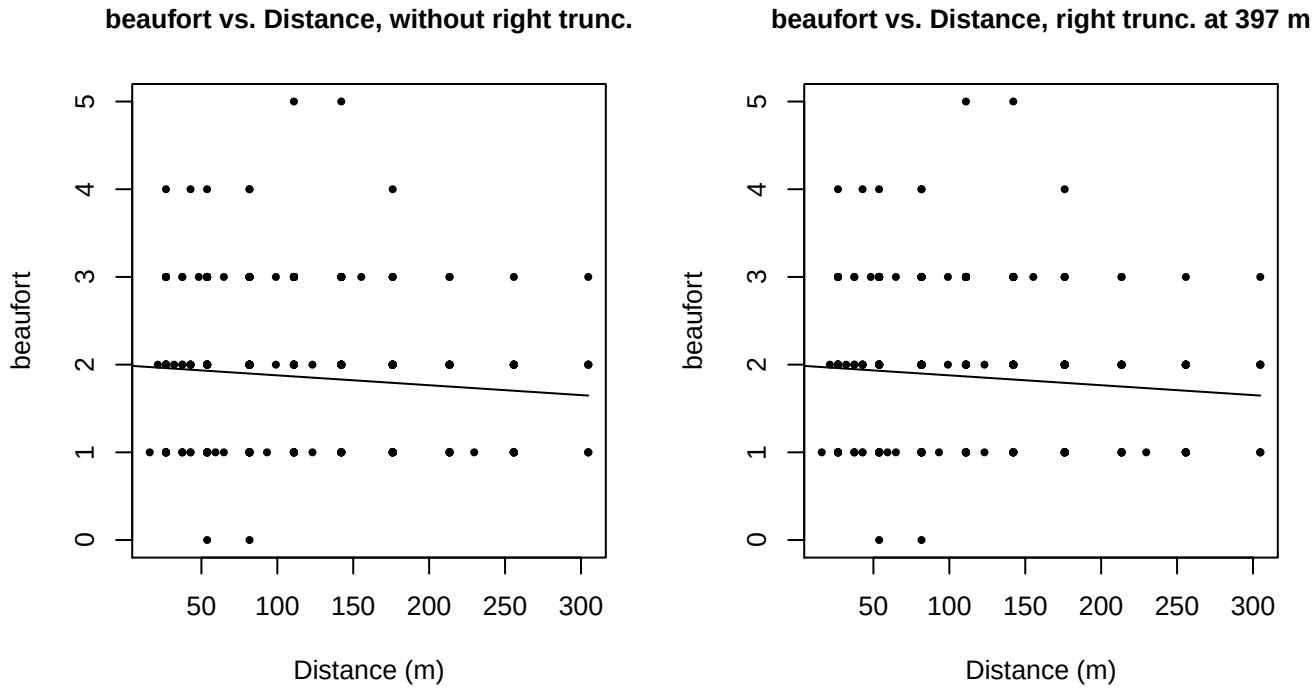

Figure 102: Scatterplots showing the relationship between Beaufort sea state and perpendicular sighting distance, for all sightings (left) and only those not right truncated (right). The line is a simple linear regression.

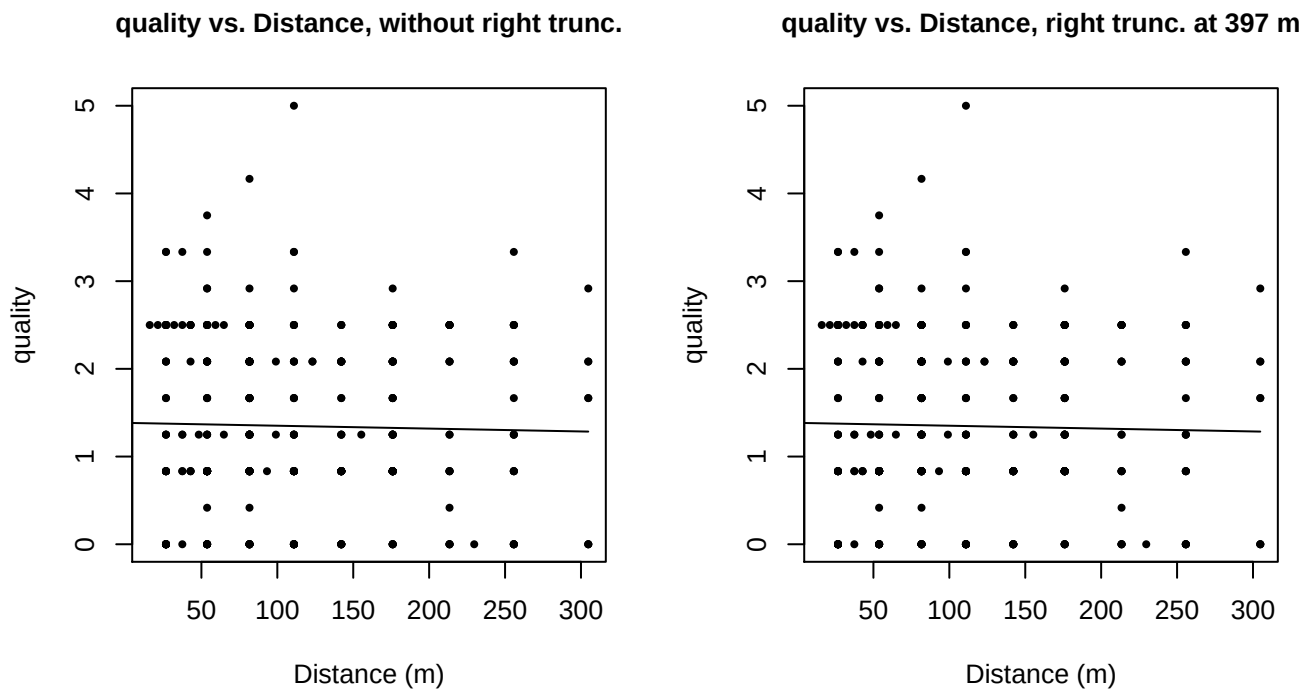

Figure 103: Scatterplots showing the relationship between the survey-specific index of the quality of observation conditions and perpendicular sighting distance, for all sightings (left) and only those not right truncated (right). Low values of the quality index correspond to better observation conditions. The line is a simple linear regression.

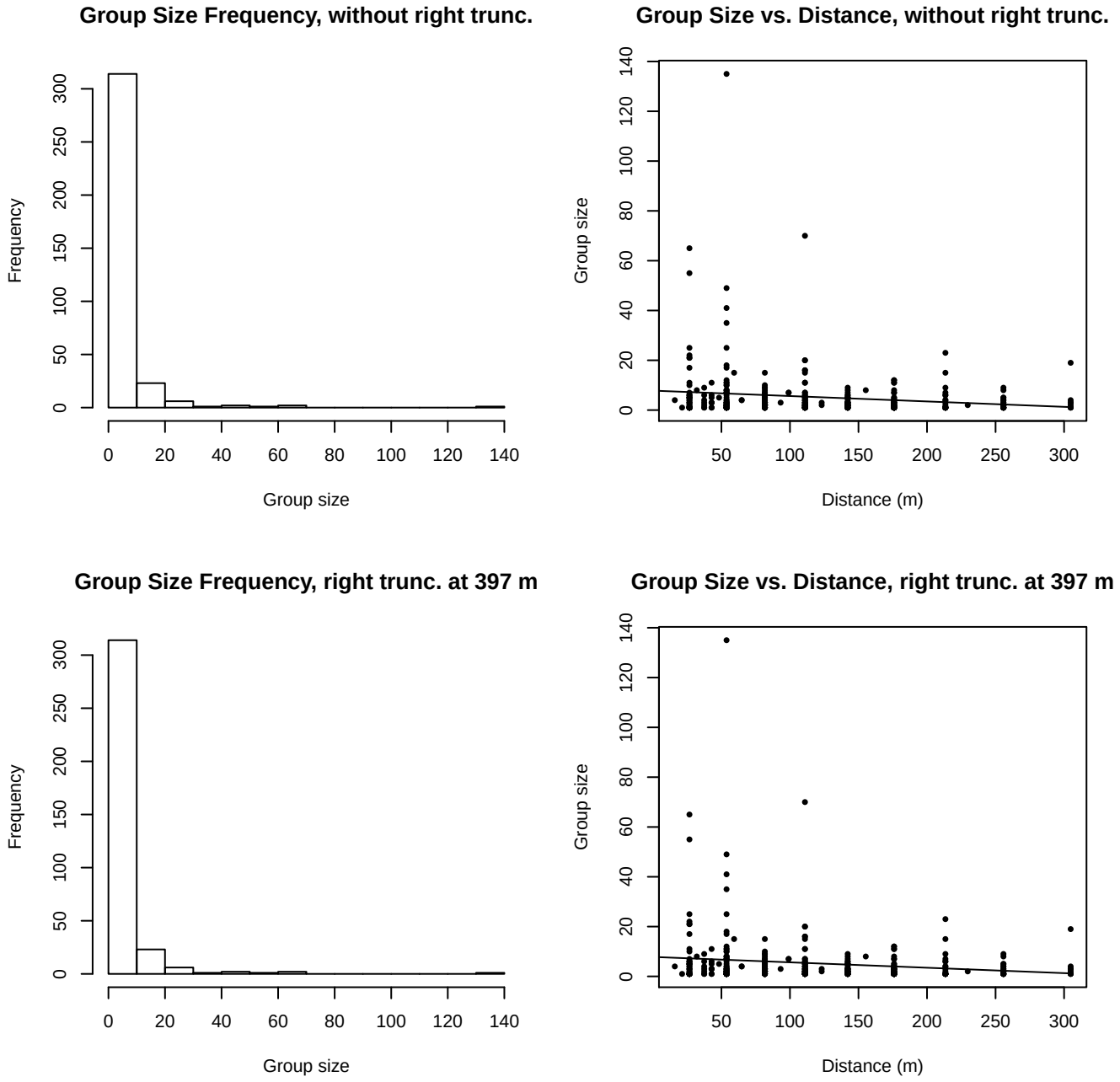

Figure 104: Histograms showing group size frequency and scatterplots showing the relationship between group size and perpendicular sighting distance, for all sightings (top row) and only those not right truncated (bottom row). In the scatterplot, the line is a simple linear regression.

Virginia Aquarium Surveys

The sightings were right truncated at 700m.

Covariate	Description
beaufort	Beaufort sea state.
quality	Survey-specific index of the quality of observation conditions, utilizing relevant factors other than Beaufort sea state (see methods).
size	Estimated size (number of individuals) of the sighted group.

Table 54: Covariates tested in candidate "multi-covariate distance sampling" (MCDS) detection functions.

Key	Adjustment	Order	Covariates	Succeeded	Δ AIC	Mean ESHW (m)
hn				Yes	0.00	313
hn	cos	3		Yes	0.70	265
hn			quality	Yes	1.27	313
hn	cos	2		Yes	1.46	282
hn			size	Yes	1.68	313
hn	herm	4		Yes	2.00	313
hr				Yes	2.81	329
hn			quality, size	Yes	2.83	313
hr			quality	Yes	4.52	327
hr			size	Yes	4.64	330
hr	poly	4		Yes	4.81	329
hr	poly	2		Yes	4.81	329
hr			quality, size	Yes	5.97	327
hr			beaufort	No		
hn			beaufort	No		
hr			beaufort, quality	No		
hn			beaufort, quality	No		
hr			beaufort, size	No		
hn			beaufort, size	No		
hr			beaufort, quality, size	No		
hn			beaufort, quality, size	No		

Table 55: Candidate detection functions for Virginia Aquarium Surveys. The first one listed was selected for the density model.

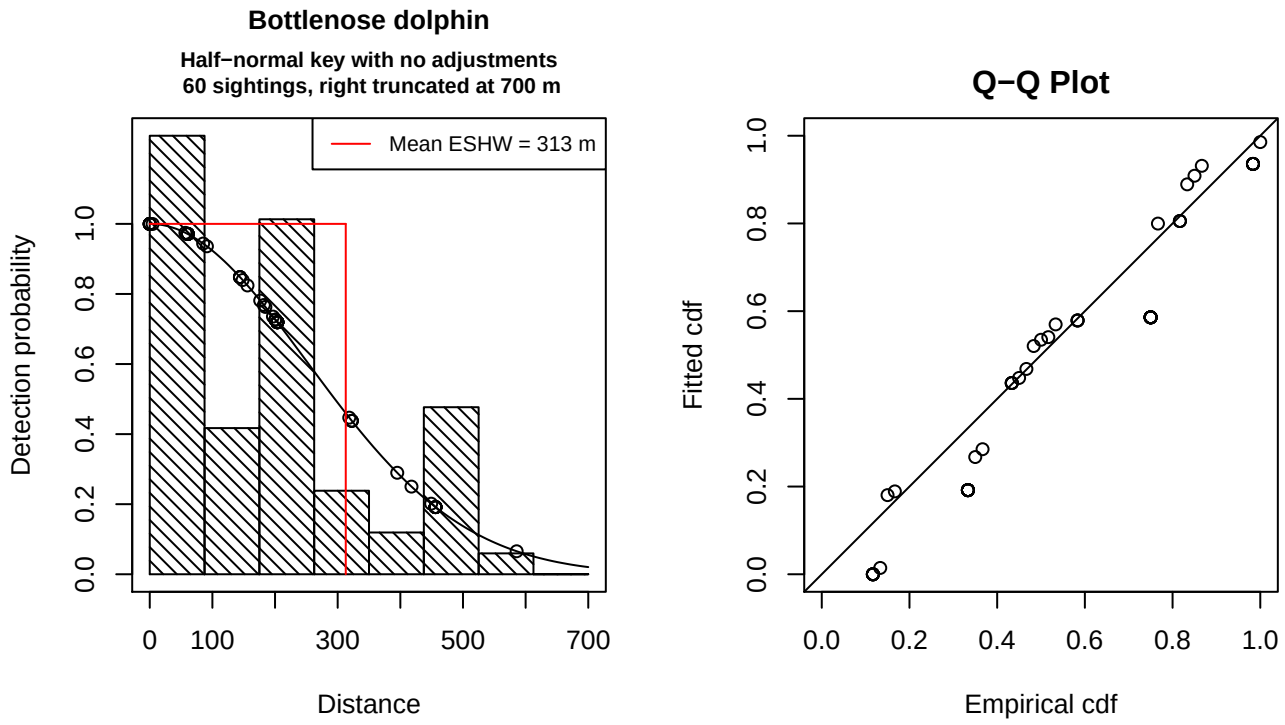

Figure 105: Detection function for Virginia Aquarium Surveys that was selected for the density model

Statistical output for this detection function:

```
Summary for ds object
Number of observations :  60
Distance range         :  0  -  700
AIC                    :  748.7597

Detection function:
 Half-normal key function

Detection function parameters
Scale Coefficients:
            estimate       se
(Intercept) 5.525393 0.103259

                       Estimate          SE         CV
Average p              0.4469979  0.04406191 0.09857298
N in covered region 134.2288301 18.46967914 0.13759845
```

Additional diagnostic plots:

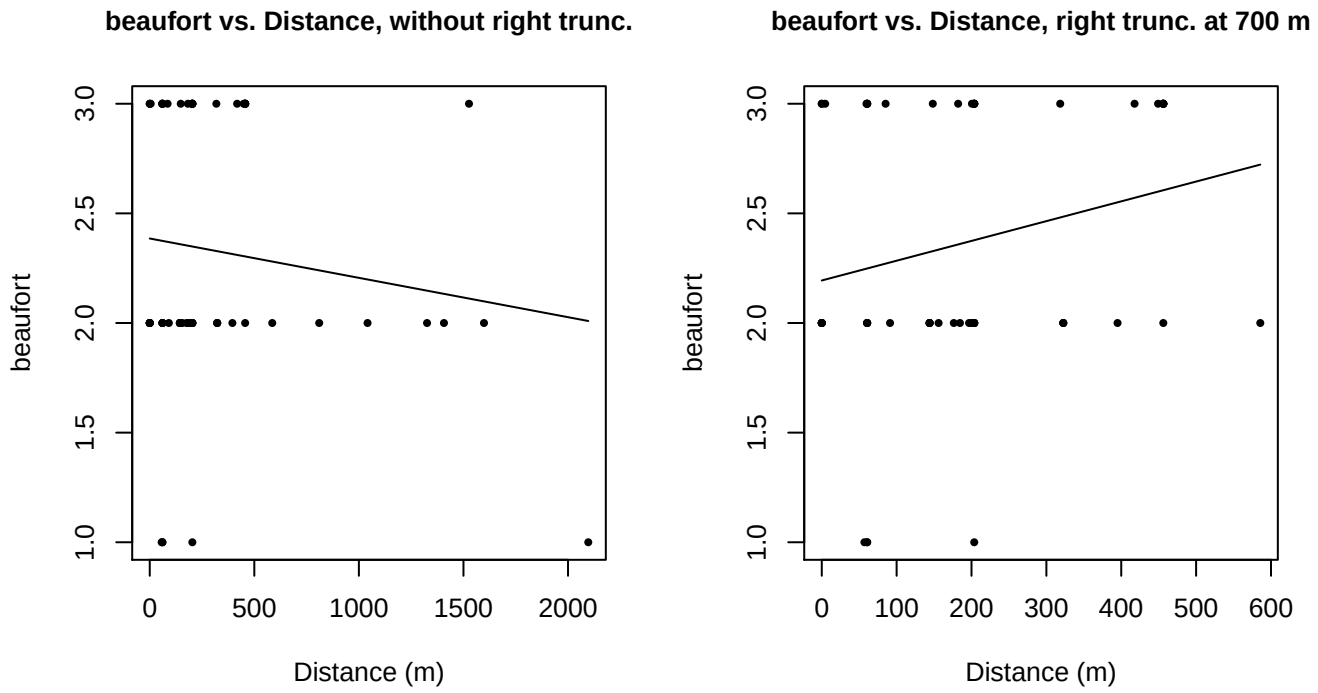

Figure 106: Scatterplots showing the relationship between Beaufort sea state and perpendicular sighting distance, for all sightings (left) and only those not right truncated (right). The line is a simple linear regression.

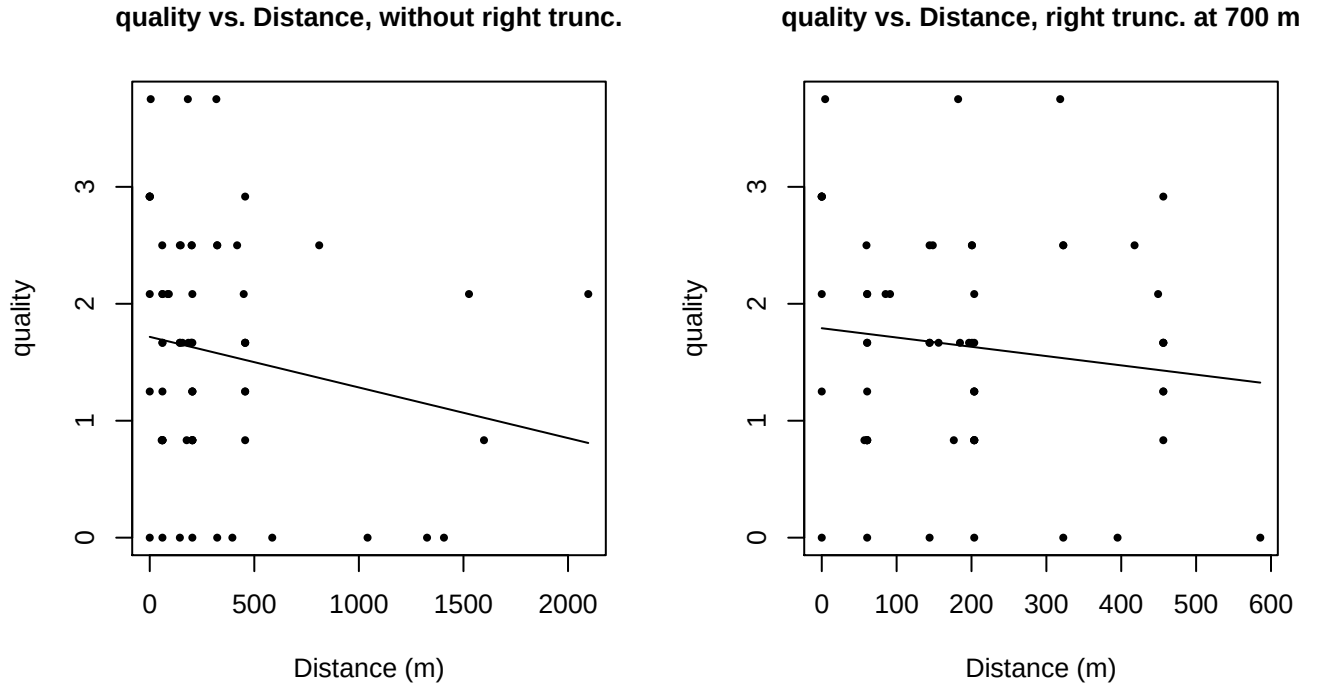

Figure 107: Scatterplots showing the relationship between the survey-specific index of the quality of observation conditions and perpendicular sighting distance, for all sightings (left) and only those not right truncated (right). Low values of the quality index correspond to better observation conditions. The line is a simple linear regression.

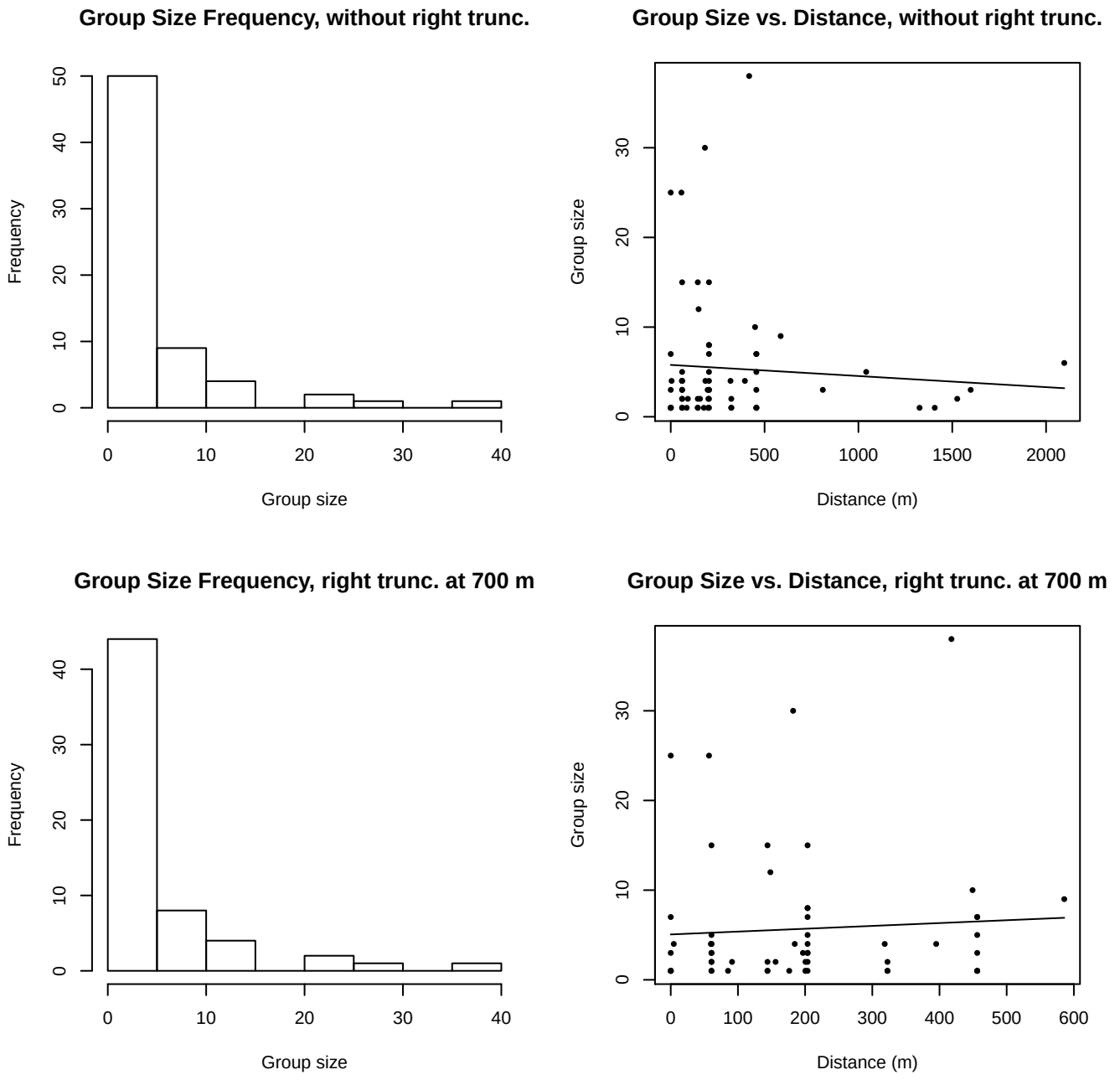

Figure 108: Histograms showing group size frequency and scatterplots showing the relationship between group size and perpendicular sighting distance, for all sightings (top row) and only those not right truncated (bottom row). In the scatterplot, the line is a simple linear regression.

NARWSS Grummans

Because this taxon was sighted too infrequently to fit a detection function to its sightings alone, we fit a detection function to the pooled sightings of several other species that we believed would exhibit similar detectability. These "proxy species" are listed below.

Reported By Observer	Common Name	n
Delphinus delphis	Short-beaked common dolphin	42
Delphinus delphis/Lagenorhynchus acutus	Short-beaked common or Atlantic white-sided dolphin	0

Delphinus delphis/Stenella	Short-beaked common dolphin or Stenella spp.	0
Delphinus delphis/Stenella coeruleoalba	Short-beaked common or striped dolphin	0
Grampus griseus	Risso's dolphin	0
Grampus griseus/Tursiops truncatus	Risso's or Bottlenose dolphin	0
Lagenodelphis hosei	Fraser's dolphin	0
Lagenorhynchus acutus	Atlantic white-sided dolphin	288
Lagenorhynchus albirostris	White-beaked dolphin	3
Lagenorhynchus albirostris/Lagenorhynchus acutus	White-beaked or white-sided dolphin	0
Stenella	Unidentified Stenella	0
Stenella attenuata	Pantropical spotted dolphin	0
Stenella attenuata/frontalis	Pantropical or Atlantic spotted dolphin	0
Stenella clymene	Clymene dolphin	0
Stenella coeruleoalba	Striped dolphin	1
Stenella frontalis	Atlantic spotted dolphin	0
Stenella frontalis/Tursiops truncatus	Atlantic spotted or Bottlenose dolphin	0
Stenella longirostris	Spinner dolphin	0
Steno bredanensis	Rough-toothed dolphin	0
Steno bredanensis/Tursiops truncatus	Bottlenose or rough-toothed dolphin	0
Tursiops truncatus	Bottlenose dolphin	6
Total		340

Table 56: Proxy species used to fit detection functions for NARWSS Grummans. The number of sightings, n, is before truncation.

The sightings were right truncated at 800m. Due to a reduced frequency of sightings close to the trackline that plausibly resulted from the behavior of the observers and/or the configuration of the survey platform, the sightings were left truncted as well. Sightings closer than 107 m to the trackline were omitted from the analysis, and it was assumed that the the area closer to the trackline than this was not surveyed. This distance was estimated by inspecting histograms of perpendicular sighting distances.

Covariate	Description
beaufort	Beaufort sea state.
quality	Survey-specific index of the quality of observation conditions, utilizing relevant factors other than Beaufort sea state (see methods).
size	Estimated size (number of individuals) of the sighted group.

Table 57: Covariates tested in candidate "multi-covariate distance sampling" (MCDS) detection functions.

Key	Adjustment	Order	Covariates	Succeeded	Δ AIC	Mean ESHW (m)
hr			quality, size	Yes	0.00	235
hr			size	Yes	5.95	231

hr			beaufort, size	Yes	7.81	233
hr			quality	Yes	11.76	213
hn			size	Yes	14.26	231
hn			quality, size	Yes	14.51	233
hn			beaufort, size	Yes	16.23	231
hr				Yes	20.06	203
hr	poly	4		Yes	21.78	200
hr			beaufort	Yes	22.05	204
hr	poly	2		Yes	22.06	203
hn				Yes	33.54	223
hn			quality	Yes	33.86	223
hn	herm	4		Yes	35.13	222
hn	cos	2		No		
hn	cos	3		No		
hn			beaufort	No		
hn			beaufort, quality	No		
hr			beaufort, quality	No		
hn			beaufort, quality, size	No		
hr			beaufort, quality, size	No		

Table 58: Candidate detection functions for NARWSS Grummans. The first one listed was selected for the density model.

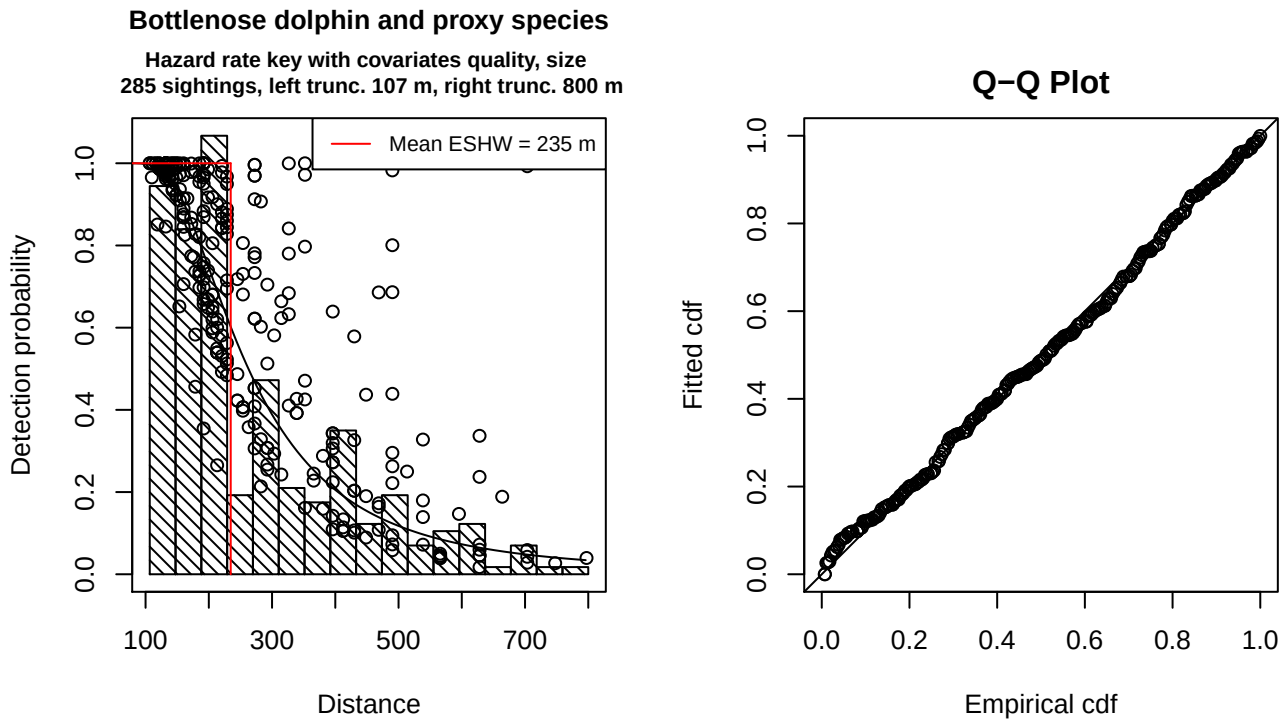

Figure 109: Detection function for NARWSS Grummans that was selected for the density model

Statistical output for this detection function:

```
Summary for ds object
Number of observations :  285
Distance range         :  106.5979  -  800
AIC                    :  3450.827

Detection function:
 Hazard-rate key function

Detection function parameters
Scale Coefficients:
             estimate         se
(Intercept)  5.5620259 0.12398130
quality     -0.2408179 0.09290192
size         0.2953779 0.09400126

Shape parameters:
            estimate        se
(Intercept) 1.119906 0.1056045

                         Estimate           SE        CV
Average p               0.2541682   0.03062592 0.1204947
N in covered region 1121.3045461 147.37019002 0.1314274
```

Additional diagnostic plots:

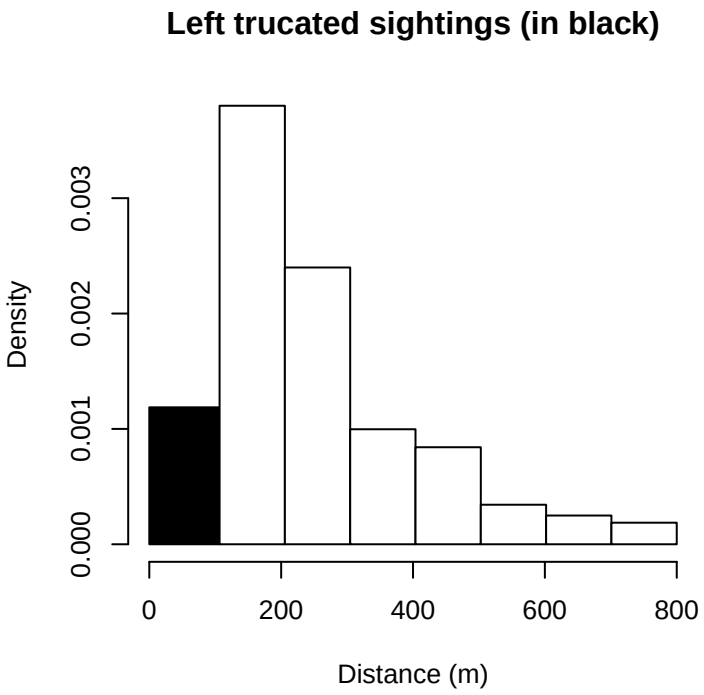

Figure 110: Density of sightings by perpendicular distance for NARWSS Grummans. Black bars on the left show sightings that were left truncated.

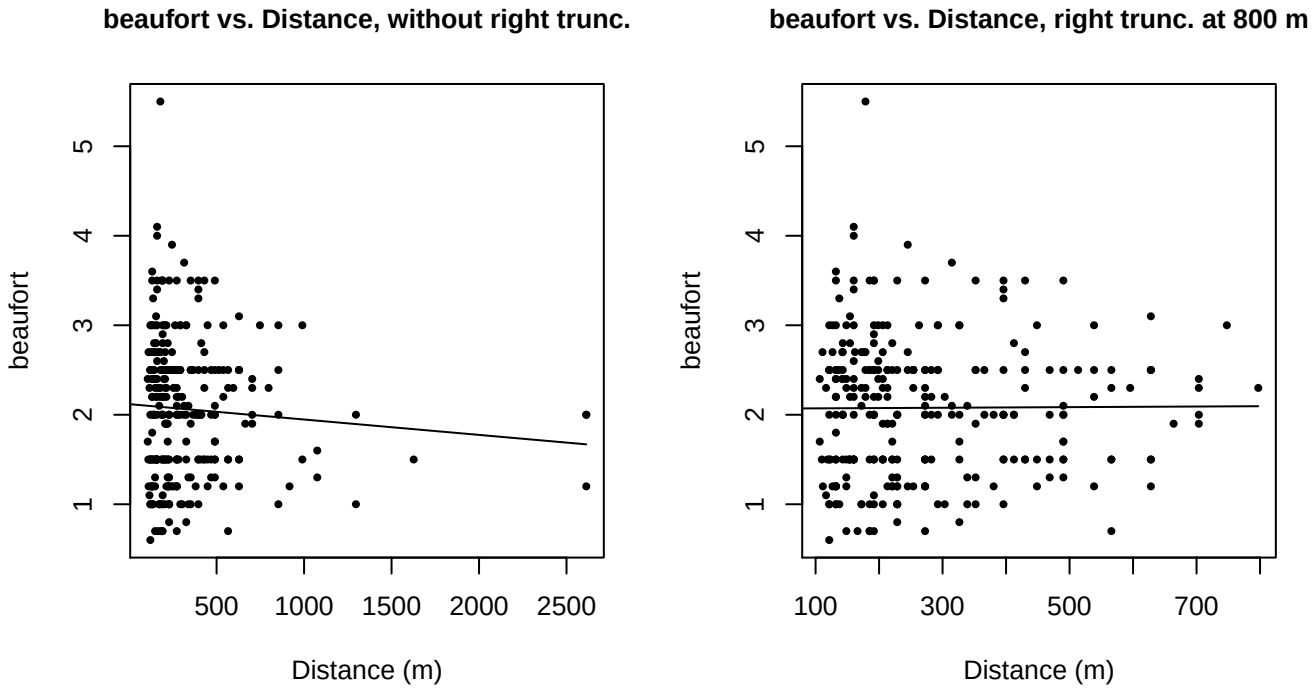

Figure 111: Scatterplots showing the relationship between Beaufort sea state and perpendicular sighting distance, for all sightings (left) and only those not right truncated (right). The line is a simple linear regression.

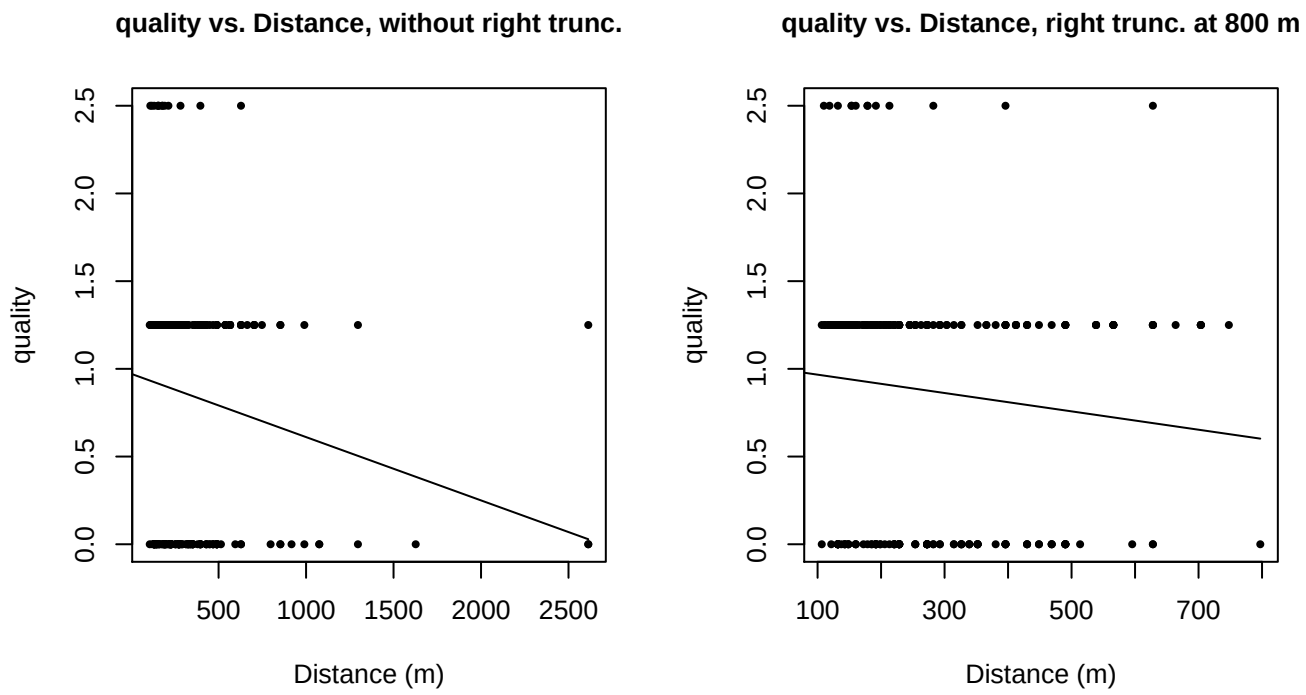

Figure 112: Scatterplots showing the relationship between the survey-specific index of the quality of observation conditions and perpendicular sighting distance, for all sightings (left) and only those not right truncated (right). Low values of the quality index correspond to better observation conditions. The line is a simple linear regression.

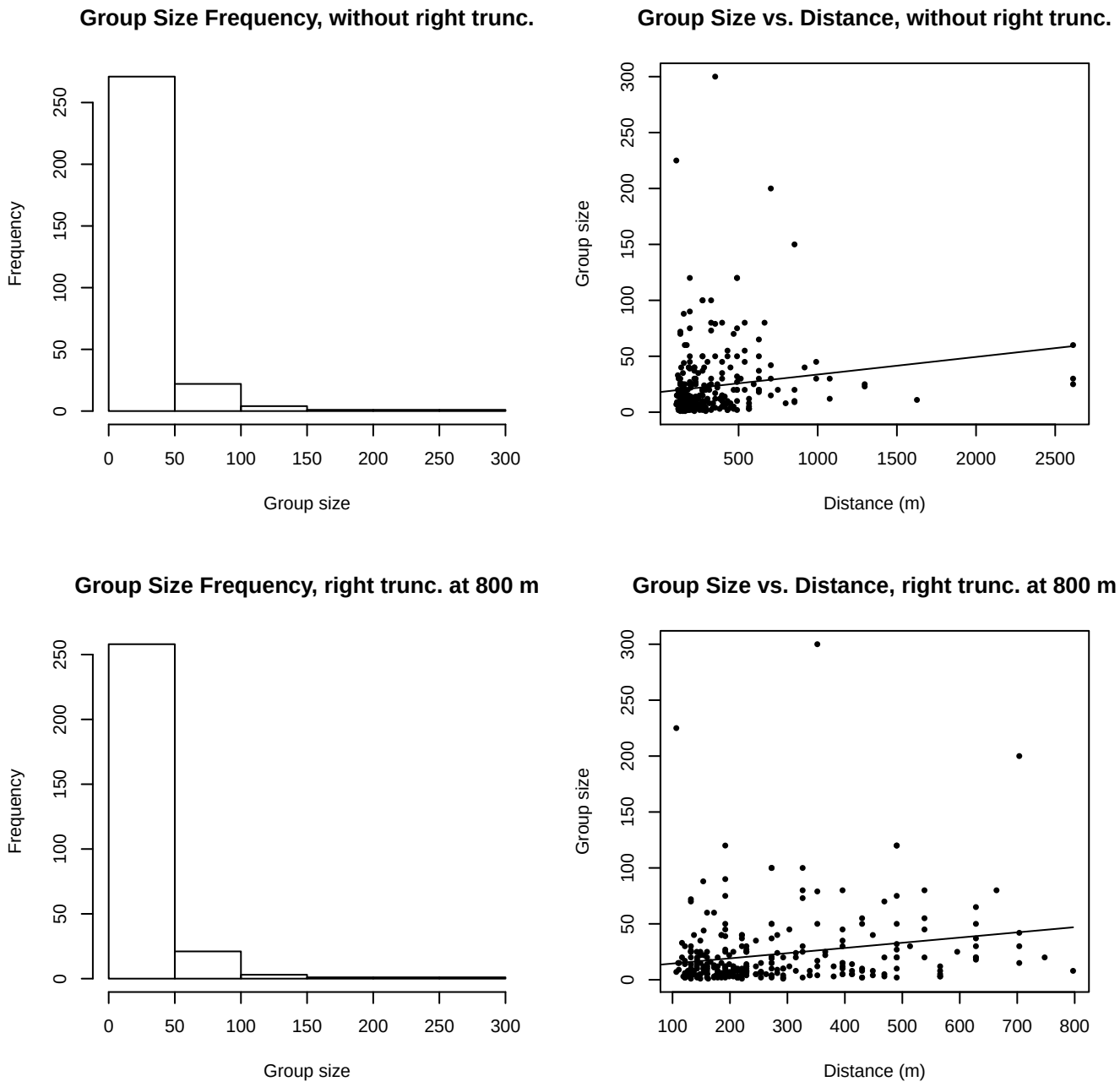

Figure 113: Histograms showing group size frequency and scatterplots showing the relationship between group size and perpendicular sighting distance, for all sightings (top row) and only those not right truncated (bottom row). In the scatterplot, the line is a simple linear regression.

NARWSS Twin Otters

Because this taxon was sighted too infrequently to fit a detection function to its sightings alone, we fit a detection function to the pooled sightings of several other species that we believed would exhibit similar detectability. These "proxy species" are listed below.

Reported By Observer	Common Name	n
Delphinus delphis	Short-beaked common dolphin	539
Delphinus delphis/Lagenorhynchus acutus	Short-beaked common or Atlantic white-sided dolphin	0

Delphinus delphis/Stenella	Short-beaked common dolphin or Stenella spp.	0
Delphinus delphis/Stenella coeruleoalba	Short-beaked common or striped dolphin	0
Grampus griseus	Risso's dolphin	86
Grampus griseus/Tursiops truncatus	Risso's or Bottlenose dolphin	0
Lagenodelphis hosei	Fraser's dolphin	0
Lagenorhynchus acutus	Atlantic white-sided dolphin	1732
Lagenorhynchus albirostris	White-beaked dolphin	4
Lagenorhynchus albirostris/Lagenorhynchus acutus	White-beaked or white-sided dolphin	0
Stenella	Unidentified Stenella	1
Stenella attenuata	Pantropical spotted dolphin	0
Stenella attenuata/frontalis	Pantropical or Atlantic spotted dolphin	0
Stenella clymene	Clymene dolphin	0
Stenella coeruleoalba	Striped dolphin	4
Stenella frontalis	Atlantic spotted dolphin	0
Stenella frontalis/Tursiops truncatus	Atlantic spotted or Bottlenose dolphin	0
Stenella longirostris	Spinner dolphin	0
Steno bredanensis	Rough-toothed dolphin	0
Steno bredanensis/Tursiops truncatus	Bottlenose or rough-toothed dolphin	0
Tursiops truncatus	Bottlenose dolphin	39
Total		2405

Table 59: Proxy species used to fit detection functions for NARWSS Twin Otters. The number of sightings, n, is before truncation.

The sightings were right truncated at 2500m. Due to a reduced frequency of sightings close to the trackline that plausibly resulted from the behavior of the observers and/or the configuration of the survey platform, the sightings were left truncted as well. Sightings closer than 160 m to the trackline were omitted from the analysis, and it was assumed that the the area closer to the trackline than this was not surveyed. This distance was estimated by inspecting histograms of perpendicular sighting distances. The vertical sighting angles were heaped at 10 degree increments up to 80 degrees and 1 degree increments thereafter, so the candidate detection functions were fitted using linear bins scaled accordingly.

Covariate	Description
beaufort	Beaufort sea state.
quality	Survey-specific index of the quality of observation conditions, utilizing relevant factors other than Beaufort sea state (see methods).
size	Estimated size (number of individuals) of the sighted group.

Table 60: Covariates tested in candidate "multi-covariate distance sampling" (MCDS) detection functions.

Key	Adjustment	Order	Covariates	Succeeded	Δ AIC	Mean ESHW (m)
hr			beaufort, size	Yes	0.00	470
hr			size	Yes	5.29	463

hr			quality, size	Yes	7.11	463
hr	poly	2		Yes	9.16	430
hr	poly	4		Yes	10.71	442
hr			beaufort	Yes	17.46	464
hr				Yes	22.55	458
hr			quality	Yes	24.49	458
hn	cos	2		Yes	33.82	434
hn	cos	3		Yes	54.89	361
hn			beaufort, size	Yes	162.73	517
hn			size	Yes	162.85	518
hn			quality, size	Yes	164.00	518
hn			beaufort, quality, size	Yes	164.45	517
hn			beaufort	Yes	185.34	516
hn				Yes	186.28	516
hn	herm	4		Yes	186.91	516
hn			beaufort, quality	Yes	187.34	516
hn			quality	Yes	188.03	516
hr			beaufort, quality	No		
hr			beaufort, quality, size	No		

Table 61: Candidate detection functions for NARWSS Twin Otters. The first one listed was selected for the density model.

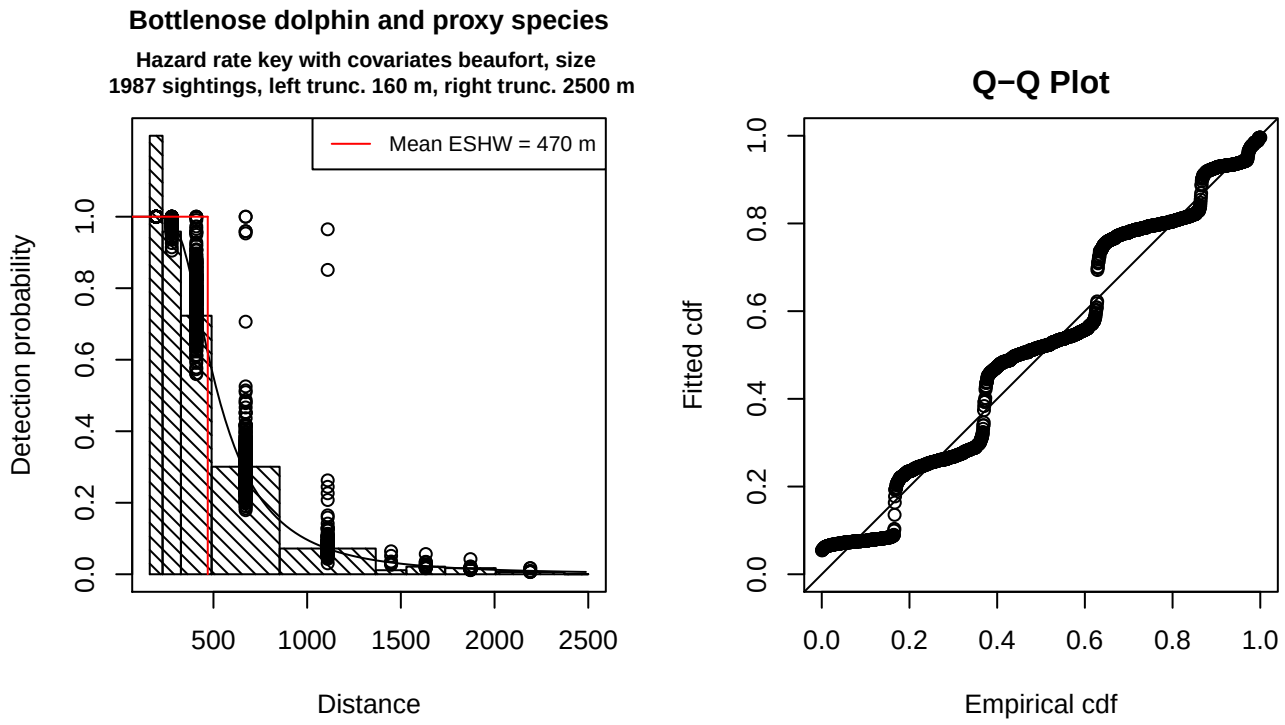

Figure 114: Detection function for NARWSS Twin Otters that was selected for the density model

Statistical output for this detection function:

```
Summary for ds object
Number of observations :  1987
Distance range         :  160.0674  -  2500
AIC                    :  6745.856

Detection function:
 Hazard-rate key function

Detection function parameters
Scale Coefficients:
               estimate         se
(Intercept)  6.26395198 0.06468196
beaufort    -0.07274292 0.02643651
size         0.08974254 0.02445737

Shape parameters:
            estimate        se
(Intercept) 1.110483 0.0356417

                        Estimate           SE         CV
Average p           1.845364e-01 5.774489e-03 0.03129187
N in covered region 1.076752e+04 4.016208e+02 0.03729928
```

Additional diagnostic plots:

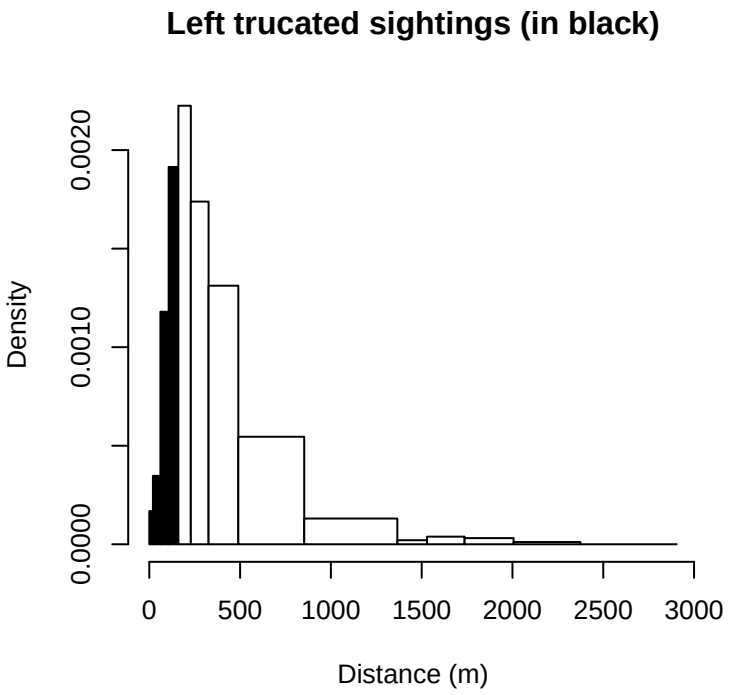

Figure 115: Density of sightings by perpendicular distance for NARWSS Twin Otters. Black bars on the left show sightings that were left truncated.

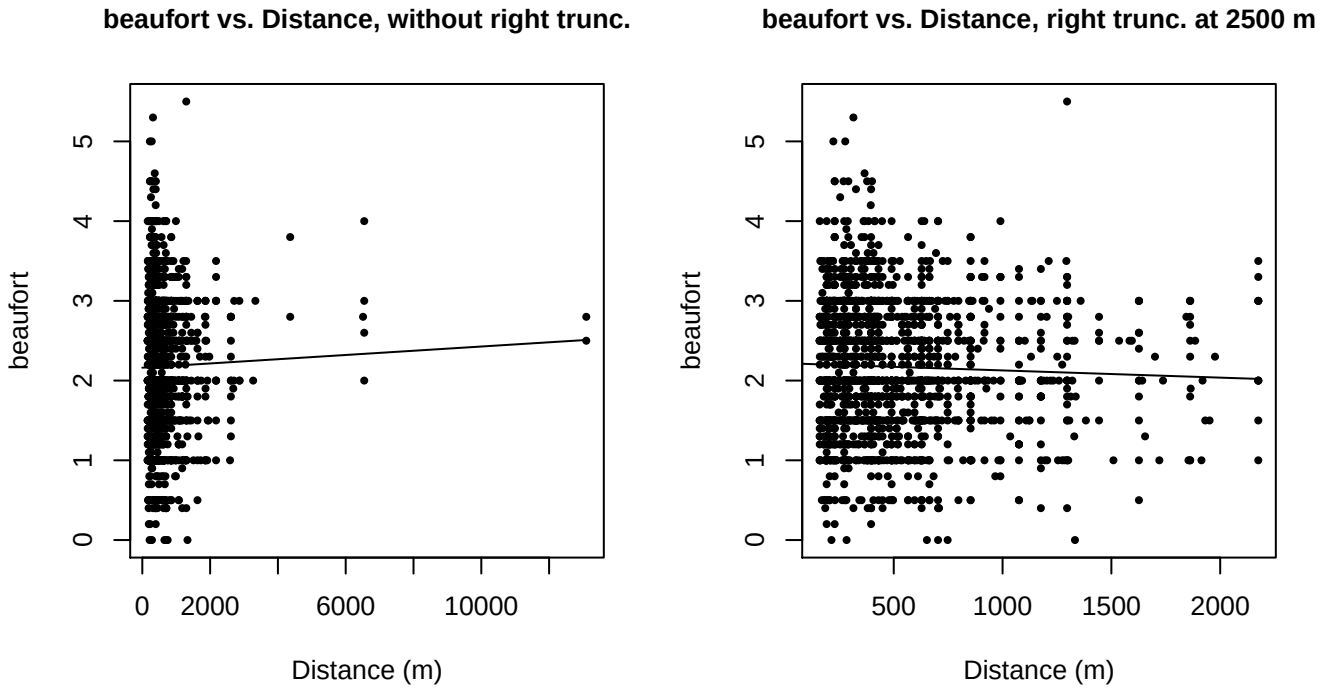

Figure 116: Scatterplots showing the relationship between Beaufort sea state and perpendicular sighting distance, for all sightings (left) and only those not right truncated (right). The line is a simple linear regression.

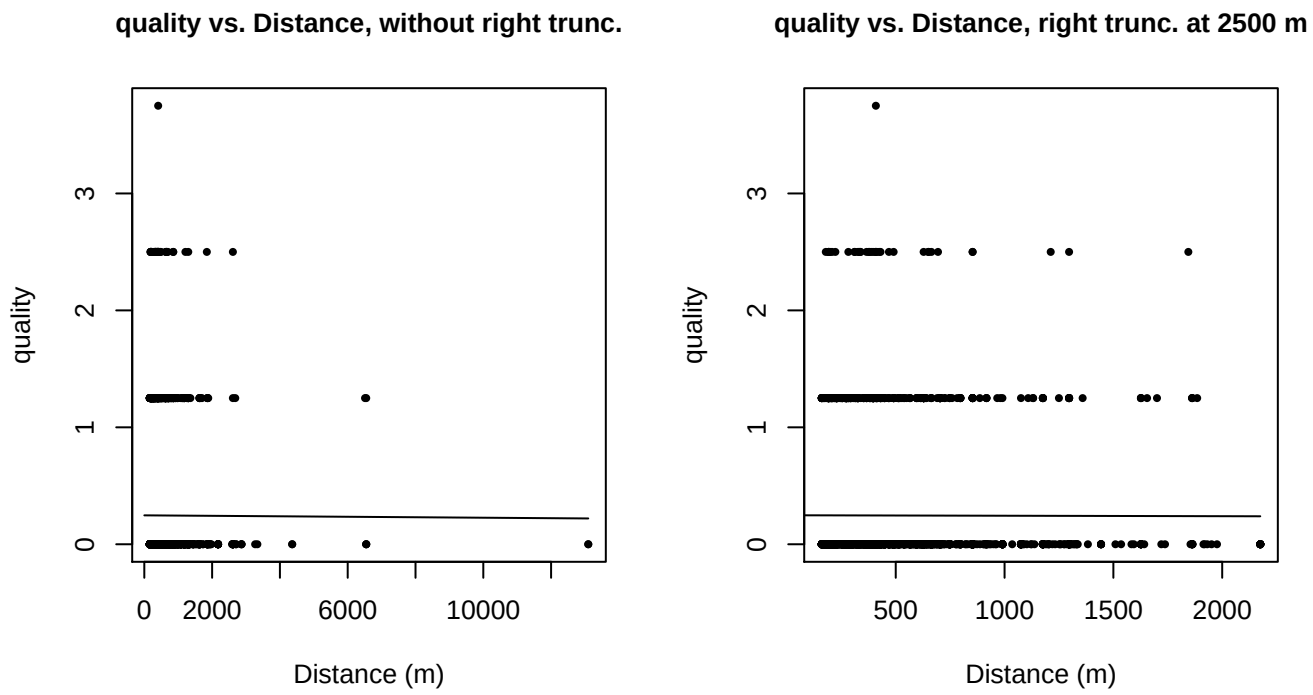

Figure 117: Scatterplots showing the relationship between the survey-specific index of the quality of observation conditions and perpendicular sighting distance, for all sightings (left) and only those not right truncated (right). Low values of the quality index correspond to better observation conditions. The line is a simple linear regression.

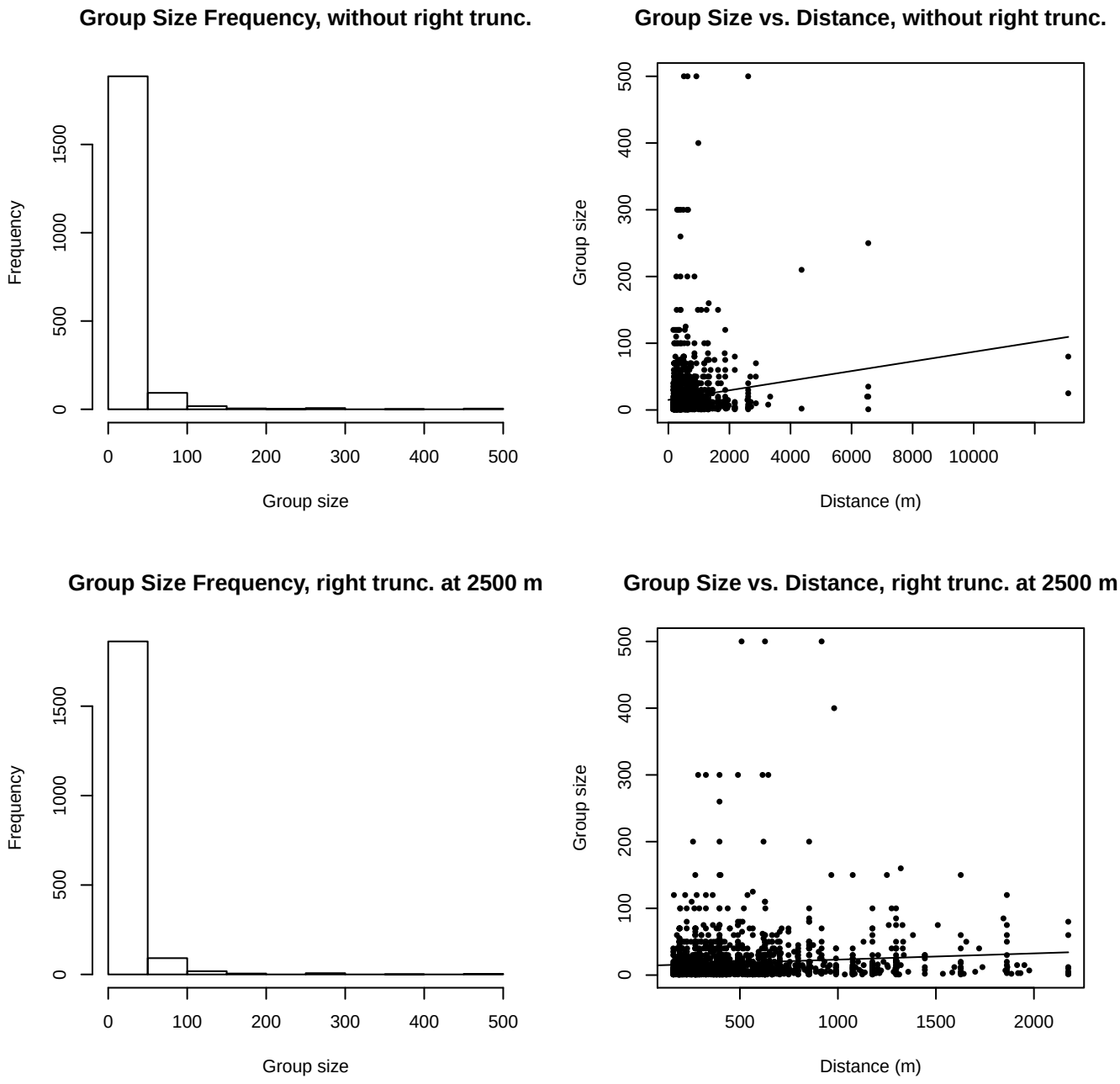

Figure 118: Histograms showing group size frequency and scatterplots showing the relationship between group size and perpendicular sighting distance, for all sightings (top row) and only those not right truncated (bottom row). In the scatterplot, the line is a simple linear regression.

g(0) Estimates

Platform	Surveys	Group Size	*g(0)*	Biases Addressed	Source
Shipboard	All	1-20	0.856	Perception	Barlow and Forney (2007)
		>20	0.970	Perception	Barlow and Forney (2007)
Shipboard	NEFSC Abel-J Binocular Surveys	Any	0.69	Perception	Palka (2006)
Shipboard	NEFSC Endeavor	Any	0.67	Perception	Palka (2006)
Aerial	All	1-5	0.43	Both	Palka (2006)
		>5	0.960	Both	Carretta et al. (2000)

Table 62: Estimates of *g(0)* used in this density model.

For shipboard surveys other than the NOAA NEFSC cruises for which Palka (2006) provided survey-specific estimates of g(0), we utilized Barlow and Forney's (2007) estimates for delphinids, produced from several years of dual-team surveys that used similar binoculars and protocols to the surveys in our study. This study provided separate estimates for small and large groups, but pooled sightings of several species together to provide a generic estimate for all delphinids, due to sample-size limitations. To our knowledge, there is no species-specific shipboard g(0) estimate that treats small and large groups separately, so we believe Barlow and Forney (2007) provide the best general- purpose alternative. Their estimate accounted for perception bias but not availability bias; dive times for dolphins are short enough that availability bias is not expected to be significant for dolphins observed from shipboard surveys.

For aerial surveys, we were unable to locate species-specific g(0) estimates in the literature. For small groups, defined here as 1-5 individuals, we used Palka's (2006) estimate of g(0) for groups of 1-5 small cetaceans, estimated from two years of aerial surveys using the Hiby (1999) circle-back method. This estimate accounted for both availability and perception bias, but pooled sightings of several species together to provide a generic estimate for all delphinids, due to sample-size limitations. For large groups, defined here as greater than 5 individuals, Palka (2006) assumed that g(0) was 1. When we discussed this with NOAA SWFSC reviewers, they agreed that it was safe to assume that the availability bias component of g(0) was 1 but insisted that perception bias should be slightly less than 1, because it was possible to miss large groups. We agreed to take a conservative approach and obtained our g(0) for large groups from Carretta et al. (2000), who estimated g(0) for both small and large groups of delphinids. We used Carretta et al.'s g(0) estimate for groups of 1-25 individuals (0.960), rather than their larger one for more than 25 individuals (0.994), to account for the fact that we were using Palka's definition of large groups as those with more than 5 individuals.

Density Models

The common bottlenose dolphin is the most abundant cetacean along the U.S. east coast, with the possible exception of the short-beaked common dolphin. Owing to its overall abundance and its distribution close to shore, the surveys used in our study reported more sightings of it than any other species–over 4600–allowing us to fit many species-specific, survey-program-specific detection functions (see Detection Functions section above).

Bottlenose dolphins exhibit the most complex population structure yet documented for any cetacean in the U.S. Atlantic or Gulf of Mexico. The U.S. Marine Mammal Protection Act (MMPA) requires that cetaceans be managed on a per "stock" basis, and defines a stock as "a group of marine mammals of the same species or smaller taxa in a common spatial arrangement, that interbreed when mature". The National Marine Fisheries Service (NMFS) is responsible for defining stocks and estimating their abundance, and periodically issues stock assessment reports that summarize the latest research and promulgate stock definitions and abundance estimates. At the time of this writing, the latest stock assessment report, dated April 2014 (Waring et al. 2014), described the western North Atlantic stocks as follows:

Two morphologically and genetically distinct morphotypes of bottlenose dolphins, known as the coastal and offshore forms, inhabit the western North Atlantic. The offshore form is larger and more robust, and consists of a single stock, which inhabits off-shelf, slope, and shelf-break waters, as well as outer portions of the continental shelf. The spatiotemporal extent and

dynamics of its on-shelf distribution (e.g. how close it comes to shore) are a topic of active research and appear to vary spatially and seasonally. The coastal morphotype consists of multiple "coastal" and "estuarine" stocks. At the time of this writing, NMFS defined five coastal stocks for the east coast, each genetically distinct. They generally inhabit the inner portions of the continental shelf, and some migrate north along the shelf in summer and return south in winter. NMFS also defined 10 estuarine stocks. These inhabit particular bays, sounds, rivers, and other estuarine systems and may be genetically distinct from each other as well as the other coastal stocks. They generally do not migrate.

There is spatiotemporal overlap between many of these stocks–between the offshore and coastal stocks, among the coastal stocks, between the estuarine and coastal stocks, and among the estuarine stocks. At present, the authors of the model presented here lack the information necessary to model each stock individually. The core problem is that there is no reliable and comprehensive way to determine which stock a given sighting belongs to. Some surveys in our study reported "coastal bottlenose dolphin" or "offshore bottlenose dolphin", but most did not, and none reported more precise detail than that. NMFS stock assessment reports and the literature discuss potential rules for classifying sightings based on geographic location, distance to shore, depth, and other variables, but these proposals do not cover all of the stocks or definitively address the overlaps between them, and there is no widespread agreement among the research community on the efficacy of proposed rules. At the present time, the only foolproof method of classifying a sighting into a stock is through genetics. Therefore we have made no attempt to model bottlenose dolphins on a per-stock basis from the visual survey, and have instead modeled the all stocks in a single model. Prior to our analysis, we discarded all estuarine survey transects, thus it is probably reasonable to assume that our model estimates the aggregate density of the offshore and coastal stocks and excludes the estuarine stocks (although some estuarine stocks are known to range into coastal areas beyond their home estuaries; presumably some of these were sighted and we failed to discard them).

As mentioned, some of the stocks are known to migrate north in summer and return south in winter. The dynamics may vary by stock and by year and are not well understood. NMFS has often described the migratory ranges and dynamics as being influenced or limited by sea surface temperature (SST). Our literature review did not reveal evidence of distinct seasonal changes in species-environment relationships, as occurred with baleen whales migrating seasonally between cold, productive feeding grounds and warm, calm calving grounds. Given the lack of evidence, we did not split the data into seasonal strata to be modeled separately, and instead relied on dynamic predictors such as SST to reproduce seasonal shifts in density within a single "year-round" model. Given the spatial overlap between stocks, we did not split the data into geographic strata either.

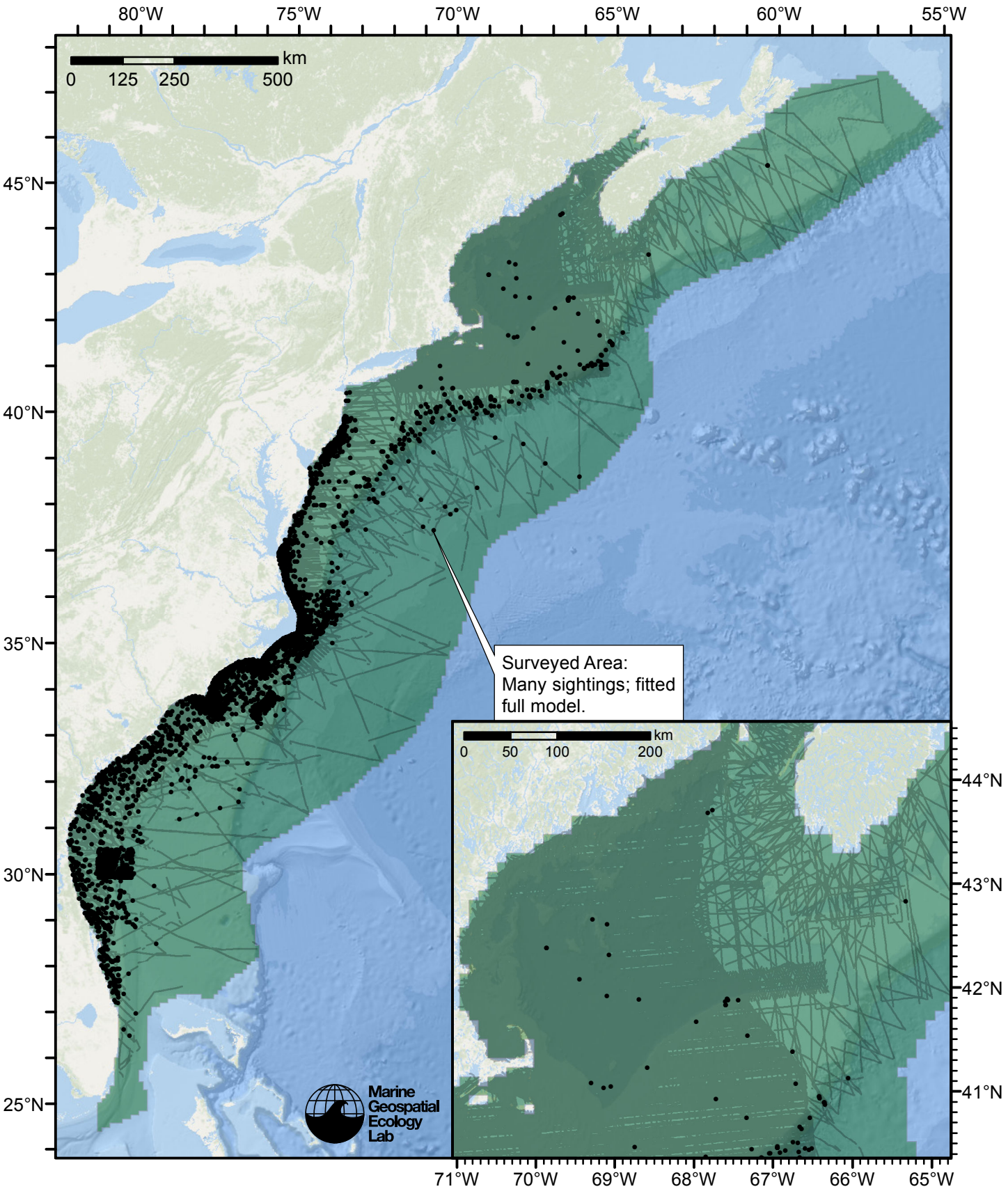

Figure 119: Bottlenose dolphin density model schematic. All on-effort sightings are shown, including those that were truncated when detection functions were fitted.

Climatological Model

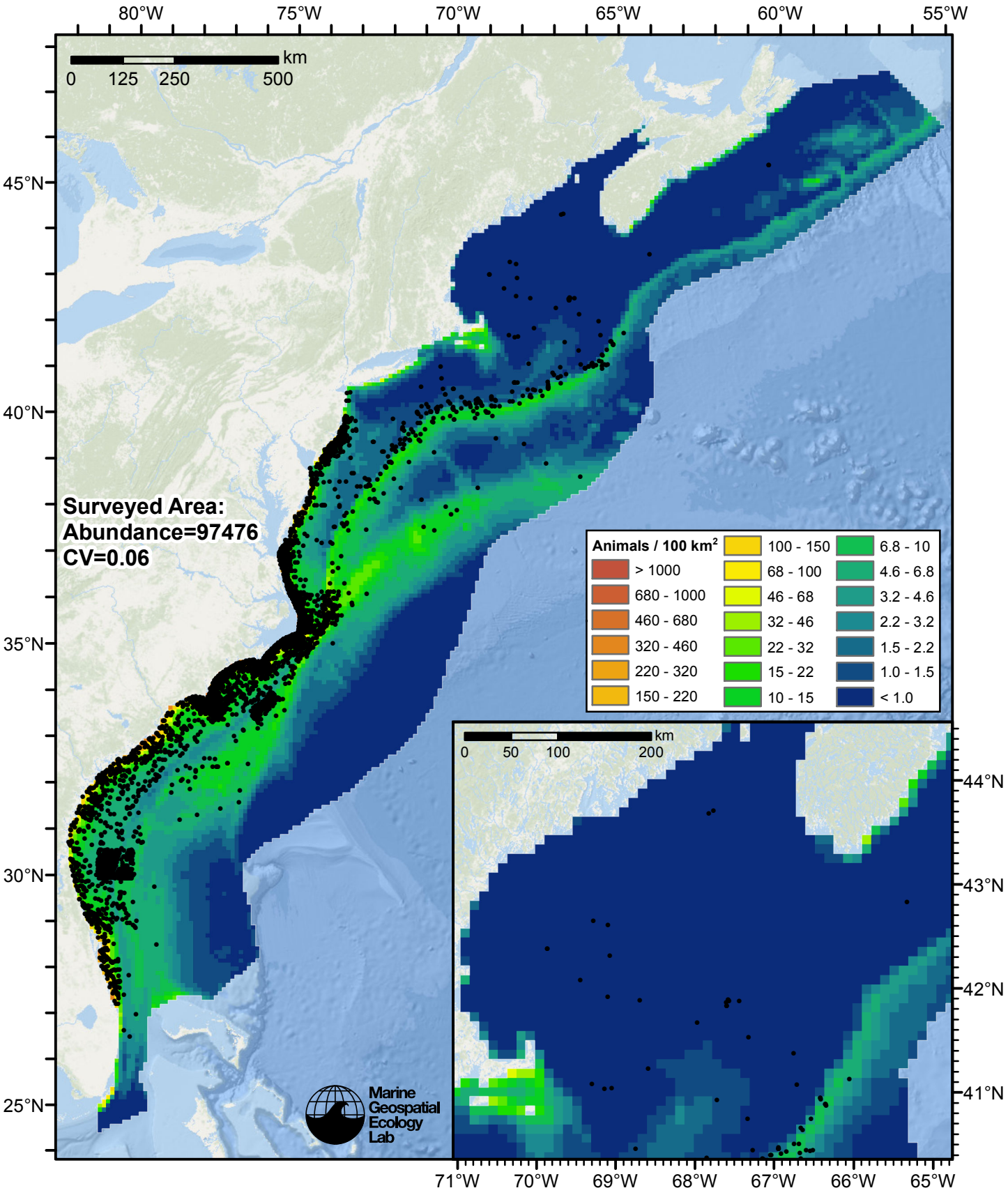

Figure 120: Bottlenose dolphin density predicted by the climatological model that explained the most deviance. Pixels are 10x10 km. The legend gives the estimated individuals per pixel; breaks are logarithmic. Abundance for each region was computed by summing the density cells occuring in that region.

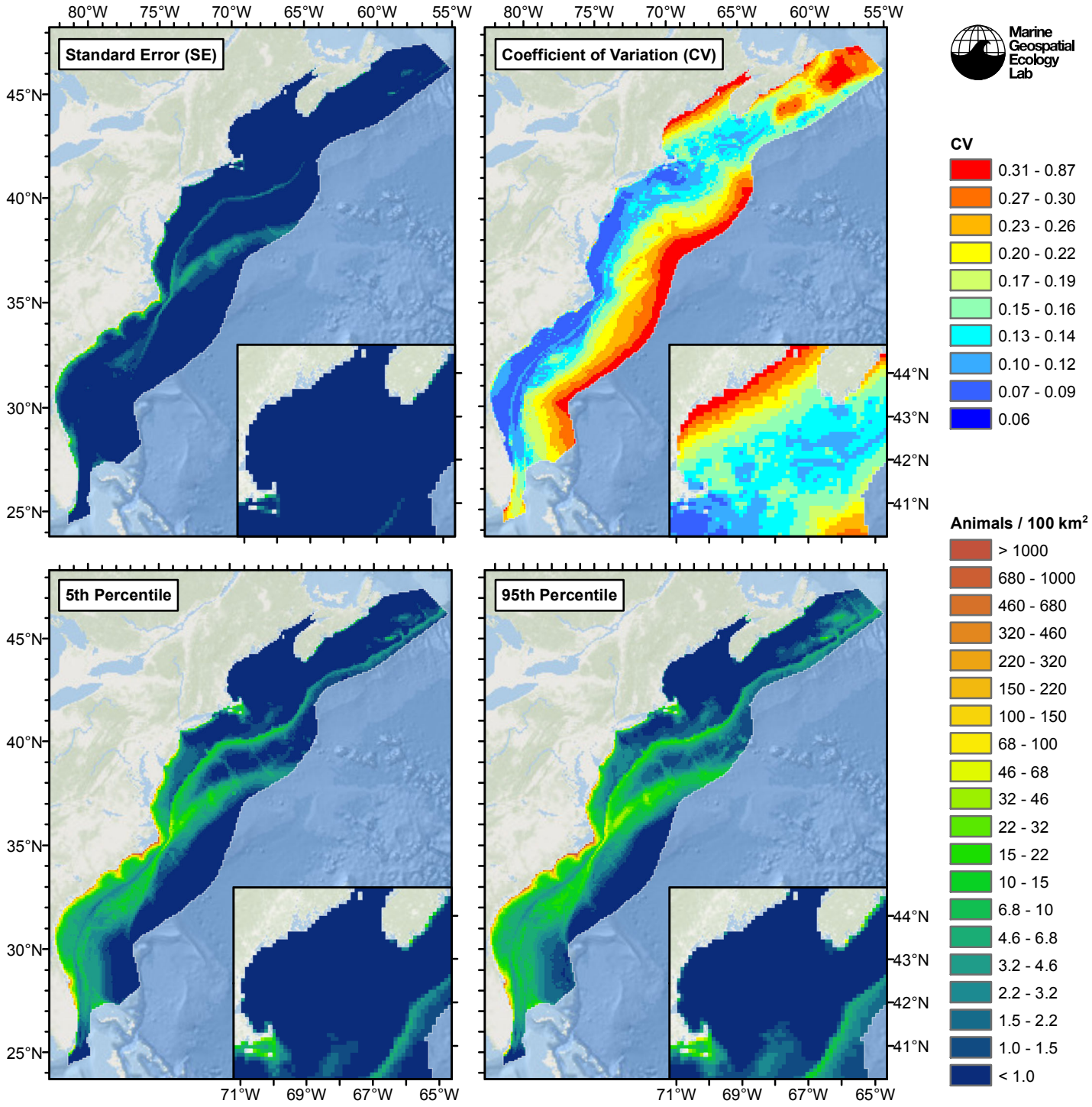

Figure 121: Estimated uncertainty for the climatological model that explained the most deviance. These estimates only incorporate the statistical uncertainty estimated for the spatial model (by the R mgcv package). They do not incorporate uncertainty in the detection functions, g(0) estimates, predictor variables, and so on.

Surveyed Area

Statistical output

```
Rscript.exe: This is mgcv 1.8-3. For overview type 'help("mgcv-package")'.


Family: Tweedie(p=1.359)
```

```
Link function: log

Formula:
abundance ~ offset(log(area_km2)) + s(log10(Depth), bs = "ts",
    k = 5) + s(sqrt(DistToShore/1000), bs = "ts", k = 5) + s(log10(Slope),
    bs = "ts", k = 5) + s(ClimSST, bs = "ts", k = 5) + s(I(ClimDistToFront2^(1/3)),
    bs = "ts", k = 5) + s(log10(pmax(ClimEKE, 1e-04)), bs = "ts",
    k = 5) + s(I(ClimDistToAEddy4/1000), bs = "ts", k = 5) +
    s(I(ClimDistToCEddy4/1000), bs = "ts", k = 5) + s(ClimChl1,
    bs = "ts", k = 5)

Parametric coefficients:
            Estimate Std. Error t value Pr(>|t|)
(Intercept) -4.46410    0.04902  -91.06   <2e-16 ***
---
Signif. codes:  0 '***' 0.001 '**' 0.01 '*' 0.05 '.' 0.1 ' ' 1

Approximate significance of smooth terms:
                                edf Ref.df      F  p-value
s(log10(Depth))               3.957      4  83.58  < 2e-16 ***
s(sqrt(DistToShore/1000))     3.783      4  38.66  < 2e-16 ***
s(log10(Slope))               3.609      4  12.15 6.41e-11 ***
s(ClimSST)                    3.861      4 123.88  < 2e-16 ***
s(I(ClimDistToFront2^(1/3)))  3.173      4  27.48  < 2e-16 ***
s(log10(pmax(ClimEKE, 1e-04))) 3.932      4  23.46  < 2e-16 ***
s(I(ClimDistToAEddy4/1000))   1.390      4  10.91 7.77e-12 ***
s(I(ClimDistToCEddy4/1000))   3.157      4 152.05  < 2e-16 ***
s(ClimChl1)                   3.851      4  41.21  < 2e-16 ***
---
Signif. codes:  0 '***' 0.001 '**' 0.01 '*' 0.05 '.' 0.1 ' ' 1

R-sq.(adj) =  0.045   Deviance explained = 37.3%
-REML =  28308  Scale est. = 55.777    n = 104236

All predictors were significant. This is the final model.
Creating term plots.
Diagnostic output from gam.check():

Method: REML   Optimizer: outer newton
full convergence after 12 iterations.
Gradient range [-0.00753176,0.000278031]
(score 28308.01 & scale 55.77694).
Hessian positive definite, eigenvalue range [0.2543896,8503.076].
Model rank =  37 / 37

Basis dimension (k) checking results. Low p-value (k-index<1) may
indicate that k is too low, especially if edf is close to k'.

                                k'   edf k-index p-value
s(log10(Depth))               4.000 3.957   0.752    0.13
s(sqrt(DistToShore/1000))     4.000 3.783   0.743    0.04
s(log10(Slope))               4.000 3.609   0.748    0.09
s(ClimSST)                    4.000 3.861   0.742    0.04
s(I(ClimDistToFront2^(1/3)))  4.000 3.173   0.741    0.04
s(log10(pmax(ClimEKE, 1e-04))) 4.000 3.932   0.750    0.10
s(I(ClimDistToAEddy4/1000))   4.000 1.390   0.739    0.02
s(I(ClimDistToCEddy4/1000))   4.000 3.157   0.743    0.04
s(ClimChl1)                   4.000 3.851   0.738    0.01
```

Predictors retained during the model selection procedure: Depth, DistToShore, Slope, ClimSST, ClimDistToFront2, ClimEKE, ClimDistToAEddy4, ClimDistToCEddy4, ClimChl1

Predictors dropped during the model selection procedure: DistTo125m

Model term plots

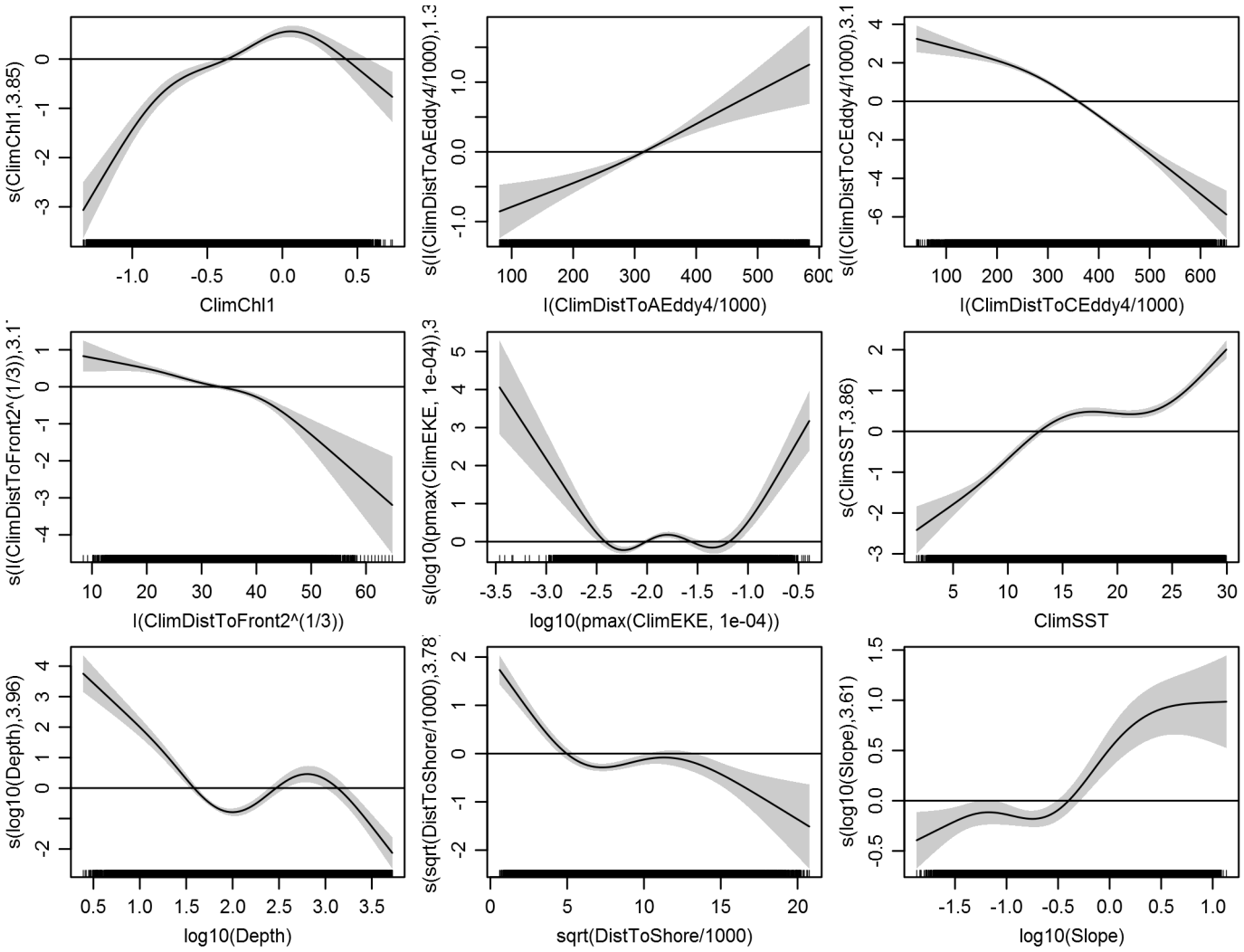

Diagnostic plots

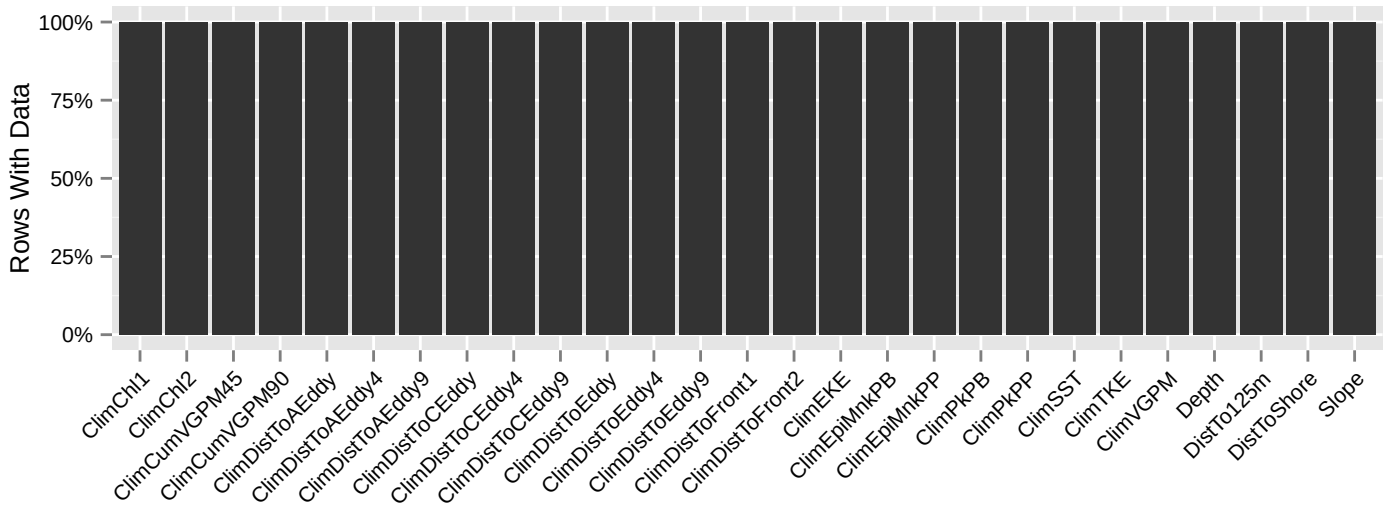

Figure 122: Segments with predictor values for the Bottlenose dolphin Climatological model, Surveyed Area. This plot is used to assess how many segments would be lost by including a given predictor in a model.

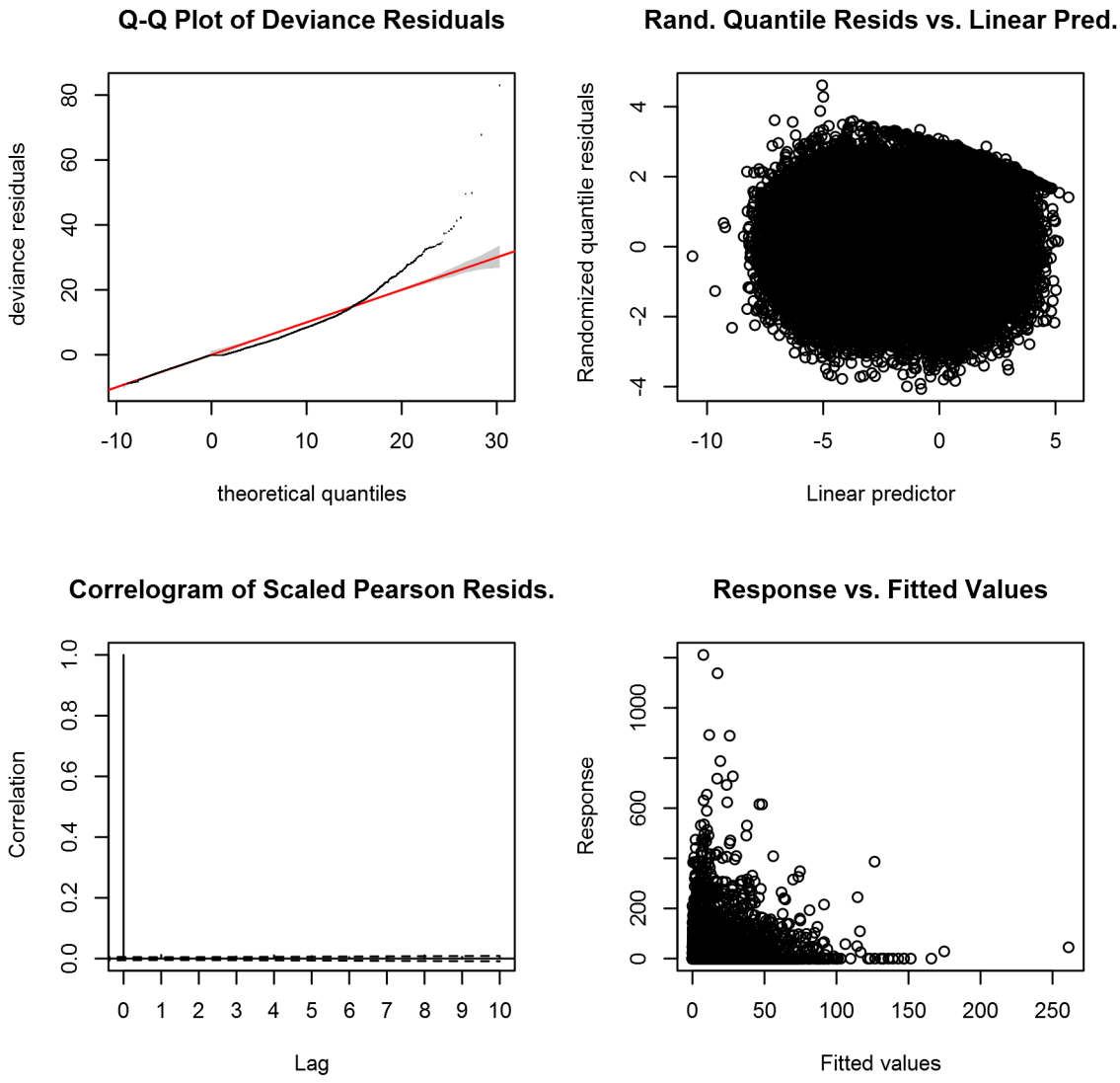

Figure 123: Statistical diagnostic plots for the Bottlenose dolphin Climatological model, Surveyed Area.

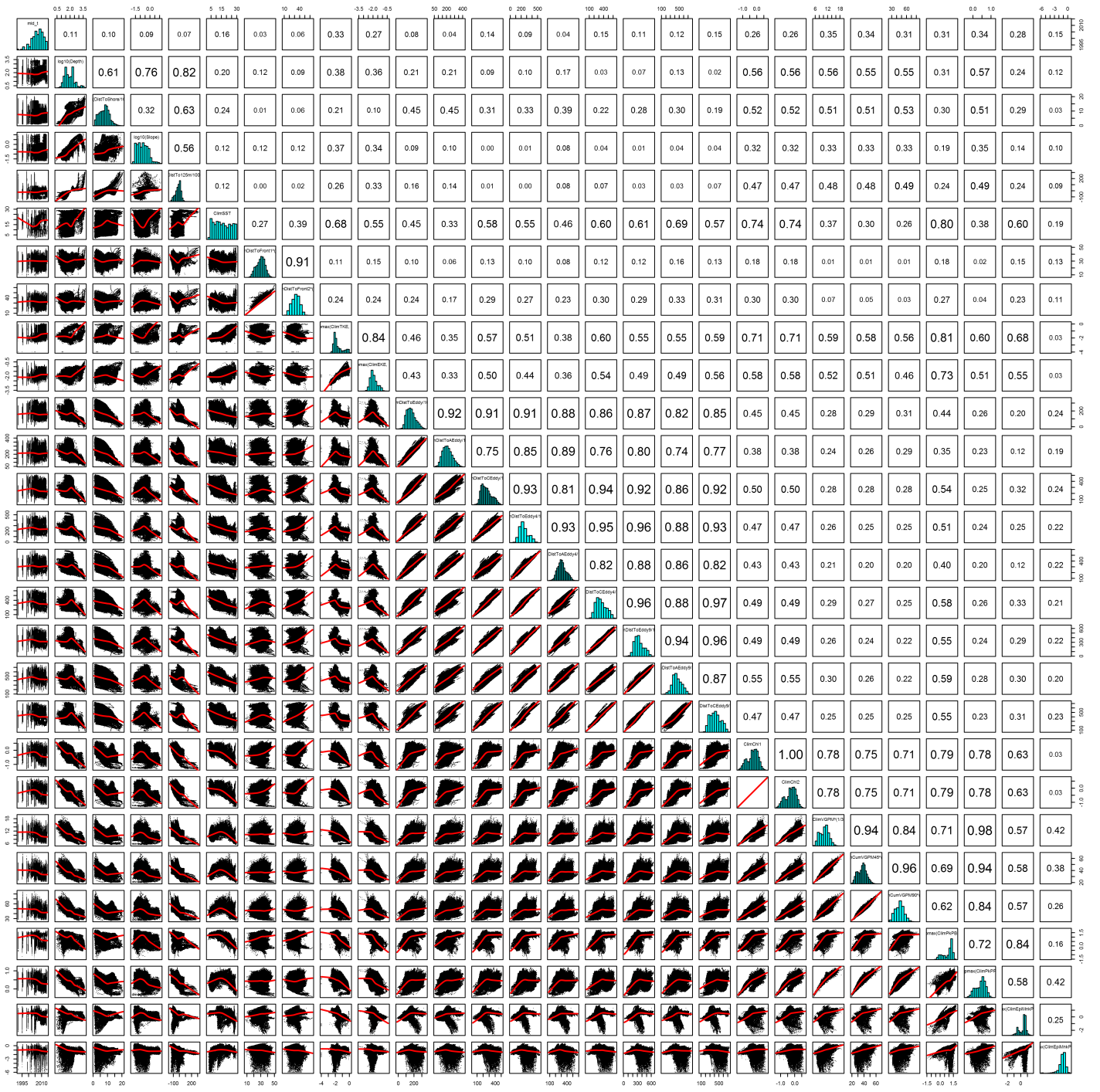

Figure 124: Scatterplot matrix for the Bottlenose dolphin Climatological model, Surveyed Area. This plot is used to inspect the distribution of predictors (via histograms along the diagonal), simple correlation between predictors (via pairwise Pearson coefficients above the diagonal), and linearity of predictor correlations (via scatterplots below the diagonal). This plot is best viewed at high magnification.

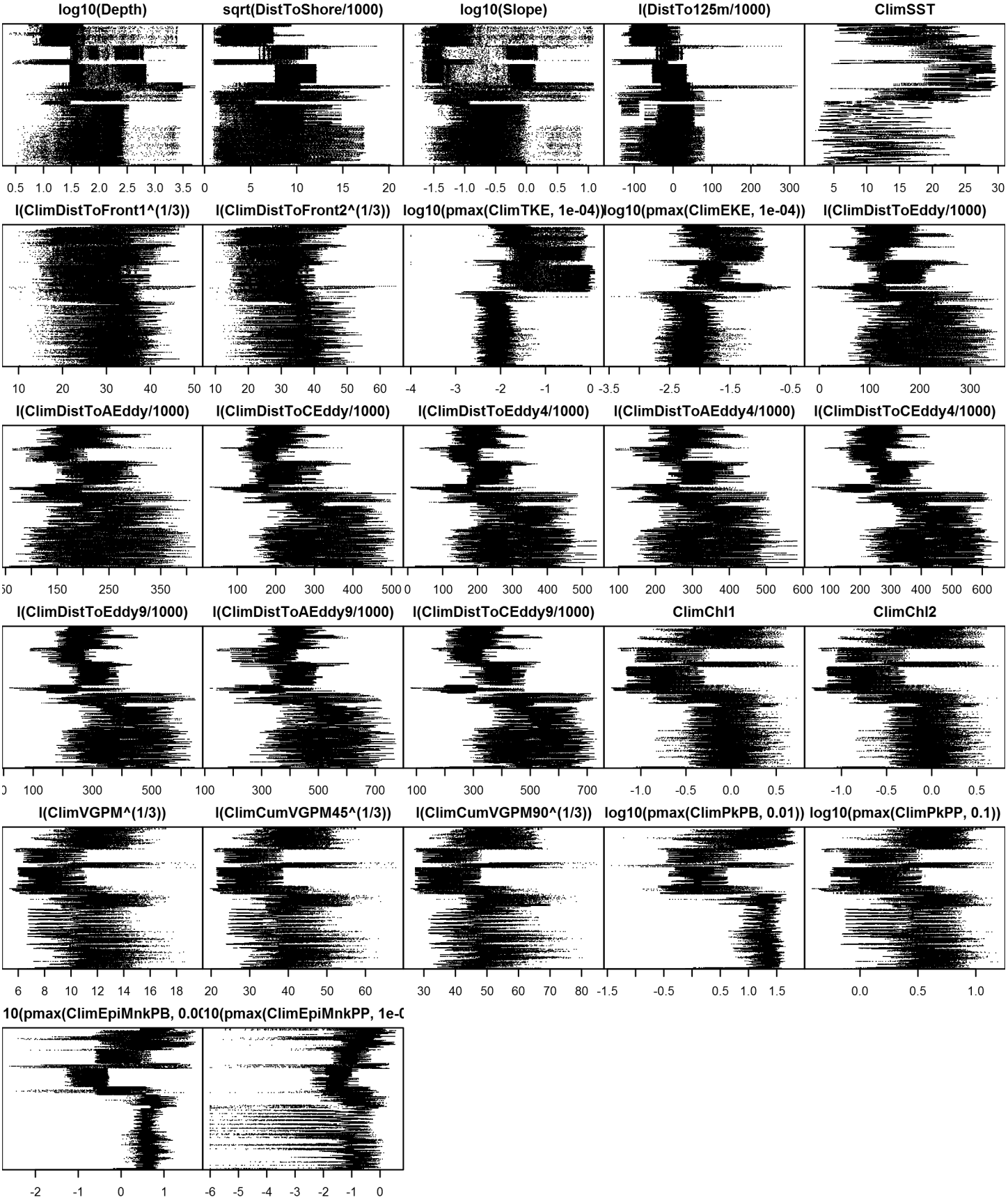

Figure 125: Dotplot for the Bottlenose dolphin Climatological model, Surveyed Area. This plot is used to check for suspicious patterns and outliers in the data. Points are ordered vertically by transect ID, sequentially in time.

Contemporaneous Model

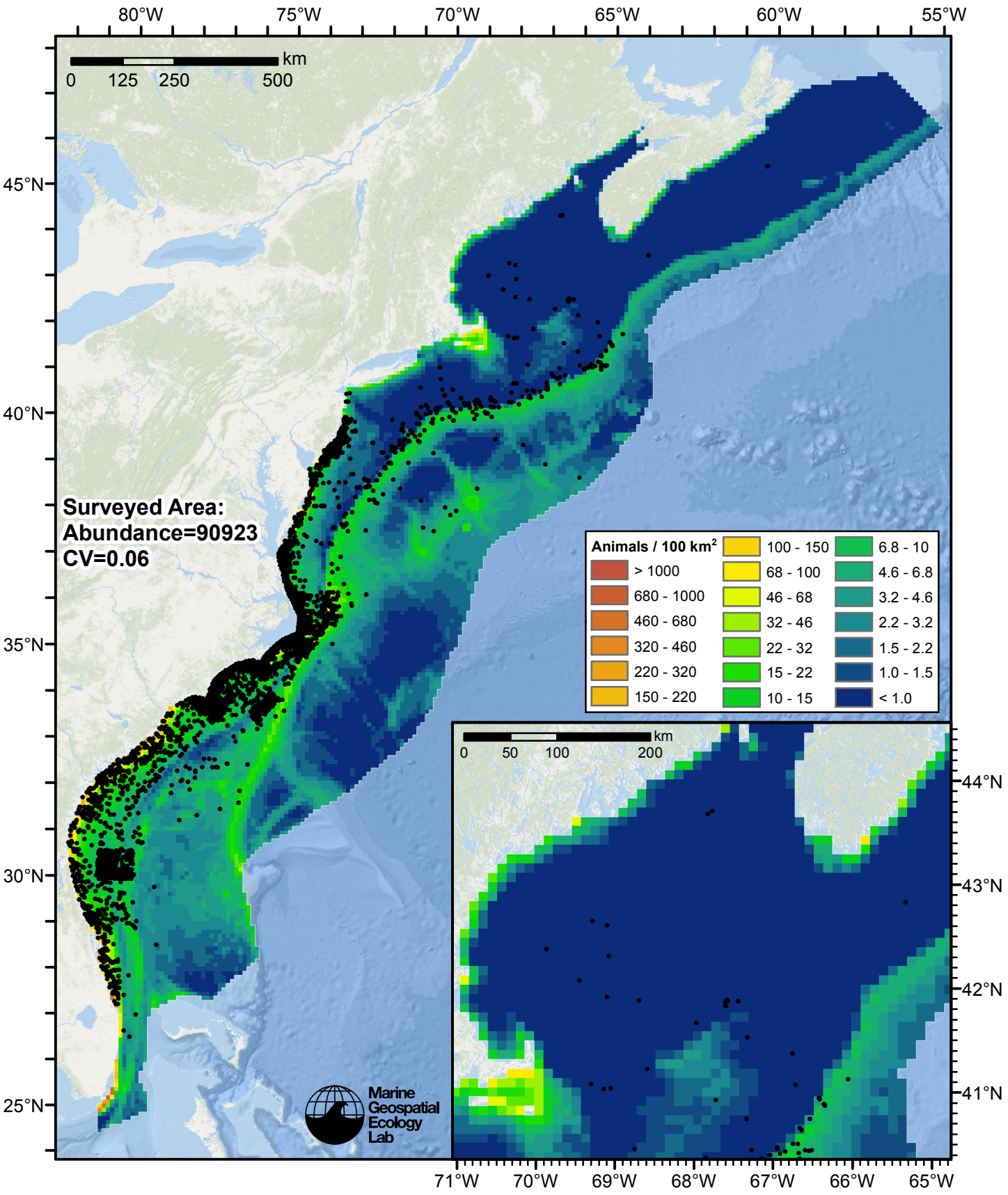

Figure 126: Bottlenose dolphin density predicted by the contemporaneous model that explained the most deviance. Pixels are 10x10 km. The legend gives the estimated individuals per pixel; breaks are logarithmic. Abundance for each region was computed by summing the density cells occuring in that region.

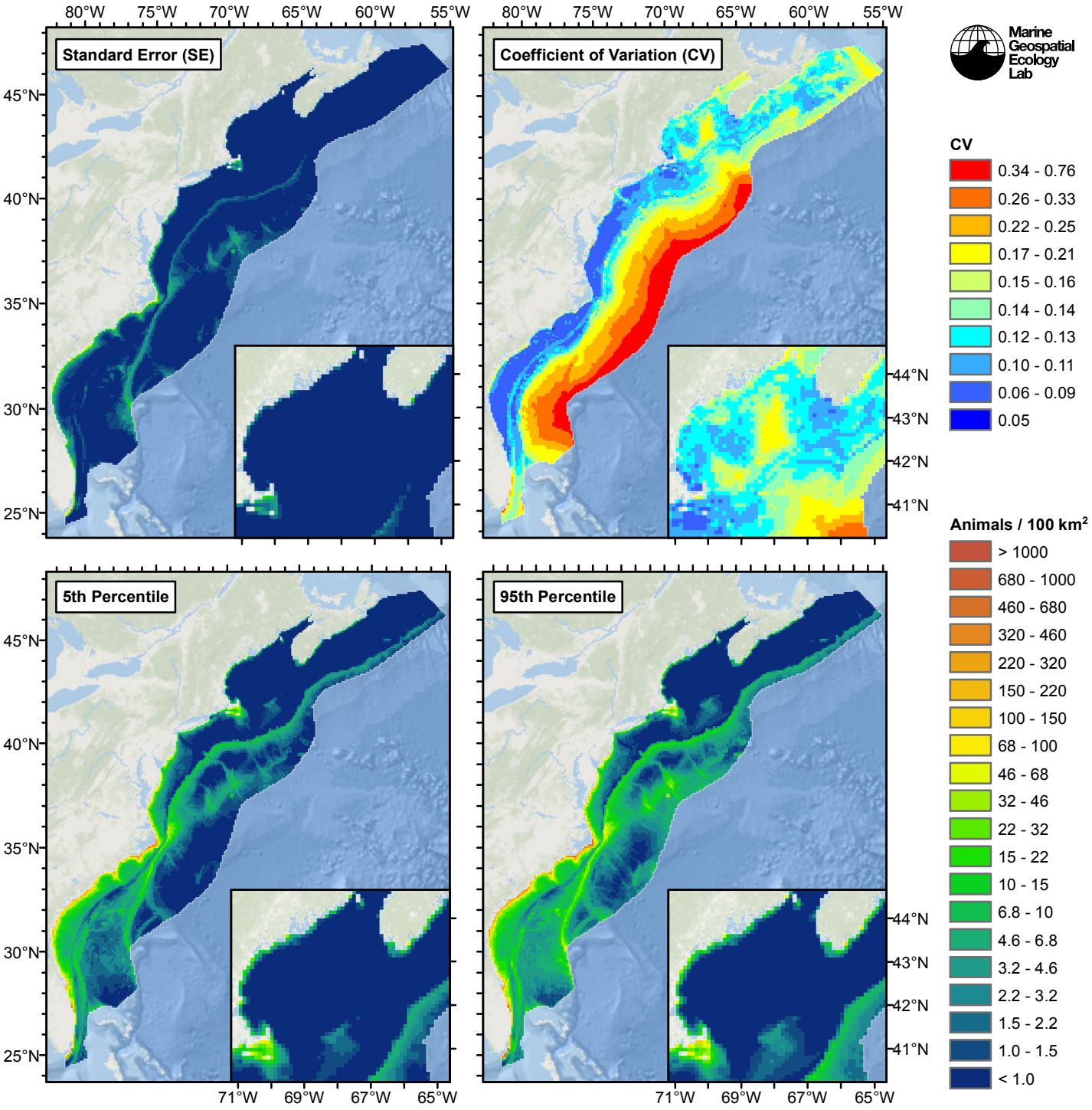

Figure 127: Estimated uncertainty for the contemporaneous model that explained the most deviance. These estimates only incorporate the statistical uncertainty estimated for the spatial model (by the R mgcv package). They do not incorporate uncertainty in the detection functions, g(0) estimates, predictor variables, and so on.

Surveyed Area

Statistical output

```
Rscript.exe: This is mgcv 1.8-3. For overview type 'help("mgcv-package")'.


Family: Tweedie(p=1.364)
```

```
Link function: log

Formula:
abundance ~ offset(log(area_km2)) + s(log10(Depth), bs = "ts",
    k = 5) + s(sqrt(DistToShore/1000), bs = "ts", k = 5) + s(log10(Slope),
    bs = "ts", k = 5) + s(I(DistTo125m/1000), bs = "ts", k = 5) +
    s(SST, bs = "ts", k = 5) + s(I(DistToFront2^(1/3)), bs = "ts",
    k = 5) + s(log10(pmax(TKE, 1e-04)), bs = "ts", k = 5) + s(I(DistToAEddy9/1000),
    bs = "ts", k = 5) + s(I(DistToCEddy9/1000), bs = "ts", k = 5) +
    s(log10(pmax(PkPP, 0.1)), bs = "ts", k = 5)

Parametric coefficients:
            Estimate Std. Error t value Pr(>|t|)
(Intercept) -4.43268    0.04751  -93.29   <2e-16 ***
---
Signif. codes:  0 '***' 0.001 '**' 0.01 '*' 0.05 '.' 0.1 ' ' 1

Approximate significance of smooth terms:
                              edf Ref.df      F  p-value
s(log10(Depth))            3.9772      4 115.99  < 2e-16 ***
s(sqrt(DistToShore/1000))  3.7799      4  32.14  < 2e-16 ***
s(log10(Slope))            3.9391      4  29.58  < 2e-16 ***
s(I(DistTo125m/1000))      3.4655      4  12.15 2.32e-11 ***
s(SST)                     3.9054      4 139.77  < 2e-16 ***
s(I(DistToFront2^(1/3)))   3.0709      4  38.48  < 2e-16 ***
s(log10(pmax(TKE, 1e-04))) 1.9977      4  46.89  < 2e-16 ***
s(I(DistToAEddy9/1000))    0.9222      4   2.01  0.00267 **
s(I(DistToCEddy9/1000))    3.9035      4  57.99  < 2e-16 ***
s(log10(pmax(PkPP, 0.1)))  3.8235      4  49.01  < 2e-16 ***
---
Signif. codes:  0 '***' 0.001 '**' 0.01 '*' 0.05 '.' 0.1 ' ' 1

R-sq.(adj) =  0.0129   Deviance explained = 34.8%
-REML =  25881  Scale est. = 59.82     n = 99937

All predictors were significant. This is the final model.
Creating term plots.
Diagnostic output from gam.check():

Method: REML   Optimizer: outer newton
full convergence after 13 iterations.
Gradient range [-0.002240532,0.001354238]
(score 25880.52 & scale 59.82007).
Hessian positive definite, eigenvalue range [0.2420412,7626.618].
Model rank =  41 / 41

Basis dimension (k) checking results. Low p-value (k-index<1) may
indicate that k is too low, especially if edf is close to k'.

                              k'   edf k-index p-value
s(log10(Depth))            4.000 3.977   0.767    0.21
s(sqrt(DistToShore/1000))  4.000 3.780   0.751    0.02
s(log10(Slope))            4.000 3.939   0.766    0.26
s(I(DistTo125m/1000))      4.000 3.466   0.773    0.40
s(SST)                     4.000 3.905   0.743    0.00
s(I(DistToFront2^(1/3)))   4.000 3.071   0.765    0.16
s(log10(pmax(TKE, 1e-04))) 4.000 1.998   0.764    0.16
s(I(DistToAEddy9/1000))    4.000 0.922   0.766    0.16
```

```
s(I(DistToCEddy9/1000))    4.000 3.904   0.771    0.34
s(log10(pmax(PkPP, 0.1)))  4.000 3.824   0.762    0.12

Predictors retained during the model selection procedure: Depth, DistToShore, Slope, DistTo125m,
SST, DistToFront2, TKE, DistToAEddy9, DistToCEddy9, PkPP

Predictors dropped during the model selection procedure:
```

Model term plots

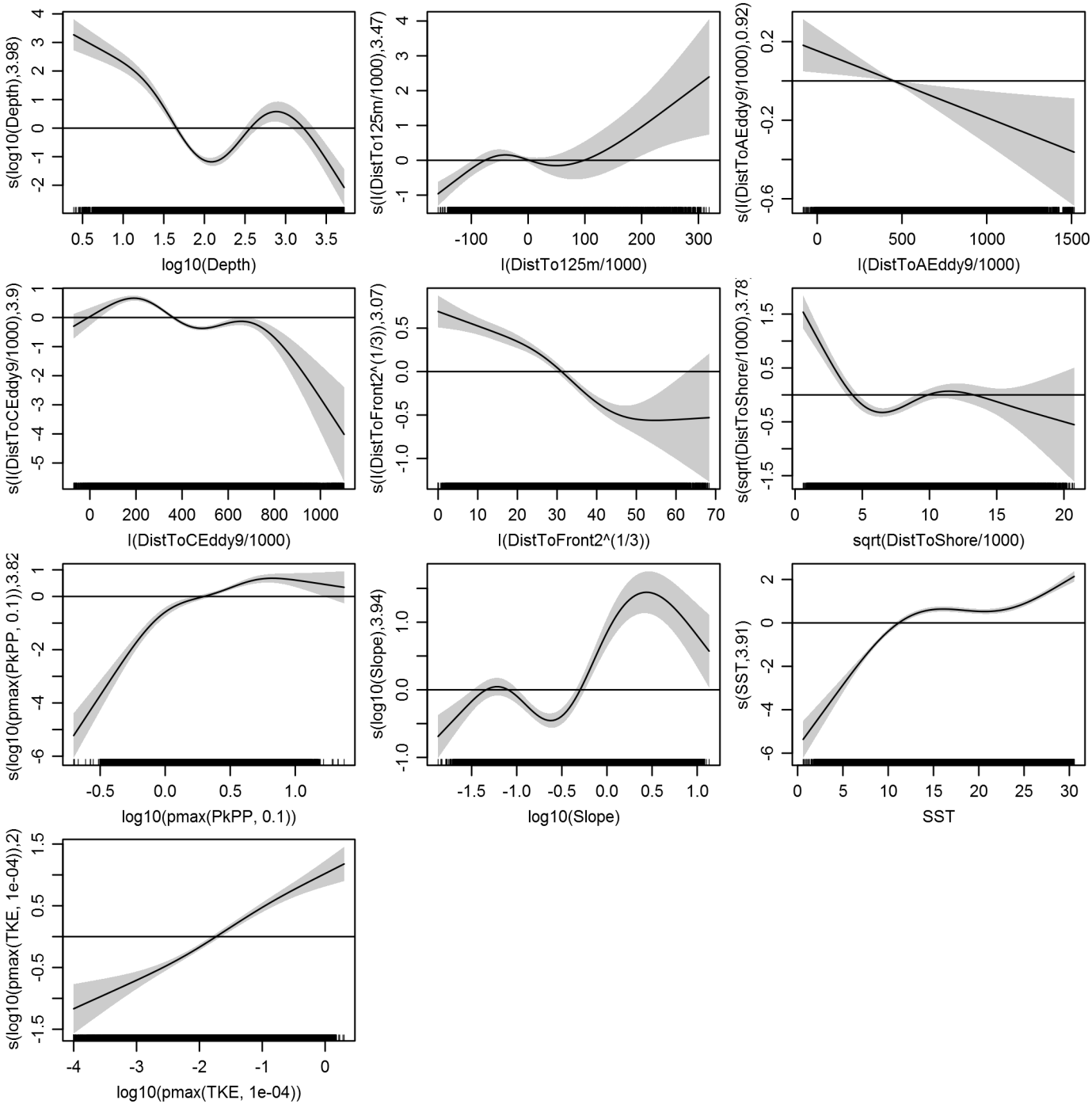

Diagnostic plots

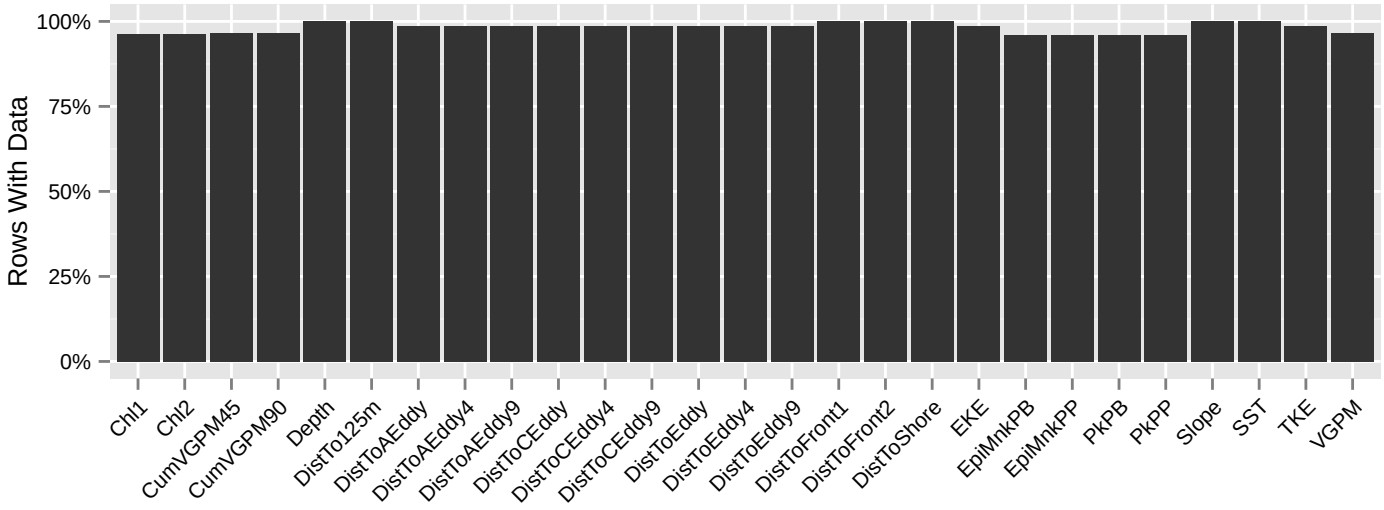

Figure 128: Segments with predictor values for the Bottlenose dolphin Contemporaneous model, Surveyed Area. This plot is used to assess how many segments would be lost by including a given predictor in a model.

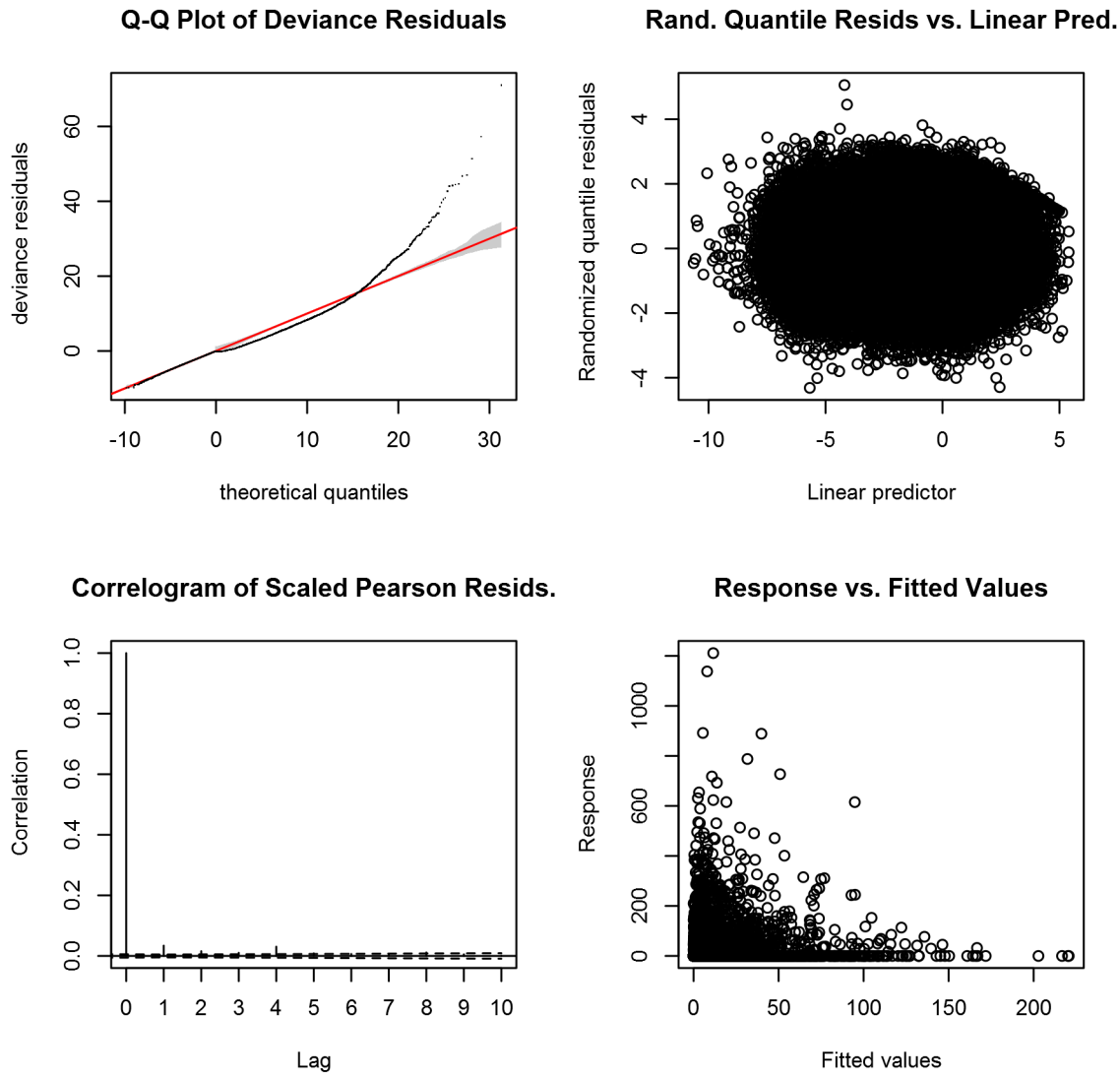

Figure 129: Statistical diagnostic plots for the Bottlenose dolphin Contemporaneous model, Surveyed Area.

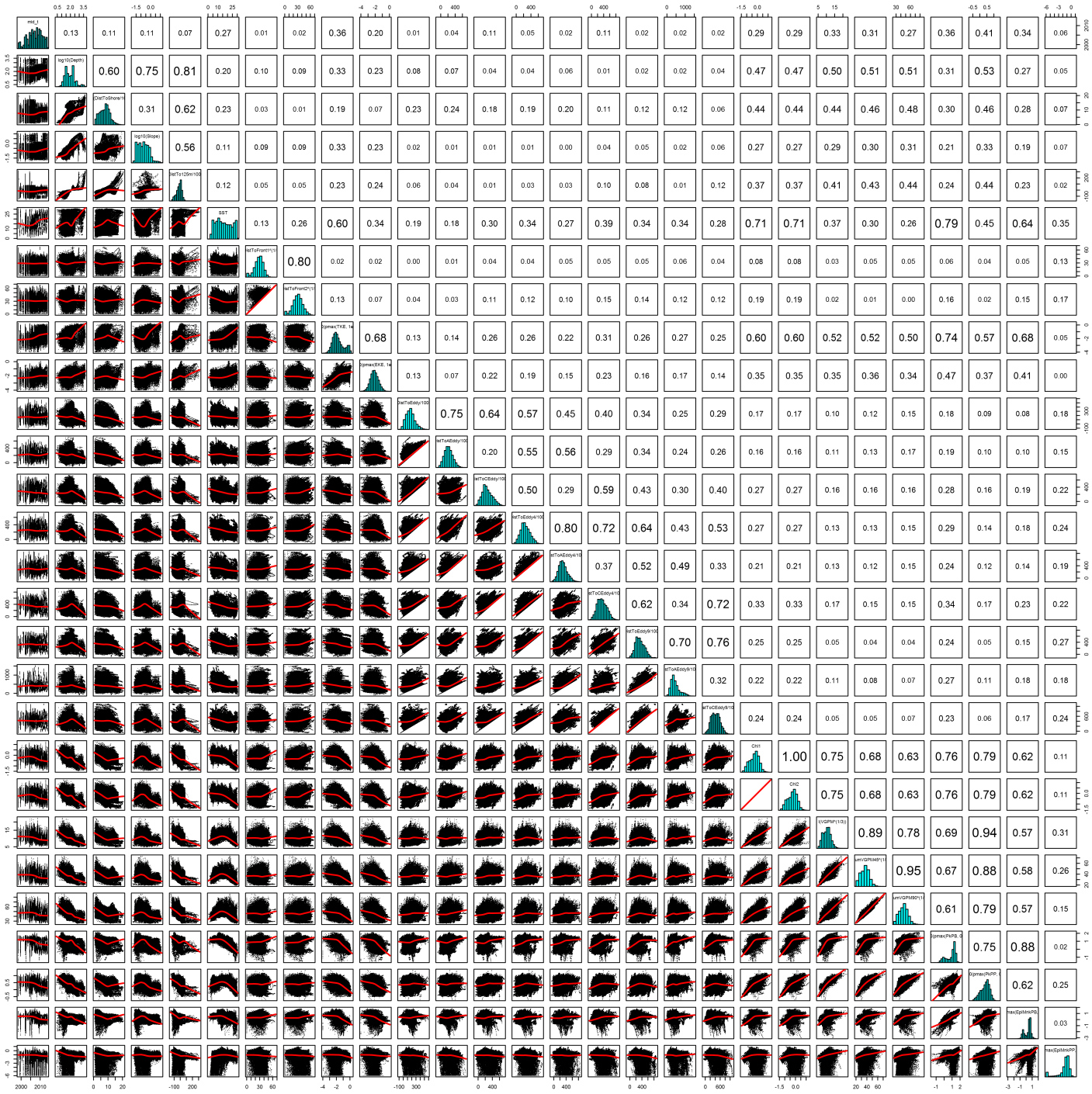

Figure 130: Scatterplot matrix for the Bottlenose dolphin Contemporaneous model, Surveyed Area. This plot is used to inspect the distribution of predictors (via histograms along the diagonal), simple correlation between predictors (via pairwise Pearson coefficients above the diagonal), and linearity of predictor correlations (via scatterplots below the diagonal). This plot is best viewed at high magnification.

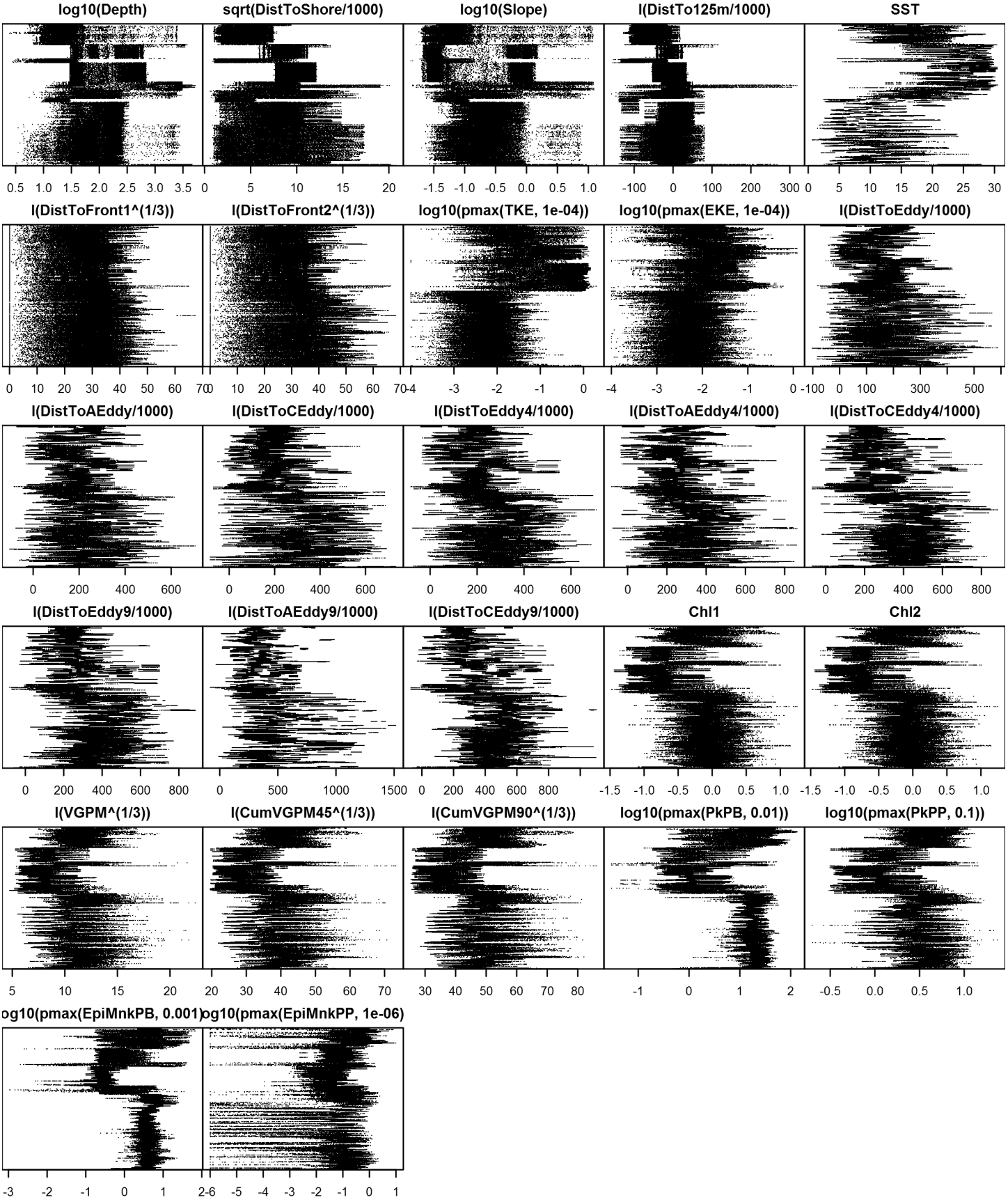

Figure 131: Dotplot for the Bottlenose dolphin Contemporaneous model, Surveyed Area. This plot is used to check for suspicious patterns and outliers in the data. Points are ordered vertically by transect ID, sequentially in time.

Climatological Same Segments Model

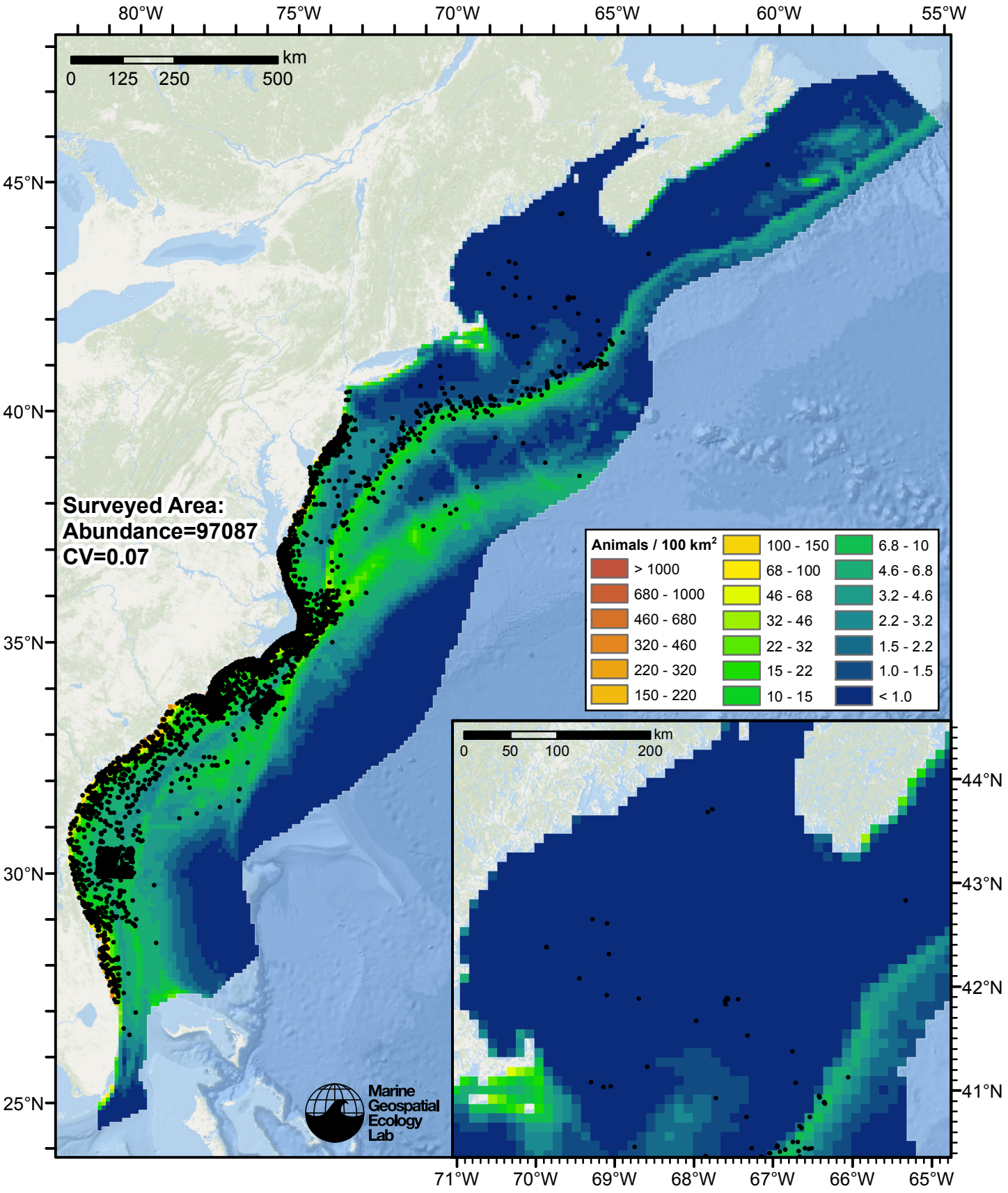

Figure 132: Bottlenose dolphin density predicted by the climatological same segments model that explained the most deviance. Pixels are 10x10 km. The legend gives the estimated individuals per pixel; breaks are logarithmic. Abundance for each region was computed by summing the density cells occuring in that region.

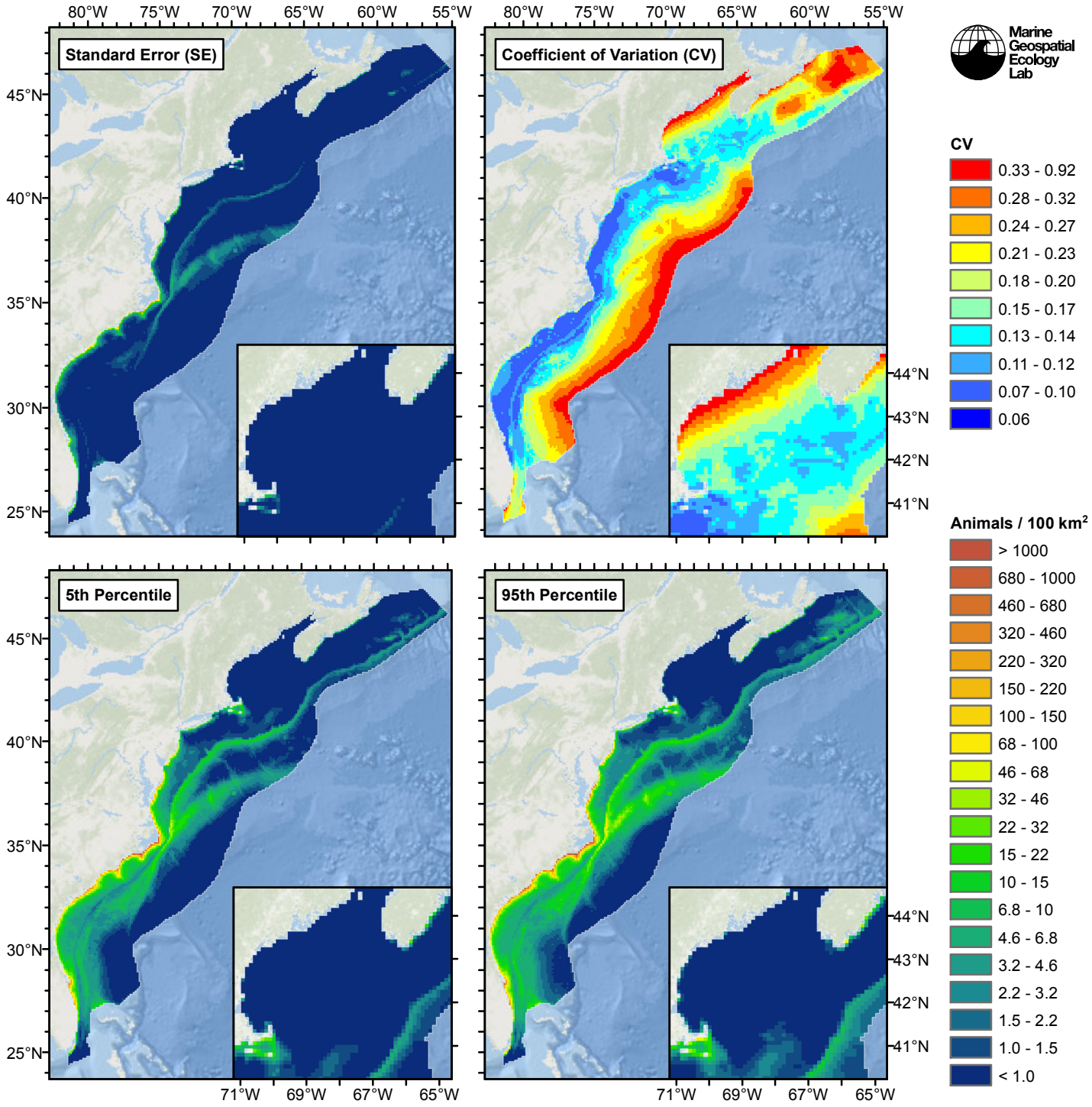

Figure 133: Estimated uncertainty for the climatological same segments model that explained the most deviance. These estimates only incorporate the statistical uncertainty estimated for the spatial model (by the R mgcv package). They do not incorporate uncertainty in the detection functions, g(0) estimates, predictor variables, and so on.

Surveyed Area

Statistical output

```
Rscript.exe: This is mgcv 1.8-3. For overview type 'help("mgcv-package")'.


Family: Tweedie(p=1.352)
```

```
Link function: log

Formula:
abundance ~ offset(log(area_km2)) + s(log10(Depth), bs = "ts",
    k = 5) + s(sqrt(DistToShore/1000), bs = "ts", k = 5) + s(log10(Slope),
    bs = "ts", k = 5) + s(ClimSST, bs = "ts", k = 5) + s(I(ClimDistToFront2^(1/3)),
    bs = "ts", k = 5) + s(log10(pmax(ClimEKE, 1e-04)), bs = "ts",
    k = 5) + s(I(ClimDistToAEddy4/1000), bs = "ts", k = 5) +
    s(I(ClimDistToCEddy4/1000), bs = "ts", k = 5) + s(ClimChl1,
    bs = "ts", k = 5)

Parametric coefficients:
            Estimate Std. Error t value Pr(>|t|)
(Intercept) -4.53297    0.05237  -86.55   <2e-16 ***
---
Signif. codes:  0 '***' 0.001 '**' 0.01 '*' 0.05 '.' 0.1 ' ' 1

Approximate significance of smooth terms:
                                edf Ref.df       F  p-value
s(log10(Depth))               3.940      4  68.247  < 2e-16 ***
s(sqrt(DistToShore/1000))     3.749      4  35.340  < 2e-16 ***
s(log10(Slope))               3.625      4  13.360 5.21e-12 ***
s(ClimSST)                    3.840      4 116.696  < 2e-16 ***
s(I(ClimDistToFront2^(1/3)))  3.536      4  25.650  < 2e-16 ***
s(log10(pmax(ClimEKE, 1e-04))) 3.927     4  20.895  < 2e-16 ***
s(I(ClimDistToAEddy4/1000))   1.146      4   7.953 6.81e-09 ***
s(I(ClimDistToCEddy4/1000))   3.240      4 143.640  < 2e-16 ***
s(ClimChl1)                   3.822      4  36.346  < 2e-16 ***
---
Signif. codes:  0 '***' 0.001 '**' 0.01 '*' 0.05 '.' 0.1 ' ' 1

R-sq.(adj) =  0.0425   Deviance explained = 37.4%
-REML =  25640  Scale est. = 57.612    n = 99937

All predictors were significant. This is the final model.
Creating term plots.
Diagnostic output from gam.check():

Method: REML   Optimizer: outer newton
full convergence after 14 iterations.
Gradient range [-0.0007473531,0.0005834007]
(score 25640.33 & scale 57.6116).
Hessian positive definite, eigenvalue range [0.4088298,7787.253].
Model rank =  37 / 37

Basis dimension (k) checking results. Low p-value (k-index<1) may
indicate that k is too low, especially if edf is close to k'.

                                k'   edf k-index p-value
s(log10(Depth))               4.000 3.940   0.706    0.00
s(sqrt(DistToShore/1000))     4.000 3.749   0.748    0.60
s(log10(Slope))               4.000 3.625   0.709    0.00
s(ClimSST)                    4.000 3.840   0.722    0.03
s(I(ClimDistToFront2^(1/3)))  4.000 3.536   0.734    0.12
s(log10(pmax(ClimEKE, 1e-04))) 4.000 3.927  0.736    0.20
s(I(ClimDistToAEddy4/1000))   4.000 1.146   0.730    0.06
s(I(ClimDistToCEddy4/1000))   4.000 3.240   0.708    0.00
s(ClimChl1)                   4.000 3.822   0.728    0.06
```

Predictors retained during the model selection procedure: Depth, DistToShore, Slope, ClimSST, ClimDistToFront2, ClimEKE, ClimDistToAEddy4, ClimDistToCEddy4, ClimChl1

Predictors dropped during the model selection procedure: DistTo125m

Model term plots

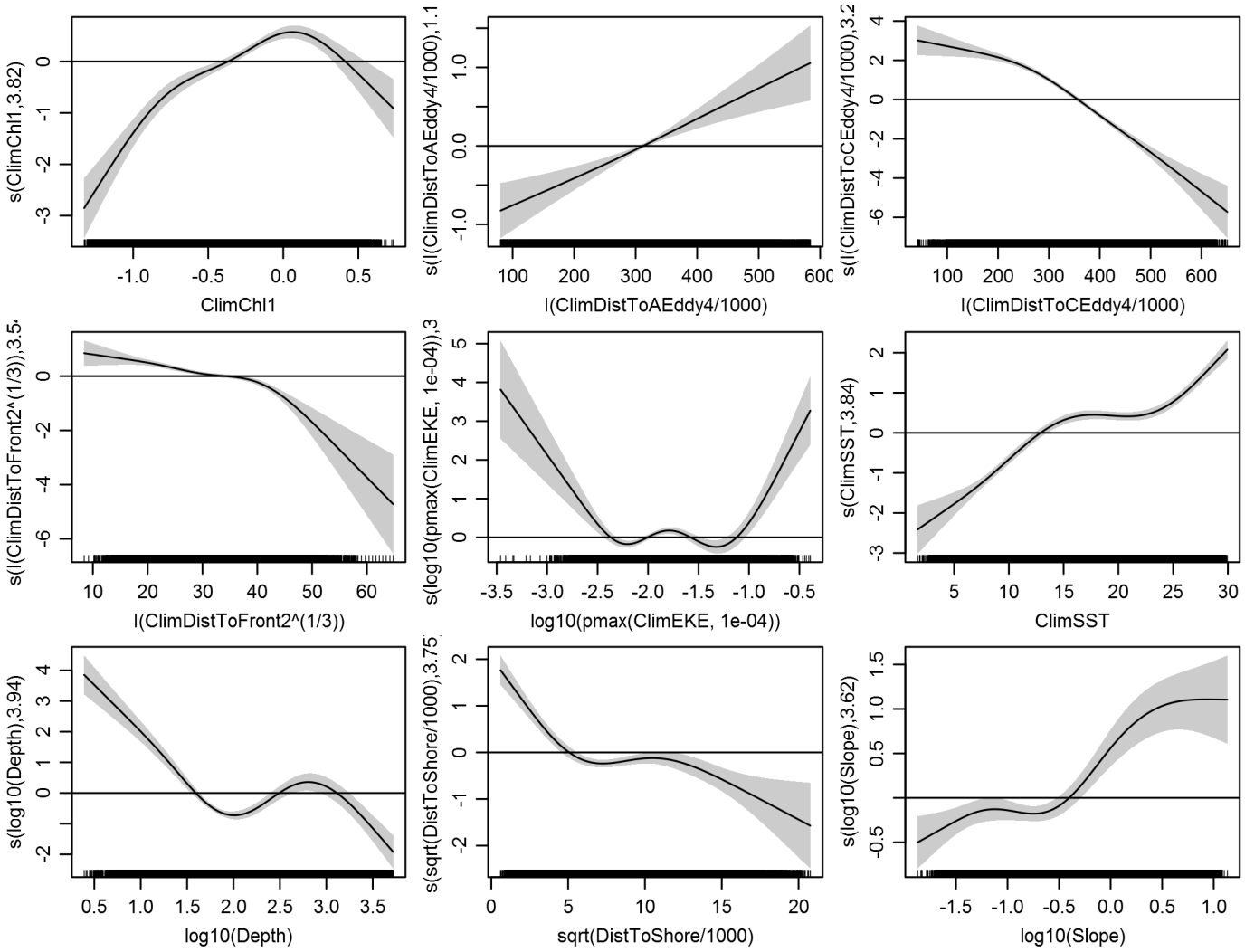

Diagnostic plots

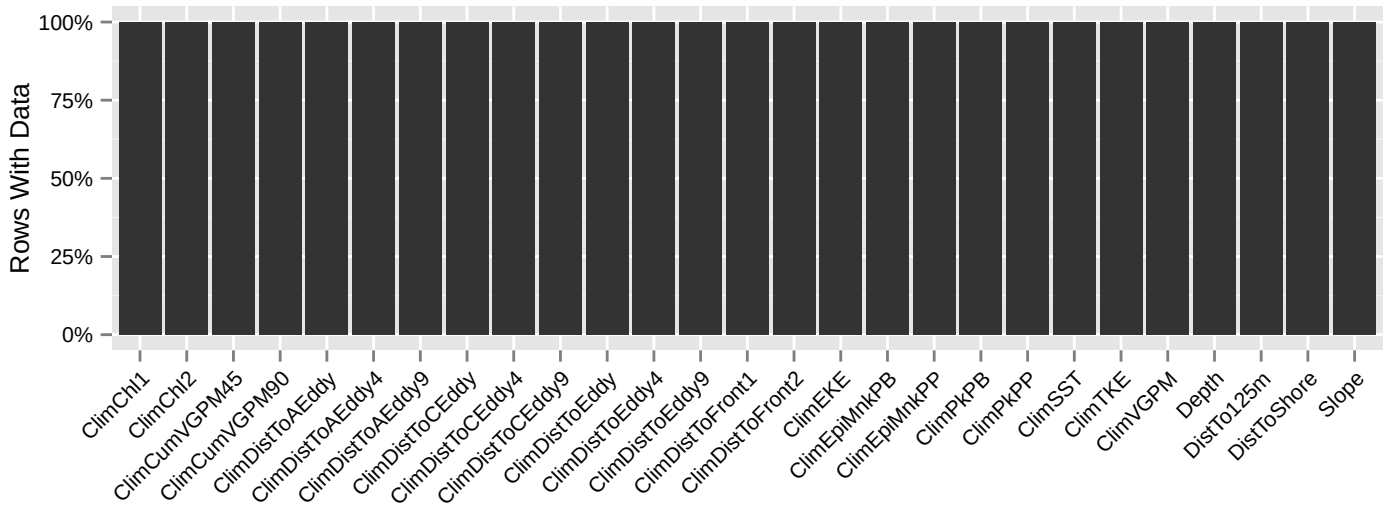

Figure 134: Segments with predictor values for the Bottlenose dolphin Climatological model, Surveyed Area. This plot is used to assess how many segments would be lost by including a given predictor in a model.

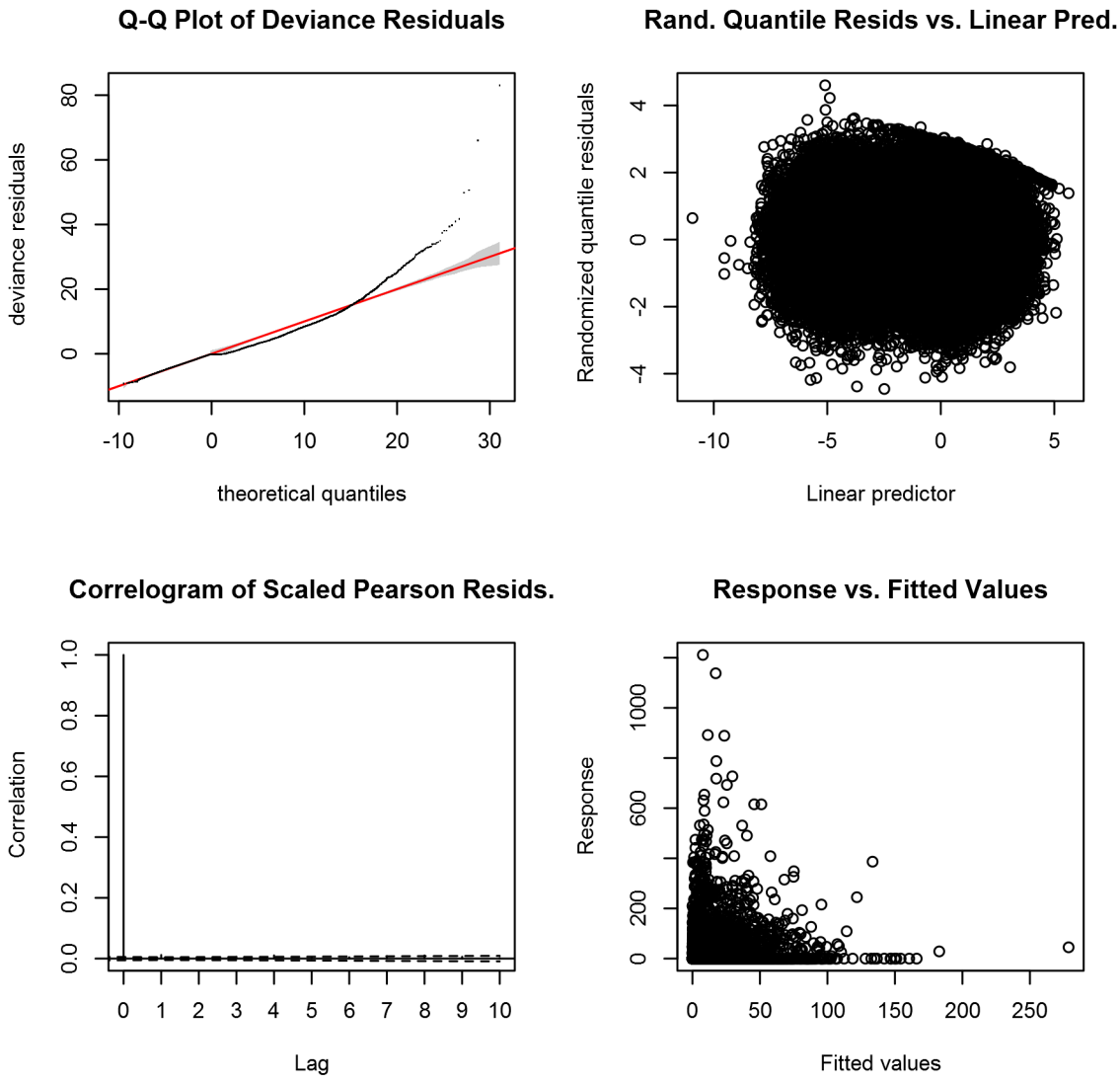

Figure 135: Statistical diagnostic plots for the Bottlenose dolphin Climatological model, Surveyed Area.

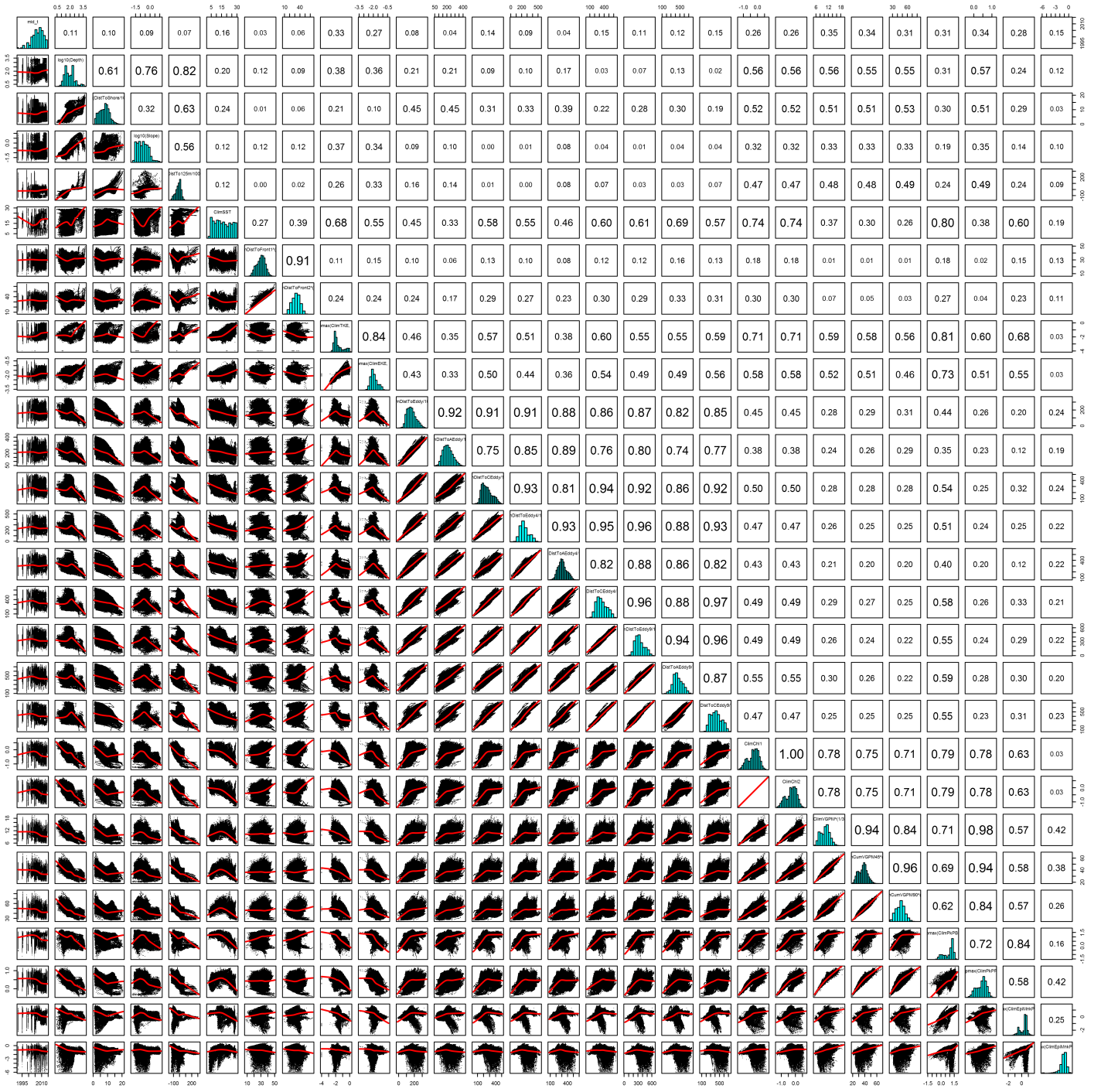

Figure 136: Scatterplot matrix for the Bottlenose dolphin Climatological model, Surveyed Area. This plot is used to inspect the distribution of predictors (via histograms along the diagonal), simple correlation between predictors (via pairwise Pearson coefficients above the diagonal), and linearity of predictor correlations (via scatterplots below the diagonal). This plot is best viewed at high magnification.

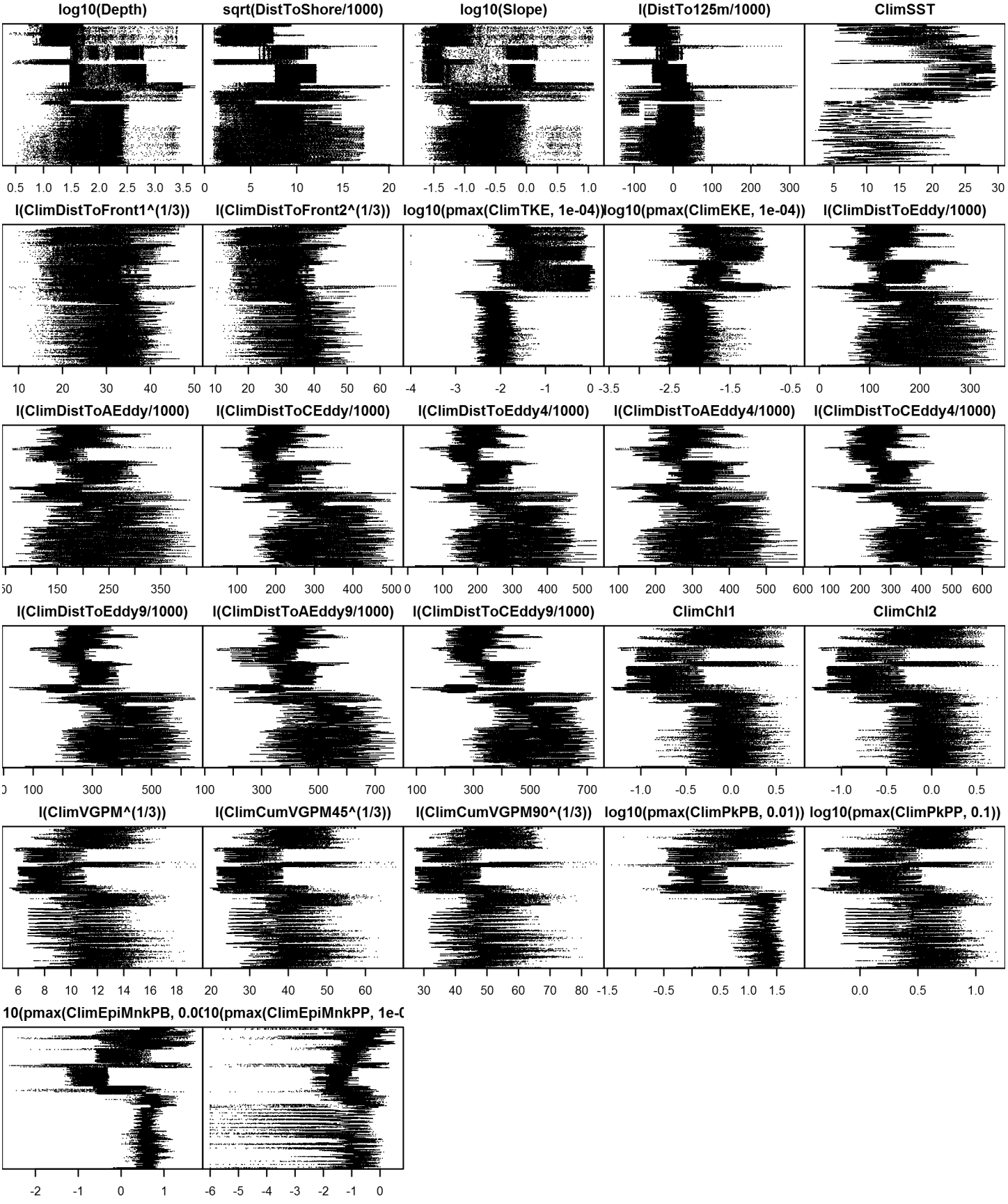

Figure 137: Dotplot for the Bottlenose dolphin Climatological model, Surveyed Area. This plot is used to check for suspicious patterns and outliers in the data. Points are ordered vertically by transect ID, sequentially in time.

Model Comparison

Spatial Model Performance

The table below summarizes the performance of the candidate spatial models that were tested. The first model contained only physiographic predictors. Subsequent models added additional suites of predictors of based on when they became available via remote sensing.

For each model, three versions were fitted; the % Dev Expl columns give the % deviance explained by each one. The "climatological" models were fitted to 8-day climatologies of the environmental predictors. Because the environmental predictors were always available, no segments were lost, allowing these models to consider the maximal amount of survey data. The "contemporaneous" models were fitted to day-of-sighting images of the environmental predictors; these were smoothed to reduce data loss due to clouds, but some segments still failed to retrieve environmental values and were lost. Finally, the "climatological same segments" models fitted climatological predictors to the segments retained by the contemporaneous model, so that the explantory power of the two types of predictors could be directly compared. For each of the three models, predictors were selected independently via shrinkage smoothers; thus the three models did not necessarily utilize the same predictors.

Predictors derived from ocean currents first became available in January 1993 after the launch of the TOPEX/Poseidon satellite; productivity predictors first became available in September 1997 after the launch of the SeaWiFS sensor. Contemporaneous and climatological same segments models considering these predictors usually suffered data loss. Date Range shows the years spanned by the retained segments. The Segments column gives the number of segments retained; % Lost gives the percentage lost.

Predictors	Climatol % Dev Expl	Contemp % Dev Expl	Climatol Same Segs % Dev Expl	Segments	% Lost	Date Range
Phys	23.0			104236		1992-2014
Phys+SST	30.9	30.7	30.9	104236	0.0	1992-2014
Phys+SST+Curr	36.5	34.0	36.7	102911	1.3	1995-2013
Phys+SST+Curr+Prod	37.3	34.8	37.4	99937	4.1	1998-2013

Table 63: Deviance explained by the candidate density models.

Abundance Estimates

The table below shows the estimated mean abundance (number of animals) within the study area, for the models that explained the most deviance for each model type. Mean abundance was calculated by first predicting density maps for a series of time steps, then computing the abundance for each map, and then averaging the abundances. For the climatological models, we used 8-day climatologies, resulting in 46 abundance maps. For the contemporaneous models, we used daily images, resulting in 365 predicted abundance maps per year that the prediction spanned. The Dates column gives the dates to which the estimates apply. For our models, these are the years for which both survey data and remote sensing data were available.

The Assumed g(0)=1 column specifies whether the abundance estimate assumed that detection was certain along the survey trackline. Studies that assumed this did not correct for availability or perception bias, and therefore underestimated abundance. The In our models column specifies whether the survey data from the study was also used in our models. If not, the study provides a completely independent estimate of abundance.

Dates	Model or study	Estimated abundance	CV	Assumed g(0)=1	In our models
1992-2014	Climatological model*	97476	0.06	No	
1998-2013	Contemporaneous model	90923	0.06	No	
1992-2014	Climatological same segments model	97087	0.07	No	

2010, 2011	Central Florida coastal stock	4895	0.71	No	No
2010, 2011	Northern Florida coastal stock	1219	0.67	No	No
2010, 2011	South Carolina/Georgia coastal stock	4377	0.43	No	No
2010, 2011	Southern migratory coastal stock	9173	0.46	No	No
2010, 2011	Northern migratory coastal stock	11548	0.36	No	No
Jun-Aug 2011	Offshore stock: central Virginia to lower Bay of Fundy (Waring et al. 2014)	26766	0.52	No	No
Jun-Aug 2011	Offshore stock: central Florida to central Virginia	50766	0.55	No	No
Jun-Aug 2011	Offshore stock: central Florida to lower Bay of Fundy, combined	77532	0.40	No	No
2010, 2011	All stocks, combined	108744			
2002, 2004	Central Florida coastal stock	6318	0.26	No	Yes
2002, 2004	Northern Florida coastal stock	3064	0.24	No	Yes
2002, 2004	South Carolina/Georgia coastal stock	7738	0.23	No	Yes
2002	Southern migratory coastal stock	12482	0.32	No	Yes
2002	Northern migratory coastal stock	9604	0.36	No	Yes
Jun-Aug 2004	Offshore stock: Maryland to Bay of Fundy (Waring et al. 2007)	9786	0.56	No	Yes
Jun-Aug 2004	Offshore stock: Florida to Maryland	44953	0.26	No	Yes
Jun-Aug 2004	Offshore stock: Florida to Bay of Fundy, combined	54739		No	Yes
2002, 2004	All stocks, combined	93945			

Table 64: Estimated mean abundance within the study area. We selected the model marked with * as our best estimate of the abundance and distribution of this taxon. For comparison, independent abundance estimates from NOAA technical reports and/or the scientific literature are shown. Please see the Discussion section below for our evaluation of our models compared to the other estimates. Note that our abundance estimates are averaged over the whole year, while the other studies may have estimated abundance for specific months or seasons. Our coefficients of variation (CVs) underestimate the true uncertainty in our estimates, as they only incorporated the uncertainty of the GAM stage of our models. Other sources of uncertainty include the detection functions and g(0) estimates. It was not possible to incorporate these into our CVs without undertaking a computationally-prohibitive bootstrap; we hope to attempt that in a future version of our models.

Density Maps

Climatological Model

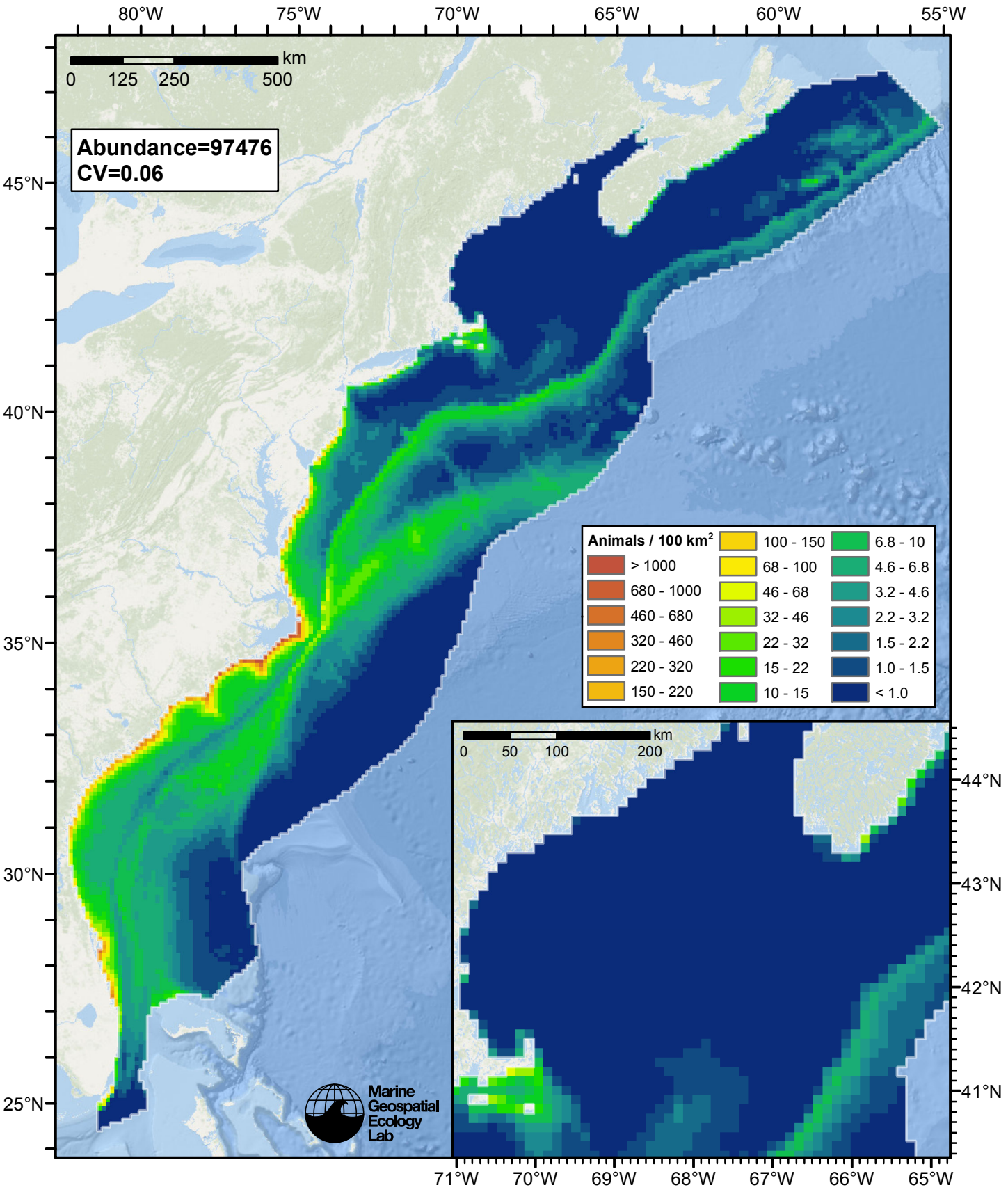

Figure 138: Bottlenose dolphin density and abundance predicted by the climatological model that explained the most deviance. Regions inside the study area (white line) where the background map is visible are areas we did not model (see text).

Contemporaneous Model

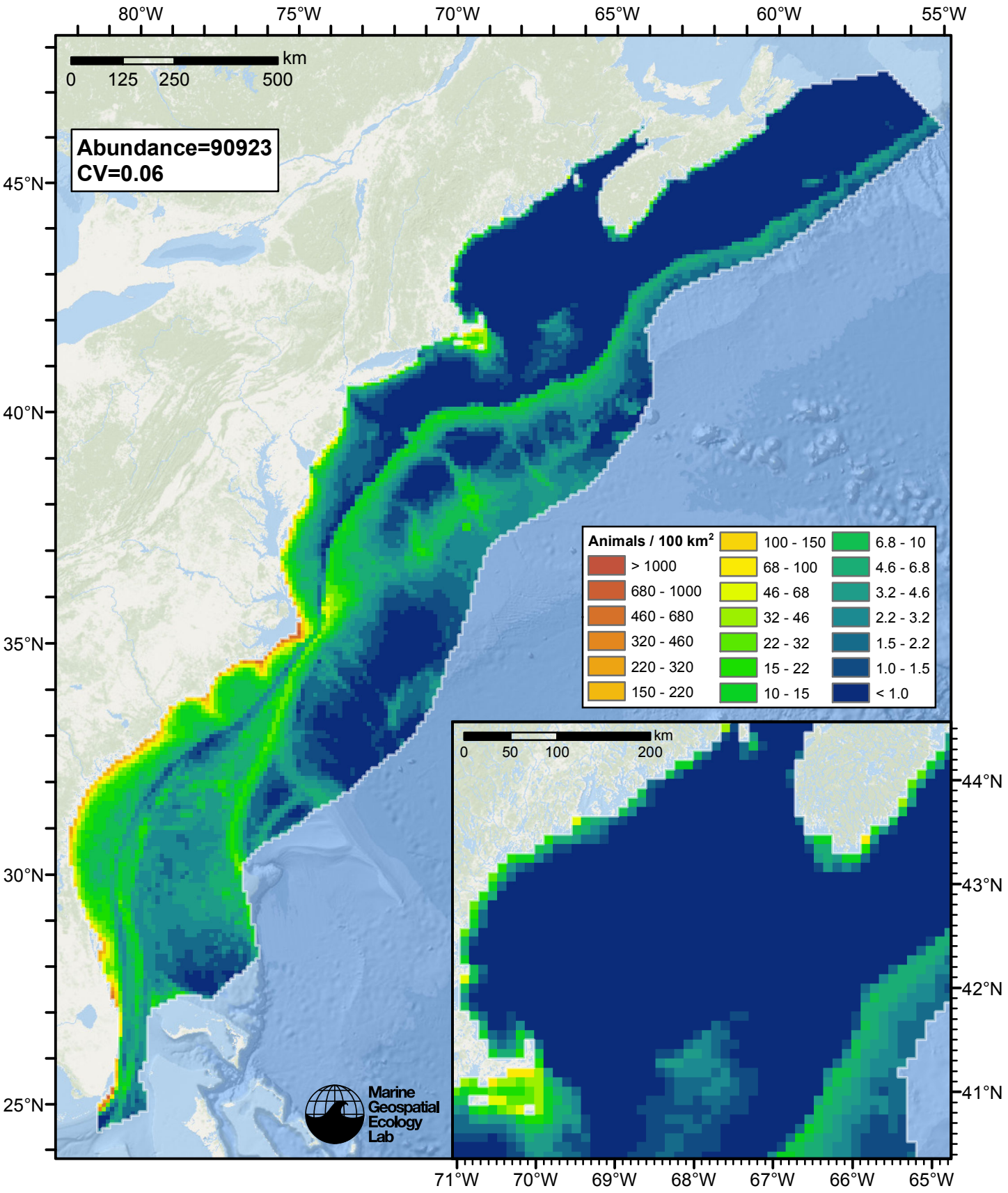

Figure 139: Bottlenose dolphin density and abundance predicted by the contemporaneous model that explained the most deviance. Regions inside the study area (white line) where the background map is visible are areas we did not model (see text).

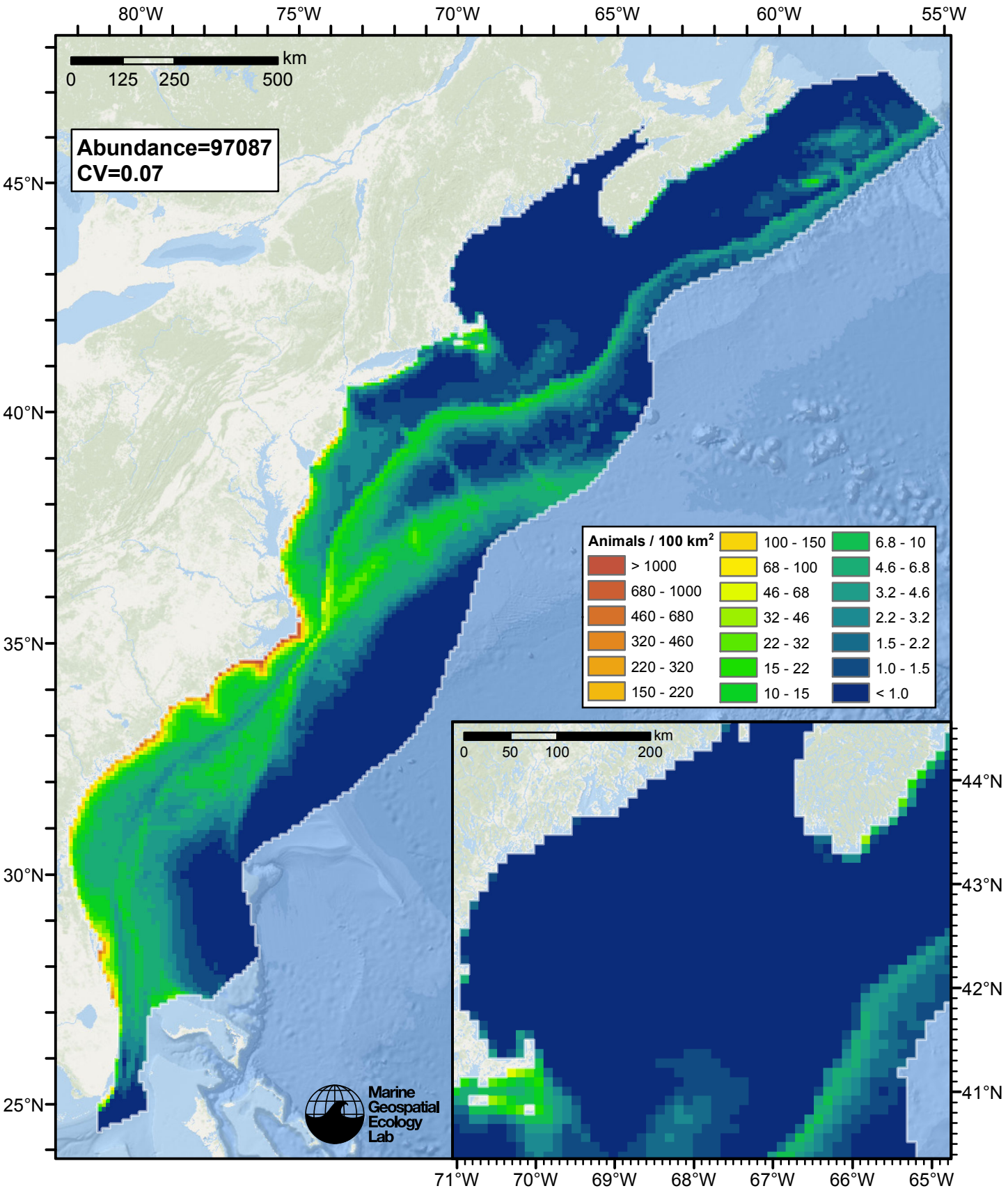

Figure 140: Bottlenose dolphin density and abundance predicted by the climatological same segments model that explained the most deviance. Regions inside the study area (white line) where the background map is visible are areas we did not model (see text).

Temporal Variability

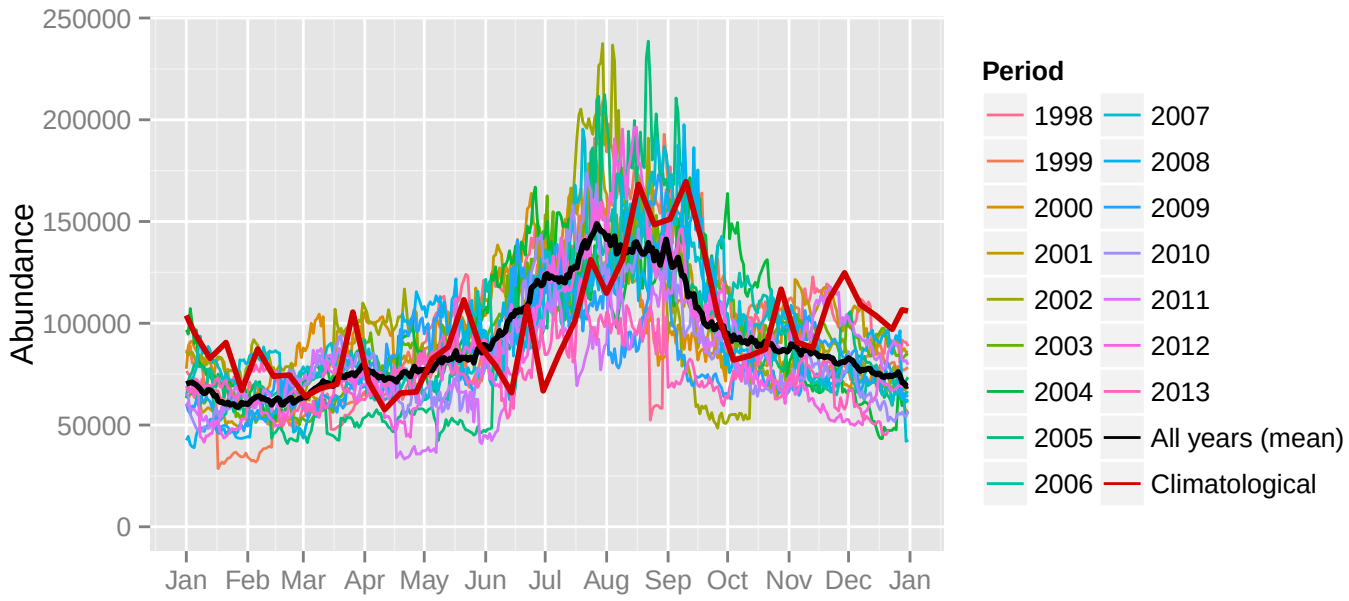

Figure 141: Comparison of Bottlenose dolphin abundance predicted at a daily time step for different time periods. Individual years were predicted using contemporaneous models. "All years (mean)" averages the individual years, giving the mean annual abundance of the contemporaneous model. "Climatological" was predicted using the climatological model. The results for the climatological same segments model are not shown.

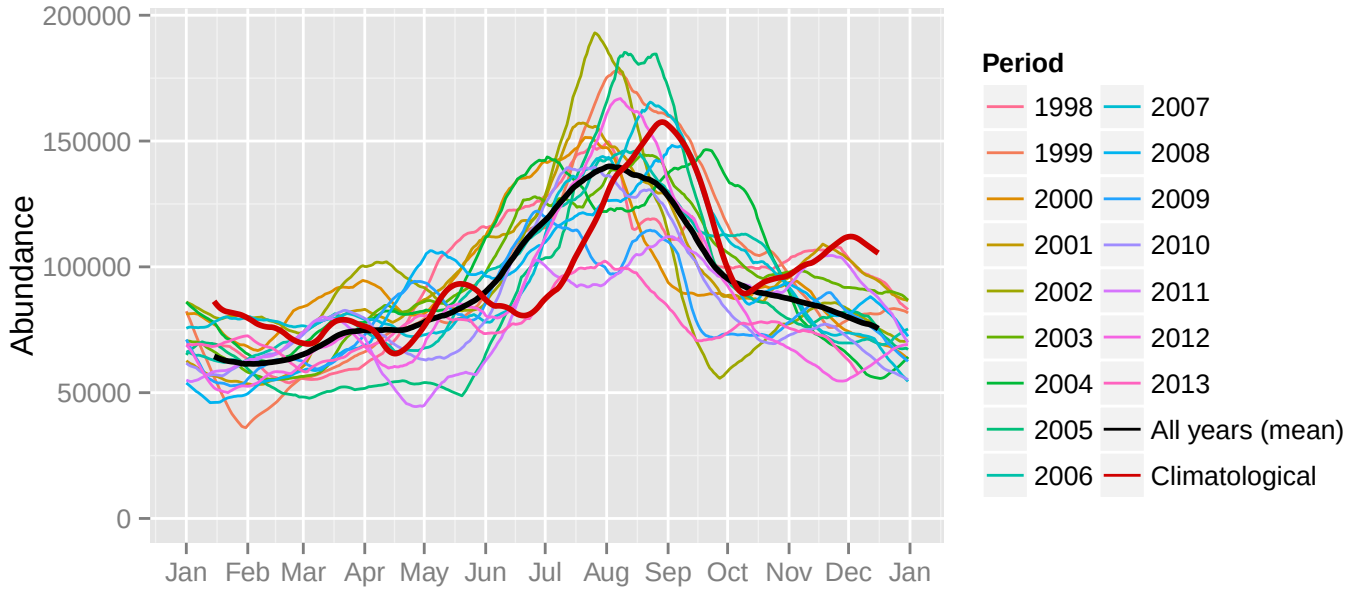

Figure 142: The same data as the preceding figure, but with a 30-day moving average applied.

Climatological Model

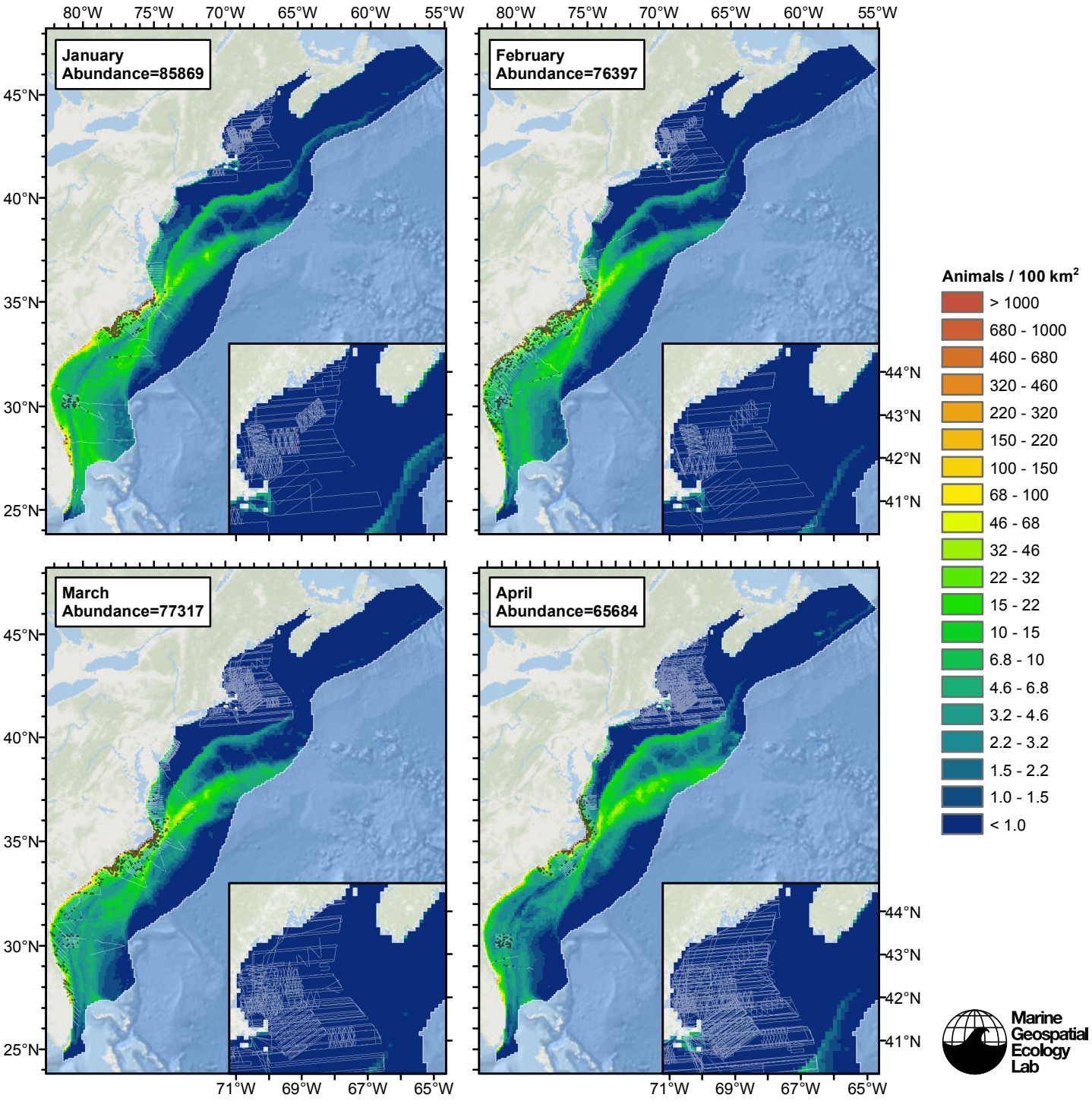

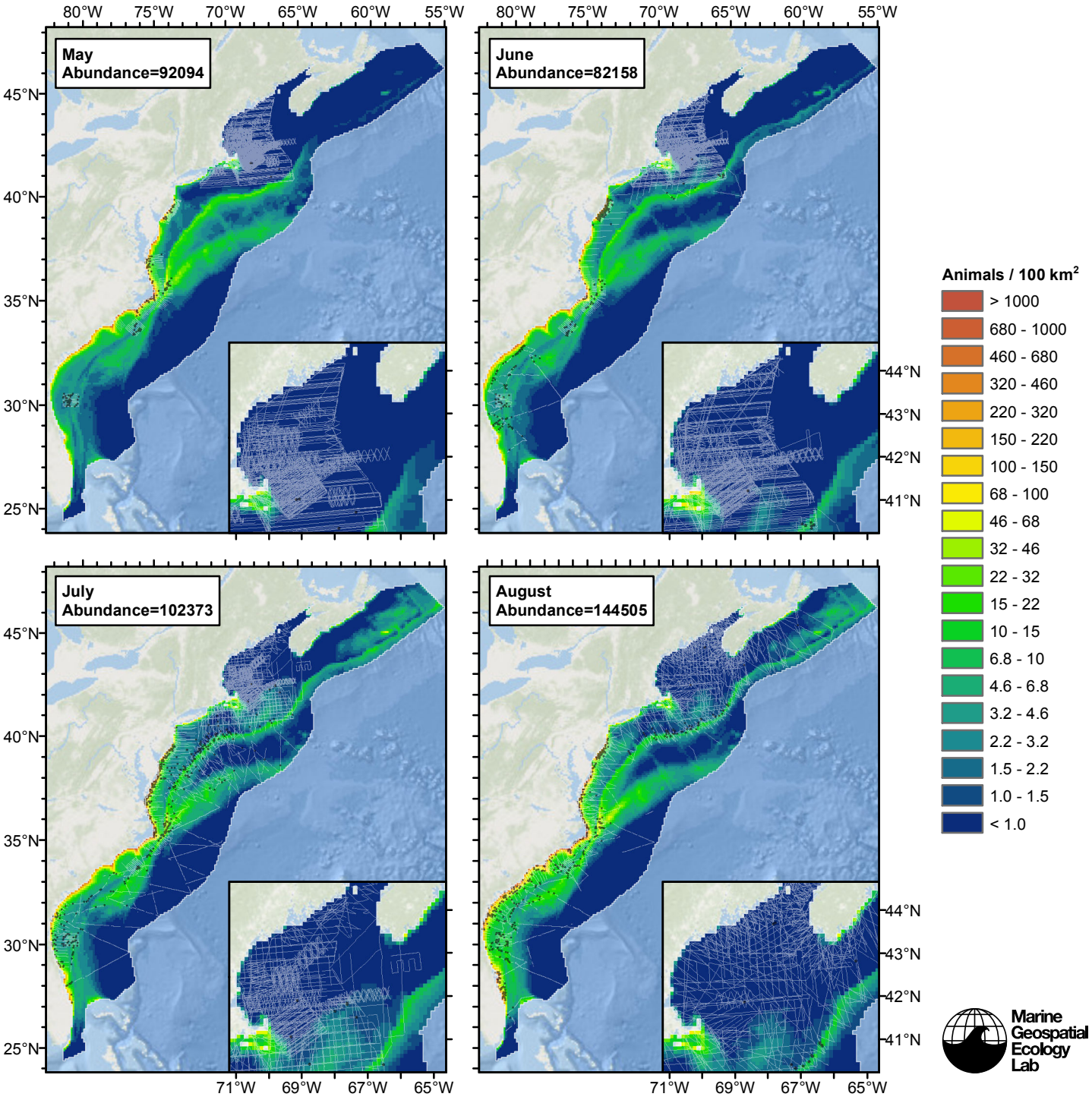
May
Abundance=92094
June
Abundance=82158
July
Abundance=102373
August
Abundance=144505
80°W
75°W
70°W
65°W
60°W
55°W
45°N
40°N
35°N
30°N
25°N
44°N
43°N
42°N
41°N
71°W
69°W
67°W
65°W
Animals / 100 km²
> 1000
680 - 1000
460 - 680
320 - 460
220 - 320
150 - 220
100 - 150
68 - 100
46 - 68
32 - 46
22 - 32
15 - 22
10 - 15
6.8 - 10
4.6 - 6.8
3.2 - 4.6
2.2 - 3.2
1.5 - 2.2
1.0 - 1.5
< 1.0
Marine
Geospatial
Ecology
Lab

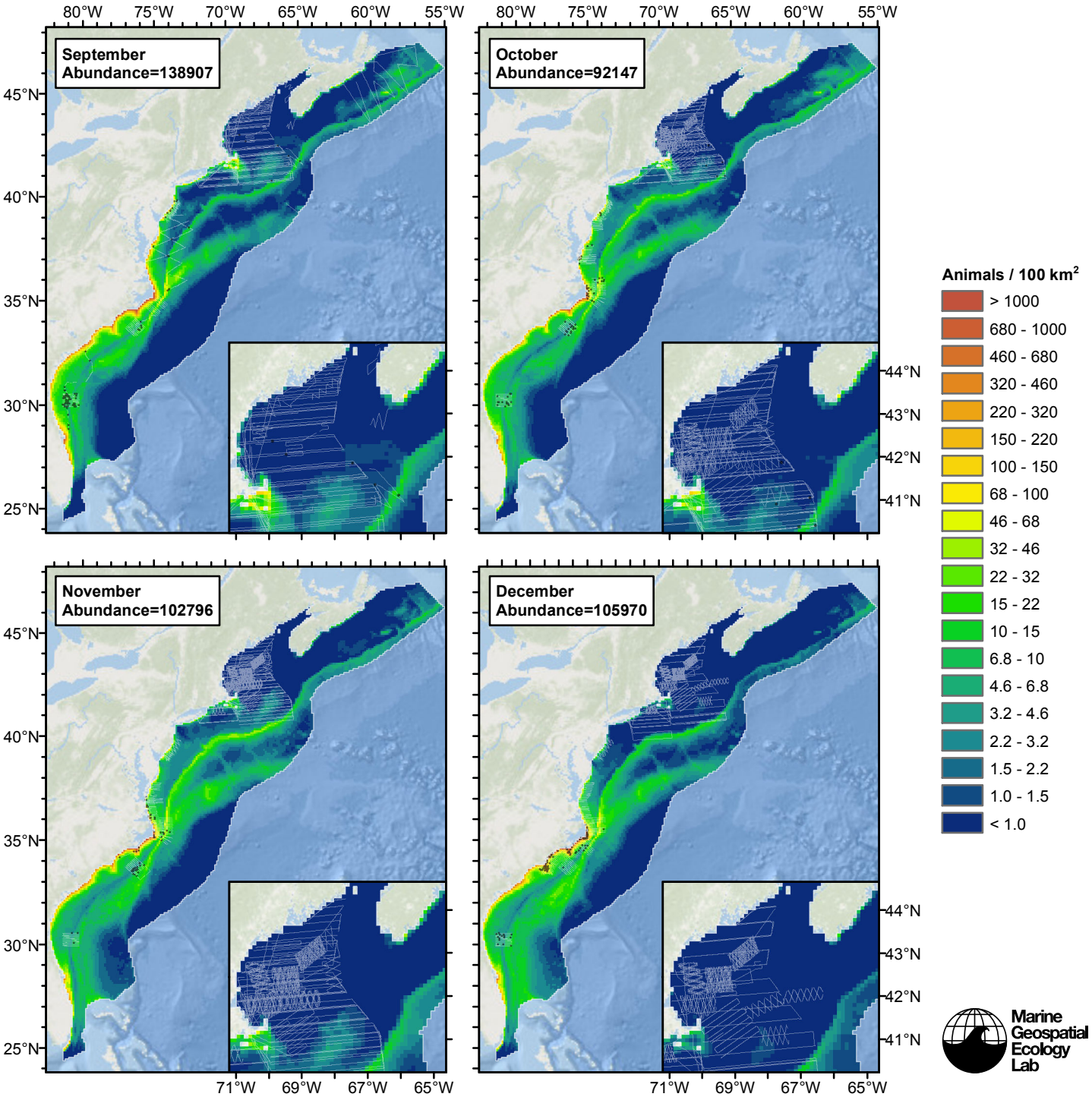
September
Abundance=138907
October
Abundance=92147
November
Abundance=102796
December
Abundance=105970
80°W
75°W
70°W
65°W
60°W
55°W
45°N
40°N
35°N
30°N
25°N
44°N
43°N
42°N
41°N
71°W
69°W
67°W
65°W
Animals / 100 km²
> 1000
680 - 1000
460 - 680
320 - 460
220 - 320
150 - 220
100 - 150
68 - 100
46 - 68
32 - 46
22 - 32
15 - 22
10 - 15
6.8 - 10
4.6 - 6.8
3.2 - 4.6
2.2 - 3.2
1.5 - 2.2
1.0 - 1.5
< 1.0
Marine
Geospatial
Ecology
Lab

Contemporaneous Model

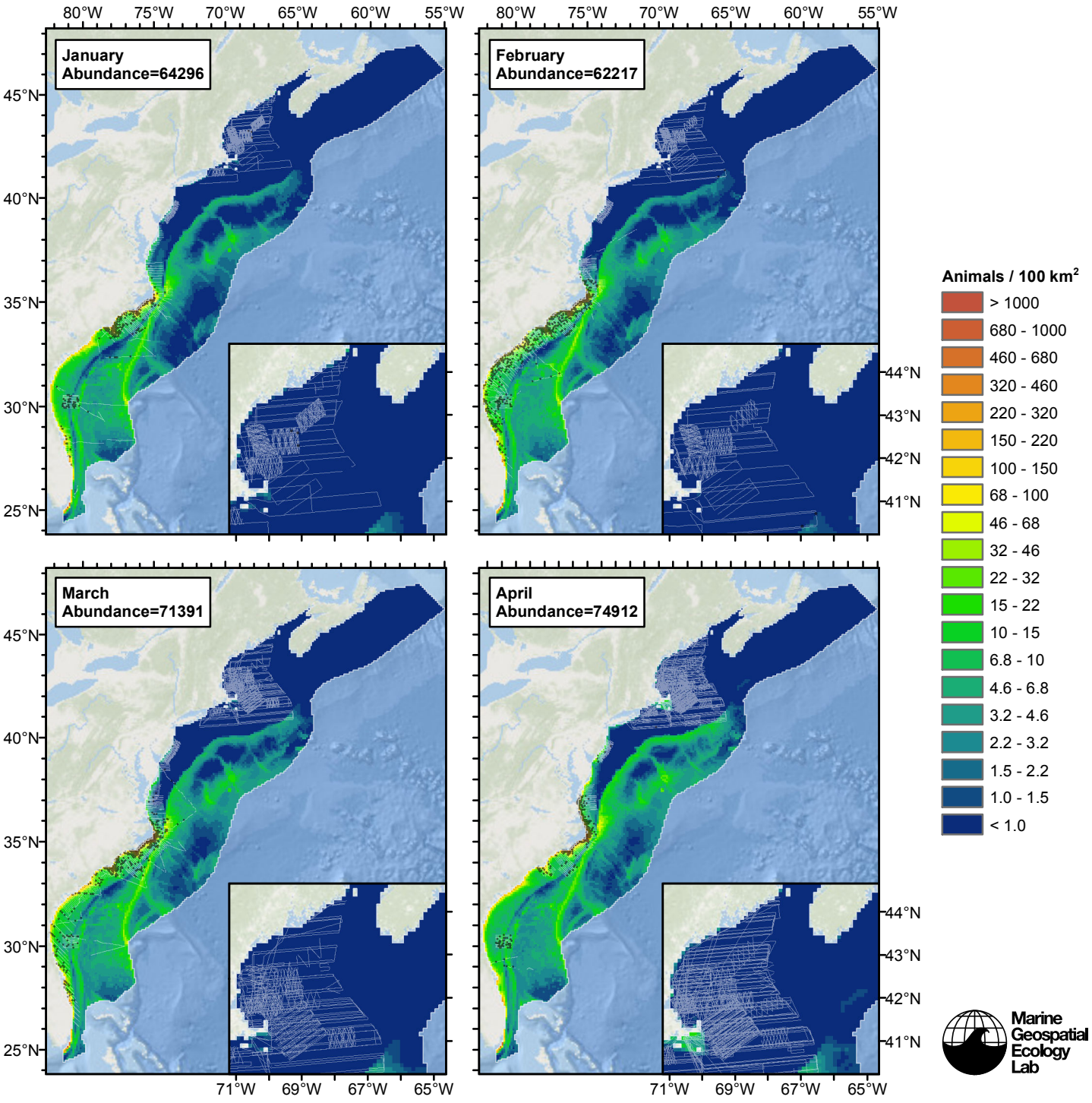

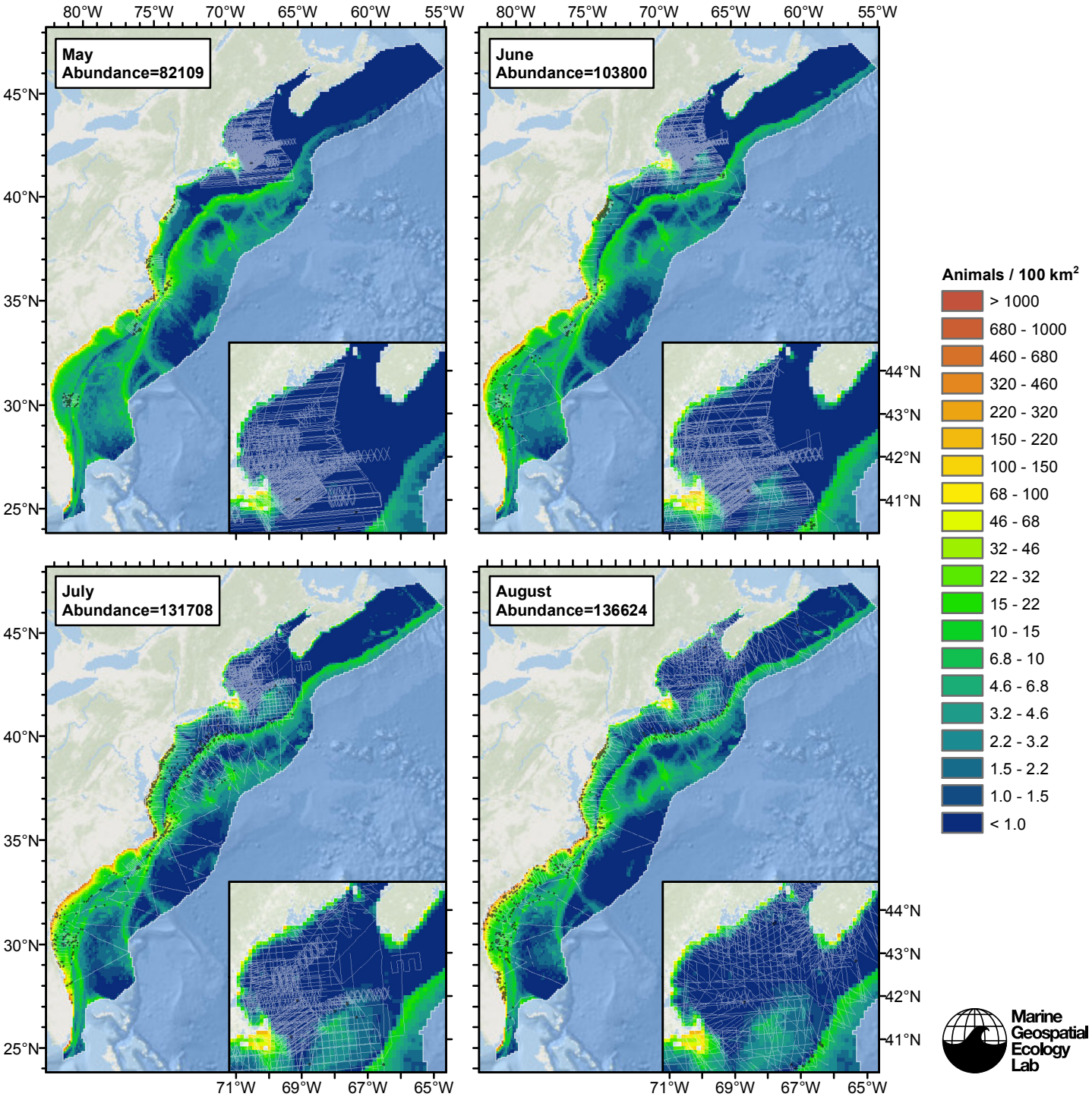
May
Abundance=82109
June
Abundance=103800
July
Abundance=131708
August
Abundance=136624
80°W
75°W
70°W
65°W
60°W
55°W
45°N
40°N
35°N
30°N
25°N
44°N
43°N
42°N
41°N
71°W
69°W
67°W
65°W
Animals / 100 km²
> 1000
680 - 1000
460 - 680
320 - 460
220 - 320
150 - 220
100 - 150
68 - 100
46 - 68
32 - 46
22 - 32
15 - 22
10 - 15
6.8 - 10
4.6 - 6.8
3.2 - 4.6
2.2 - 3.2
1.5 - 2.2
1.0 - 1.5
< 1.0
Marine
Geospatial
Ecology
Lab

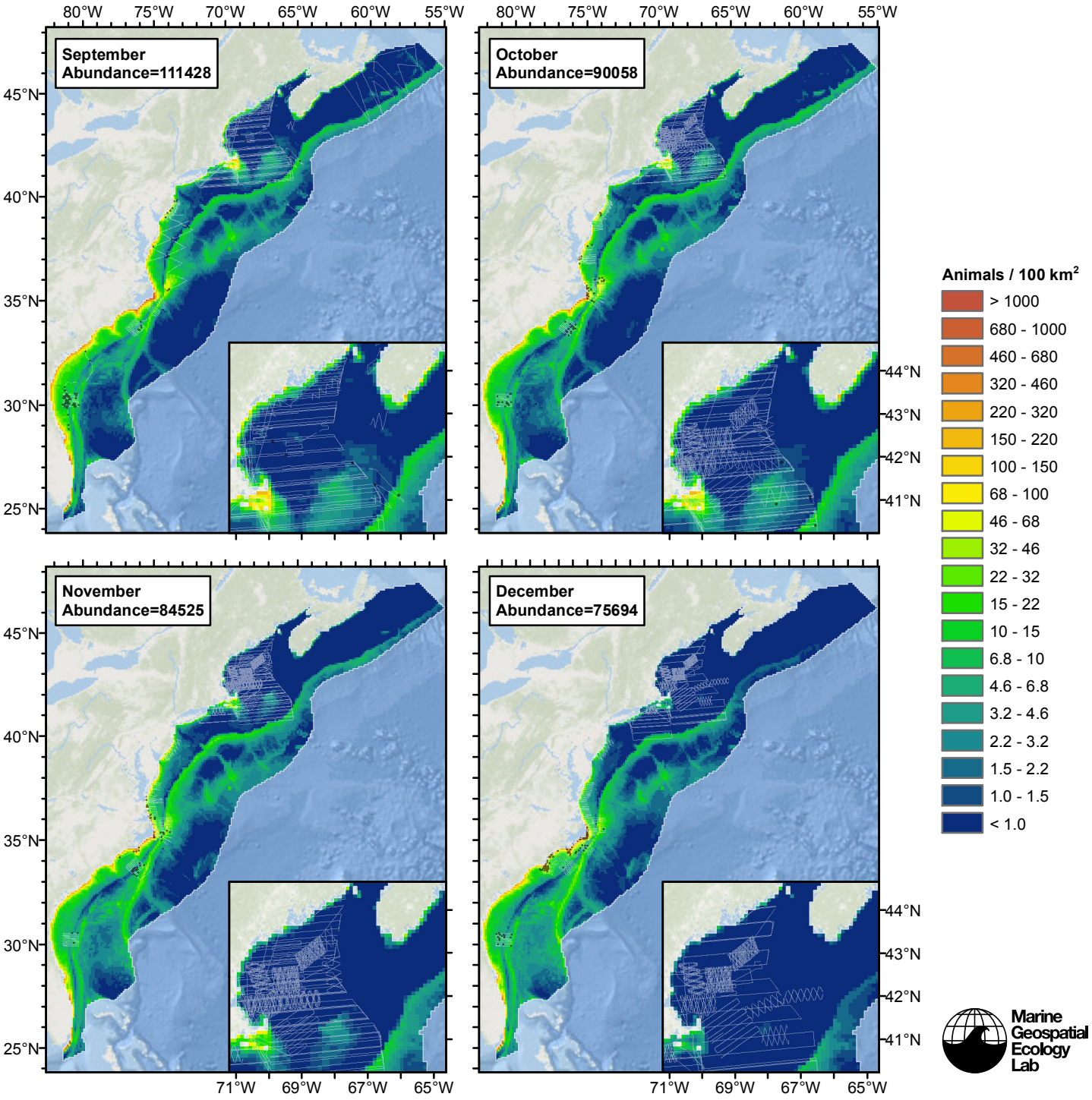
September
Abundance=111428
October
Abundance=90058
November
Abundance=84525
December
Abundance=75694
80°W
75°W
70°W
65°W
60°W
55°W
45°N
40°N
35°N
30°N
25°N
44°N
43°N
42°N
41°N
71°W
69°W
67°W
65°W
Animals / 100 km²
> 1000
680 - 1000
460 - 680
320 - 460
220 - 320
150 - 220
100 - 150
68 - 100
46 - 68
32 - 46
22 - 32
15 - 22
10 - 15
6.8 - 10
4.6 - 6.8
3.2 - 4.6
2.2 - 3.2
1.5 - 2.2
1.0 - 1.5
< 1.0
Marine
Geospatial
Ecology
Lab

Climatological Same Segments Model

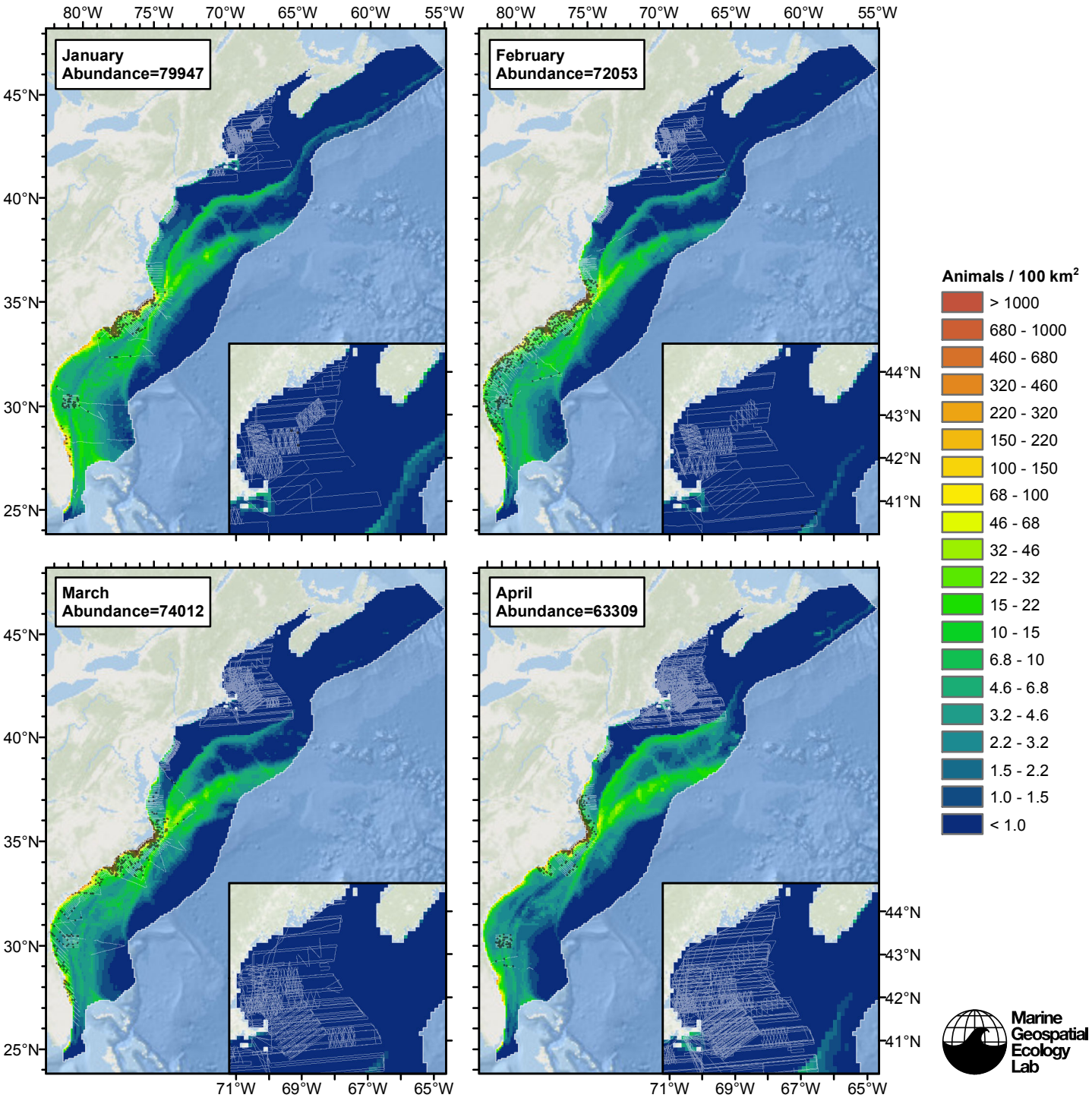

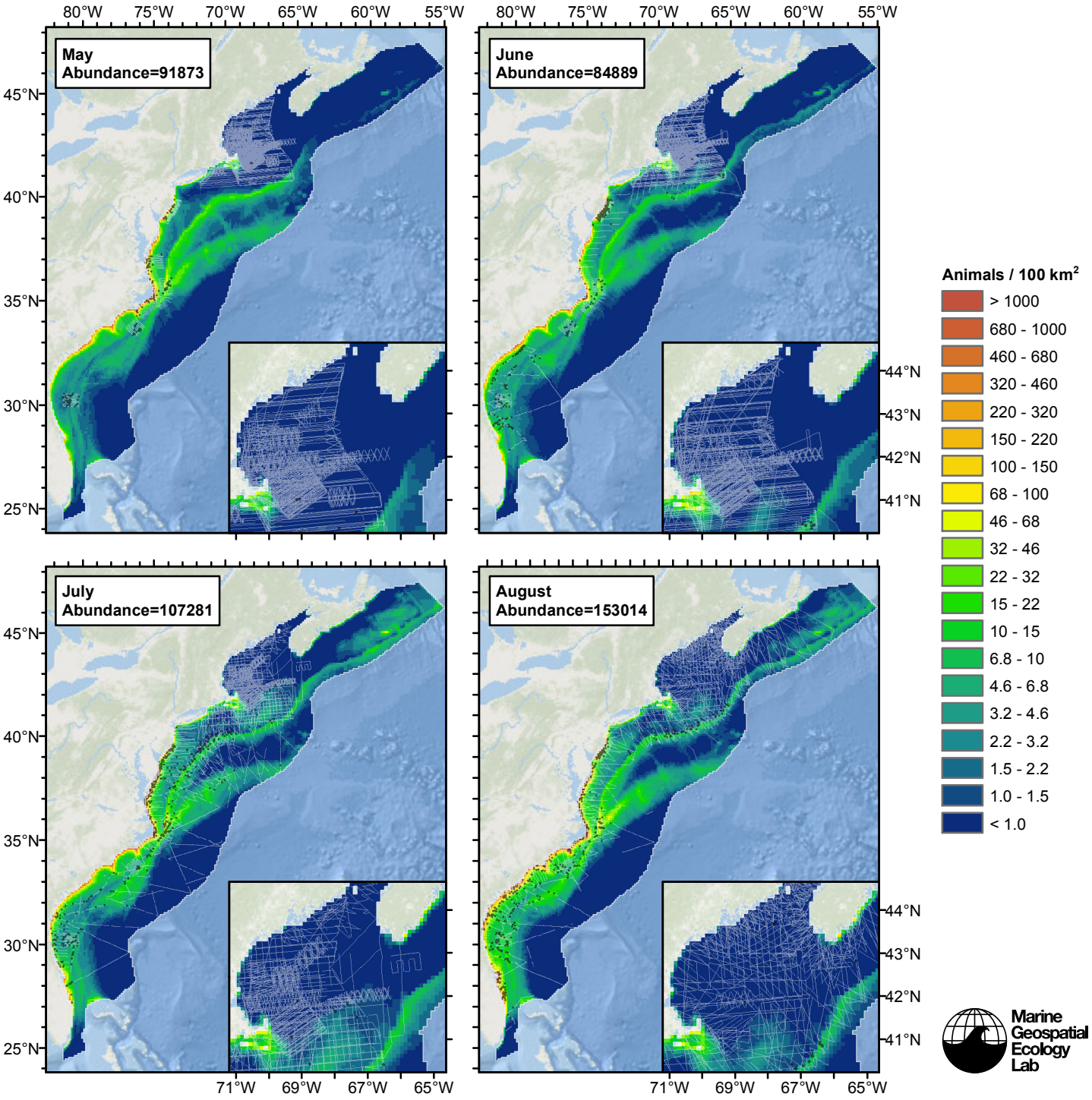
May
Abundance=91873
June
Abundance=84889
July
Abundance=107281
August
Abundance=153014
80°W
75°W
70°W
65°W
60°W
55°W
45°N
40°N
35°N
30°N
25°N
44°N
43°N
42°N
41°N
71°W
69°W
67°W
65°W
Animals / 100 km²
> 1000
680 - 1000
460 - 680
320 - 460
220 - 320
150 - 220
100 - 150
68 - 100
46 - 68
32 - 46
22 - 32
15 - 22
10 - 15
6.8 - 10
4.6 - 6.8
3.2 - 4.6
2.2 - 3.2
1.5 - 2.2
1.0 - 1.5
< 1.0
Marine
Geospatial
Ecology
Lab

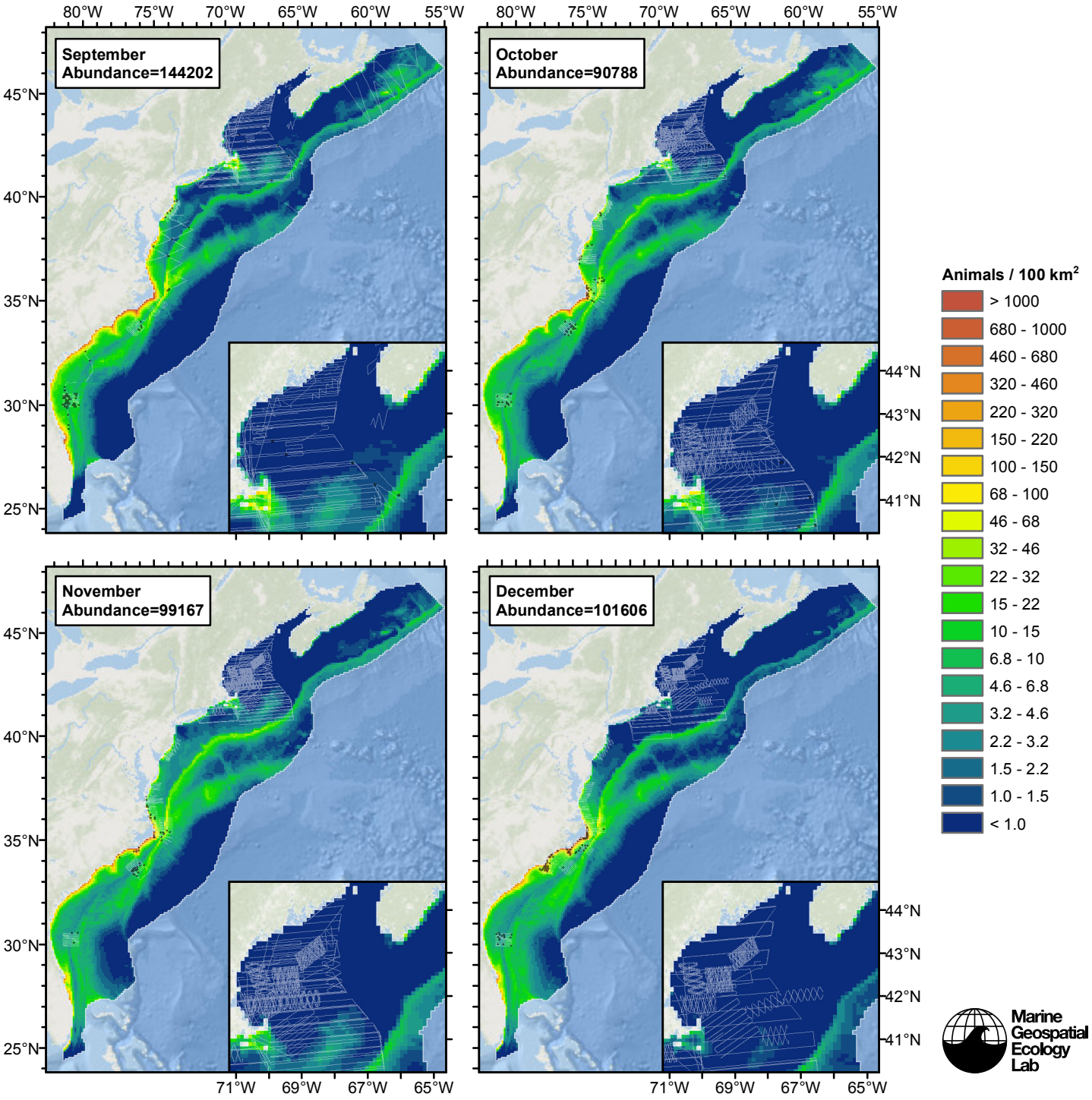

Discussion

Models fitted with climatological estimates of dynamic predictors consistently explained more deviance than models fitted with contemporaneous estimates. However, the best climatological models and the best contemporaneous model predicted very similar spatial distributions (Figs. 134-136) and mean abundances estimates fell within 10% of each other (Table 62). The contemporaneous model predicted higher abundance along the shore in the far north–e.g. in Maine and Canada–which was not supported by the sightings or the literature. Owing to this error, and to the climatological models' higher explanatory power, we selected the climatological model fitted to all segments as our best estimate of the distribution and abundance of bottlenose dolphins.

When summarized at a monthly time step, the model predicted spatiotemporal shifts in density that roughly matched the the

north-in-summer, south-in-winter movements described by Waring et al. (2014) (see Temporal Variability section above), although the total abundance estimate was noisy when predicted at a finer time step (Figs. 137, 138), and we are unsure whether total abundance across the study area should vary seasonally or remain constant. The model predicted that total abundance varied seasonally, with peak summer abundance more than doubling the winter low. If this prediction was correct, it would require seasonal movement of large numbers of animals into and out of the study area. For example, in winter, dolphins would have to move inshore to estuaries or exit the study area to the south or east.

Despite our lack of confidence about the large seasonal variation in study-area-wide abundance, we found the concordance the model showed with the seasonal spatial dynamics described in the literature to be compelling enough to recommend that the monthly predictions be used for management and marine spatial planning applications. For example, the predictions reproduced documented seasonal patterns in near-shore density along mid-Atlantic states. By utilizing the monthly predictions, marine spatial planners siting activities in the mid-Atlantic area can factor these seasonal patterns into their decision making processes, e.g. by deferring activities harmful to bottlenose dolphins to winter months.

Since 2000, NMFS has published two sets of coast-wide abundance estimates. As noted above, we believe our model plausibly represents the aggregate density of the offshore stock and five coastal stocks. For these in aggregate, NMFS estimated an abundance of 93,945 in 2002-2004 and 108,744 in 2010-2011 (Table 62). NMFS surveys occurred in the months of June-August. Our model estimated a year-round mean abundance of 97,476 (Table 62) and a June-August mean abundance of 109,679. This latter estimate concurs very well with NMFS's 2010-2011 estimate, providing further evidence that our model offers a plausible depiction of bottlenose dolphin distribution.

Although NMFS's 2010-2011 estimate was 16% higher than their 2002-2004 estimate, NMFS reported an inability to estimate trends for the abundance for any stock, stating for most stocks that:

> There are limited data available to assess population trends for this stock. The estimates from the 2002/2004 and 2010/2011 surveys are not significantly different from each other; however, it should be noted that the relatively large CVs limit the power to detect significant differences. The statistical power to detect a trend in abundance for this species is poor due to the relatively imprecise estimates and long survey interval.

Although our abundance estimate yielded a relatively low CV (0.06), owing to the large number of surveys it considered, we caution that this CV is an underestimate, as it did not incorporate uncertainty in the detection functions or g(0) estimates (see Methods in our main paper), as NMFS's estimates usually do. Had we incorporated those uncertainties, it is likely that our CV would have been large enough that NMFS's 2002-2004 estimate would have fallen within our expanded confidence intervals. In sum, we believe the evidence is insufficient to identify a trend in bottlenose dolphin abundance, owing to the the issues NMFS raised as well as the likelihood that neither our nor NMFS's abundance estimates are significantly different from each other.

Finally, because our model estimated aggregate density of multiple stocks, model users may face a practical problem utilizing our results to estimate impacts to individual stocks. The solution to this probably requires that each pixel of our predicted density surfaces be apportioned to the stock or stocks that occupy that pixel on that month. We recognize that this is nontrivial, and akin to solving the problem of classifying a sighting into a stock based on geography and time. Model users should consult with NMFS about the best way to approach this problem.

References

Barlow J, Forney KA (2007) Abundance and density of cetaceans in the California Current ecosystem. Fish. Bull. 105: 509-526.

Carretta JV, Lowry MS, Stinchcomb CE, Lynn MS, Cosgrove RE (2000) Distribution and abundance of marine mammals at San Clemente Island and surrounding offshore waters: results from aerial and ground surveys in 1998 and 1999. Administrative Report LJ-00-02, available from Southwest Fisheries Science Center, P.O. Box 271, La Jolla, CA USA 92038. 44 p.

Hiby L (1999) The objective identification of duplicate sightings in aerial survey for porpoise. In: Marine Mammal Survey and Assessment Methods (Garner GW, Amstrup SC, Laake JL, Manly BFJ, McDonald LL, Robertson DG, eds.). Balkema, Rotterdam, pp. 179-189.

Palka DL (2006) Summer Abundance Estimates of Cetaceans in US North Atlantic Navy Operating Areas. US Dept Commer, Northeast Fish Sci Cent Ref Doc. 06-03: 41 p.

Waring GT, Josephson E, Fairfield-Walsh CP, Maze-Foley K, eds. (2007) U.S. Atlantic and Gulf of Mexico Marine Mammal Stock Assessments – 2007. NOAA Tech Memo NMFS NE 205; 415 p.

Waring GT, Josephson E, Maze-Foley K, Rosel PE, eds. (2014) U.S. Atlantic and Gulf of Mexico Marine Mammal Stock Assessments – 2013. NOAA Tech Memo NMFS NE 228; 464 p.